



STATENS GEOTEKNISKA INSTITUT  
SWEDISH GEOTECHNICAL INSTITUTE



# Investigations and Load Tests in Clay Till

ROLF LARSSON

Report 59

LINKÖPING 2001

<b>Rapport/Report</b>	Swedish Geotechnical Institute SE-581 93 Linköping
Order	SGI Literature service Tel: +46 13 20 18 04 Fax: +46 13 20 19 09 E-mail: <a href="mailto:info@swedgeo.se">info@swedgeo.se</a> Internet: <a href="http://www.swedgeo.se">http://www.swedgeo.se</a>
ISSN	0348-0755
ISRN	SGI-R--01/59--SE
Project number SGI	10325
Dnr SGI	1-9905-310
©	Swedish Geotechnical Institute



STATENS GEOTEKNISKA INSTITUT  
SWEDISH GEOTECHNICAL INSTITUTE

# Report No 59

## Investigations and Load Tests in Clay Till

Results from a series of investigations and load tests  
in the test field at Tornhill outside Lund in southern Sweden

Rolf Larsson

## Preface

This report deals with the results of a research project concerning investigations and evaluation of properties in clay till. The investigations in this part of the project have been preceded by a comprehensive literature survey reported in SGI Varia 480 "Lermorän - en litteraturstudie. Förekomst och geotekniska egenskaper". Thereafter, a series of investigations have been performed at the research field at Tornhill outside the city of Lund in southwestern Sweden. Different types of soundings and in situ tests have been tried out for this type of soil. The results have been compared to each other and to results from laboratory tests concerning properties and classification of the soils. A number of in situ and laboratory tests have also been performed and compared to the results from large-scale field loading tests.

The research project has been financed jointly by the Swedish Council for Building Research (BFR), Grant No. 1997 0396, and the Swedish Geotechnical Institute.

The author wishes to express his thanks to all those who have participated and co-operated in the project. Special thanks go to Ann Dueck for her invaluable help in making available both the test field and results from previous investigations, to Mats Svensson, Magnus Palm and Fredrik Leveen at Lund University for their co-operation in the tests concerning the use of surface wave and resistivity measurements, to Ulf Ekdahl at PEAB Grundteknik AB for making available the results from previous pressuremeter tests and the calculation procedure, to Lennart Eriksson at Skanska Teknik AB for providing results from previous pressuremeter tests, to the staff at the PEAB supply depot at Stångby outside Lund for their most valuable help with all the practical arrangements in connection with the load tests, and to Gunnar Tornhill at Tornhill Farm for his kind support and co-operation. Many other colleagues, both at the Swedish Geotechnical Institute and other institutions, have also been involved and contributed to the project to various extents. Finally, the successful execution of the project is largely a result of the skill and dedication of the staff at the Institute's division for Field and Measuring Techniques.

Linköping, December 2000

Rolf Larsson

# Contents

## Preface

<b>Reader's guide to this report</b> .....	8
--	---

<b>Summary</b> .....	9
----------------------	---

<b>Chapter 1: Introduction</b> .....	13
--------------------------------------	----

Purpose and background of the investigation .....	13
---	----

Scope of the investigation .....	13
----------------------------------	----

<b>Chapter 2: The test field</b> .....	16
--	----

2.1 Location .....	16
--------------------	----

2.2 Soil conditions .....	16
---------------------------	----

2.21 Geology .....	16
--------------------	----

2.22 Hydrogeology .....	17
-------------------------	----

2.23 Initial tests to determine geotechnical conditions .....	17
---	----

Field tests .....	17
-------------------	----

CPT-tests .....	19
-----------------	----

Dynamic probing tests .....	20
-----------------------------	----

Field vane tests .....	20
------------------------	----

Ground water observations .....	20
---------------------------------	----

2.24 Laboratory tests .....	23
-----------------------------	----

Classification .....	23
----------------------	----

Determination of mineral composition .....	24
--	----

Water content .....	26
---------------------	----

Soil plasticity .....	26
-----------------------	----

Density .....	27
---------------	----

Particle density .....	25
------------------------	----

Void ratio .....	28
------------------	----

Degree of saturation .....	28
----------------------------	----

Oedometer tests and triaxial tests .....	28
--	----

2.3 Other previous investigations in the test field .....	29
---	----

<b>Chapter 3: Field investigations</b> .....	30
--	----

3.1 General .....	30
-------------------	----

3.2 Groundwater observations .....	31
------------------------------------	----

3.3 Soundings .....	31
---------------------	----

3.31 CPT-tests .....	31
----------------------	----

3.32 Seismic CPT-tests .....	32
------------------------------	----

3.33 Dynamic probing tests .....	36
----------------------------------	----

3.34 Soil-rock drilling .....	38
-------------------------------	----

3.4	In situ tests .....	40
3.41	SASW measurements .....	40
3.42	Resistivity measurements .....	41
3.43	Field vane tests .....	42
3.44	Dilatometer tests .....	42
3.45	Pressuremeter tests .....	45
	Preparation of test cavities .....	45
	Menard pressuremeter .....	46
	New pressuremeter .....	46
	Results .....	48
	Menard parameters .....	48
	Evaluation of creep effects .....	52
	Evaluation of shear strength .....	53
	Evaluation of moduli at small strains .....	55
3.5	Sampling .....	65
3.51	Tube sampling .....	65
3.52	Core drilling .....	66
<b>Chapter 4: Experience from the field tests .....</b>		<b>69</b>
4.1	Ground water observations .....	69
4.2	Soundings .....	69
	CPT-tests .....	69
	Dynamic probing tests .....	69
	Soil-rock drilling .....	69
	Seismic CPT-tests .....	69
4.3	In situ tests .....	70
	Resistivity measurements .....	70
	Field vane tests .....	70
	Dilatometer tests .....	70
	Pressuremeter tests .....	70
4.4	Sampling .....	71
	Open tube sampling .....	71
	Core drilling .....	71
<b>Chapter 5: Laboratory tests .....</b>		<b>73</b>
5.1	Routine tests .....	73
	General .....	73
	Classification .....	73
	Grain size distribution .....	76
	Density .....	76
	Dry density .....	76
	Particle density .....	78
	Natural water content .....	78
	Liquid limit .....	78
	Clay content .....	78
	Void ratio .....	79
	Degree of saturation .....	79
5.2	Oedometer tests .....	81

5.3	Triaxial tests .....	90
	Moduli from triaxial tests .....	100
<b>Chapter 6: Experiences from the laboratory tests .....</b>		<b>103</b>
6.1	Handling of soil samples .....	103
6.2	Routine tests .....	103
6.3	Oedometer tests .....	103
6.4	Triaxial tests .....	104
<b>Chapter 7: Plate loading tests .....</b>		<b>105</b>
7.1	Principle of the plate loading tests .....	105
7.2	Installation of plates and instrumentation .....	106
7.3	Installation of the reaction system .....	108
7.4	Installation of the loading system .....	109
	Measuring system .....	109
	Loading procedure .....	110
<b>Chapter 8: Results of the plate load tests .....</b>		<b>111</b>
8.1	General .....	111
8.2	0.5 x 0.5 metre plate .....	111
8.3	1 x 1 metre plate .....	116
8.4	2 x 2 metre plate .....	120
8.5	Settlement distribution in the load tests .....	124
8.6	Comments on the plate load tests .....	125
<b>Chapter 9: Comparison between predicted and measured settlements and bearing capacity .....</b>		<b>127</b>
9.1	Settlements .....	127
	Oedometer tests .....	127
	Dilatometer tests .....	127
	Pressuremeter tests .....	129
	Menard procedure .....	129
	Briaud procedure .....	129
	Ekdahl and Bengtsson procedure .....	135
	Calculations using the alternative interpretation of the new pressuremeter tests .....	138
	Calculations based on the results of triaxial tests .....	138
	Calculation with moduli from seismic cone tests .....	138
	Comments on the settlement calculations .....	142
9.2	Bearing capacity .....	145
	Comments on the calculations of bearing capacity .....	148
<b>References .....</b>		<b>149</b>
<b>Appendix: Calculation methods for prediction of settlements and bearing capacity .....</b>		<b>155</b>

# Reader's guide to this report

## Why this report is special

This book contains a review of the usefulness of different investigation and calculation methods when applied to clay tills. It focuses on the practical application and use of the most rational ways of solving the engineering problems encountered. It describes the possible sources of error when using different methods, and limitations in the ability to penetrate stiffer and coarser clay tills. The report also describes various problems encountered during the execution of the test programme.

## The goal of this report

The goal of this report is to recommend suitable methods for investigating clay tills, the special precautions that should be observed when using the methods, and the way in which the results should be interpreted. The report also contains recommendations for the way in which bearing capacity and settlements for shallow foundations should be calculated in this type of soil.

## Who should read this report and why

This report will provide the reader with an insight into the advantages and shortcomings of the investigation and calculation methods normally employed in clay tills.

The report will be useful for **geotechnical engineers** planning investigations for selecting the most appropriate methods, giving instructions on how they should be carried out, specifying what supplementary investigations and observations should be made, and stating how the results should be interpreted. It is useful in helping **field engineers** understand how the methods work in this type of soil, what precautions need to be taken and why it is important to follow certain special procedures. It also provides guidance to **designers** when selecting calculation methods

and parameters that are relevant for the design life of the construction.

Finally, the report offers **clients** for geotechnical investigations and design an insight into the relevance of different methods and procedures, thereby enabling a better understanding of the quality of various procedures.

## How this report is organised

The report opens with a summary setting out the main results and recommendations. It continues with a detailed description of the investigations and tests performed, and the results of these. The results of the investigations and the practical experiences and observations gathered in connection with these are summarised in special chapters, which also contain more detailed recommendations on how the investigations should be performed.

Finally, the results obtained with various methods of calculation of settlements and bearing capacity of shallow foundations are compared to the results obtained in the large-scale loading tests in the field. A description of these calculation methods is given in an appendix



# Summary

## Site investigations

Clay till can be very heterogeneous and varying in composition and stiffness. At the same profile, there can be several layers of different origin and composition deposited on top of each other. In the test field at Tornhill, there are three layers with different types of clay till on top of bedrock of clay shale. These are from top to bottom; Baltic clay till, Mixed clay till and North-east clay till. Only a few types of drilling and sounding methods can be used to penetrate every type of clay till. Soil-rock drilling with multi-channel registration of drilling parameters can be used to determine the main stratigraphy both in different types of clay till and the underlying bedrock. A coarse relative measure of certain properties in the main layers can also be obtained. Of the normal sounding methods, only the super-heavy dynamic penetration methods can be used to penetrate every clay till, and then only with special equipment for reduction of the rod friction.

In the softer and more fine-grained Baltic and Mixed clay tills, CPT-tests can be used to determine the stratigraphy and shear strength properties. The classification obtained by using the CONRAD presentation and interpretation programme has been improved with regard to clay tills, but it is still somewhat uncertain in this very mixed-grained material. CPT-tests in clay tills should be performed with robust cones and should include measurement of inclination. The penetration pore pressures should also be measured, preferably with grease-filled slot filters.

Dilatometers can be pushed into the same type of clay tills and many of the results appear to be relevant, provided that the proper interpretation methods are used. However, the experience gathered from dilatometer tests in this type of soil is very limited.

The pressuremeter test is well proven also for clay till, the main problem being to create a good test cavity with a minimum of disturbance in this type of soil. This can be achieved with ordinary methods in the softer and more fine-grained clay tills, but in coarser soils, such as the underlying North-east till, special methods have to be applied.

Some geophysical methods have been tried out. In particular, measurement of the variation in soil resistivity by geo-electrical surface measurements was found to be a good supplement to the ordinary soundings and drillings for mapping of the soil conditions.

Monitoring of the groundwater conditions showed that problems often occur with slow responses in open systems and formation of gas in closed systems. No significant negative pore pressures were found, except in the slopes of the excavation.

## Sampling and laboratory tests

Continuous sampling can be performed in all types of clay till and the underlying bedrock by means of core drilling. A 100% recovery ratio was obtained with the Geobor-S equipment, although great skill was required on the part of the operator to achieve this. The core samples provide a very good basis for a detailed mapping of the profile. However, the combined effects of water flushing during drilling, bending actions during handling and transport in slender plastic containers, and the actions necessary for extrusion and trimming of the samples in the laboratory often create excessive disturbance affecting the strength and stiffness properties of the soil. Disturbed/remoulded samples can be taken by screw auger, but they may not be fully representative of the soil mass.

More undisturbed samples can be taken with thin-walled tube samplers. These samples become limited lengths and are not continuous, but the stiffer tubes and a better handling procedure minimize their further disturbance.

Classification tests in the laboratory are cumbersome since sieving and sedimentation analyses are often required for a proper classification. Determination of relevant bulk densities and water contents requires fairly large specimens. Determination of the degree of saturation can often be complex since measuring errors in the determination of specimen volume and wet and dry masses have a considerable influence in very dense soils. The particle densities measured in the fine-grained material used in the sedimentation analyses may also be non-representative of the larger soil mass.

Oedometer tests require large oedometers because of the heterogeneous soil. It is preferable to use oedometers with the same inner diameter of the oedometer ring as the sampling tube, into which the specimen can be pushed directly. This minimises the trimming and disturbance effects. Because of the large diameters of the specimens and the high stresses required in these tests, high capacity loading arrangements are required.

Triaxial tests also require large specimens because of the heterogeneous soil. When the soil contains a large proportion of coarse particles, even the 102 mm diameter core sample may be too small. However, because of the heterogeneity of the soil, a specimen may also contain separate layers of different materials, which complicates the tests and their interpretation. Trimming is difficult and should be limited in order to avoid unnecessary further disturbance and drying of the specimen. Trimming of the end surfaces must be performed very carefully and often results in the length of the specimen becoming shorter than intended. Friction free end caps should be used. The often recommended arrangement with pins protruding from the end caps into the specimen to prevent it from sliding on the cap cannot be used. It is therefore very important for the end

surfaces to be parallel. The specimen should normally be reconsolidated to its preconsolidation stresses and then brought to its in situ stress condition. Care should then be taken in order to avoid overconsolidating the specimen and thereby giving it properties that it does not exhibit in the field. The often used method of estimating the preconsolidation stresses from information such as the results from field vane tests is therefore questionable, and requires great caution together with close observations of the deformations during the consolidation stages.

### Determination of shear strength

Determination of undrained shear strength in clay till is often performed with Danish field vane tests. The spread in the test results is normally large, as was found in this test field. The undrained shear strength can also be estimated from the net cone resistance in CPT-tests. An empirical cone factor of about 11 has been reported for clay tills from calibrations against the results from field vane tests. This was found also in this investigation. A rough estimate may be obtained also from dynamic probing tests. The interpretation of undrained shear strength from such tests proposed by Butcher et al. (1995) on the basis of results from tests in stiff clays in the U.K. appears to be useful also in the investigated clay tills.

A number of methods have been proposed for evaluation of shear strength from pressuremeter tests. Of these methods, those proposed by Menard (1975) and Mair and Wood (1987) yielded values very similar to the field vane tests. The Gibson and Anderson (1961) method yielded significantly higher values and the method proposed by Briaud (1992) yielded much lower values. The results from pressuremeter tests are time-dependent and the above findings were obtained for the traditional Menard procedure for pressuremeter tests.

Triaxial tests on specimens reconsolidated for the preconsolidation pressures determined in oedometer tests and then unloaded to in situ stresses yielded undrained shear strengths that were about

60 % of those measured by the vane. Strengths similar to those measured by the vane would have been obtained if the procedure of estimating the preconsolidation pressure empirically from the results of the vane tests and consolidating the samples for these stresses had been employed. However, this would have led to arguing in circles in order to match the two types of determinations, which in this context were intended to be independent.

The plate load tests in the investigation proved to be drained and no results from an undrained full-scale failure exist to evaluate the relevance of the determined undrained strengths.

The drained and effective shear strength parameters were determined by triaxial tests. The results correspond well to what is estimated by empirical relations elaborated for other types of clay in Sweden, (Larsson et al. 1985). They also appear to be fairly relevant when comparing them with the results of the large-scale load tests.

### **Determination of deformation characteristics**

Determination of the preconsolidation pressure and oedometer modulus has been performed in oedometer tests in the laboratory. Determination of the preconsolidation pressure required a large number of tests and application of several evaluation methods in order to find probable values and their variation with depth. The evaluated preconsolidation pressures deviated strongly from values evaluated empirically on the basis of field vane tests.

The oedometer moduli evaluated both in the normally consolidated range and in unloading re-loading loops were in good agreement with what would empirically be estimated on the basis of soil type and grain size distribution. The evaluated parameters enabled a modification of the re-loading moduli with respect, for example, to unloading of the soil caused by the excavation before installation of the test plates.

The dilatometer tests yielded similar moduli,

even if the relatively low values in the Mixed till indicated a certain excessive disturbance in this type of soil. These moduli could not be modified in the same way as the oedometer moduli.

Pressuremeter moduli have been evaluated from Menard type pressuremeter tests and the values appear to be appropriate. However, these moduli can only be used in the related semi-empirical calculation methods.

New pressuremeter equipment and test procedures as proposed by Briaud (1992) and Ekdahl and Bengtsson (1996) have been tried. They were found to yield consistent results and to be well suited to supplying moduli and other parameters for calculation of strains in the soil mass.

Tests were also performed with seismic cone tests and surface shear wave tests (SASW) in order to determine the initial shear modulus. This was found to be rather difficult in this heterogeneous type of soil mass. A relatively consistent picture could be obtained by compilation of the results from several seismic cone tests, but the scatter in the results in and between the individual tests was unusually large.

### **Load tests**

Three large-scale plate load tests were performed. The load was applied in steps with durations of mainly 2–6 hours and the results in terms of pore pressure dissipation and time-settlement curves indicated that the tests could be considered as drained. The load-settlement curves indicated yield stresses that corresponded fairly well to the preconsolidation pressures evaluated in the oedometer tests. However, at this stage also the bearing capacity calculated from the drained shear strength parameters was approached, and it is difficult to estimate the degree to which these two aspects interact.

The failure loads and the relative settlements for a given ground pressure differed between the plates. Investigations after the tests also showed that the soil conditions below the plates differed significantly in spite of the fact that they were

relatively closely spaced in a row. In 1974, Hartlén recommended that footings on clay till should be designed as stiff continuous slabs or rafts in order to even out the different properties in the ground. This recommendation was thus found to be prudent.

### Comparison between calculated and measured settlements and bearing capacity

#### Settlements

The method yielding the best correspondence between measured and calculated settlements was the traditional method using theory of elasticity, moduli from oedometer tests and the empirical correction proposed by Jacobsen (1967). However, the cost of obtaining the relevant moduli is fairly high.

Relatively good results were also obtained using the same method but replacing the oedometer test results by results from dilatometer tests in the field, which is considerably less costly.

Traditional pressuremeter tests according to Menard (1975) and the related calculation method yielded settlements that were fairly relevant for normal ground pressures. However, the curvature of the load-settlement curve cannot be estimated by this method. The newer Briaud (1995) method of evaluating the same type of test and calculation of settlements yielded better correlation with the measured values throughout the test. This assumes that the transformation factors proposed by Larsson (1997) and the time exponent as measured in the pressuremeter tests are applied. However, the very large settlements and almost brittle failure after yield in the tests could not be estimated in this way.

The new calculation method proposed by Ekdahl and Bengtsson (1996) using theory of elasticity and moduli varying with strain and time produced relatively good results. However, the results are dependent not only on moduli but also on assumptions about stress transfer between the plate and the surrounding soil and the shear

strength in the soil. The original method is based on new pressuremeter tests according to Briaud (1992) and Ekdahl and Bengtsson (1996). In this case, it has also been used together with another type of modulus reduction and an alternative interpretation of the modulus and its variation with stress in unloading and reloading. The correlation with the measured values deteriorated and improved respectively to some extent. The correlations depend very much on the assumptions about strength and stress transfer.

The same calculation method has been applied to the results from the triaxial tests. The calculated load-settlement relations took the same shape as the measured relations, but the calculated settlements were generally too large.

Finally, the same type of calculations have been made with moduli determined in seismic CPT-tests together with empirical relations for their decrease with increasing strains and an estimate of probable time effects. Similar load-settlement curves were obtained compared with the other calculations, even if the calculated response in this case generally became stiffer. However, the influence from the crude assumptions regarding strain and time dependency is so great that the relevance of these calculations must be questioned.

#### Bearing capacity

The ultimate bearing capacity was predicted fairly well using the general bearing capacity equation and drained shear strength parameters. The corresponding calculations using undrained shear strength yielded values that were too high. Also calculations using the Menard procedure for results from pressuremeter tests yielded exaggerated bearing capacities.

The bearing capacity in terms of allowable settlements was predicted fairly well with settlement calculation methods, which take the curved load-settlement relation into account. The accuracy of the predictions follows the ability of the methods to correctly predict the settlements at fairly large loads and settlements.

# 1. Introduction

## **Purpose and background of the investigation**

Clay tills occur in many places in Sweden although the extent and thickness of the deposits are often limited. Since clay till is a fertile soil, most of these areas are used for agriculture. The most extensive deposits are located in the province of Skåne in the southernmost part of the country.

Construction on and in clay tills using increasingly advanced designs has expanded greatly in connection with the new Öresund Link to Denmark; both in the development of the infrastructure associated with this project and general development in the area. This has led to a need for better knowledge of the local clay tills and their properties, together with efficient methods of investigating them. This investigation addresses some of these questions.

A major part of the research forming the basis for current practice in the investigation of clay tills and calculation of settlements and bearing capacity was carried out in the 1960's and early 1970's, primarily by Moust Jacobsen in Denmark and Jan Hartlén in Sweden. Progress in investigation methods and design methods has continued since then. The results have partly been utilised in large infrastructure projects in Denmark, while research and development with respect to Swedish conditions has been more limited. In Sweden, practice when investigating clay tills has largely relied upon the methods and empirical relations proposed by Hartlén (1974). More traditional investigation methods such as the Danish field vane test and Menard-type pressuremeter tests, have also been used to some extent. However, projects concerning the development of new techniques have recently been initiated and carried out by local contractors, primarily PEAB AB and Skanska Teknik AB,

and a test field for investigations in clay till has been established by Lund University. Laboratory investigations performed as part of the last project have recently led to a licentiate thesis (Dueck 1998).

The current investigation was carried out in order to obtain a more comprehensive picture of the usefulness and potential for different investigation methods, both more traditional methods and newer equipment developed since the 1960's. The aim was also to make an evaluation of certain newly proposed design methods. Funds for this purpose were allocated by the Swedish Council for Building Research and the Swedish Geotechnical Institute in 1997.

## **Scope of the investigation**

The project began with a thorough survey of the existing literature on clay tills. The study was supplemented with international experiences from other stiff clays, which to some extent may be relevant also for clay tills. On the basis of this study, a mapping of the occurrence, origin and composition of clay tills in Sweden was performed. The reported experience regarding properties and investigation methods was synthesised and both parts were reported in SGI Varia No. 480 "Lermorän -en litteraturstudie. Förekomst och geotekniska egenskaper." (Clay till – a literature survey. Occurrence and geotechnical properties.).

The following part of the project reported here comprised extensive investigations using every available and possibly relevant method, in addition to large-scale plate loading tests in the test field for clay till at Tornhill. The test field was made available by the Department of Soil Mechanics and Foundation Engineering at Lund University, which is responsible for its administration.

The present investigation has thus been aimed at investigating the usefulness of the different investigation methods in clay till and determining necessary modifications, if any, to the existing interpretation methods. The aim has also been to investigate the present methods of calculating the bearing capacity of shallow foundations and settlements in this type of soil. The final goal has been to find a recommendation as to which investigation method or combination of methods should be used in different types of clay tills, the special precautions that should be observed in connection with investigations in this type of soil, methods/procedures for evaluating different soil properties and methods/procedures for calculating bearing capacity and settlements for shallow foundations.

The test field was well suited for the intended purpose since the soil profile is varied and contains three of the major types of clay till in the area: Baltic clay till, Mixed clay till and North-east clay till. This layering sequence is also typical for the area and a large part of the region. However, the variation in properties between the tills is too great to permit the use of most of the test methods in all three types of till. The North-east till is so coarse and stiff that only a few methods can be used to penetrate it. The focus of the investigations therefore lies on the upper two types of clay till. After the investigations, a series of three large-scale plate load tests was performed in the test field. The plates were excavated to the normal foundation level. Nevertheless, the zone of influence from these tests was also confined to the upper two types of clay till. Although the results were unanimous in certain respects, the variation both vertically and laterally in the upper soil layers was so great that a detailed evaluation of the different design methods cannot be made from this limited number of load tests.

All references to evaluated properties, soil classifications etc. from field and laboratory tests in this report refer to established methods used in Swedish practice unless otherwise stated.

The test and interpretation methods commonly used in Sweden are described in the following publications:

*Test and interpretation methods commonly used in Sweden.*

Test method	Test procedure	Inter-pretation	Publication
Dynamic probing test type HfA	X	X X	<b>Bergdahl (1984)</b> . Geotekniska undersökningar i fält. SGI Information No. 2 <b>Bergdahl et al. (1993)</b> . Plattgrundläggning. Svensk Byggtjänst.
CPT-test tests.	X X	X	<b>Swedish Geotechnical Society SGF (1993)</b> . Recommended standard for CPT- <b>Larsson (1992)</b> . The CPT-test. SGI Information No. 15.
Field vane shear test	X	X	<b>Danish Geotechnical Society, DGF Feltekomité (1993)</b> . Referenceblad for vingeforsog. Referenceblad 1.
Seismic cone test	X X	X	<b>Campanella et al (1986)</b> . Seismic cone penetration test. Proc. In Situ 86. ASCE. <b>Larsson and Mulabdic (1991)</b> . Shear moduli in Scandinavian Clays. SGI Report No. 40.
Dilatometer test	X X	X	<b>Swedish Geotechnical Society SGF (1993)</b> . Recommended standard for dilatometer tests. <b>Larsson (1990)</b> . Dilatometerförsök. SGI Information No. 10. <b>Powell and Uglov (1988)</b> . The interpretation of dilatometer tests in U.K. clays. Penetration testing in the U.K. Thomas Telford, London.
Pressuremeter test	X X	X X X X	<b>Baguelin et al. (1978)</b> . The Pressuremeter and Foundation Engineering. Trans. Tech. Publications. <b>Mair and Wood (1987)</b> . Pressuremeter testing - methods and interpretation. Ciria. <b>Briaud (1995)</b> . Pressuremeter Method for Spread Footings on Sand. The Pressuremeter and its New Avenues. Balkema. <b>Larsson (1997)</b> . Investigations and load tests in silty soil. SGI Report No. 54.
New pressuremeter tests	X X	X X	<b>Briaud (1992)</b> The Pressuremeter. Balkema. <b>Ekdahl and Bengtsson (1996)</b> Ny metod att beräkna sättningar vid plattgrundläggning. Väg- och Vattenbyggaren.
Pore pressure measurements	X		<b>Tremblay (1990)</b> . Mätning av grundvattennivå och portryck. SGI Information No. 11
Plate load tests	X X	X X	<b>Bergdahl (1984)</b> . Geotekniska undersökningar i fält. SGI Information No. 2 <b>Bergdahl et al. (1993)</b> . Plattgrundläggning. Svensk Byggtjänst.
Classification	X	X	<b>Karlsson and Hansbo (1984)</b> . Soil Classification. Swedish Council of Building Research, T21:1982.
Bulk density	X	X	<b>Swedish standard SS 02 71 14</b>
Water content	X	X	<b>Swedish standard SS 02 71 16</b>
Liquid limit	X	X	<b>Swedish standard SS 02 71 18</b>
Plastic limit	X	X	<b>Swedish standard SS 02 71 18</b>
Sedimentation test	X	X	<b>Swedish standard SS 02 71 24</b>
Oedometer test with incremental loading	X	X	<b>Swedish standard SS 02 71 29</b>

## 2. The test field

### 2.1 LOCATION

The test field is located in southern Sweden north of the city of Lund, about 1 km outside the limits of the built-up areas of the city. The land belongs to the municipality of Lund and since 1993 has been let to the Department of Soil Mechanics and Foundation Engineering at Lund University as a test field for geotechnical investigations and experimental installations. In the same year, the department thoroughly investigated the field in a project sponsored by the Swedish Council for Building Research (Dueck 1994). Since then, it has been open for research projects aimed at improving knowledge of clay tills, in addition to developing design and investigation methods such as the current project. The test field is under the administration of the above department.

The test field is named Tornhill after the neighbouring farm. It is a former market garden surrounded by cultivated farmland. Most of the field is open grass-covered land, but its former use can be seen from the remaining apple, cherry and pear trees surrounding the open spaces. There is a thin cover of topsoil on top of the clay till and remains of shallow drainage installations can also be found in the ground. The area is very flat.

### 2.2 SOIL CONDITIONS

#### 2.2.1 Geology

The test site is located in the south-western part of the province of Skåne, where several different types of clay till have been deposited on top of each other during different periods of the last glaciation. This ended approximately 13,000 years ago.

The bedrock at the site consists of clay shale. Further away, to the north-east of the site, the bedrock consists mainly of primary crystalline rocks, while to the south-west, it contains mostly

sedimentary rocks such as limestone, chalk and sandstone. The bottom layers of the clay till were deposited during a period when the ice cover moved in from the north-east and consequently they principally contain material originating from the types of rock found in this area. The ice cover then retreated and readvanced several times, and the direction of the ice movement also changed. During the last stage of the glaciation, the ice approached from the south-west direction and consequently the top layers contain a large proportion of material originating from sedimentary rocks. This material was more easily crushed and ground down by the ice and the layers are therefore also more fine-grained. In the limestone and chalk, flint had been created and the till contains various amounts of this material. In Sweden, this clay till is called Baltic clay till, since the ice approached from areas that are now covered by the Baltic Sea. The layering of the soil is complicated by the fact that during certain periods of the glaciation the area was free from ice and sediments were then deposited. In succeeding stages of the ice movement, these sediments and the upper layers of underlying previously deposited till were partly mixed into the new deposits of till.

The geological soil profile at the test site can thus roughly be divided into bedrock of clay shale, a North-east clay till dominated by material originating from crystalline rock, an intermediate layer of a mixture of North-east clay till, sedimentary deposits of sand and silt and Baltic clay till, and on top, a layer of Baltic clay till. The composition within these main layers varies considerably both with depth and laterally owing to the formation process. In particular, the intermediate layer may contain layers or pockets classified as clay till, silt till or even sand till, depending on the amount of sediment they contain. Also pockets of cleaner sand or silt are found. This is



also valid for the upper layer of Baltic clay till but to a lesser extent. The sand and silt pockets appear to be isolated and unconnected, judging from the results of nearby soundings and from ground water observations during pumping tests.

In the test field, the thickness of the Baltic clay till is about 3 metres and the intermediate layer is also about 3 metres thick. The thickness of the North-east till and the depth to the bedrock varies. In the part of the test field where the current investigation was carried out, the North-east till was about 8 metres thick and the depth to bedrock was thus about 14 metres. In a borehole at the neighbouring farm, the depth to bedrock had been found to be 16 m and on the opposite side of the test field it had been found to be 24 metres.

This type of profile is common for a larger area encompassing the cities of Malmö, Lund and Eslöv. However, the thickness of the different layers varies. The combined thickness of the upper two layers varies between about 3 and 15 metres, and the thickness of the underlying North-east till varies even more. The composition of the bedrock also varies and over most of this larger area it consists of sedimentary rock and mainly limestone. Bearing these variations in mind, the results from the test field may be useful in the larger region.

## 2.22 Hydrogeology

The clay till is very low-permeable. Rain and meltwater therefore penetrate the ground very slowly. On the other hand, the underlying bedrock is normally much more pervious and the ground water pressure is here highly affected by the level of depressions in the ground in the surroundings and by the sea level in Öresund bordering south-west Skåne. In the test field, this results in a free ground water level in the upper soil layers which varies seasonally between ground level and a depth of approximately 2 metres. In the upper two main layers and the upper parts of the North-east till, the pore water pressure increases more or less hydrostatically from this free ground water level. At greater depths,

the pressure level drops towards a new and considerably lower hydrostatic ground water head in the bedrock.

Due to the very low porosity of the soil and a high degree of saturation, the amount of water required for changing the ground water level is very limited and thereby also, for example, the amount required for changing the bearing capacity in the upper layers. Since the former shallow drainage system has ceased to function, the parts that are slightly shallower than the surrounding area often become flooded during snow melting and periods of heavy rain.

## 2.23 Initial tests to determine the geotechnical conditions

### Field tests

The geotechnical conditions in the test field were investigated in 1993 (Dueck 1994). CPT-tests covering the main open area were performed in a grid pattern with 12 metres between the test points, *Fig. 1*. Supplementary tests were also performed in other parts of the field. Dynamic probing tests were performed at three points and the level of the bedrock was determined on one side of the field with rock drilling equipment. The undrained shear strength of the clay till was measured at two points in the field using a Danish field vane.

The ground water conditions were observed with a number of piezometers and in open holes at various locations in the field.

Disturbed samples were taken by continuous flight auger down to 10 metres depth at four points. This sampling has been supplemented by “undisturbed” sampling in a later investigation by Dueck (1997). The latter samples were taken with both a Danish type of piston sampler (American tube) and by core drilling using a triple tube core sampler of the Geobor-S type.

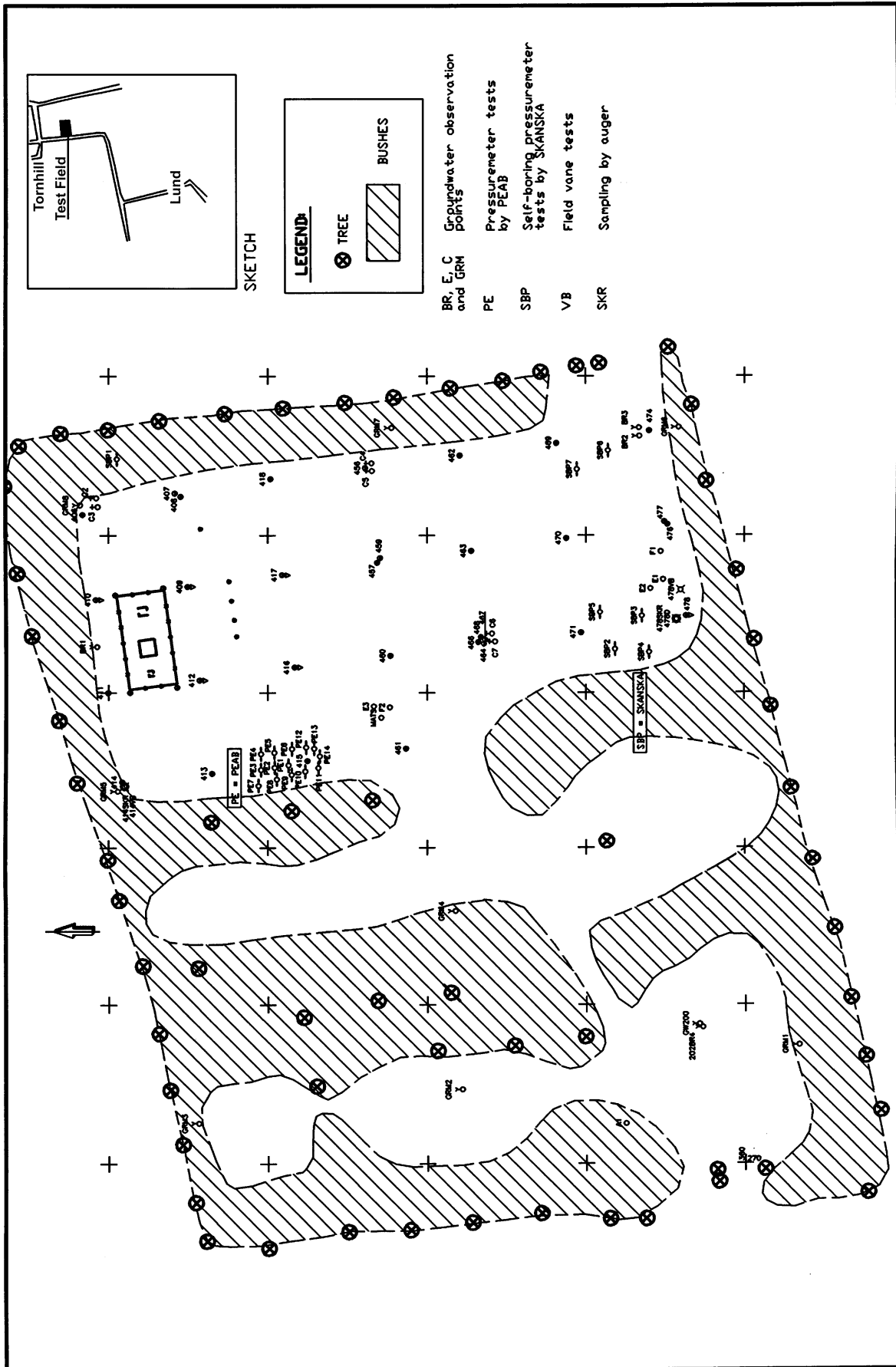


Fig. 1. Layout of the test field and the investigation points.

**CPT-tests**

Altogether, 25 CPT-tests were performed in the initial investigations. The tests were performed using a standard 5-ton CPT-probe with 1000 mm<sup>2</sup> cross sectional area. The pore pressure was measured at the standard position behind the shoulder of the tip using a slot filter filled with grease, which has become common practice in CPT-tests in this type of soil.

The test results generally confirmed the picture of the layering in the profile with a thin layer of top soil on top of about 3 metres of a relatively

stiff soil, followed by about 3 metres of a somewhat less stiff layer. Thereafter, the stiffness of the soil rapidly increased and all tests stopped at about 7 metres depth, below which penetration was impossible with the equipment used, *Fig. 2*. Apart from this unanimous general picture, the results were heavily scattered with large dips and peaks in an inconsistent pattern. Part of these anomalies can be expected to be related to coarse particles of gravel and stone sizes, and part may be assumed to originate from embedded pockets of sand and silt. However, it is very difficult to distinguish between these possibilities.

**CPT - test**

- |                 |                 |                 |                 |                 |                 |                 |
|-----------------|-----------------|-----------------|-----------------|-----------------|-----------------|-----------------|
| 01 Tornhill 406 | 05 Tornhill 411 | 09 Tornhill 415 | 13 Tornhill 456 | 17 Tornhill 462 | 21 Tornhill 470 | 25 Tornhill 407 |
| 02 Tornhill 478 | 06 Tornhill 412 | 10 Tornhill 416 | 14 Tornhill 459 | 18 Tornhill 463 | 22 Tornhill 471 |                 |
| 03 Tornhill 409 | 07 Tornhill 413 | 11 Tornhill 417 | 15 Tornhill 460 | 19 Tornhill 468 | 23 Tornhill 474 |                 |
| 04 Tornhill 410 | 08 Tornhill 414 | 12 Tornhill 418 | 16 Tornhill 461 | 20 Tornhill 469 | 24 Tornhill 477 |                 |

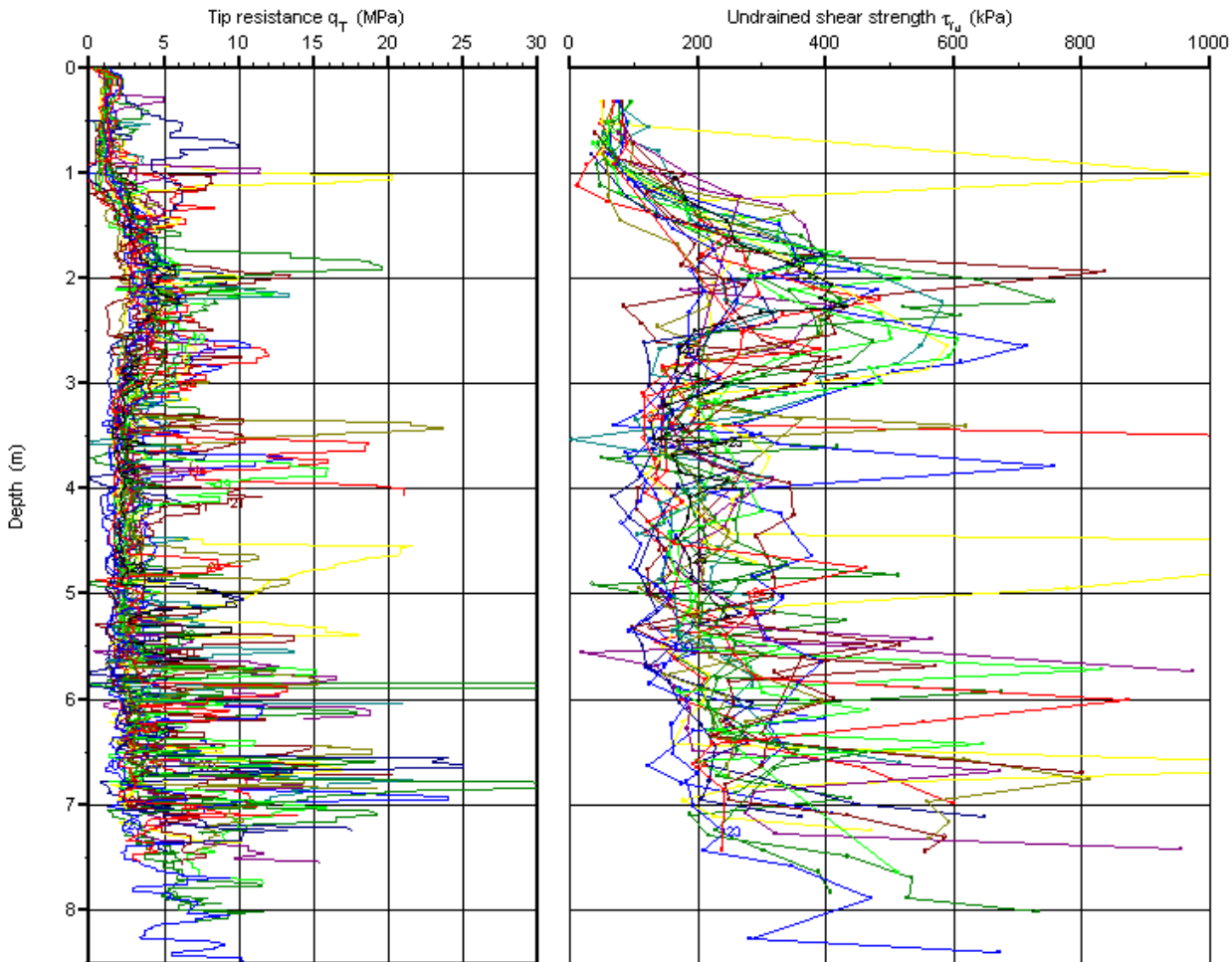


*Fig. 2. Compilation of the results from the CPT-tests in the test field.*

Existing charts for classification of soils on the basis of results from CPT-tests indicated soils ranging between silty clay and sand, with a concentration on silt. Since these charts classify “soil type behaviour” rather than grain size distribution and since clay tills in many respects behave in a similar manner to silt, this may be seen as a relatively fair classification. Since then, the results from these tests together with other tests in clay till and the results from numerous investigations in silts have enabled an improved classification to be made. This has been incorporated in the CPT programme CONRAD, used mainly in Sweden, *Fig. 3*. However, the possibilities of separating various types of clay till from each other and from silt on the basis of CPT-tests alone are still limited.

### Dynamic probing tests

The dynamic probing tests were performed with a rather crude method and did not yield any detailed information, except that the penetration resistance increased rapidly from about 7 metres depth. With this method, the tests penetrated to about 8 metres depth, i.e. slightly more than the CPT-tests.

### Field vane tests

The field vane tests showed a profile with an undrained shear strength of generally 300 to 400 kPa between 1.5 and 3 metres depth, dropping to about 200 kPa between 3 and 5 metres depth and then increasing again. The scatter in the measured strength values was considerable. A comparison between these results and the results from the CPT-tests indicates that a cone factor  $N_{KT}$  of between 10 and 12 would be appropriate, *Fig. 4*. Cone factors of this size have been suggested from various Danish investigations in clay till, (Kammer Mortensen et al 1991, Jørgensen and Denver 1992, Luke 1996).

### Ground water observations

The pore pressures and groundwater levels were studied in six closed piezometers of the BAT type and in three open standpipes installed at different locations in the test field and at depths between 3 and 5 m. The results were not quite consistent. This was probably due to problems with a considerable time lag in the open standpipes and with formation of gas at two of the closed piezometers. However, after an observation period of one year, it was concluded that the ground water table in this part of the profile appeared to vary between ground level in early spring and a depth of about 2 m during summer and early autumn.

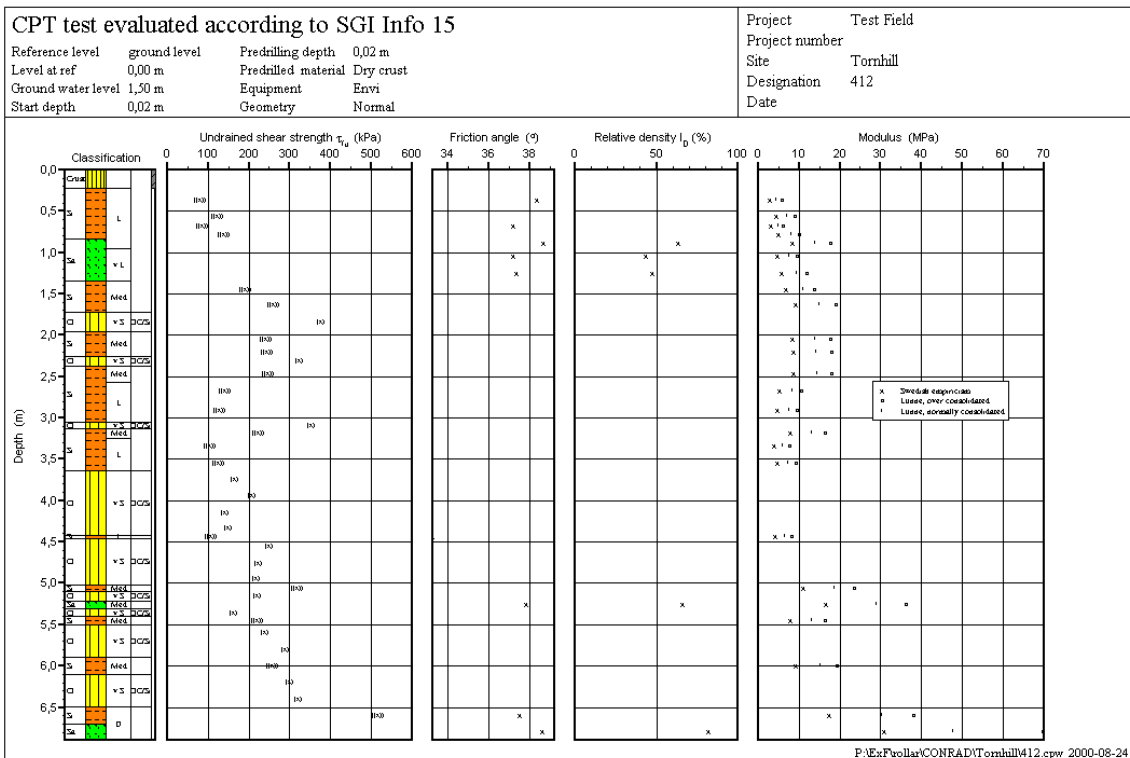
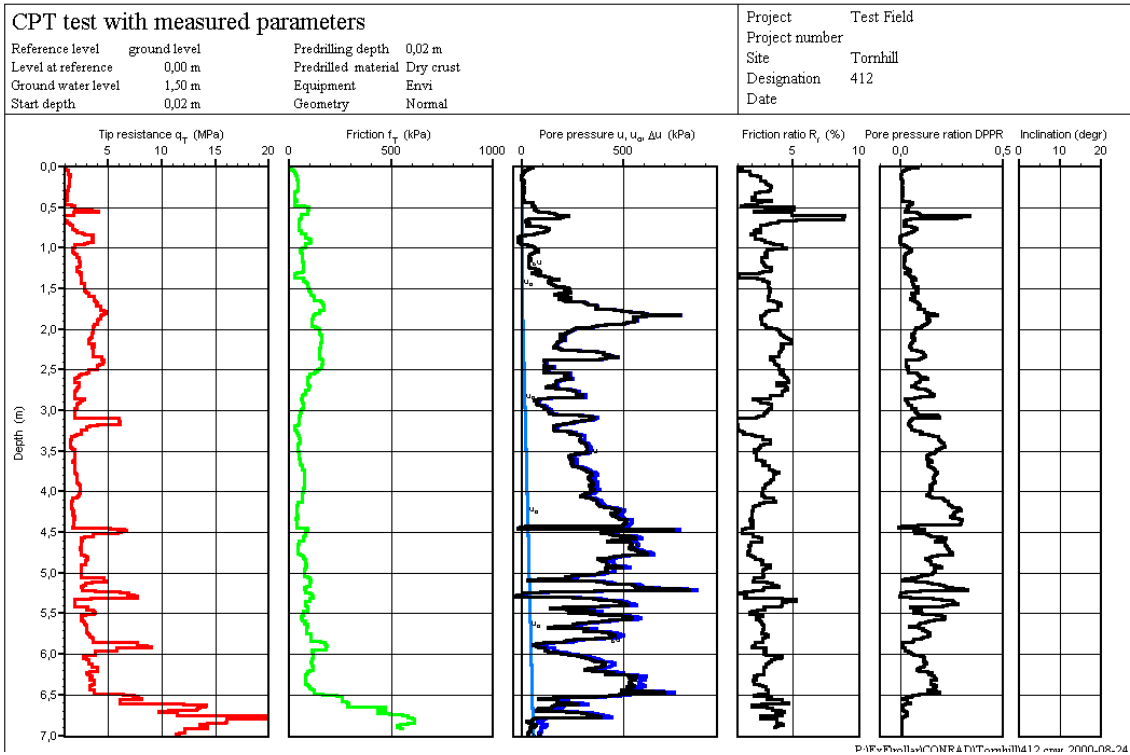


Fig. 3. Examples of CPT-test results presented and evaluated using the CONRAD programme.  
a) Test point 412.

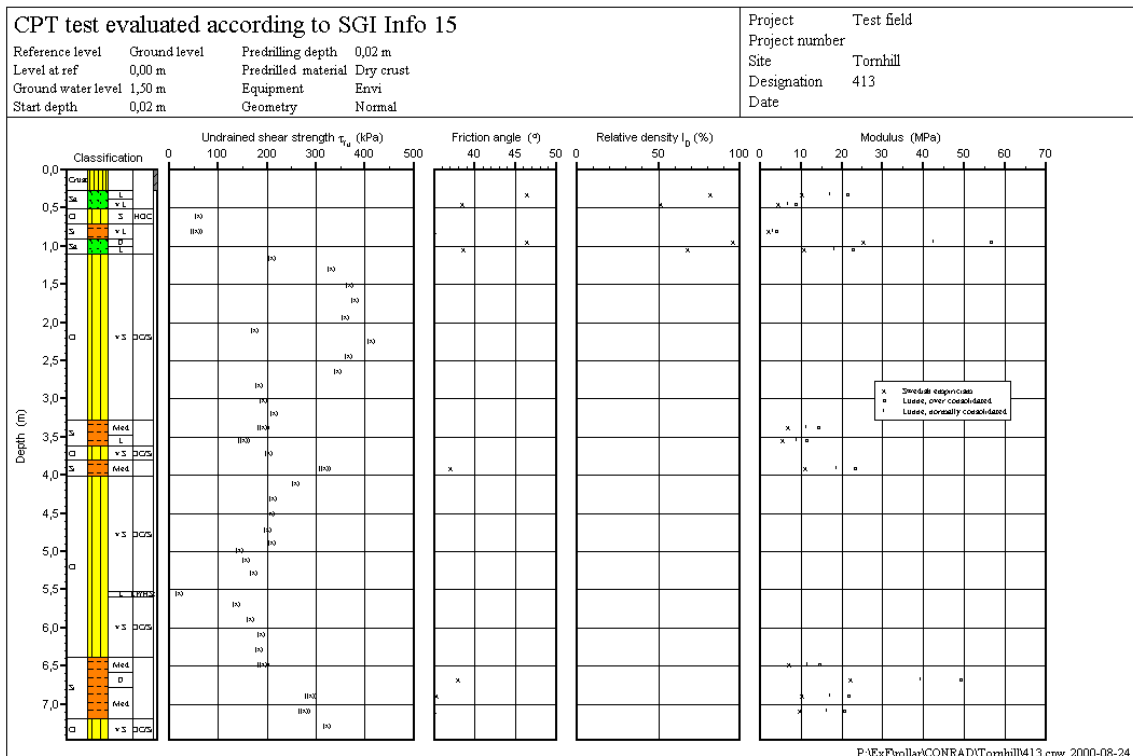
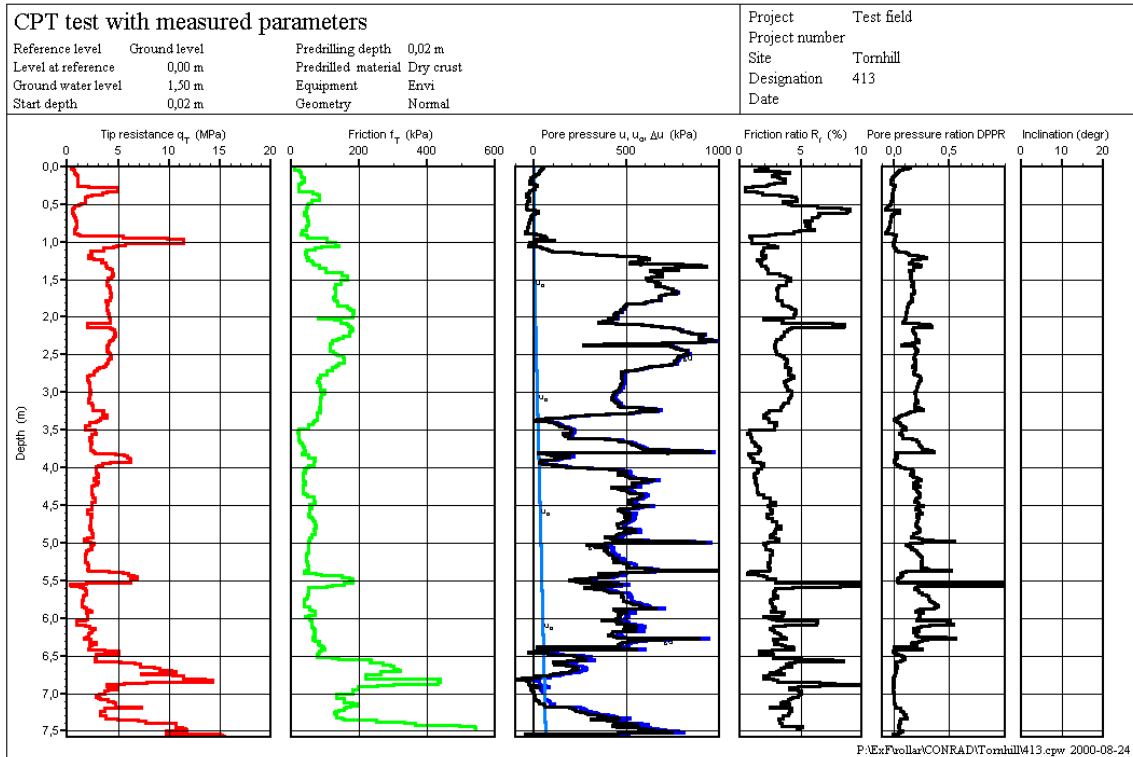


Fig. 3. Examples of CPT-test results presented and evaluated using the CONRAD programme.  
 b) Test point 413.

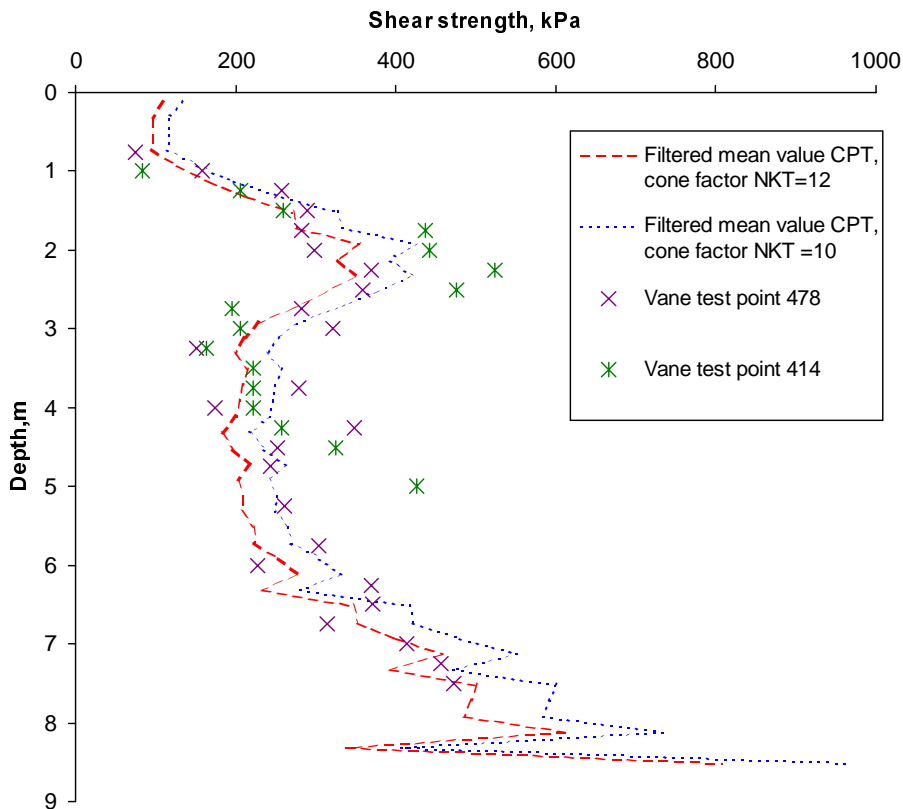


Fig. 4. Results from the field vane tests compared to an average curve for the CPT tests. The shear strength from the CPT-tests has been evaluated from  $c_u = (q_T - \sigma'_{v0})/N_{KT}$

## 2.24 Laboratory tests

### Classification

The soil samples taken with the continuous flight auger were carefully divided into different layers with different compositions and the thickness of the individual layers was measured. Each layer was then classified with respect to colour and soil type. The profiles were found to consist of 0.3 – 0.4 metre of black topsoil on top of 2.5 metres of brown clay till. Further down, the clay till becomes grey and below about 7 metres it is dark grey, with the colour strongly affected by the underlying clay shale. Embedded in the clay till are layers or lenses of silt, sand or gravel. At some levels, the material has been lost and may be assumed to have been friction soil. The thickness of these layers range from a few millimetres to a few decimetres. The amounts and levels vary from point to point. No exact measure of the amount of such coarser layers can be given, but

from the reported classification it may be estimated that layers of silt and coarser soil constitute about 5 – 20 % of the profiles down to 7 metres depth.

Only the layers of clay till have been examined further. They contain varying amounts of sand and silt, as well as some gravel. Cobbles and stones, if present, are not taken by the auger but remain in the ground. In general, the grain sizes in the till increase with depth, but in the upper 6 metres there is a large variation. Various amounts of chalk were also observed in this material. Below about 6 metres depth, the material becomes significantly coarser, at the same time as it changes colour and reveals a significant amount of gravel size particles of mainly clay shale. The grain size distribution for 32 different layers was determined by sieving and sedimentation analyses. *Fig. 5.*

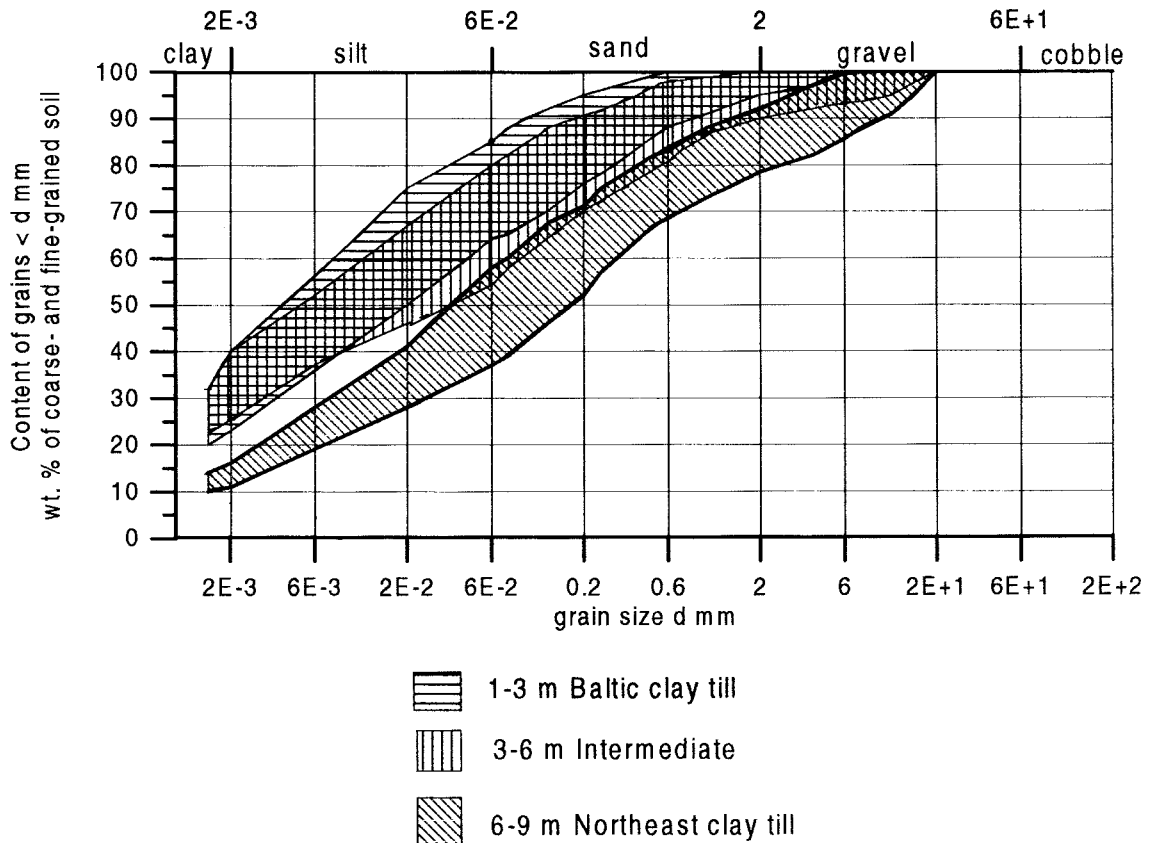


Fig. 5. Measured grain size distributions in the clay till (Dueck 1994).

**Determination of mineral composition**

The mineral composition was determined for both the coarser grains in the gravel fraction and the finer clay particles. For the gravel fraction, 100 grains with sizes between 2 and 6 mm were randomly selected from each tested layer. A petrographic analysis was then made of each grain to determine its mineral content. The grains were divided into granite, dolorite, flint, clay shale, limestone, sandstone, quartz and calcite, and the relative percentages were determined in 26 different layers. From these determinations, it was observed that there is a significant change in the composition of the grains at a depth of 6 – 7 metres. Above this level, there is a large content of limestone and flint, which is not found below this depth. Instead, the grains originating from clay shale and crystalline rock are totally dominant at greater depths, Fig. 6.

The mineral composition of the particles in the clay fraction was analysed by X-ray diffraction. Such determinations were made on material from six selected layers. These analyses are qualitative rather than quantitative and no exact amounts or percentages can be determined. It was found that significant amounts of illite and kaolinite were present in all the samples. Similar amounts of chlorite were found in all samples, except in the shallowest sample from about 1.5 metre depth. Varying amounts of smectite were also found in most samples and small amounts of quartz and feldspar were found in all samples. A very schematic picture of the variation is shown in Fig. 7.



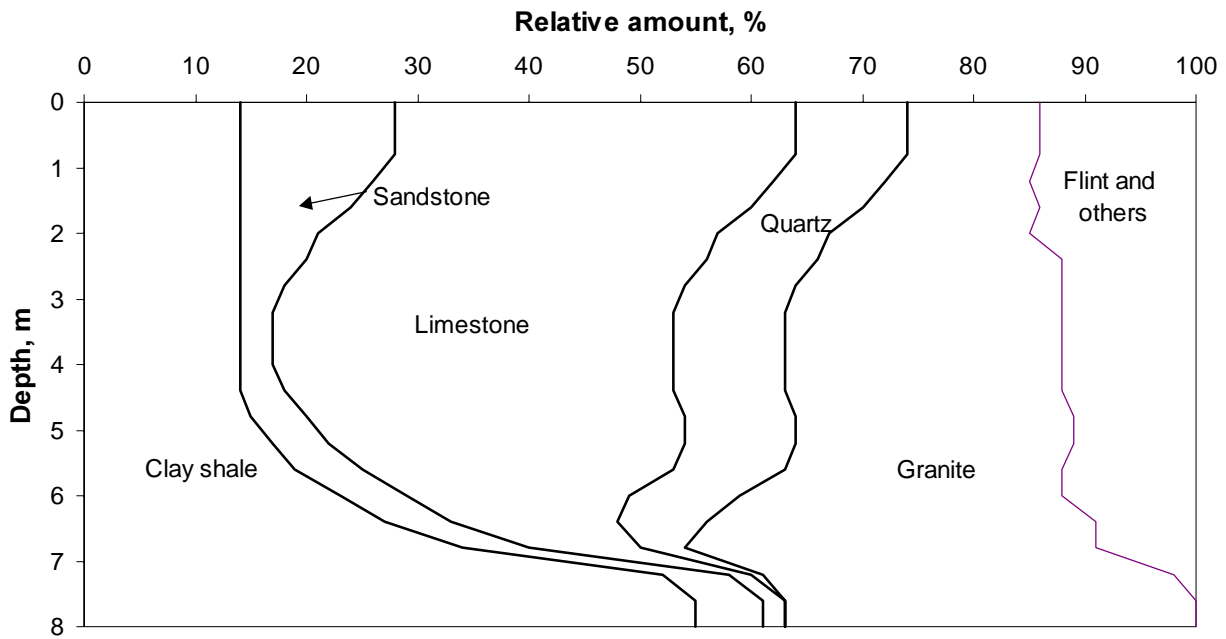


Fig. 6. Schematic variation in the mineral composition of the gravel size particles.

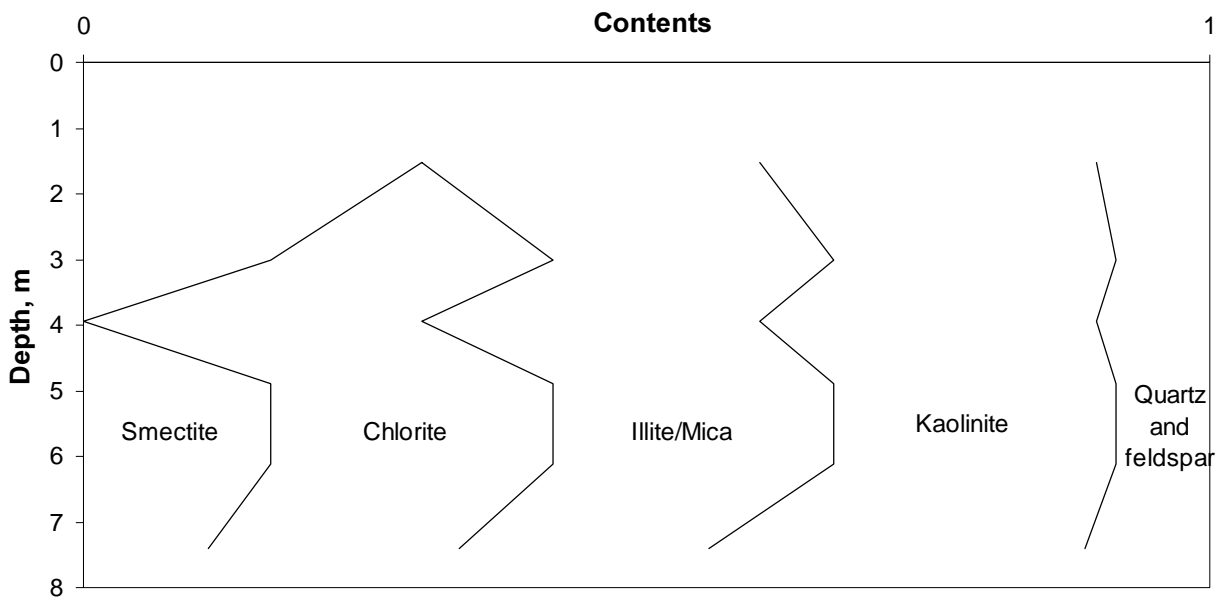


Fig. 7. Schematic variation of the mineral content in the clay size particles. The relative amounts are not to scale.

**Water content**

The natural water content was determined in the layers of clay till. Although there is a large scatter in these determinations, the water content generally decreases with depth from between 13 and 23 % in the upper 3 metres to about 10 % at 8 metres depth. Below this level, it appears to be fairly constant, but the determinations are few and the scatter is still considerable. At some levels, the initial determinations have later been supplemented by determinations from samples taken with piston sampler and by core drilling. The values from the latter determinations generally agree with the results from the first tests, but do not reduce the scatter, *Fig. 8*.

**Soil plasticity**

The liquid limit was measured for most of the different clay till layers and the plastic limit was measured for a few of them. Similar to the water content, there is a large scatter in the determinations of the liquid limit, which varies between 20 and 45 % in the upper layers and decreases to about 20 % at 8 metres depth, *Fig. 9a*. The plasticity index was found to vary between 5 and 25 %. Dueck (1994) found a good correlation

between the clay content and the liquid limit, *Fig. 9b*. The plasticity index is normally not determined or used in Swedish practice, but according to the determinations made, the plasticity index in the clay till at Tornhill can be estimated from the liquid limit using the formula  $I_p = 0.79 (w_L - 0.12)$ , *Fig. 9c*.

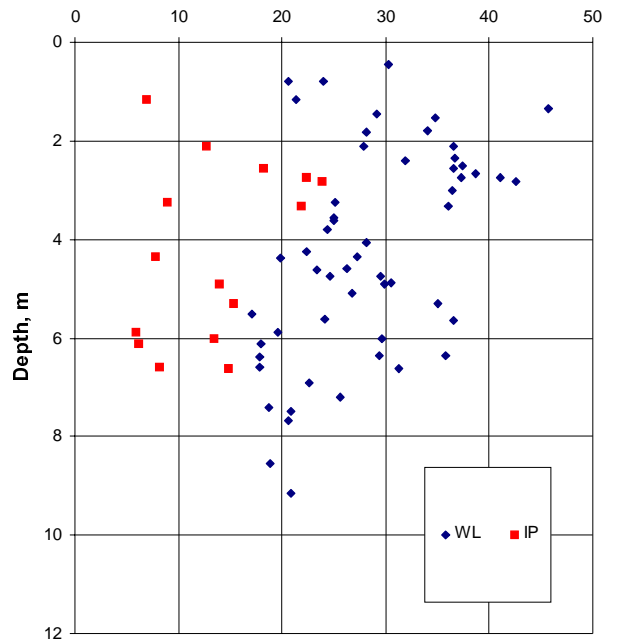


*Fig. 9. Consistency limits for the soil profile at Tornhill.  
a) Measured liquid limits and plasticity index.*

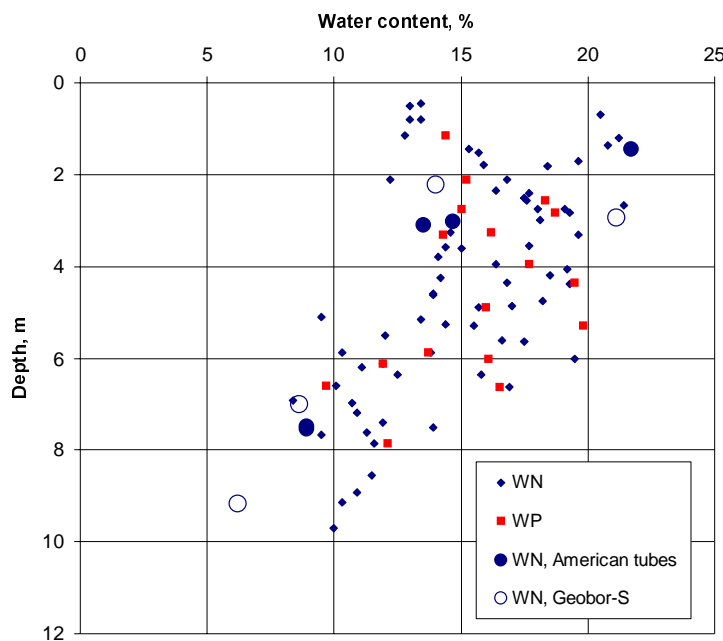


*Fig. 8. Water contents measured in the samples from the clay till.*

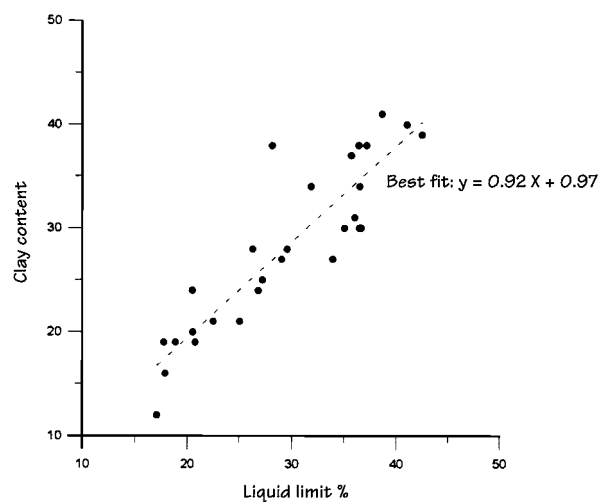


*Fig. 9. Consistency limits for the soil profile at Tornhill.  
b) Relation between liquid limit and clay content.*

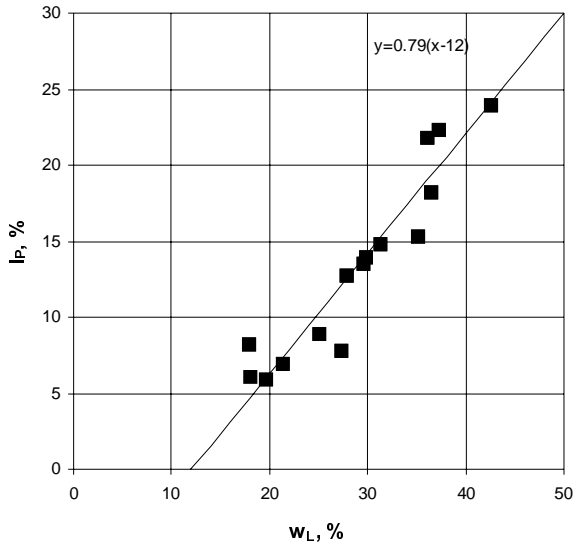


Fig. 9. Consistency limits for the soil profile at Tornhill.  
c) Relation between liquid limit and plasticity index.

### Density

The determined values of the bulk density of the soil also vary considerably. This may be due partly to remoulding effects at sampling and partly to the method of determining the property, which was made on lumps of the soil according

to Archimedes' principle. The average value was found to be  $2.13 \text{ t/m}^3$ , which is a fairly normal value for this type of soil. However, the maximum scatter of the values is  $1.82 - 2.55 \text{ t/m}^3$ , which is much too great. The average density of  $2.13 \text{ t/m}^3$  appears to be relevant down to a depth of 6 metres, whereupon it increases to about  $2.3 \text{ t/m}^3$  from 7 metres depth and downwards, Fig. 10. In the figure, the most extreme values have been omitted and the data have also been supplemented with the later determinations made by Dueck (1997) on samples taken with piston sampler and core drilling.

### Particle density

The particle density has been determined on a number of specimens from different layers of the clay till, both on the first samples taken with the auger and on the samples in the later investigations. In all these determinations, a constant value of  $2.72 \text{ t/m}^3$  was obtained. This is somewhat surprising in view of the variation in mineral composition and the value is also among the highest that have been reported for this type of soil. Later determinations by Dueck (1997) yielded values between  $2.71$  and  $2.74 \text{ t/m}^3$ , with an average of  $2.72 \text{ t/m}^3$ .

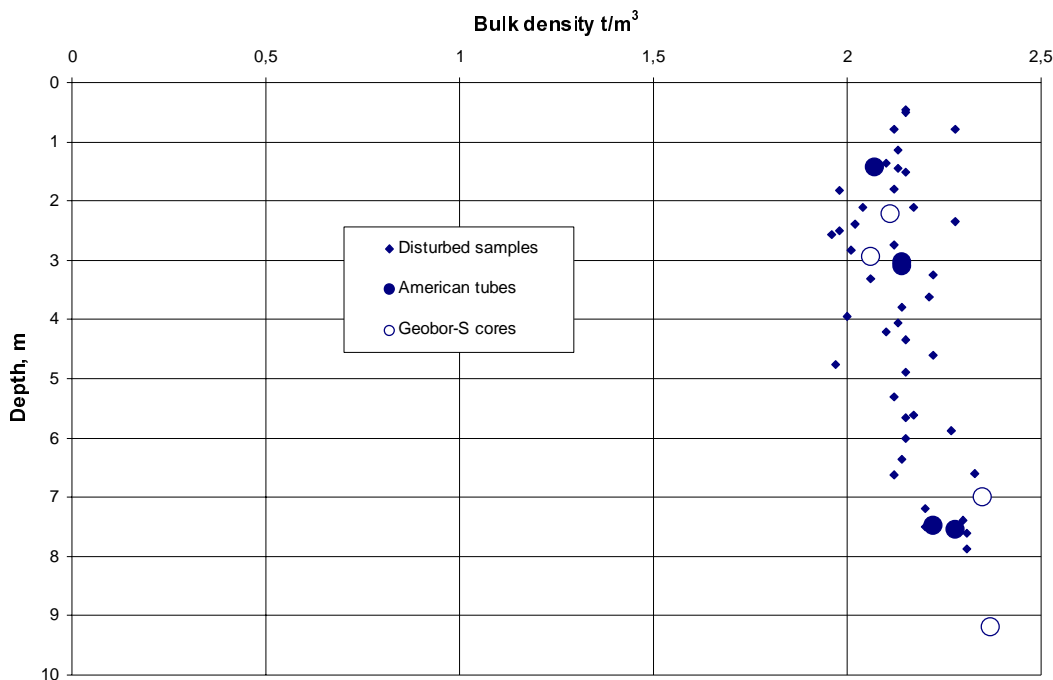


Fig. 10. Measured densities in the soil profile at Tornhill.

**Void ratio**

The calculated void ratio in the clay till varies between 0.4 and 0.6 in the upper part of the profile and decreases to about 0.3 from 7 metres depth and downwards. Both the dry density and the particle density affect the calculated void ratio. An excessively high particle density results in an exaggerated calculated value of the void ratio. In *Fig. 11*, the most extreme values, which are also related to extreme values of bulk density, have been omitted.

**Degree of saturation**

The degree of saturation has been calculated from the determinations mentioned above. It is sensitive to a number of parameters and values between 55 and 190 % have been calculated in this way. The extreme values relate to extreme values of bulk density. After a separation of the obviously erroneous values, the remaining data yield saturation ratios between 80 and 100 %. Also the calculated values from the latter samples taken with piston sampler and core drilling are in the same range, *Fig. 12*. In this case, the maximum possible error resulting from an excessive particle density is about 10 %. The results thus indicate that the clay till has a high degree of

saturation, but that it is not necessarily fully saturated, even below the free ground water level. Hartlén (1974) has previously reported similar observations. However, these findings for the clay till in the test field were not supported in the present investigation.

**Oedometer tests and triaxial tests**

Oedometer tests and triaxial tests, mainly on two levels in the test field, have been performed by Dueck in the latter investigation reported in 1997. The tests were performed at Aalborg University using the techniques and equipment developed at this institution. The results showed a large difference in the preconsolidation and the shear strength between the upper Baltic till and the underlying North-east till. The soil in the profile is overconsolidated or heavily overconsolidated. The results will be discussed further together with those from the present investigation.

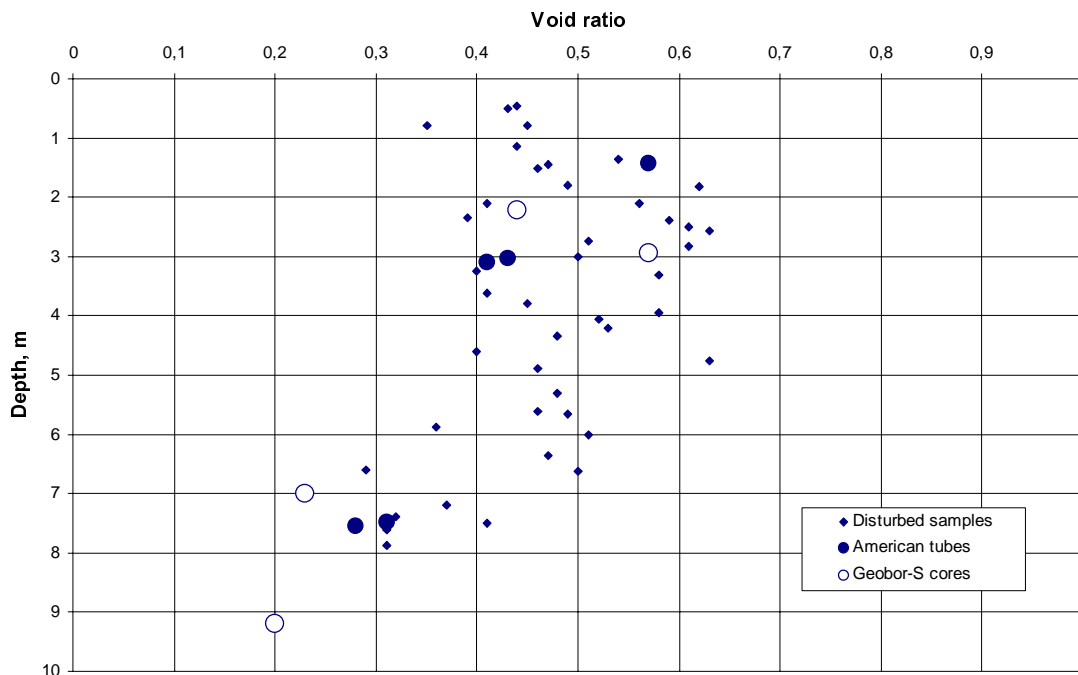


*Fig. 11. Calculated values of the void ratio in the soil profile at Tornhill.*

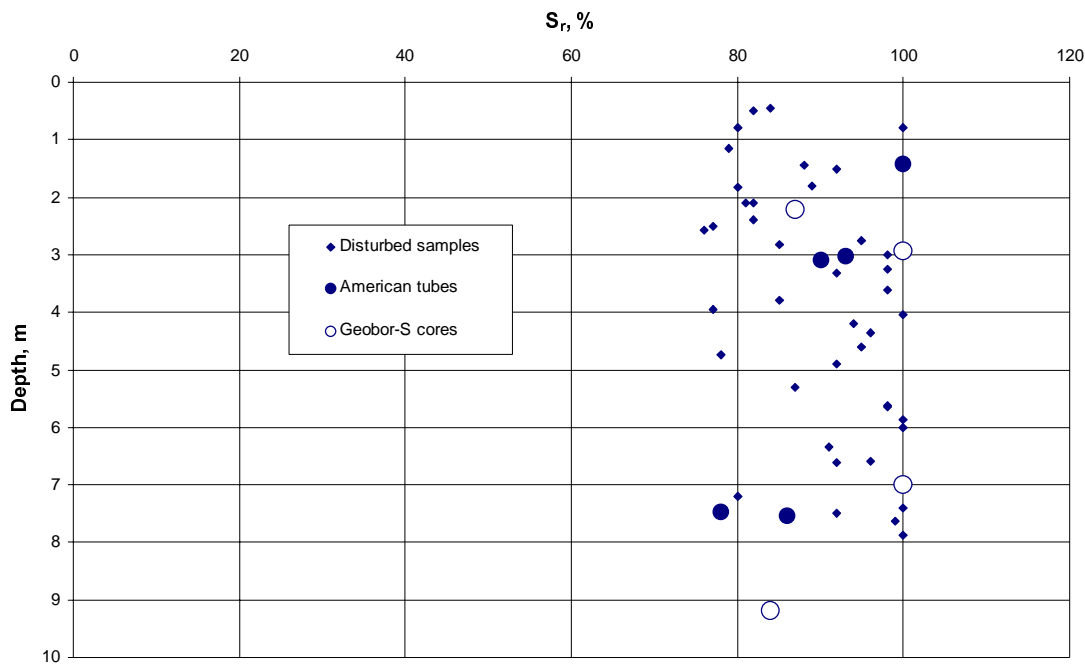


Fig. 12. Calculated values of degree of saturation in the soil profile at Tornhill.

### 2.3 OTHER PREVIOUS INVESTIGATIONS IN THE TEST FIELD

Apart from the two investigations by Dueck (1994 and 1997), the test field has been used for a number of investigations before the present project. In 1995, Jonsson et al used the field for testing the Geobor-S coring system and developing the technique for taking continuous samples in clay till. The results from that investigation form a basis for the technique used for sampling with the Geobor-S system in later investigations and among them also the present project.

The field has since then been used in two investigations aimed at developing the technique for pressuremeter testing in clay till. In the first project, (Ekdahl and Bengtsson 1996), a comprehensive test series was performed in the Baltic clay till at about 2 metres depth, together with a series of small-scale plate load tests. These tests used a TEXAM pressuremeter and mainly followed the guidelines given by Briaud (1992). The results led to a proposal for a new testing

technique, a model for the variation in elastic modulus at unloading and reloading of the Baltic clay till and a proposal for a new method of calculating settlements of shallow foundations in clay till. The proposed testing technique has mainly been followed in one of the pressuremeter test programmes in the present project.

The second project in the test field concerning pressuremeter testing was carried out by Skanska Teknik (1998). In this project, a self-boring Cambridge pressuremeter was used and the aim was to investigate the effectiveness of the self-boring technique and the stress-strain properties of the soil. The results showed that in this type of material, which is relatively rich in flint and gravel size particles, the self-boring technique was successful at only half of the test points, in spite of the fact that drilling was only performed down to about 2 metres depth. At the points where it was possible to install the probe, the tests showed that the stress strain curve could be represented by a hyperbolic function such as those proposed by Duncan and Chang (1970) and Hardin and Drnevich (1972).

### 3. Field investigations

#### 3.1 GENERAL

The field investigations in the present project comprised ground water observations, soundings, in situ tests and sampling. The purpose of these investigations was to determine:

- the applicability of different methods and equipment to these particular types of soil
- the relevance and repeatability of the results
- the quality of the soil samples obtained with different methods

The results of the field investigations and the laboratory tests on the samples were then to be compared to each other and to the results of the large-scale load tests. In order to obtain as relevant data as possible, most of the test points were located along the perimeter of the test area with an even spacing, *Fig. 13*. However, certain operations had to be moved some distance away. For example, sampling with the Geobor-S core drilling equipment, which uses large amounts of water for flushing while drilling, was performed some 15 metres away. Some of the pressuremeter tests also had to be moved to a safe distance from the machinery installing the tie rods for the subsequent load tests.

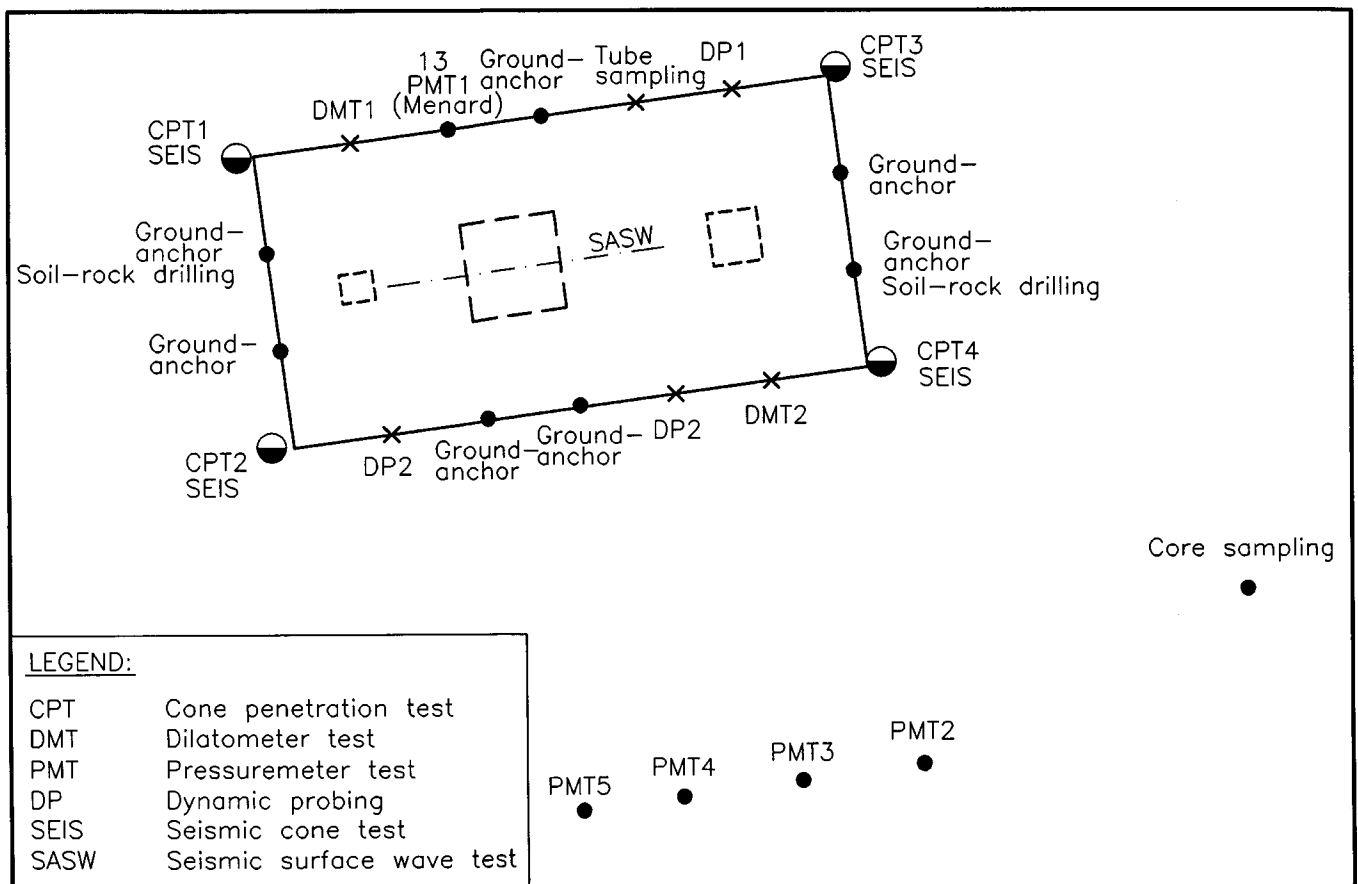


Fig. 13. Layout of the field tests.

## 3.2 GROUNDWATER OBSERVATIONS

The ground water level had previously been observed to vary between ground level and a depth of 2 metres, being highest from late autumn to early spring and lowest during summer and early autumn. After the first year with frequent observations, the readings had become more sporadic. In early spring 1999, the ground water observations were renewed before the field investigations started. These were scheduled to take place later in the spring and the plate load tests were to be performed during the summer. Before performing the actual groundwater observations, the function of the various observation points was checked. The pipes for the piezometers were rinsed and flushed to remove accumulated dirt, and attempts were also made to remove any entrapped gas. The water levels in the open standpipes were altered and the process of re-establishing natural conditions was studied. It was observed that the function of the piezometers in many cases was uncertain and that it took a considerable time for the water levels in the open standpipes to return to their original positions.

The spring of 1999 was wet in this part of the country. When the actual observations started in March, the lower parts of the area were flooded and most of the piezometers and open standpipes showed groundwater levels close to the ground surface. These conditions prevailed throughout the period of investigation and sampling activities. The ground surface dried out during drier spells, but was repeatedly soaked by heavy rainstorms. At the end of May, when the preparations for the load tests approached, an attempt was made to lower the ground water table locally in the area chosen for the present investigation. This was made by excavating two pumping holes down to about 2 metres depth on each side of the test area. The effect of continuously pumping out the water in these holes was very limited. In spite of the fact that a large pocket of sand was found in one of the holes, these efforts had practically no effect on the water levels at the surrounding observation points, i.e. the piezometers and open standpipes and all the open holes from the various investigations. This was also the case when

the distance between the pumping hole and the observation point was only a few metres.

The load tests were to be performed during the summer, which was the period when the ground water level had been expected to be below the excavation depth. However, these more favourable conditions did not occur, neither could they be achieved by artificial means within the available time. The excavation for the load tests therefore had to be carried out under more normal wet conditions and the groundwater had to be dealt with in a conventional way.

## 3.3 SOUNDINGS

### 3.3.1 CPT-tests

An extensive programme of CPT-tests had already been performed. These tests had been performed with an ordinary 5-ton probe and Swedish lightweight crawler drill rig. The pore pressure measurements during the tests had been carried out using a slot filter and grease as pressure transmitting medium. All these tests stopped at about 7 metres depth owing to insufficient penetration force.

The new CPT-tests were performed in the area chosen for the present investigation to ensure that the conditions here were the same as in the rest of the field. Four tests were performed, one in each corner of the test area. At the same time, the investigations were also aimed at determining the possibility of penetrating further using heavier machinery and a more robust probe. For this purpose, a 10-ton probe and a heavy crawler rig were used. Investigations were also made to find whether it would be possible to register the corresponding pore pressure response using ordinary filters and glycerine in the probe.

The CPT-tests penetrated to about the same depth as before. A check of the results showed that the reason for the stop was not that the tip resistance was too great, but that the side friction was very high. In fact, the side friction was so high that it would not be worthwhile trying to inject drilling mud above the probe because the

friction against the probe itself would still be too high for the maximum capacity of the probe and the pushing equipment. The maximum capacity of the friction sleeve had already been reached. It was thus concluded that CPT-tests penetrate the Baltic clay till and the intermediate mixed clay till, but not the North-east till. The use of stronger cones, heavier pushing equipment and lubrication of the drill rods is unlikely to change this situation as long as the standard requirements for the CPT-tests have to be fulfilled.

The results from the new CPT-tests were also fully compatible with the previous tests with respect to the variation in tip resistance and sleeve friction. The same average pattern was obtained and the same irregularities in terms of occasional peaks in the tip resistance were found, *Fig. 14*. The evaluation of undrained shear strength using a cone factor  $N_{KT}$  of 11 yielded the same stiffer zone between 1.5 and 2.5 metres depth, with a strength of about 300 kPa. The evaluated strength then became constant around 180 kPa

between 3 and 6 metres depth, whereupon it rapidly increased.

The new CPT-tests also confirmed previous findings that the ordinary pore pressure measuring system with a porous filter and a liquid as pressure transmitting medium performs very poorly in this type of soil. This result was obtained in spite of great efforts to saturate the fluid, filter and system within the practical limits that usually apply to ordinary investigations on land.

### 3.32 Seismic CPT-tests

In the new series of CPT-tests, measurement of the shear wave velocity was performed with a seismic CPT probe and related equipment from Geotech AB. The tests were performed in the usual way as described by Campanella et al (1986). This means that the penetration was stopped at regular intervals and the travel time for the shear wave from the ground surface to the current depth of the probe was measured. The waves were generated by horizontal blows from a sledgehammer on a beam pressed against the ground surface. The measurements at each level were duplicated with blows on the beam-ends from opposite directions. Because of the shallow depth of penetration and the heterogeneous soil mass, a distance of 0.5 metre between the measuring depths was chosen. This was intended to give a more detailed picture of the variation in the soil layers, but tended instead to make the interpretation more problematic.

The signals in this material contained a large amount of noise, which made a filtering process necessary. A filtering and evaluation programme written by Eric Baziw for Geotech AB was used for this purpose. After filtering, the signals became clear, although some problems still remained when examining the results in detail, *Fig. 15*. Considering the whole soil volume, the results were uniform, with almost exactly the same travel time for the shear wave from the ground surface down to 7 m depth. However, when studying the travel times between the different test levels within the soil mass, certain anomalies were observed. It thus happened that

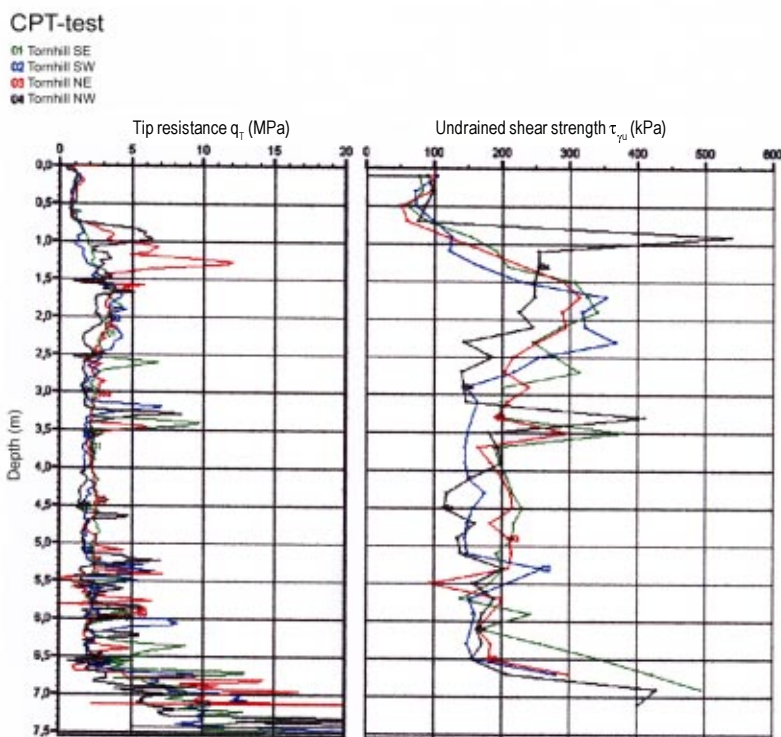


*Fig. 14. Results from the four CPT-tests in the corners of the test area.*



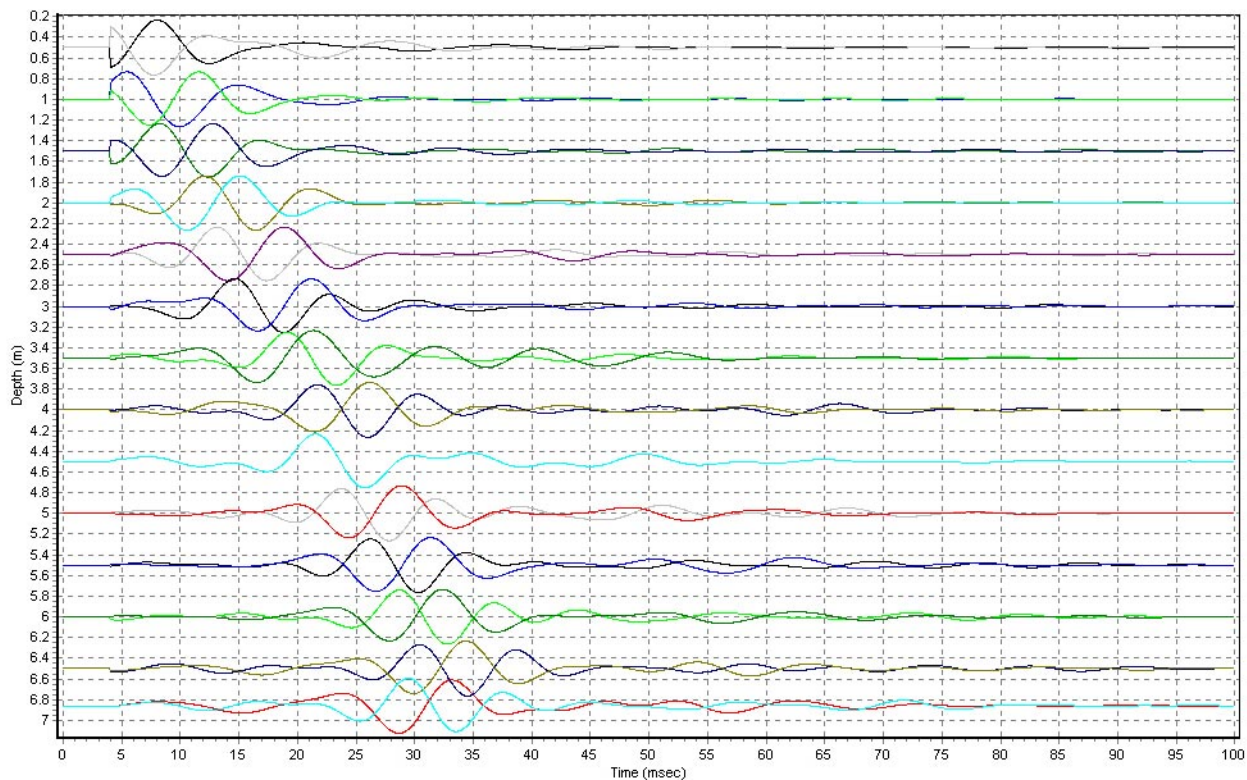


Fig. 15. Arrival times at different depths in a seismic CPT-test at Tornhill.

the travel time down to one level could be shorter than the travel time to the level just above. Furthermore, this could be true for waves created with blows from one direction, but not from the opposite direction. It is not possible to judge whether this is a result of all the embedded objects in the soil mass, such as silt and sand pockets, stones and possibly slices of rock material, which can be the same size as the distance between the test depths. The problem was largely overcome by increasing the distance between the compared depths to 1 metre, but a fully uniform picture required averaging over the whole soil layer from 0 to 7 metres depth. A considerable amount of averaging was thus required to obtain a clear picture.

The results from the different holes differ considerably also after a certain averaging, but plotted together they still yield a fairly consistent picture. The general trend for the time of first arrival versus depth is the same in all four tests, Fig. 16. In spite of the scatter, the evaluated shear wave

velocities in the different depth intervals also yield a consistent picture, which strongly resembles the evaluated variation in undrained shear strength, Fig. 17.

The shear wave velocity,  $v_s$ , is used to calculate the initial shear modulus by the relation  $G_0 = \rho v_s^2$ . In this case, the average values of  $v_s$  have been used. The variation in initial shear modulus thus estimated is shown in Fig. 18.

The initial shear modulus for other Scandinavian clays has been found to be related to the undrained shear strength and the liquid limit of the soil (Larsson and Mulabdic 1991). The initial shear modulus can thus be estimated from

$$G_0 \approx \frac{504 \cdot c_u}{w_L}$$

This relation was obtained mainly in normally consolidated or only slightly overconsolidated soils. Investigations by Andersen et al (1988)

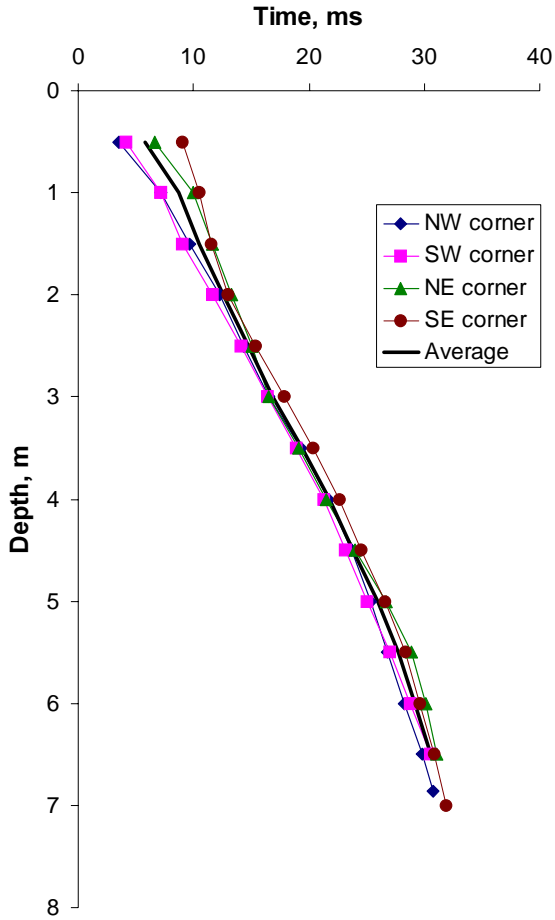


Fig. 16. Time of first arrival of the shear wave versus depth.

have shown that the relation between shear modulus and undrained shear strength varies with the overconsolidation ratio. The relation decreases with increasing overconsolidation ratio, OCR, and an approximate correction factor for the overconsolidation ratio,  $m$ , would be

$$\mu \approx 1 - 0,4 \cdot \log OCR \geq 0,4$$

The initial shear modulus in overconsolidated clays could then be calculated from

$$G_0 \approx \mu \cdot \frac{504 \cdot c_u}{w_L}$$

The initial shear modulus at Tornhill has been estimated in this way using the undrained shear strength obtained by field vane tests and CPT-tests together with the liquid limits estimated from an averaging of the scattered results in the first investigation (Dueck 1994).

The preconsolidation pressures,  $\sigma'_c$ , and overconsolidation ratios have been estimated in two ways; from the results from the oedometer tests presented in Chapter 5 and from a Danish empirical relation with the undrained shear strength (Steenfeldt and Foged 1992).

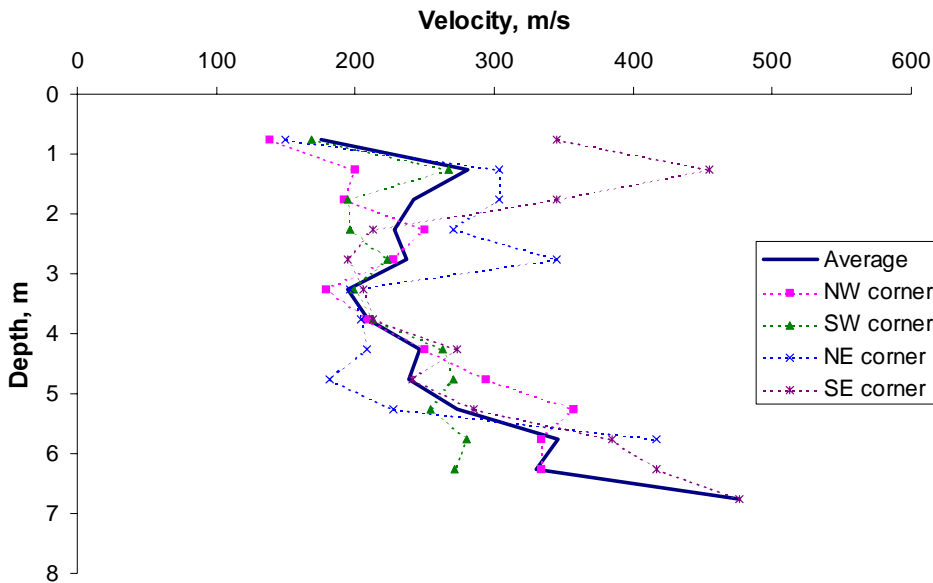


Fig. 17. Variation in shear wave velocity versus depth.

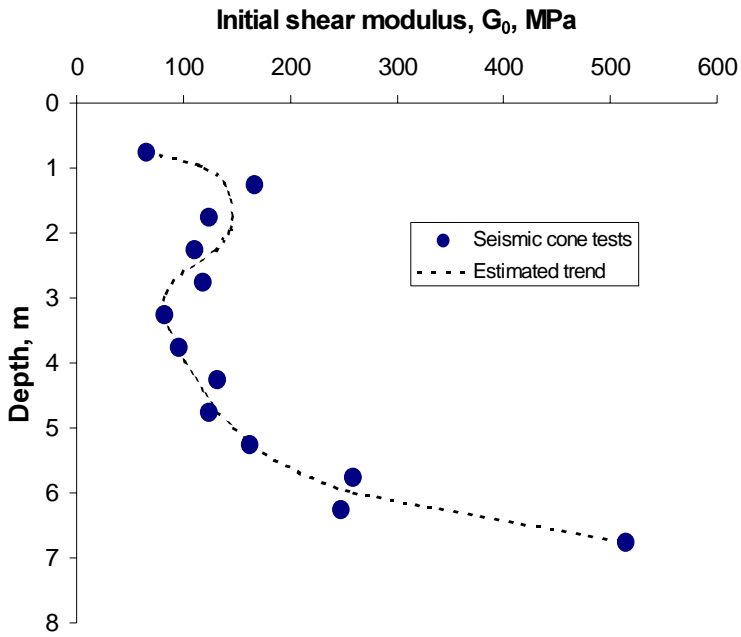


Fig. 18.  
Variation in initial shear modulus with depth at Tornhill.

$$\sigma'_c \approx \sigma'_0 \left( \frac{c_u}{0.4 \cdot \sigma'_0} \right)^{1/0.85}$$

These two ways of estimating the preconsolidation pressure yield very different results in this case, with the latter method giving preconsolidation pressures 1.5–2.5 times higher than the oed-

ometer tests, which will be discussed later. However, the sensitivity of the correction factor for the initial shear modulus is limited for changes in overconsolidation ratios of this size. The initial shear modulus has been calculated using both types of estimation of the preconsolidation pressure, and the results are shown and compared to the results of the seismic cone tests in Fig. 19.

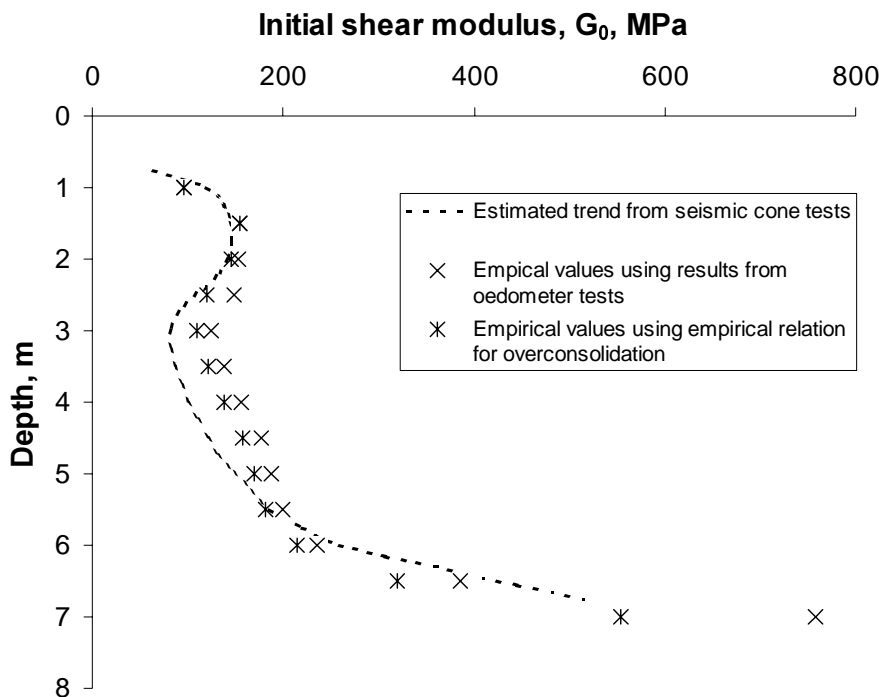


Fig. 19.  
Comparison between empirically estimated shear moduli and results from the seismic cone tests.

As can be seen in the figure, a consistent picture was obtained of the variation in the initial shear modulus. However, it must be emphasised that the procedure for obtaining this picture was not straightforward. The estimation of the shear modulus from the seismic cone tests involved averaging the results from several tests and the empirical estimation involves averaging a large number of determinations of shear strength and liquid limit and the combination of two empirical relations. The apparently very good correlation between the measured and the empirically estimated values in the figure may thus not be typical.

### 3.33 Dynamic probing tests

Dynamic probing tests were performed in both the initial investigation (Dueck 1994) and the current investigation. In both cases, the tests were performed according to the Swedish Hfa method, (Bergdahl 1984). This method uses a tip with a diameter of 45 mm and cone angle of 90°, and a weight of 63.5 kg with a free fall of 0.5 m. Penetration is registered as the number of blows for each 0.2 metre of penetration. The method

falls between the international DPH and DPSH methods. The specific work per blow is 167, 200 and 238 kJ/m<sup>2</sup> for the DPH, Hfa and DPSH methods respectively.

Investigations in stiff clay and clay till by Butcher et al (1995) have shown that lighter dynamic probing methods are to be preferred since they yield a better resolution of the soil properties. However, the initial investigations using the Hfa method penetrated only to about 8 metres, which was marginally more than the CPT-tests. One reason for this was the very high friction against the rods. The Hfa method stipulates that the friction against the rods should be measured at regular intervals and accounted for in the interpretation. A special torquemeter has been designed for this purpose. In the initial investigations, a much cruder and subjective measure was used to estimate the rod friction. However, also this method clearly showed that the friction was considerable, Fig. 20. Butcher et al (1995) recommend a reduction of the rod friction by pumping in slurry above the tip.

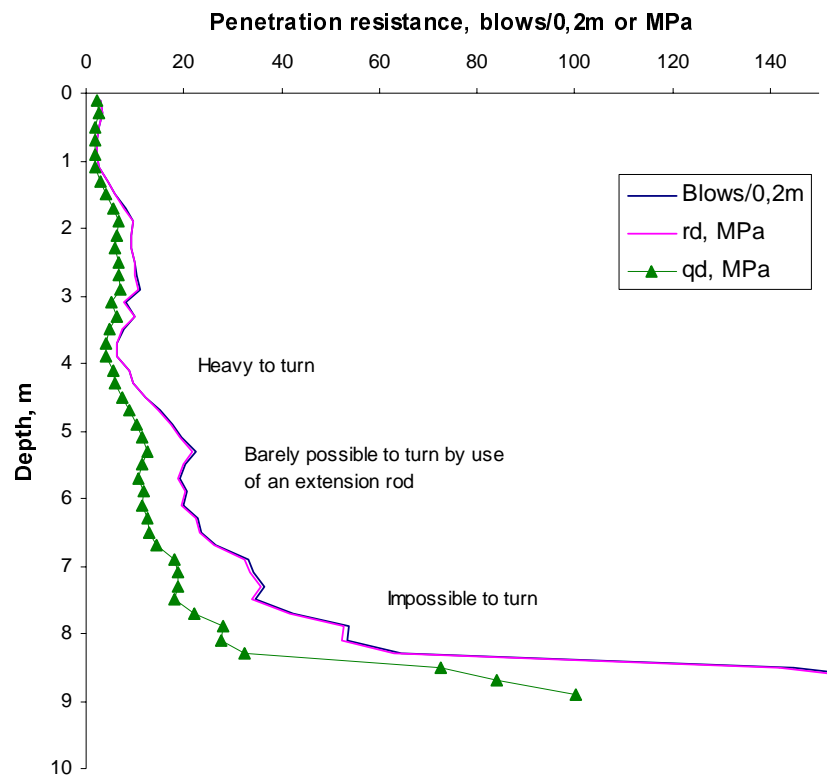


Fig. 20. Results from the early dynamic probing tests, average of three tests (after Dueck 1994)

The new investigations were performed in order to study the possibility of penetrating further and obtaining more reliable results if a suitable method was used. The new soundings were therefore performed with a slip coupling between the tip and the rods. This coupling enabled the rods to be retracted 0.2 metre at regular intervals and a direct measure of the friction in terms of the number of blows required to ram them down the same distance again. Hollow rods were used and bentonite slurry was pumped out at the coupling. The crawler drill rig was used and this enabled a further reduction of the friction by extensive rotation of the rods, if necessary.

Three probing tests were carried out in this way. The reduction in friction already became significant at a depth of about 3.5 metres. Two of the tests penetrated all the way to about 14 metres depth, where they stopped on the bedrock. The third test stopped at about 7.5 metres depth, where the sound from the drill rods appeared to indicate a large boulder.

It was thus possible also to penetrate the North-east till when suitable equipment was used. A somewhat higher stop criterion than normal had to be employed since extra hammering was sometimes necessary to pass larger objects in the ground. However, it was fairly easy to distinguish these from a real stop. The rod friction was considerable when passing certain layers, particularly at the interface between the North-east till and the overlying layers. This friction was almost eliminated when the mud lubrication had become fully effective after further penetration and rotation of the rods.

It is thus concluded that dynamic probing can be performed in every type of clay till in this area, provided that a suitable method is used. Friction reduction is necessary, but even then it must be expected that some tests will stop at a higher level because of large embedded objects in the soil mass. The suggestion of using lighter penetration methods could not be followed if the whole soil profile was to be investigated, since it was barely possible to penetrate the soil even

with the heavy to super heavy method employed.

The results from a dynamic probing test can be presented in terms of blows for a certain interval of penetration depth or by the variation in the resistance numbers  $r_d$  or  $q_d$  with depth. The resistance numbers are calculated from

$$r_d = \frac{MgH}{Ae}, Pa \quad \text{and} \quad q_d = r_d \frac{M}{M + M'}, Pa$$

where

- $M$  = mass of the falling weight, kg
- $g$  = acceleration of gravity = 9.81 m/s<sup>2</sup>
- $H$  = height of free fall, m
- $A$  = cross sectional area of the tip, m<sup>2</sup>
- $e$  = average penetration per blow within the depth interval, m
- $M'$  = total mass of sounding rods, anvil and guide tube, kg

For the Hfa method, the parameter  $r_d$  expressed in MPa is numerically approximately equal to the number of blows per 0.2 metre of penetration, which is normally reported in Sweden, *Fig. 21*.

The parameter  $q_d$ , also called the dynamic tip resistance, accounts for the mass of the parts of the equipment involved. This parameter has been found to be independent of the equipment and method and is thus most suitable for describing the stiffness of stiff clays and clay tills (Butcher et al 1995). According to these authors, the shear strength of the soil can be calculated from

$$c_u = q_d/22$$

This gives a very good correlation with the strengths determined by field vane tests and CPT-tests also for the clay till at Tornhill. The authors furthermore suggest that the parameter  $q_d$  should be approximately equal to the tip resistance in CPT-tests. This was not found at Tornhill. Instead, the relation between the two values was almost constant at 2.0. This is also reflected in the factor 22 in the formula above and the cone factor  $N_{KT} \approx 11$ .

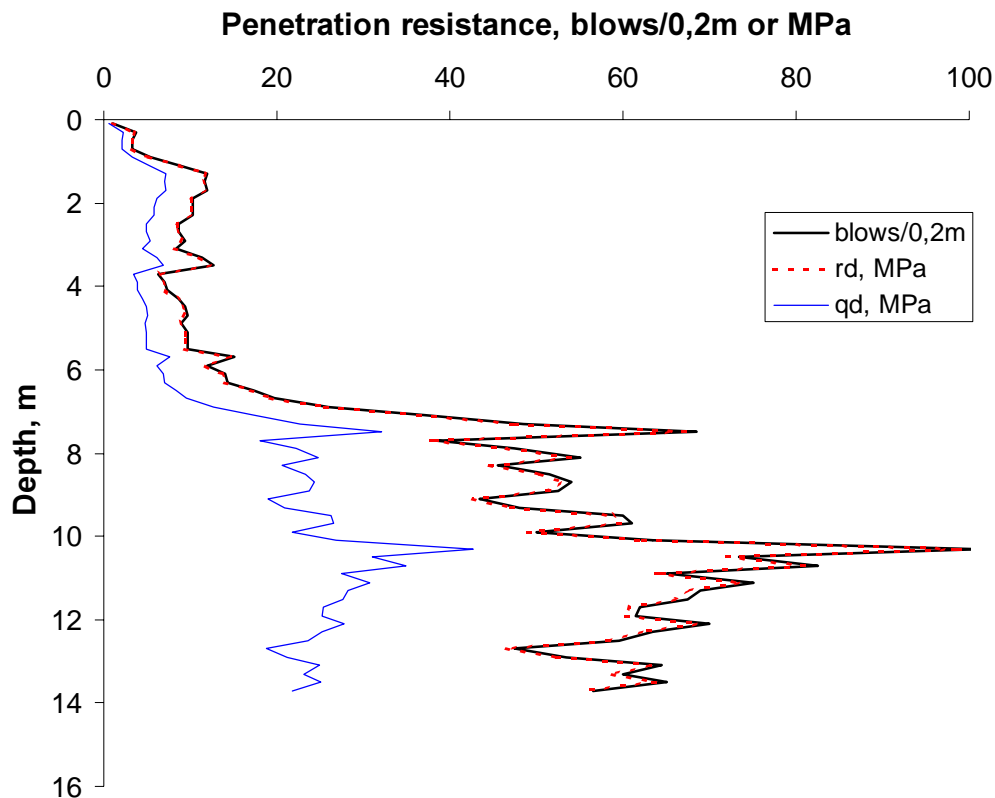


Fig. 21. Results from the new dynamic probing tests at Tornhill – average of the tests. (The parameter  $r_d$  is plotted in the figure, but is difficult to detect since it is almost completely obscured by the curve for blows/0.2 m).

### 3.34 Soil-rock drilling

Soil-rock drilling is normally performed when the content of stones and cobbles is so high that neither CPT-tests nor dynamic probing tests penetrate or when the soundings are to be continued into the underlying bedrock. The method has recently been developed in such a way that six additional and independent drilling parameters can be registered continuously. The parameters, which are registered together with depth and rate of penetration, are:

- Applied static vertical force, kN
- Applied torque (measured as pressure in the hydraulic device providing the rotation and torsion force), MPa.
- Speed of rotation, rpm

- Pressure of flushing medium, MPa
- Flow of flushing medium, litres/min
- Applied hammering energy (measured as pressure in the hydraulic hammer), MPa

(The Field Committee of the Swedish Geotechnical Society 1998)

The drillings are normally performed with constant settings of the pump for the flushing medium, the rate of rotation and the applied vertical force and hammering energy. However, when very different materials are encountered, the settings may have to be altered in order to reduce or increase the rate of penetration. Two such drillings were carried out at Tornhill with slightly different settings. The results from one of these are shown in *Fig. 22*.

Löpnummer 1 Datum 19990427 Objekt nummer tornhill  
 Nr 1025 Starttid 07:31 Företagsnummer 11nv.2ms  
 Serienummer ENVI-28 Företag SGI  
 Förborringsdjup 0.00 m Metod 60-6 kanals borr

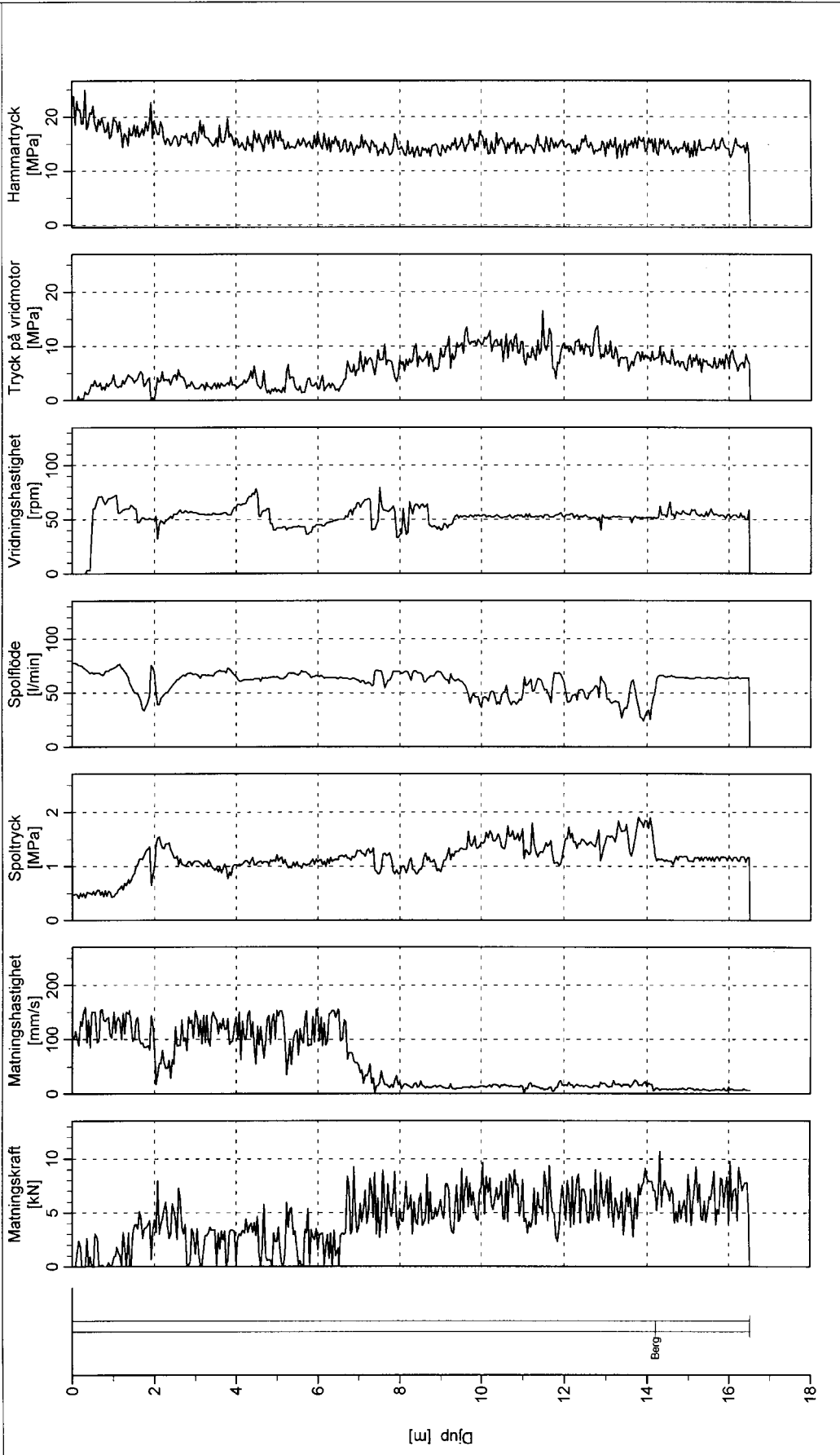


Fig. 22. Results from a soil-rock drilling at Tornhill.

From the results, it can be seen that the soil is softer and more permeable in the top metre of soil, that there is a peak in stiffness and a dip in permeability between 1.5 and 2.5 m depth, and that the properties are thereafter fairly similar down to 6.5 metres depth. In this latter layer, there is a large scatter in vertical force and rate of penetration, indicating a heterogeneous material. At 6.5 metres depth, the character of the material changes considerably. The material becomes much stiffer, which is indicated by a tenfold decrease in rate of penetration in spite of a doubling of the applied static force. The torque required to rotate the rods at the same speed also increases by a factor of 3 – 4. The material appears to be less permeable since the pressure in the flushing medium increases and the flow drops. The bed-rock is then found at 14 metres depth. This can be seen mainly in an even lower rate of penetration and a considerably more homogeneous material with respect to permeability. Soil-rock drilling is found to be a fast and effective way of establishing the soil-rock profile in this type of material. It also yields a fairly good qualitative picture of the relative stiffness of the material in the profile. However, it is not yet possible to evaluate any quantitative parameters from the results.

### 3.4 IN SITU TESTS

#### 3.4.1 SASW measurements

Measurement of the variation of the Raleigh wave velocity in the test field at Tornhill was performed in a separate joint project between the University of Lund and SGI (Svensson 2000). In this project, SASW measurements have been performed in a number of test fields where the initial shear wave velocity has been determined by seismic cone tests. The aim of this project was to determine the accuracy that would be obtained with the method, which is simpler in certain respects, and the effectiveness of recent attempts to improve the interpretation by using “forward modelling techniques”.

The tests at Tornhill were performed at the same time as the investigations in the current project and involved a larger area covering the present test area and its surroundings, *Fig. 23*. The results of the SASW measurements proved to be rather difficult to interpret. The ordinary and simplest method of interpretation yielded values of the shear wave velocity that had a trend similar to those evaluated from the seismic cone tests, but were considerably lower. When a more ad-



*Fig. 23.*  
*SASW measurements in progress.*



vanced interpretation method was employed, another similar trend was obtained, but with considerably higher values. The combined results from all the test fields indicated that the interpretation of SASW measurements was quite satisfactory in homogeneous clay profiles with continuously increasing stiffness with depth. However, in heterogeneous, considerably layered profiles with irregularly varying stiffness, as at Tornhill, the accuracy of the interpretation is still limited.

### 3.42 Resistivity measurements

Measurements of the soil resistivity in the field have recently been performed in a diploma project at Lund University (Leveen and Palm, 2000). The measurements have been performed both as vertical resistivity soundings using an RCPT probe and as geo-electrical surface measurements. The electrical resistivity was found to vary between 10 and 130  $\Omega\text{m/m}$ , which is typical for relatively fine-grained soils. The variation in resistivity with depth reflects the composition of the soil layers. The lowest values are found in the most homogeneous fine-grained soil in the

Baltic clay till between about 0.4 and 3 m depth, and the resistivity then increases with depth as the soil becomes coarser in the mixed clay till and the North-east till below. Various thinner layers within the main layers can also be discerned, *Fig. 24*.

The variation in thickness of the various layers and their uneven lateral distribution is illustrated by the results from the geo-electrical surface measurements, *Fig. 25*. A number of different test set-ups and interpretation techniques have been used. These methods have various advantages and limitations in terms of vertical and lateral resolution. However, in principle, they all yielded good illustrations of the heterogeneous composition of the soil and the great variation in extent and thickness of the soil layers above the North-east till, particularly in the Baltic clay till with its large embedded pockets of coarse material. This picture is very helpful for understanding the variation in the test results and the relevance of individual test results for the larger soil mass.

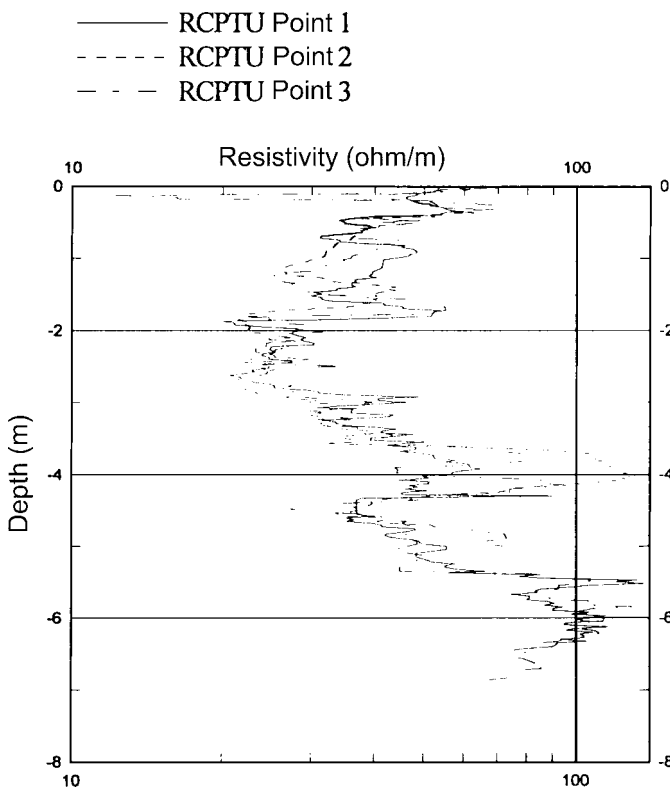


*Fig24.*  
Variation in measured soil resistivity with depth in RCPT. (Leveen and Palm 2000)

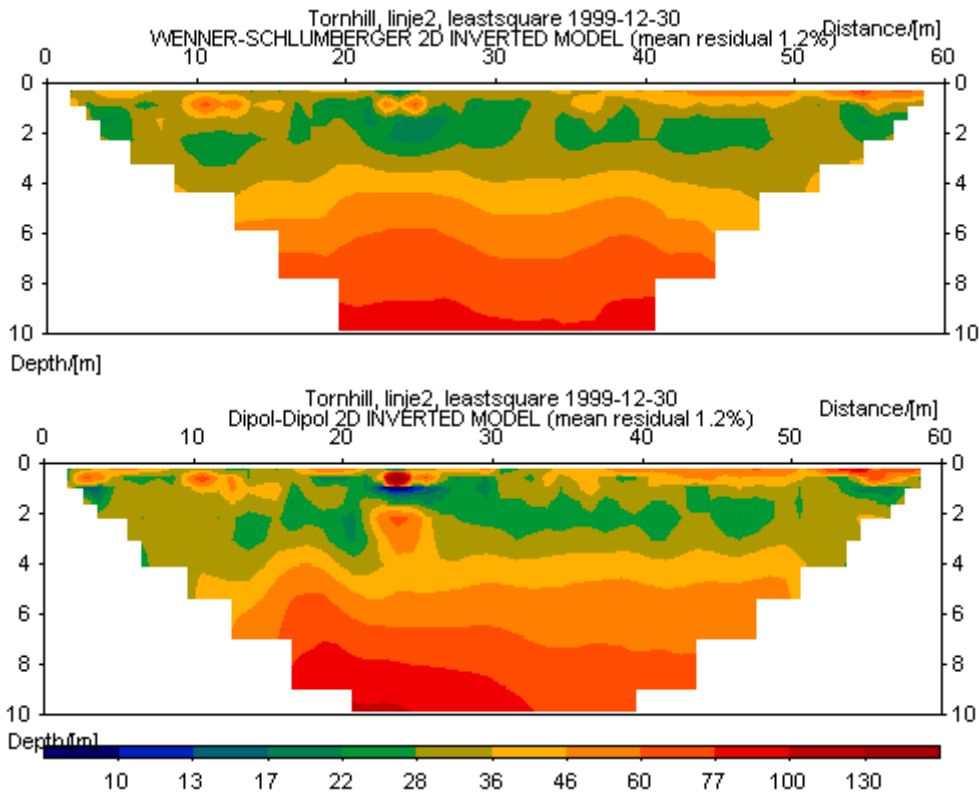


Fig. 25. Results of geo-electrical surface measurements at Tornhill. (Leveen and Palm 2000)

### 3.43 Field vane tests

Field vane tests were performed in the initial investigations (Dueck 1994) with the Danish field vane (DGF Feltekomité 1993). This equipment is designed for tests in clay till and is more robust than ordinary field vanes. The tests confirmed that the Danish relation between field vane tests and CPT-test results could be applied also in the test field at Tornhill. According to Steenfelt and Sørensen (1995), the CPT-test can be considered superior to the field vane test for determination of the undrained shear strength. This is primarily a result of less scatter in the results. No further field vane tests were therefore performed in the current project.

### 3.44 Dilatometer tests

Two dilatometer tests were performed in the test area. The dilatometer penetrated down to 6.6 and 7.4 metres without blows, which is approximately the same depth as for the CPT-tests. No attempt was made to ram it down further, since this was only expected to damage the equipment.

The tests were performed according to the standard procedure, e.g. SGF 1995, with the exception that the pressure readings were taken and stored electronically by a computer with the readings triggered by the signals from the dilatometer. The results from the two tests were surprisingly consistent in spite of the heterogeneous soil, Fig. 26. The same pattern as for the other types of tests was observed, with a peak in the stiffness between 1.5 and 2.5 metres depth, a fairly constant stiffness between 3 and 6 metres depth, and thereafter rapidly increasing values. The results are more scattered between 5 and 6.5 metres

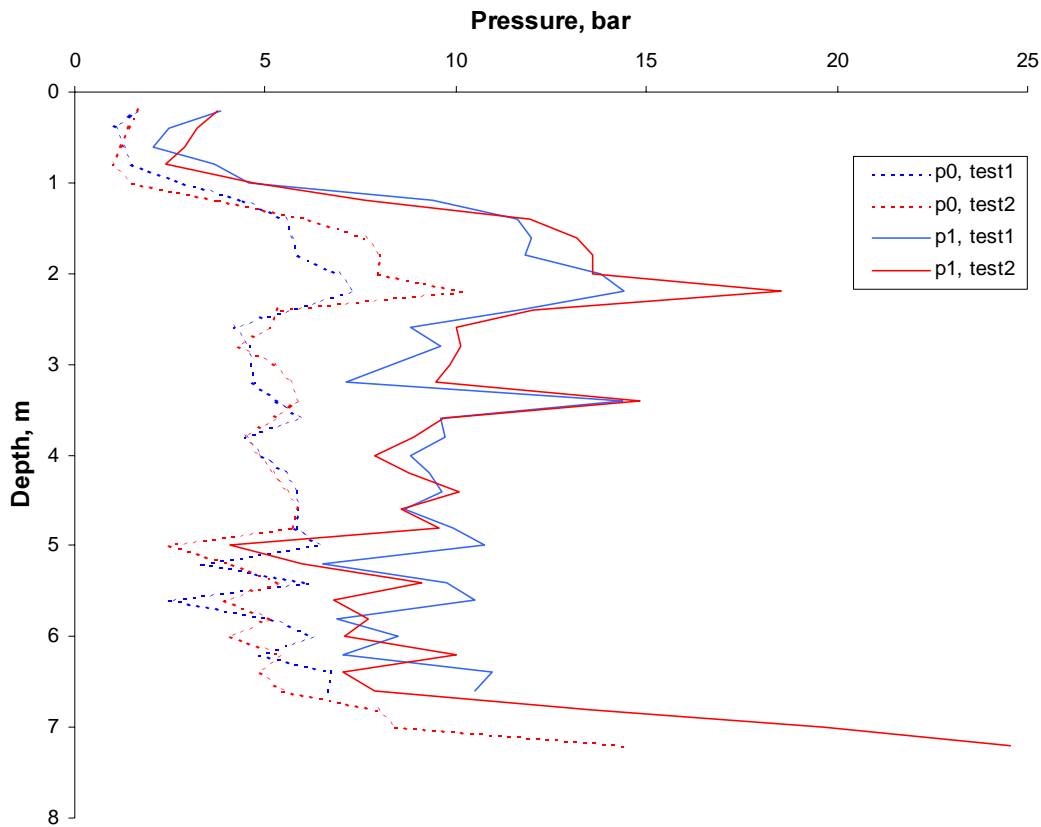


Fig. 26. Zero pressures,  $p_0$  and expansion pressures,  $p_p$ , in the dilatometer tests.

depth, which probably reflects a more heterogeneous soil and larger disturbance effects.

The results were interpreted using the SWEDILL interpretation programme according to the guidelines given in SGI Information No. 14. The soil classification was fairly accurate in designating the soil in the upper part as very stiff clay and the soil below as stiff silty clay with occasional layers of silt or sand.

The undrained shear strengths followed the same trend as the vane tests and the CPT-tests, but the values were only about half those from the other tests. This was valid regardless of whether the Marchetti (1980) evaluation or the evaluation proposed by Larsson (1989) was used. However, the evaluation proposed by Roque et al (1988) on the basis of results from Norwegian very silty clays and clayey silts would have yielded shear strength values closer to those from the other tests.

The evaluated coefficients of earth pressure ranged from about 5 in the upper layer of Baltic clay till to 1.5 – 2 in the intermediate layer of mixed till below, Fig. 27a. This is in the same range as was later obtained from the pressuremeter tests and from empirical relations with the preconsolidation pressures measured in the laboratory. The estimated overconsolidation ratios were very high in the upper layer, but in this case are very dependent on the evaluation method. The empirical methods normally used for evaluating overconsolidation ratios in clays refer to soil profiles where very high values are found only in dry crusts and other fissured soils. These methods strongly overestimate high overconsolidation ratios in non-fissured soils. Based on British experience from non-fissured soils, Powell and Uglow (1988) proposed that the overconsolidation ratio, OCR, could be evaluated from

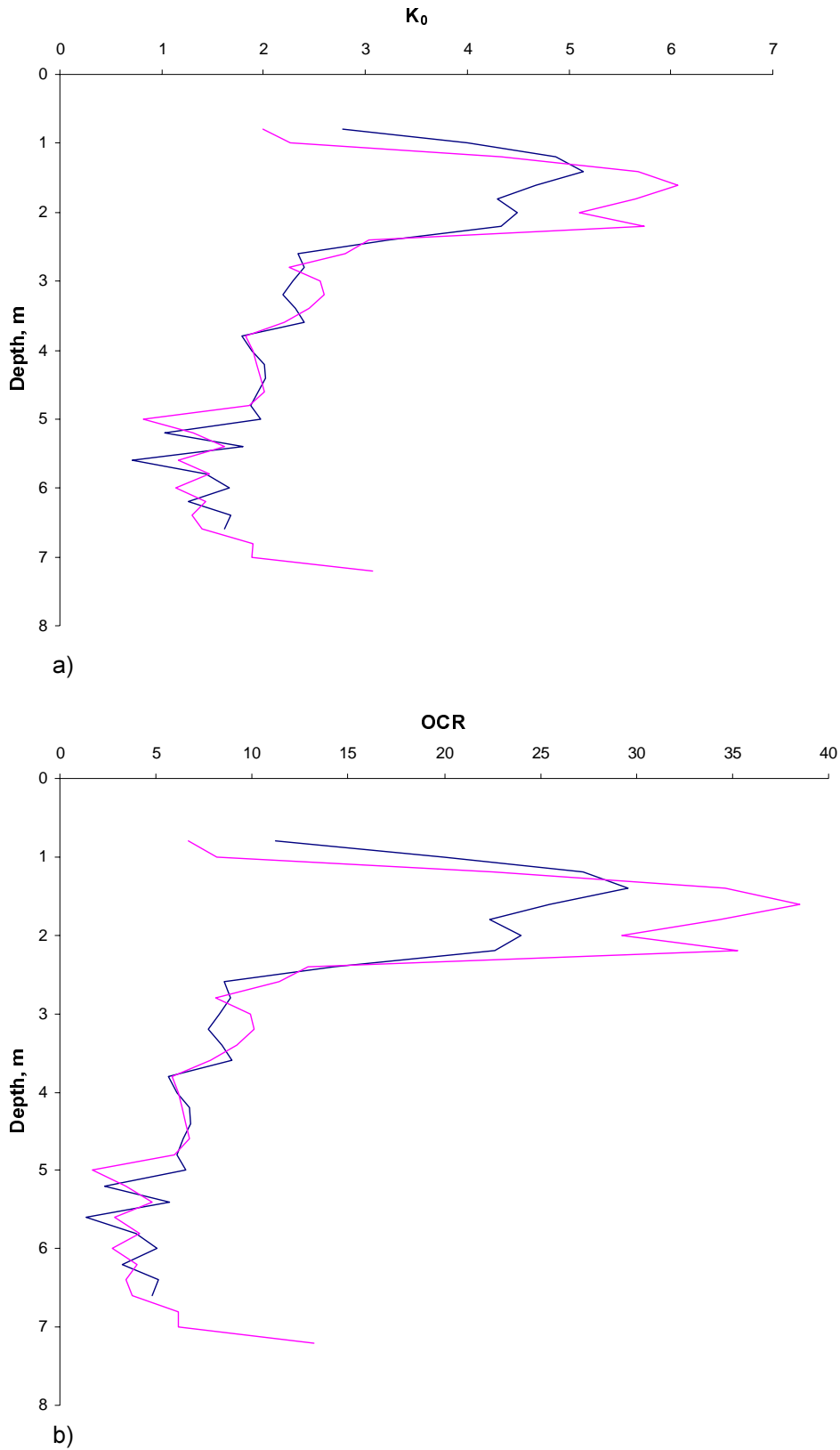


Fig. 27. Evaluated coefficient of horizontal earth pressure and overconsolidation ratio from the horizontal stress index measured in the two dilatometer tests at Tornhill.  
 a) coefficient of horizontal earth pressure.  
 b) overconsolidation ratio.

$$OCR \approx 0.24K_D^{1.32}$$

where  $K_D$  is the horizontal stress index evaluated from the dilatometer test. This has been applied to the data from Tornhill and the results show overconsolidation ratios in the order of 25 to 30 in a layer between 1.5 and 2.5 metres depth, decreasing to about 6.5 below 3 metres depth.

These values are of about the same size as those obtained from the preconsolidation pressures estimated from oedometer tests, but only about half of what is estimated from the field vane tests using Danish empiricism, *Fig. 27 b*.

The evaluated compression moduli (oedometer moduli) show a peak in the stiff layer of Baltic clay till with values around 80 MPa and then decrease to values around 30 MPa in the intermediate mixed clay till, *Fig. 28*.

The results from the dilatometer tests were thus consistent and yielded what appear to be fairly relevant soil parameters. The main exceptions are that the undrained shear strength estimated with

the ordinary methods is only half of what is obtained from field vane and CPT-tests, and that a special empirical relation for non-fissured clays had to be employed for the overconsolidation ratio. However, it was possible to penetrate only the upper two types of clay till.

### 3.45 Pressuremeter tests

Pressuremeter tests were performed with two types of equipment; the ordinary Menard type of pressuremeter and new equipment similar to the TEXAM pressuremeter. In both cases, the tests were performed in predrilled holes using thick bentonite slurry to stabilise the holes.

### Preparation of test cavities

Two methods were tried to prepare the test cavities; the original tool designed by Menard and a special screw auger (Joelson screw) with a hollow stem and hollow drill rods through which bentonite slurry can be pumped when the auger is retracted. The original Menard tool proved to give slightly better test cavities. However, when larger objects were encountered in the ground,

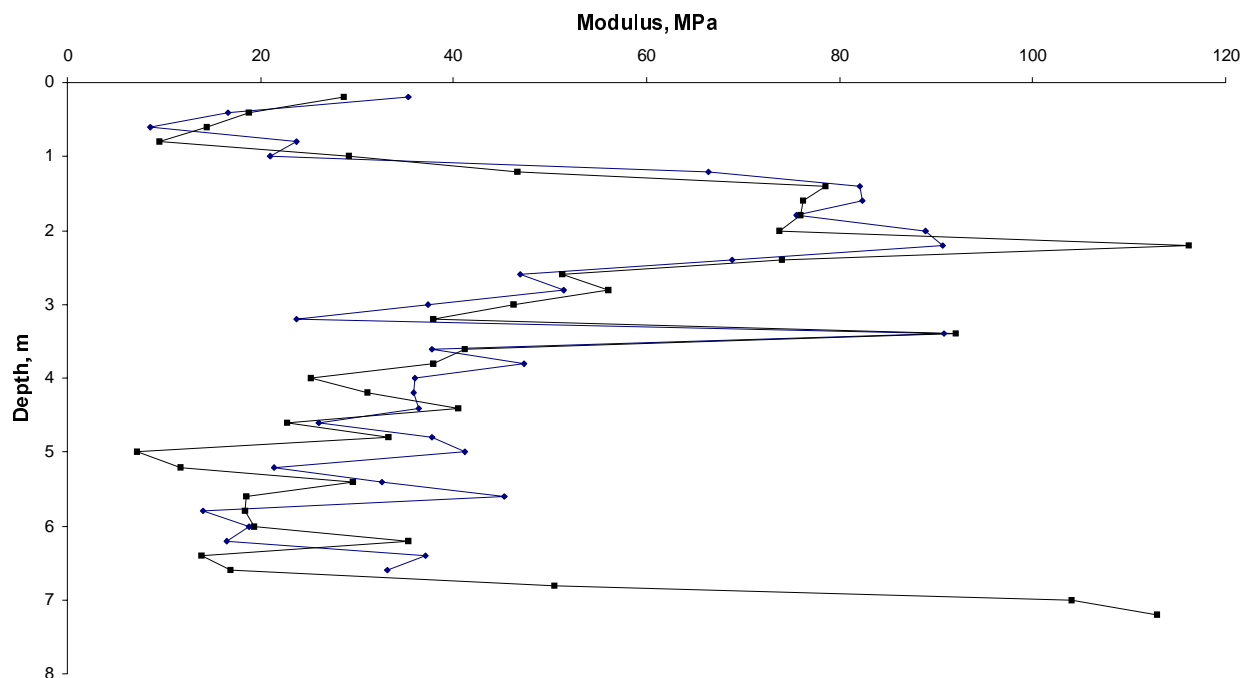


*Fig. 28. Evaluated moduli, M, from the dilatometer tests at Tornhill.*

this tool created holes that were misaligned. A combination of both tools often proved to be the best solution. The auger was then used to prepare a straight hole down to just above the test level and thereafter the Menard tool was used to prepare the test cavity. It was also found very important to insert the probe in the test cavity and start the test immediately after preparation of the cavity. The walls of the cavity deteriorated rapidly and any significant delay meant that the test was performed in a cavity of inferior quality.

### Menard pressuremeter

The tests with the Menard pressuremeter were performed with a probe fitted with a “canvas cover”, which is a relatively thick and stiff rubber membrane. This outer cover was chosen because of the relatively high amount of sharp flint particles in the ground. Although it causes a relatively high pressure correction, careful and repeated calibrations showed that this correction could be determined accurately.

The tests with this pressuremeter were performed in three holes with a vertical distance between the test levels of 1 metre. The first hole was primarily used to elaborate the method of preparing the test cavities and some of the results from this hole were therefore discarded. The other two holes were prepared in such a way that tests were performed at every metre depth in one hole and at depths of 1.5 m, 2.5 m and so on in the other, in order to obtain, as far as possible, a continuous profile. The maximum testing depth was 6 metres. Below this depth, it was not possible to create test cavities with the method employed. To perform tests in the underlying North-east till, tests would have to be performed inside slotted drilling tubes or in cavities created with a special, more elaborate technique developed for this material by Ekdahl et al.(1996). Since no reference data would be obtained for this soil from the later plate load tests, this was not considered relevant for the present project.

The tests were performed according to the ordinary procedure with new pressure increments applied every minute and readings of the volume

changes after 30 and 60 seconds. About 12 pressure increments were used in each test. No attempts were made to cycle the stress and measure unload-reload moduli in these tests.

### New pressuremeter

The other type of pressuremeter test was performed with equipment designed along the guidelines given by Briaud (1992) and which in principle works in the same way as the TEXAM pressuremeter. The probe was an ordinary Menard probe from which the inner rubber membranes and the gas supply tube had been removed. The probe was thus converted to a mono-cell covered by a canvas cover and completely saturated with water. The cell had a diameter of 56.4 mm and a length of 408 mm, giving an  $L/D$  ratio of approximately 7.2.

The probe was connected to a stainless hydraulic cylinder in which the piston was operated by a turning wheel through a play-free gearbox. The position of the piston was measured accurately by a pulse counter on the wheel axis. A pressure transducer in the pressure pipe to the probe measured the pressure in the system. The signals from the pulse counter and the pressure transducer were recorded by a computer, *Fig 29*.

The probe and the system were first saturated. The probe was then inserted into a tight fitting steel tube and the system was leak tested. This tube was also used to zero the volume reading system in the field tests and to test the correction for system compressibility. The volume measurement was then checked by expanding the probe and studying its shape and change in radius. It was found that the canvas cover expanded very evenly with practically parallel sides of the expanded probe and very small radii at the fixed ends. The translation of the volume change as measured by the movement of the piston into change of radius of the probe was thus a straightforward procedure.

The system was calibrated for pressure corrections because of resistance in the rubber membrane and loss of pressure because of water flow.



Fig. 29. Performing a test with the new pressuremeter at Tornhill.

The calibration was performed with constant water flow at different rates, by stopping the expansion at regular intervals and letting the pressure stabilise, and by repeating this process with reversed water flow and deflation of the probe. A correction was thus obtained which accounted for the resistance in the rubber membrane, hysteresis effects at reversal of the volume change and combined rate effects on both the resistance in the rubber membrane and the pressure loss because of the flow velocity in the pressure pipe, Fig. 30.

Briaud (1992) proposed various test procedures for evaluating the modulus at unloading and reloading, its dependence on stress level and strain level in the cycle, and the time dependence (creep effects) on the results. Based on this, Ekdahl and Bengtsson (1996) proposed a test procedure that would enable the most comprehensive evaluation of parameters from a single test. In this procedure, the probe is expanded at a fairly constant rate. The expansion is halted at regular intervals in order to read off a stabilised pressure after 15 seconds. Unloading and reloading cycles are also performed at regular intervals in the ex-

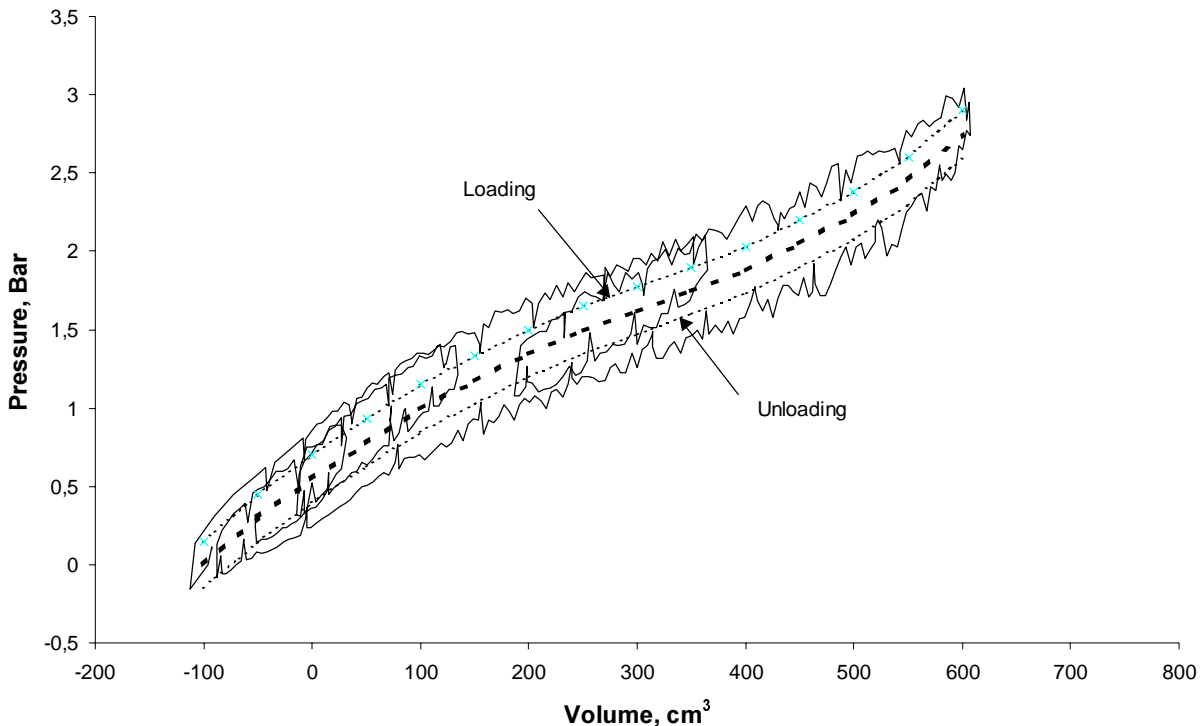


Fig. 30. Calibration curve for pressure corrections to be applied to the new pressuremeter. Volume readings refer to the zero reading in the steel tube.

pansion. At least three series of such cycles are performed, each series consisting of three cycles with three different fixed amounts of volume change. The amounts of volume change are pre-selected with consideration to the probe size in such a way that the strains within the cycle remain “elastic”. A minimum of nine unload-reload cycles are thus performed in each test. At one stage, the expansion is changed in such a way that the pressure is kept constant and the further expansion due to creep effects is recorded for about ten minutes. If the creep within the “elastic” part is to be investigated, this should ideally be performed within the unloading-reloading loop. In the current series of tests, the procedure was carried out after the loop had been completed and the expansion had more or less returned to the virgin curve in practically the same way as recommended by Briaud for ordinary pressuremeter tests. This procedure was followed in all tests with the new equipment, *Fig. 31*. The only deviation was that the volume change and pressure were recorded continuously.

This was done during both volume changes and stops for about 15 seconds at regular intervals, both at loading and unloading, in order to study the influence of creep on the recorded stress-strain relations. Each test performed in this way occupied about two hours. The tests were performed in two adjacent boreholes with the test depths overlapping each other in the same way as for the tests with the Menard pressuremeter.

## Results

### ■ *Menard parameters*

The traditional parameters evaluated from a pressuremeter test are the in situ horizontal stress  $p_0$ , the yield pressure  $p_y$  or  $p_{fl}$ , the limit pressure,  $p_L$ , and the pressuremeter modulus  $E_M$ . In the Menard pressuremeter test, the in situ horizontal stress and the yield pressure are evaluated using the shape of the pressuremeter curve (the plotted pressure-volume change relation), and the curve for creep versus pressuremeter pressure. The creep is then evaluated as the difference between

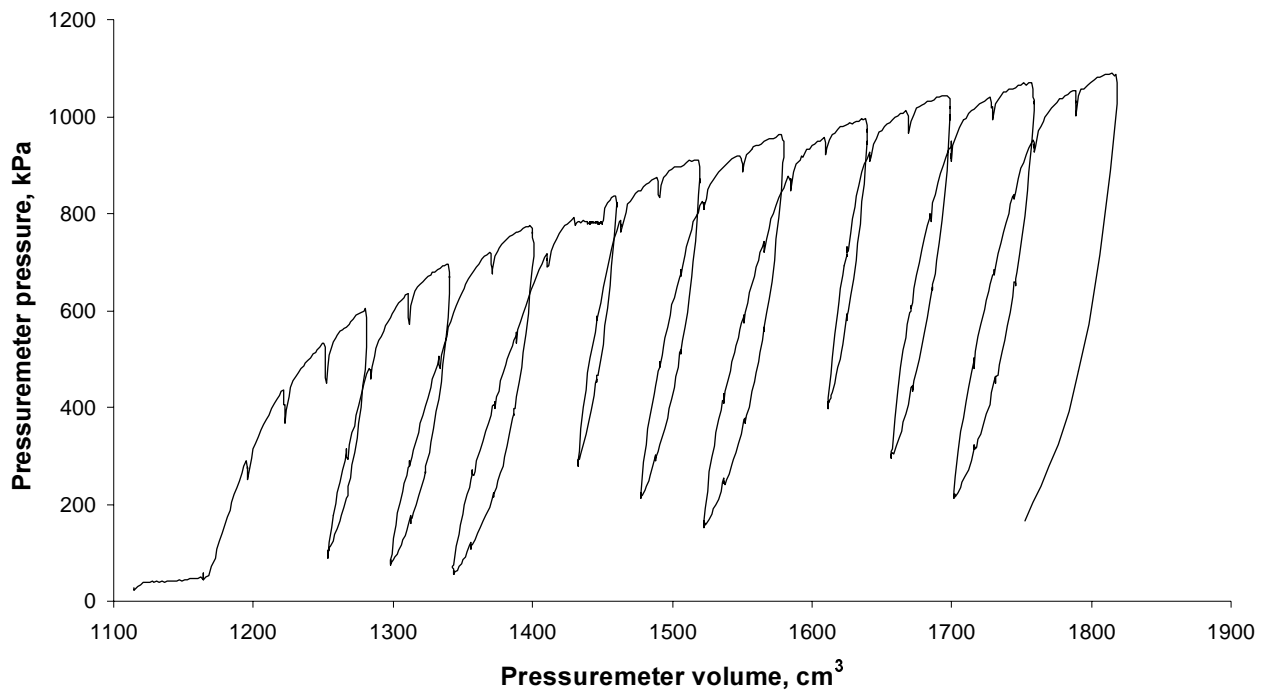


*Fig. 31. Example of a test at Tornhill with the new pressuremeter.*



the volume readings taken 30 and 60 seconds after the application of the pressure increment. The in situ horizontal pressure is interpreted as the pressure when the stress-volume change relation becomes linear after an initial expansion of the probe required to bring it into full contact with the cavity walls. The interpretation of this point is facilitated by the fact that the creep-pressure curve becomes a minimum at the same point in ideal tests. The yield pressure is evaluated at the point where the stress-volume change relation leaves the straight line relation. The pressure at this point should coincide with the pressure where the creep-pressure relation changes and the creep rate starts to increase significantly. The initial volume of the test cavity is evaluated from the initial volume of the pressuremeter probe plus the volume increase required for the probe to make full contact with the cavity walls. The limit pressure is then evaluated as the pressure at which the initial volume of the test cavity has been doubled. Finally, the pressuremeter modulus is evaluated from the slope of the straight pressure – volume change relation and the current volume of the cavity in this stage, *Fig. 32*.

Pressuremeter tests performed according to the new procedure have to be interpreted in a somewhat different way. No creep curve is obtained from these tests. However, the creep that occurs during the test significantly influences the results, and these effects are much larger in a test that lasts for about two hours than in a test lasting only about ten minutes. Furthermore, the results from the new tests are influenced by the effects of the repeated unloading-reloading cycles, which result in extra volume changes and may also influence the limit pressure. The in situ horizontal pressure must therefore be interpreted solely from the shape of the pressure-volume change curve (or pressure radius change curve). For this case, it has been suggested that the horizontal stress should be evaluated at the point of minimum radius of the curve before it attains its straight relation (Briaud 1992), *Fig. 33*.

The volume of the test cavity is then determined by extrapolation of the straight pressure- radius change relation to the estimated in situ horizontal pressure. The yield pressure also has to be estimated solely from the shape of the pressure –

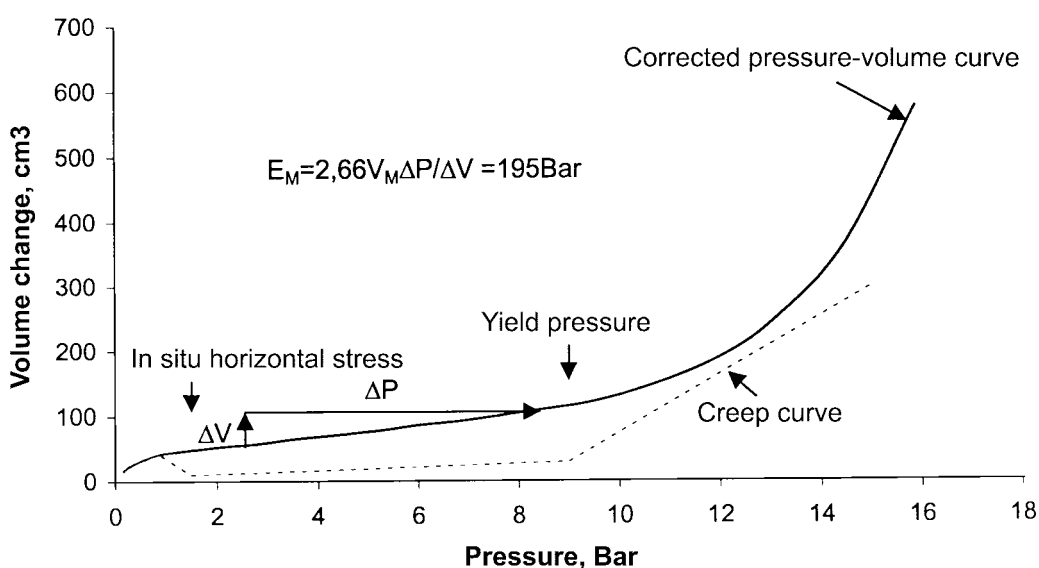


*Fig. 32. Evaluation of parameters from a Menard pressuremeter test.*

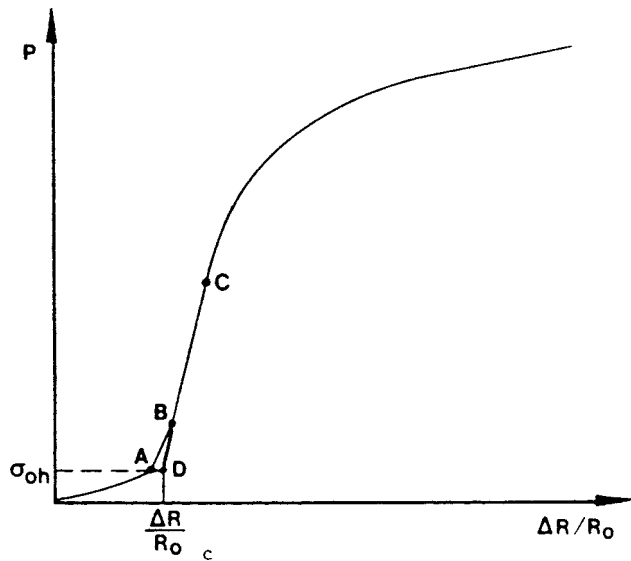


Fig. 33. Evaluation of in situ horizontal stress and initial radius of the test cavity. (Briaud 1992)

volume change curve, which makes it somewhat more uncertain. The evaluation can be performed as a subjective interpretation of the point at which the relation leaves the straight line, at the intersection of extrapolated parts of the curve before and after yield (which is difficult since the curve after yield is not a straight line) or at the point of minimum radius of the curve. Here, the latter interpretation has been chosen. The interpretation is complicated further by the fact that it is sensitive to the rate at which the test has been performed and to possible interfering effects of unloading and reloading loops. The pressuremeter modulus is evaluated in the same way as the Menard tests, but the limit pressure has to be evaluated using another procedure. Otherwise, the evaluated limit pressures consistently become considerably lower than those evaluated from the tests performed according to the Menard procedure.

Mair and Wood (1987), have presented a procedure for estimating the limit pressure at infinite expansion of the cavity, when  $\Delta V/V = 1$ . In this procedure  $\Delta V/V$ , the volume change versus the current volume is plotted in a logarithmic scale against the pressuremeter pressure. The relation

becomes a straight line, which is extrapolated to  $\Delta V/V = 1$  and the limit pressure is read off. In this plot, the limit pressure according to the Menard procedure corresponds to the pressure at  $\Delta V/V = 0.5$ . This procedure has been applied to the tests according to the Menard procedure as a supplement to the manual extrapolation and interpretation of the pressuremeter curve and thus provides a more objective estimation of the limit pressure. It has also been applied to the tests performed according to the new procedure and both the Menard criterion and the criterion  $\Delta V/V = 1$  have been applied to the latter tests.

The results in terms of horizontal stresses, which are very sensitive to the quality of the test cavity, show a certain degree of scatter, Fig. 34. However, if a few odd values are sorted out there is a consistent trend for the in situ horizontal stresses corresponding to  $K_0$ -values of 3 to 4 in the upper layers to decrease to about 1.5 between 3.5 and 5.5 metres depth and then to increase again. As a comparison, previous tests with a self-boring Camcometer had yielded  $K_0$ -values of about 5 at 1.9 metres depth and 6 to 12 at 2.9 metres depth (Skanska Teknik 1998).

The yield pressures from both tests give a fairly consistent picture of the variation with depth, but the values from the new type of test are generally lower than the values from the Menard tests, Fig. 35. The typical picture with a peak between 2 and 2.5 metres depth is found for both types of test.

The limit pressures show a clear trend versus depth, which is similar to the yield pressures. In order to achieve compatibility between the two types of tests, the limit criteria  $\Delta V/V = 1$  has to be applied to the latter type. Also when this is done, the yield pressures from the new type of pressuremeter tests in general become somewhat lower, Fig. 36.

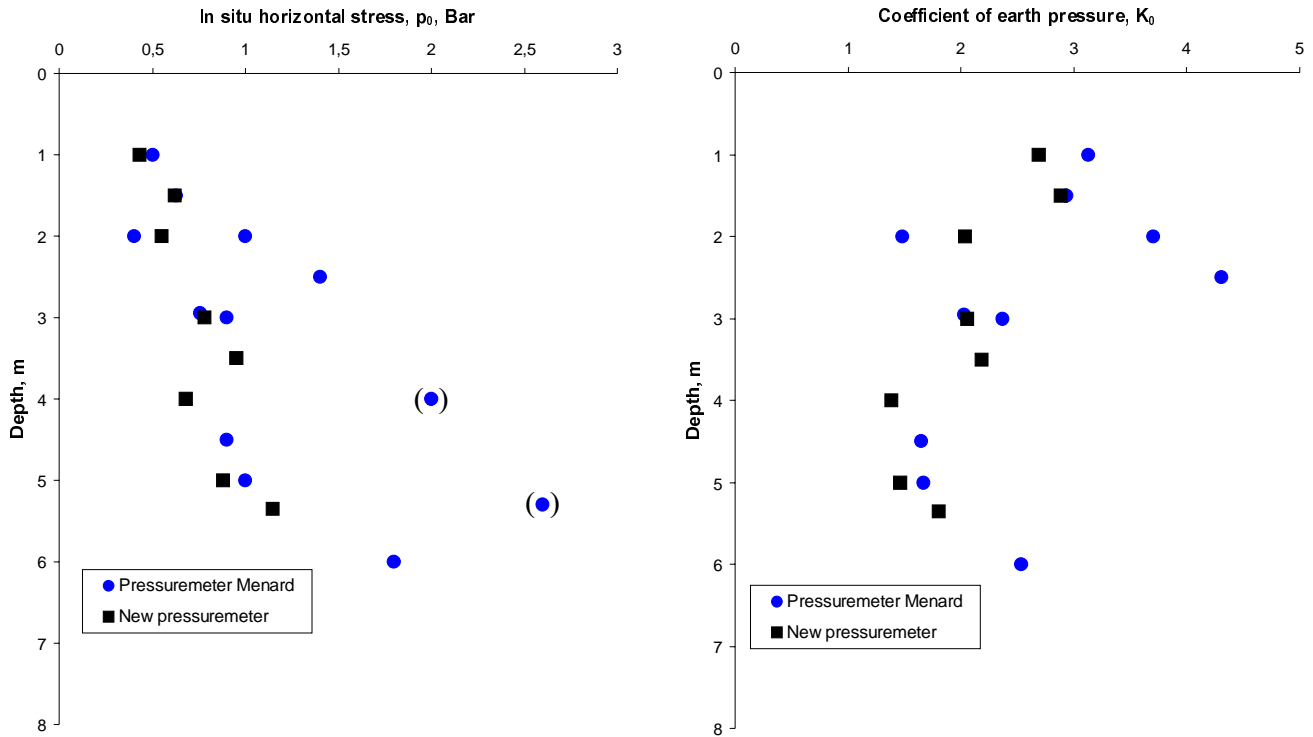
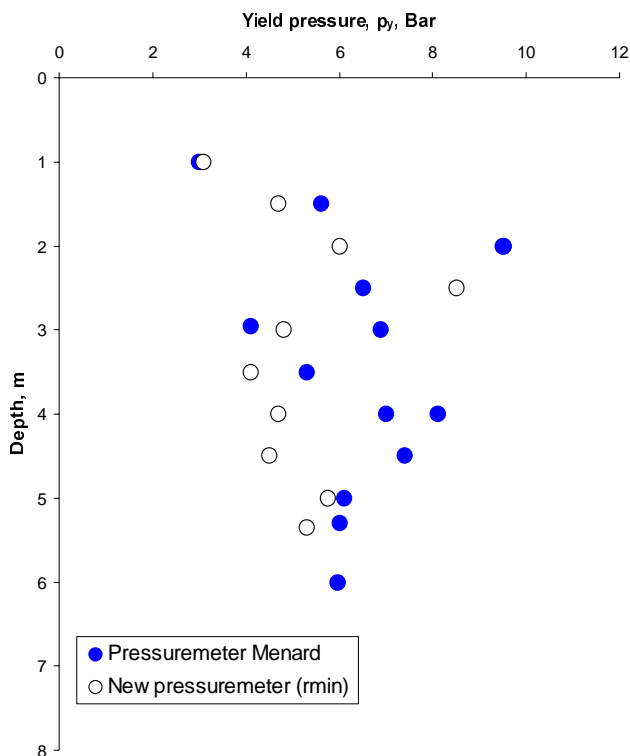


Fig. 34. Evaluated in situ horizontal stresses and coefficients of earth pressure from pressuremeter tests at Tornhill.



The pressuremeter moduli evaluated from the two types of tests fell within the same scatter band and no significant difference was observed. The pattern with peak values between 2 and 2.5 metres depth, decreasing to a lower and fairly constant value between 3.5 and 5.5 metres depth, is repeated, *Fig. 37*.

Fig. 35. Evaluated yield pressures from the pressuremeter tests at Tornhill.

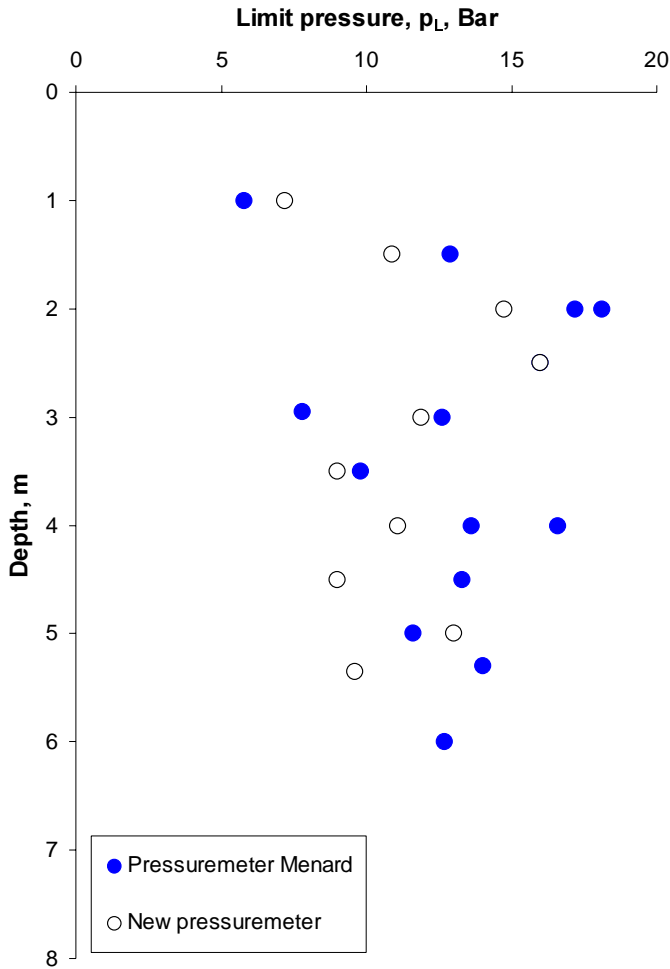


Fig. 36. Evaluated limit pressures from the pressuremeter tests at Tornhill.

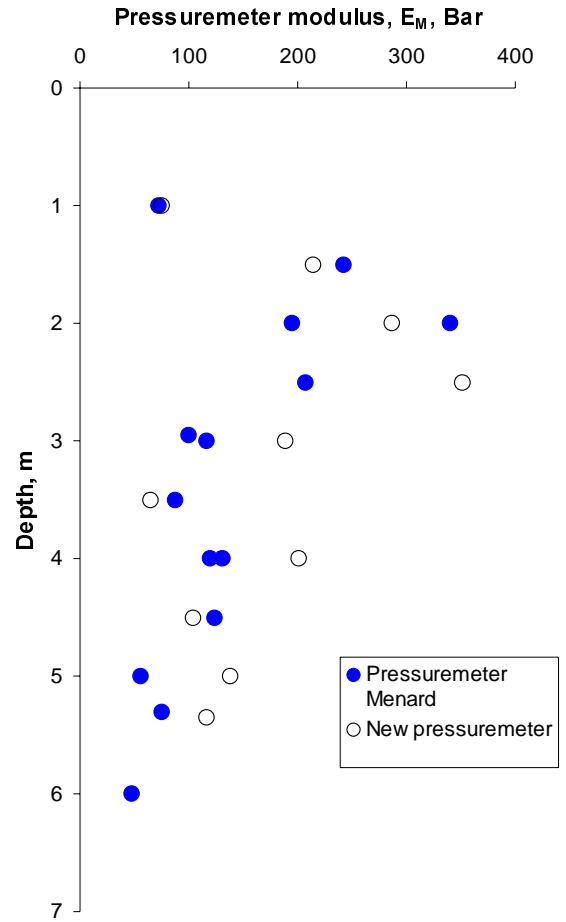


Fig. 37. Evaluated pressuremeter moduli from the pressuremeter tests at Tornhill.

■ **Evaluation of creep effects**

The parameters measured in a Menard type of pressuremeter test relate to a loading time of one minute. For a longer duration, the volumetric expansion during the stress increment will increase with time. This creep effect is approximately a function of the logarithm of the time and can be written in different ways. Schmertmann (1978) proposed that creep effects be written as

$$\varepsilon = \varepsilon_1 \left( 1 + \alpha \log \frac{t}{t_1} \right)$$

Riggins (1981) proposed that the creep effects be written as

$$E = E_0 \left( \frac{t}{t_0} \right)^{-n_t}$$

and in the pressuremeter test the creep exponent  $n_t$  is evaluated from

$$\Delta R_{C_t} = \Delta R_{C_{(1 \text{ minute})}} \left( \frac{t, \text{ minutes}}{1 \text{ minute}} \right)^{n_t}$$

Both approaches have been used to evaluate the creep parameters from the holding periods during the tests with the new pressuremeter. The results were fairly constant with depth, yielding an average value of  $\alpha$  of 0.114 and an average value of  $n_t$  of 0.047. Briaud (1995) proposed that a creep exponent twice that determined in pressuremeter tests be applied when calculating settlements of footings.

■ **Evaluation of shear strength**

A number of different ways have been proposed to estimate the undrained shear strength in cohesive soils on the basis of pressuremeter test results. The traditional way of interpreting the shear strength is by using the equation:

$$c_u = \frac{p_L - p_0}{1 + \ln \frac{G}{c_u}}$$

Use of the formula requires knowledge of the rigidity index  $G/c_u$ , which is rarely known precisely. Instead, an empirical relation is normally used. For most practical estimations, the value of  $p_L$  determined according to Menard has been used together with a value of the “pressuremeter constant” ( $1+G/c_u$ ) of 5.5. Mair and Wood (1987) point out that a theoretically correct evaluation should use  $p_L$  evaluated using the limit criteria  $\Delta V/V = 1$  and that the pressuremeter constant should rather be approximately 6.2.

Briaud recommends that the undrained shear strength be evaluated from the empirical relation:

$$c_u = 0.21 p_a \left( \frac{p_L - p_0}{p_a} \right)^{0.75}$$

where  $p_a$  is the atmospheric pressure.

Gibson and Anderson (1961) presented a method of interpreting the expansion of a cylindrical cavity in an ideal elastic-perfectly plastic material. Using this method, the undrained shear strength can be interpreted as the slope of the pressuremeter curve when plotted as  $\ln(\Delta V/V)$  versus the pressuremeter pressure, i.e. in the same plot as used for evaluation of  $p_L$ , *Fig. 38*.

Ideally, the curve should be corrected for initial deformations due to unloading of the cavity before it becomes reloaded by the probe, but this is not necessary when relatively large deformations are used for the interpretation. More elaborate

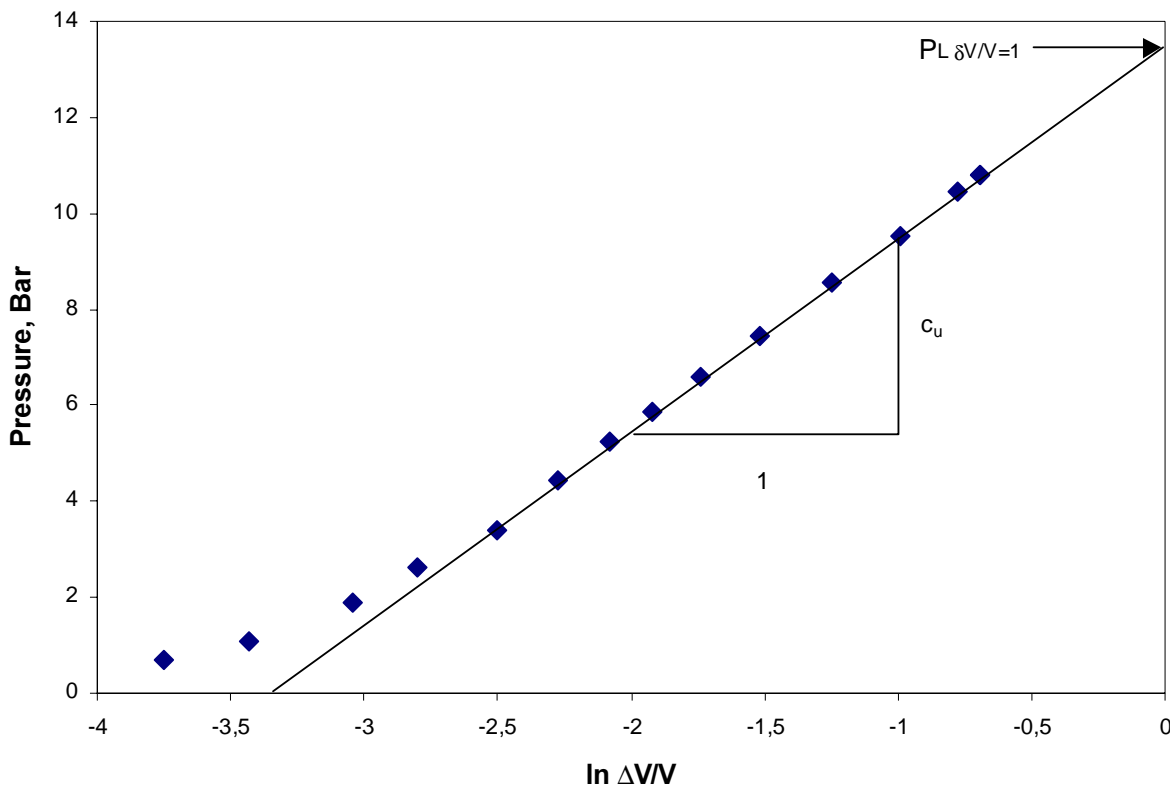


Fig. 38. Evaluation of undrained shear strength according to Gibson and Anderson (1961). Example of a pressuremeter test in clay till.

interpretations along similar lines yielding stress strain relations also for soils exhibiting peak strength followed by strain softening have been presented by authors such as Palmer (1972, Ladanyi (1972) and Baguelin et al. (1972). These methods have not been employed here since no tendencies for peak strengths could be detected in the pressuremeter curves.

The undrained shear strengths evaluated from the Menard type pressuremeter tests are shown together with the results from the CPT-tests and the field vane tests in Fig. 39. As can be seen in the comparison, the strength values evaluated

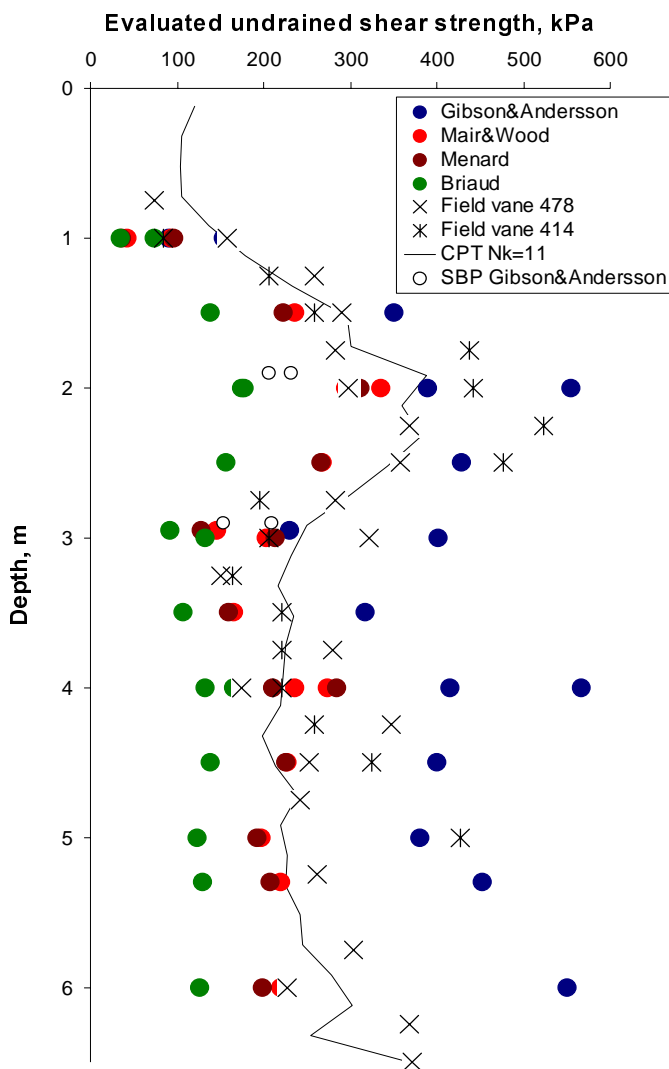


Fig. 39. Evaluated undrained shear strength from Menard type pressuremeter tests at Tornhill.

according to Menard or Mair and Wood are about equal and in general compatible with the reference data. The strength values evaluated according to Briaud are only about half of the reference data and the values evaluated according to Gibson and Anderson generally become higher than the reference data. The difference increases with depth and becomes up to about two times.

The results from the pressuremeter tests according to the new procedure have been interpreted in the same way. In this case, the best correspondence with the reference data was obtained with the Gibson and Anderson method. The results obtained with the Menard and the Mair and Wood methods corresponded to about two thirds of those in the reference data and values obtained by the Briaud method equalled less than half those in the reference data, Fig. 40.

From the results, it is obvious that the results of the pressuremeter tests are rate and procedure dependent, and that the interpretation method should be chosen accordingly. The Menard interpretation has traditionally been used together with the Menard procedure and both this and the more objective Mair and Wood procedure appear to yield relevant strength values also in the present case. Slower tests yield lower limit pressures and consequently also lower strengths when interpreted with these methods. For the new testing procedure, the Gibson and Anderson method yielded the best correlation with the reference data. However, this method does not either account for rate or creep effects and an even slower testing rate might result in excessively low values being evaluated also with this method, whereas an increased testing rate would result in excessively high values. So far, no method has been presented which takes the testing rate into account.

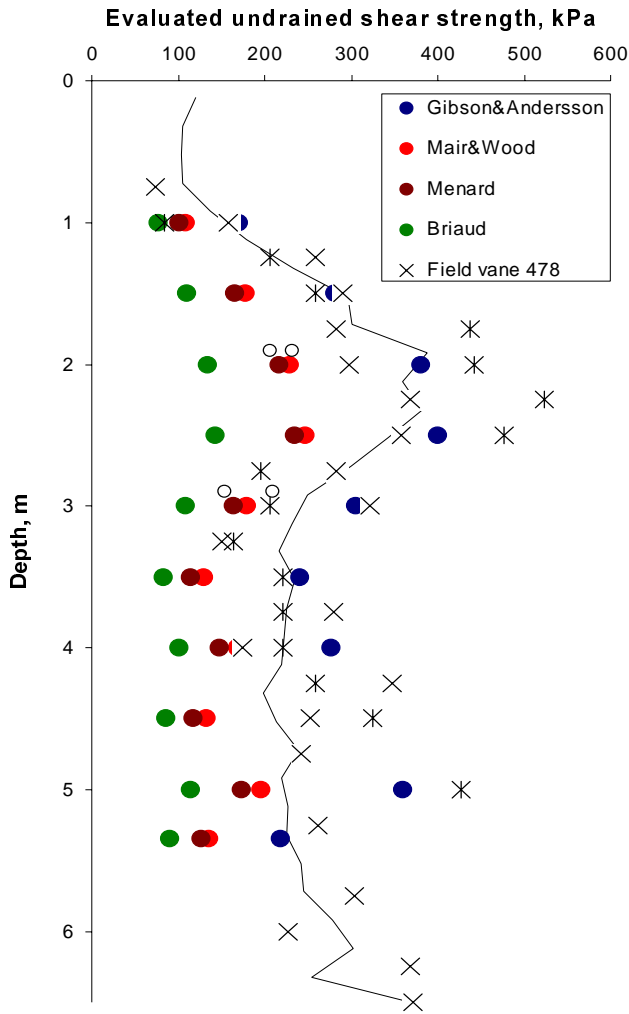


Fig. 40. Evaluated undrained shear strength from the new type of pressuremeter tests at Tornhill.

#### ■ Evaluation of moduli at small strains

The purpose of the new equipment was to enable measurement of moduli at small strains in unloading-reloading loops. This requires very careful calibration and measurement of the volume changes, which the equipment and calibration was designed to provide. Correction was thus made for stresses in the rubber membrane, including hysteresis and rate effects, pressure loss due to flow in the pressure pipe and system compressibility. Furthermore, the expansion and deflation was stopped for about 15 seconds at several stages also in the unloading-reloading loops in order to check that no significant errors occurred because of loading rate.

The initial volume and radius of the cavity,  $V_0$  and  $R_0$ , have been determined by the method for evaluation of in situ horizontal stress described above. The relative increase in cavity radius  $\Delta R/R_0$  has then been calculated and the pressuremeter curves have been plotted as pressure versus this parameter, Fig. 41. The curves have been studied carefully and relevant minimum and crossover points for the loops have been selected.

Unload-reload loops are affected by creep and hysteresis effects that have to be accounted for in some way. The creep effects are most pronounced at the start of the unloading cycle, where the pressuremeter pressure decreases even if the volume is kept constant, and at the end of the reloading cycle where significant creep starts again. The “elastic” part of the curve, which is relatively unaffected by creep effects, may be assumed to be between the lowest pressure at unloading and the point where the reloading curve intersects the unloading curve. This is also the point to which the creep effects tend to take the virgin loading curve when the expansion is stopped and the pressure decreases because of creep and stress relaxation. A condition for the strains remaining elastic at unloading in a clay is that the decrease in pressure in the loop does not exceed twice the undrained shear strength (Wroth 1982). This has been checked for the test data and the loops have then been evaluated as an unloading from the pressure at the crossover point to the minimum pressure in the loop and reloading again.

There is a significant hysteresis effect within the loops and the moduli for the reloading loops have been determined as secant moduli for the whole loop or from the point at the minimum pressure in the loop to the particular pressure or strain under consideration. When the unloading curve has been studied, the secant moduli have been calculated from the crossover point.

The current radius of the cavity,  $R_c$ , has been calculated continuously and the cavity strain in the loops,  $\epsilon_c$ , has been calculated as  $\Delta R_c/R_c$ . The secant shear modulus,  $G$ , is then calculated as

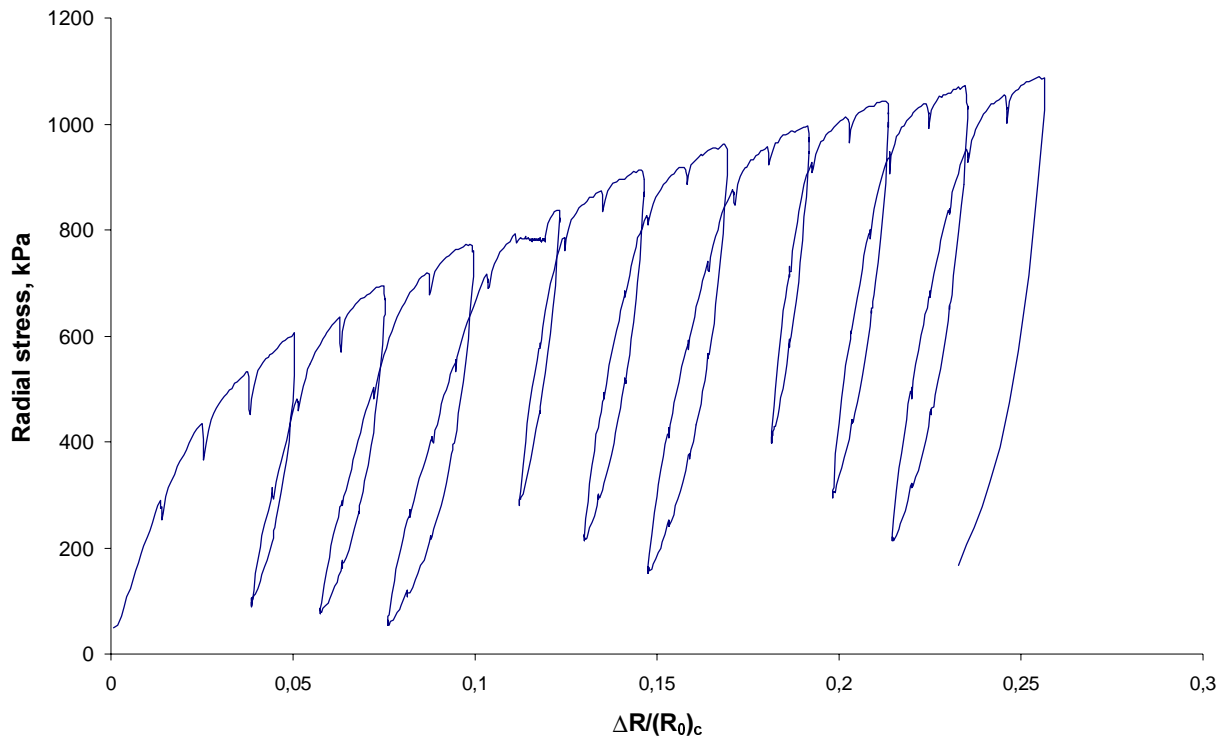


Fig. 41. Pressuremeter curve from 2 metres depth at Tornhill presented as radial stress versus relative increase in cavity radius.

$$G = \frac{\Delta p}{2\Delta\epsilon_c}$$

The shear modulus can be converted into modulus of elasticity, E, by

$$E = 2G(1 + \nu)$$

where Poisson's ratio  $\nu$  is generally assumed to be 0.33.

The cavity strain,  $\epsilon_c$ , is the strain at the cavity wall, and the shear strain in the surrounding soil decreases with distance from the wall. According to Briaud et al (1987), the average shear strain in the affected soil mass can be estimated as  $0.32 \epsilon_c$ . Jardine (1991) has proposed another empirical way of translating the cavity strains to shear strains. According to this method, the shear strain,  $\epsilon_s$ , that corresponds empirically to the same shear modulus as measured in this type of pressuremeter test can be calculated from

$$\epsilon_s \approx \frac{\epsilon_c}{1.2 + 0.8 \log\left(\frac{\epsilon_c}{10^{-5}}\right)}$$

The shear modulus and the modulus of elasticity are stress and strain dependent. The strain dependence is often written as a hyperbolic function (Kondner 1963):

$$\frac{1}{E} = a + b\epsilon, \text{ secant modulus}$$

and the stress dependence as an exponential function (Janbu 1963):

$$E = k \left( \frac{p'}{p_a} \right)^n, \text{ tangent modulus}$$

where  $p'$  is the mean effective normal stress and  $p_a$  is the atmospheric pressure.



If  $p'$  is taken as the average effective stress in the stress interval for which the modulus is valid, the shear modulus or modulus of elasticity at any stress and strain can be written as

$$G = \frac{\left(\frac{p'}{p_a}\right)^n}{a_G + b_G \varepsilon}$$

and

$$E = \frac{\left(\frac{p'}{p_a}\right)^n}{a_E + b_E \varepsilon}$$

These formulas then provide secant moduli.

The mean effective normal stress in the soil is

$$p' = \frac{\sigma'_1 + \sigma'_2 + \sigma'_3}{3}$$

which in the pressuremeter case becomes

$$p' = \frac{\sigma'_r + \sigma'_\theta + \sigma'_v}{3}$$

where  $\sigma'_r$ ,  $\sigma'_\theta$  and  $\sigma'_v$  are the effective radial, circumferential and vertical stresses.

However, only the initial vertical stress and the radial pressure at the cavity wall are known. According to Briaud et al. (1987), a reasonable estimate of the mean effective normal stress in the soil mass around the pressuremeter can be obtained from

$$p' = \frac{0.8\sigma'_r + \sigma'_v}{3}$$

and the relevant mean stress for a secant modulus evaluated in a loop should be calculated from the mean radial stress in the interval for which the modulus is determined.

The stresses in the equations above are effective stresses and, in fine-grained soils, the pore pressures should ideally be measured and an estimate made of the radial pore pressure distribution.

This could not be done in the current tests and the evaluation had to be made under the assumption that the initial pore pressures remained fairly constant during the test. The relevance of this assumption is difficult to judge, but it was noted that the tests were rather slow and that the pore pressures developed in the later plate load tests were very low.

The stress dependence of the moduli can be determined from loops with equal strains. This has been done for all the tests. The intention of the procedure using series of loops with equal volumetric deflation of the probe in loops belonging to the different series was to provide data from loops with equal strains but at different stress levels. However, also the current radius of the cavity increases as the test proceeds and the strains therefore become somewhat different in this way. This led to a certain extra scatter in the results and uncertainty in the evaluation. In this case, the pressure and volume changes were recorded continuously and it was thus possible to select portions with equal strains within all loops and to plot the data together. This procedure provided fairly good relations when the moduli at relatively small strains were considered, *Fig. 42*. However, the scatter increases significantly when larger strains are considered and the relations also appear to change somewhat.

The strain dependence of the moduli was then estimated. It was possible to do this from loops with almost equal effective mean stresses, which the test procedure was also designed to produce. The estimation could also be made by first normalising the moduli for the estimated stress dependence as

$$k_G = \frac{G}{\left(\frac{p'}{p_a}\right)^n} \quad \text{or} \quad k_E = \frac{E}{\left(\frac{p'}{p_a}\right)^n}$$

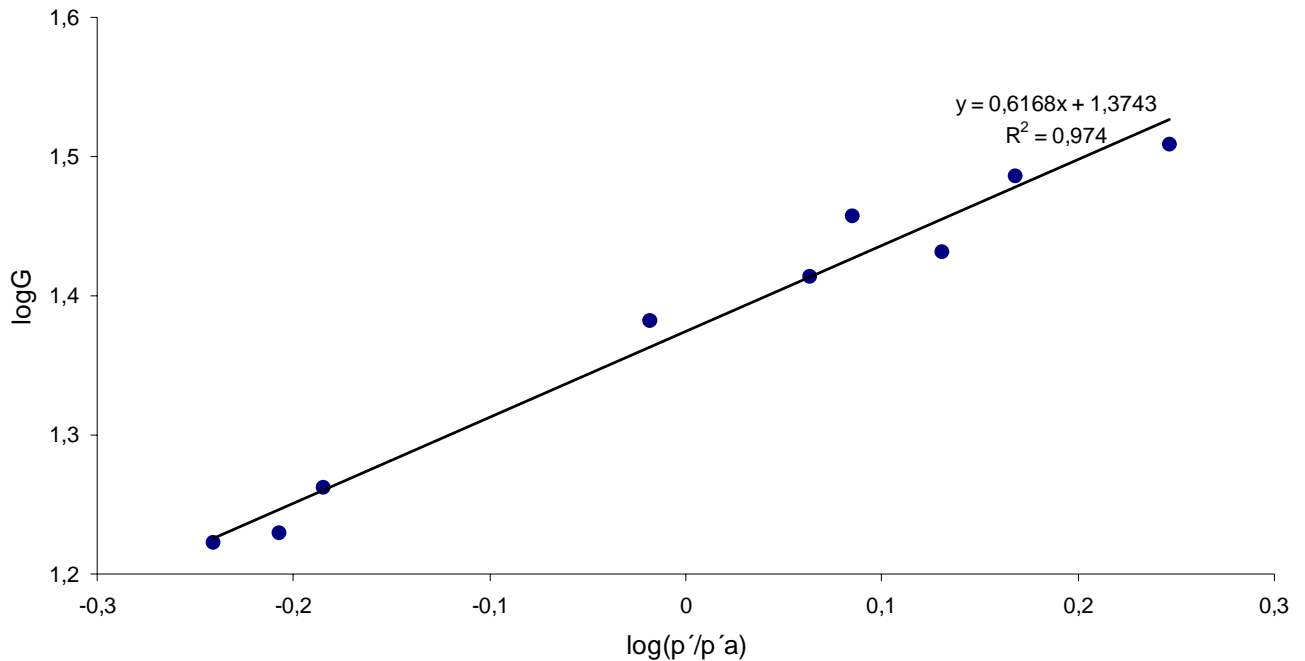


Fig. 42. Shear moduli versus normalised effective mean stress at a cavity strain of 0.002 at 2 metres depth at Tornhill.

and the inverse of the normalised modulus was then plotted against the corresponding strain. This was done in different ways depending on how the relevant shear strain was estimated. Fig. 43 shows two such plots, one for modulus of elasticity versus shear strain estimated according to Briaud et al (1987) and the other for shear modulus versus shear strain estimated according to Jardine (1991). As can be seen in the figure, a fairly good correlation can be obtained for both types of relation, but the strain dependence differs significantly depending on the method used to estimate the shear strain.

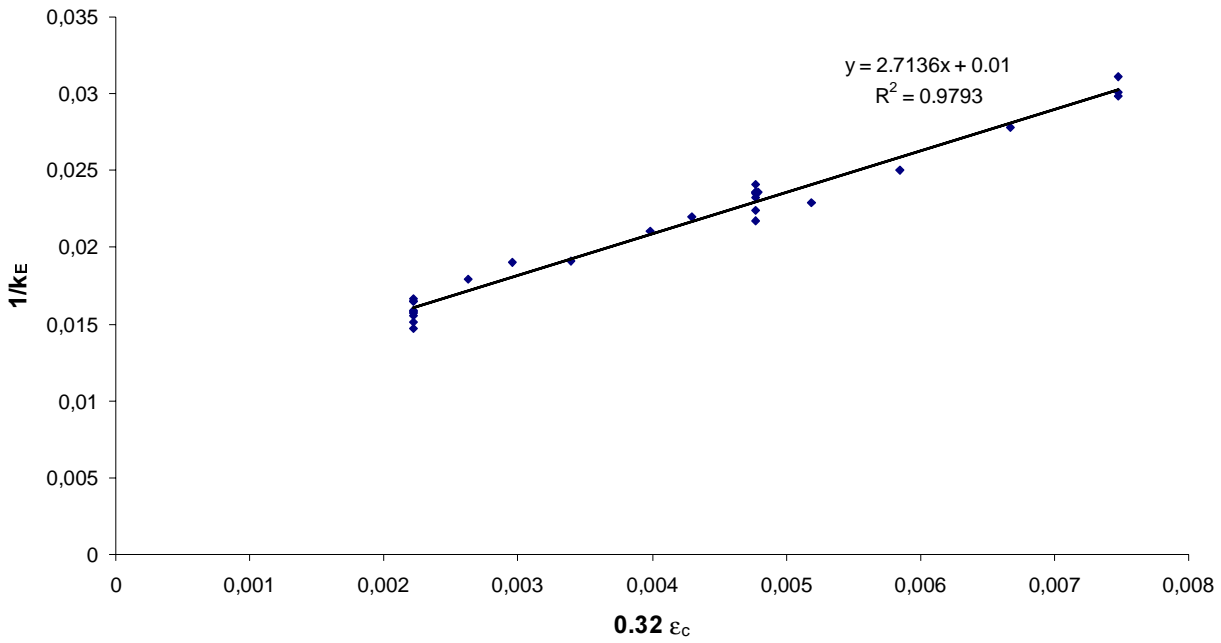
Three parameters are evaluated in this way:

- $n$ , which describes the stress dependence of the modulus
- $a$ , which is a measure of the initial stiffness of the soil
- $b$ , which is a measure of the strain dependence of the modulus

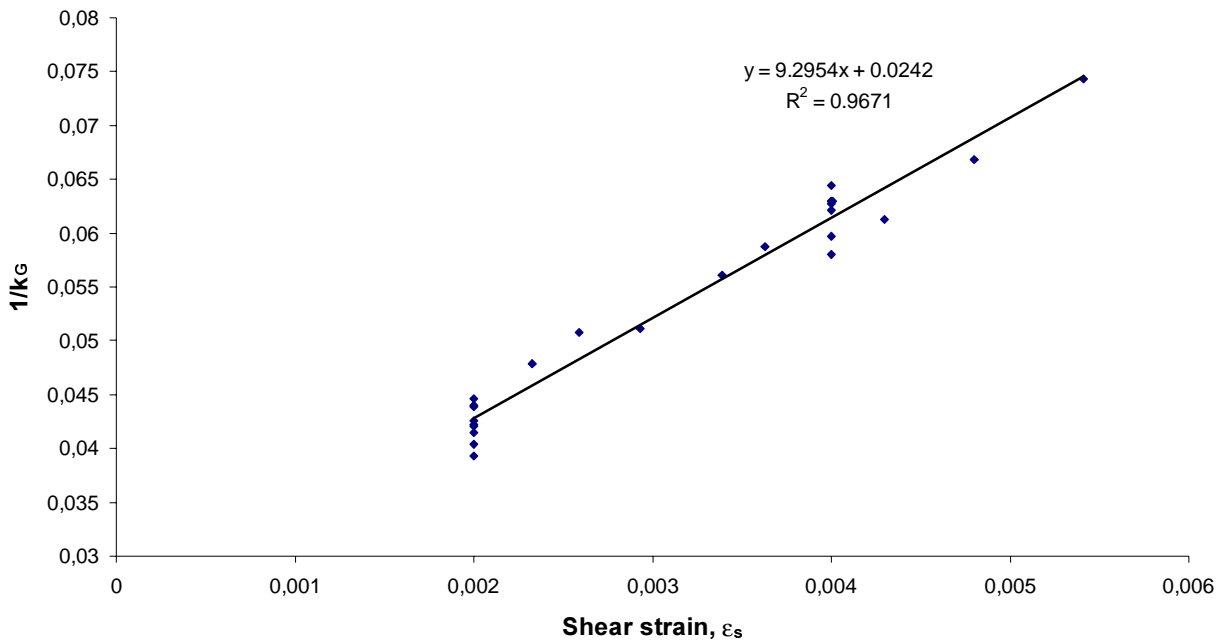
A high value of  $n$  entails a high sensitivity of the modulus to stress level, a high value of  $a$  entails a low initial stiffness and a high value of  $b$  entails a high sensitivity of the modulus to strain level. The evaluated parameters are listed in Tables 1 and 2.

Table 1. Evaluated parameters for the modulus of elasticity with respect to shear strains estimated according to Briaud et al. (1987).

Depth, m	$n$	$a$	$b$
1	0.930	0.0186	2.39
1.5	0.640	0.0089	3.25
2	0.617	0.0100	2.71
2.5	0.456	0.0085	2.62
3	0.676	0.0119	3.08
3.5	0.732	0.0138	3.67
4	0.580	0.0127	3.13
4.5	0.621	0.0172	3.00
5	0.992	0.0104	3.91
5.35	0.726	0.0135	2.82



a)



b)

Fig. 43. Evaluation of strain dependence for the moduli at 2 metres depth at Tornhill.  
 a) Modulus of elasticity versus shear strain estimated according to Briaud et al. (1987)  
 b) Shear modulus versus shear strain estimated according to Jardine (1991).

Table 2. Evaluated parameters for the shear modulus with respect to shear strains estimated according to Jardine (1991).

Depth, m	n	a	b
1	0.930	0.0443	8.75
1.5	0.640	0.0207	11.48
2	0.617	0.0242	9.30
2.5	0.456	0.0195	9.27
3	0.676	0.0272	11.15
3.5	0.732	0.0330	12.17
4	0.580	0.0305	10.89
4.5	0.621	0.0417	10.66
5	0.992	0.0246	10.72
5.35	0.726	0.0333	9.67

A comparison of the data reveals that the initial stiffness becomes about 10 % lower when the strains are evaluated according to Jardine (1991). It also decreases somewhat faster with strain when evaluated in this way.

A study of the parameters versus depth shows that the stress dependence of the modulus (parameter  $n$ ) appears to be somewhat lower in the layer of Baltic clay, which in general has the highest clay content, Fig. 44a. All values are within the normal limits between 0.38 and 1.45 reported by Briaud et al. (1983). The initial stiffness (the inverted value of parameter  $a$ ) shows a pronounced peak between 1.5 and 2.5 metres depth in agreement with what has been found in all other tests, Fig. 44b, and the parameter  $b$  shows a somewhat lower strain dependence in the upper layers, Fig. 44c.

These evaluated parameters should ideally enable an estimation of the moduli at any stress and strain level. However, this assumes that the models used correctly describe the soil behaviour. A comparison between the moduli estimated continuously for the reloading loops and those calculated with the evaluated factors shows that this model corresponds fairly well to the measured moduli within the shear strain region 0.002 - 0.01, Fig. 45.

It should be observed that the shear strains in the higher region are no longer “elastic” strains within the unload-reload loop, but include plastic strains in the loading path after the crossover point has been passed.

A further comparison with the estimated values can be made by calculating the modulus at zero strain using the estimated parameters and in situ stresses, which ideally would yield a measure of the initial shear modulus. This gives a variation in shear modulus that more or less reflects that evaluated from the seismic cone tests, but the former values are only about a third of the latter, Fig. 46.

Thus, the model described above reproduces fairly well the shear modulus as measured within a certain strain interval. For very small strains, which constitute the major part of the loop, the fit is poor and the model overpredicts the values in relation to measured values. However, there is another way of describing what is happening in unload-reload cycles on soils, which has previously been found useful in evaluating oedometer tests (Larsson 1981). According to this method, the swelling of the soil at unloading can be described by a swelling index,  $a_s$ . The relative expansion,  $\epsilon_{swell}$  of the soil can then be calculated from

$$\epsilon_{swell} = a_s \ln \frac{\sigma'_{max}}{\sigma'_{min}}$$

where  $\sigma'_{max}$  and  $\sigma'_{min}$  are the maximum and minimum effective vertical stresses in the loop. The secant reloading modulus,  $Mr_l$ , then becomes

$$Mr_l = \frac{\sigma'_{max} - \sigma'_{min}}{\epsilon_{swell}}$$

The same approach has been applied to the loops in the pressuremeter tests using the radial pressure instead of the effective vertical stress. The evaluated shear modulus has thus been plotted against the parameter  $(p_{max} - p_{min}) / \ln(p_{max}/p_{min})$  and a corresponding swelling index has been evaluated, Fig. 47. In this way, a very consistent picture was obtained with an almost constant relation between the two parameters.

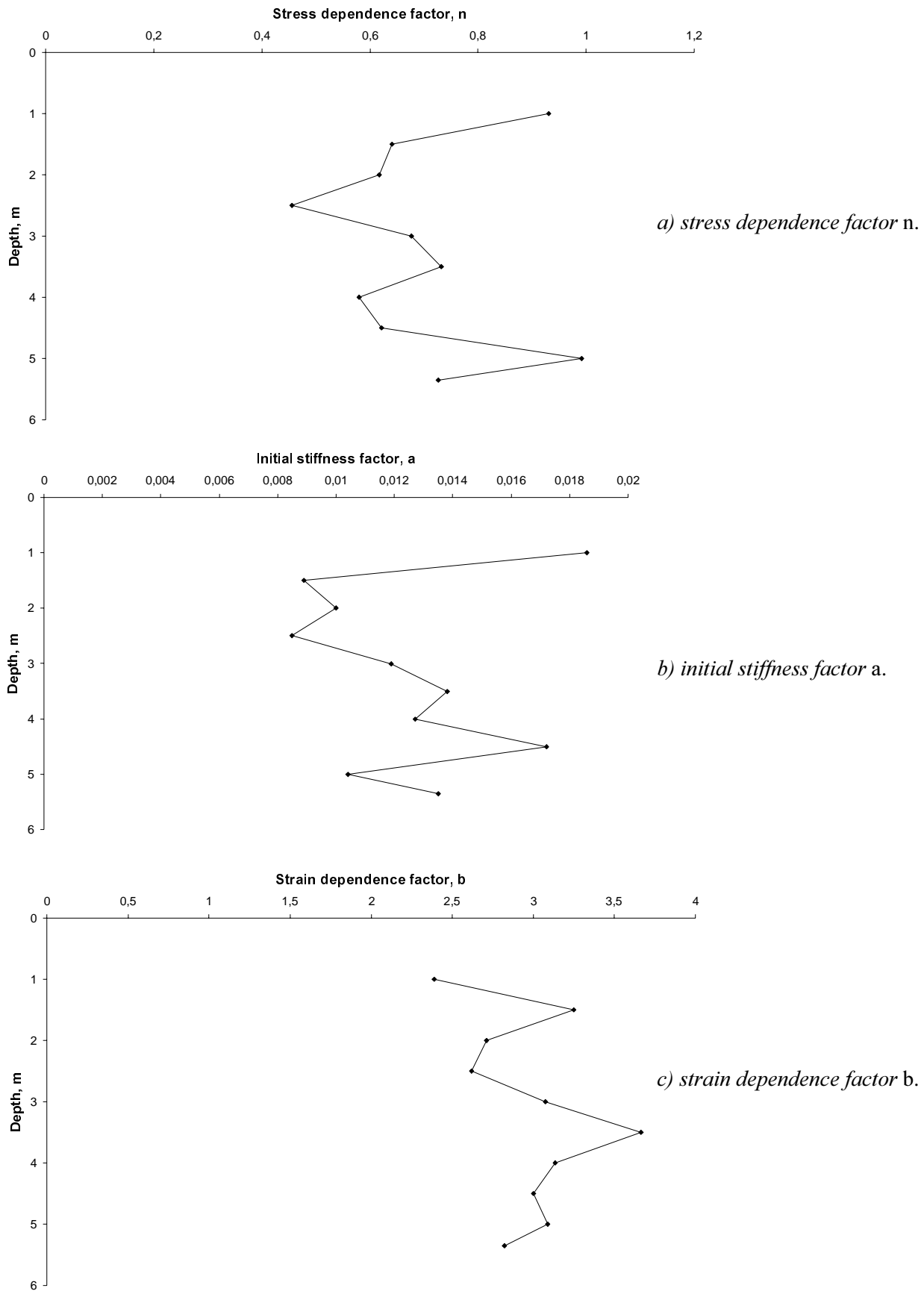


Fig. 44. Evaluated parameters for the shear modulus versus depth at Tornhill.

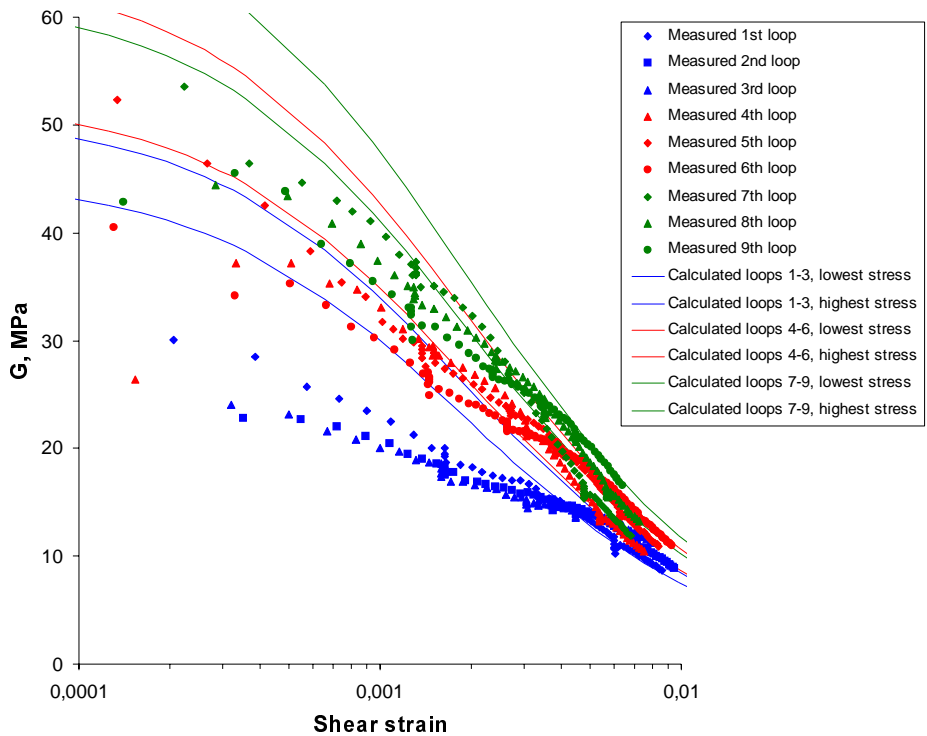


Fig. 45. Comparison between the evaluated shear moduli in the different unloading-reloading loops and the estimated relations between modulus and shear strain at 2 metres depth at Tornhill. The evaluated curves are shown in three groups, each representing one of the unload-reload series in the tests. The estimated curves are shown as upper and lower boundaries corresponding to the maximum and minimum mean stresses in the loops within each series.

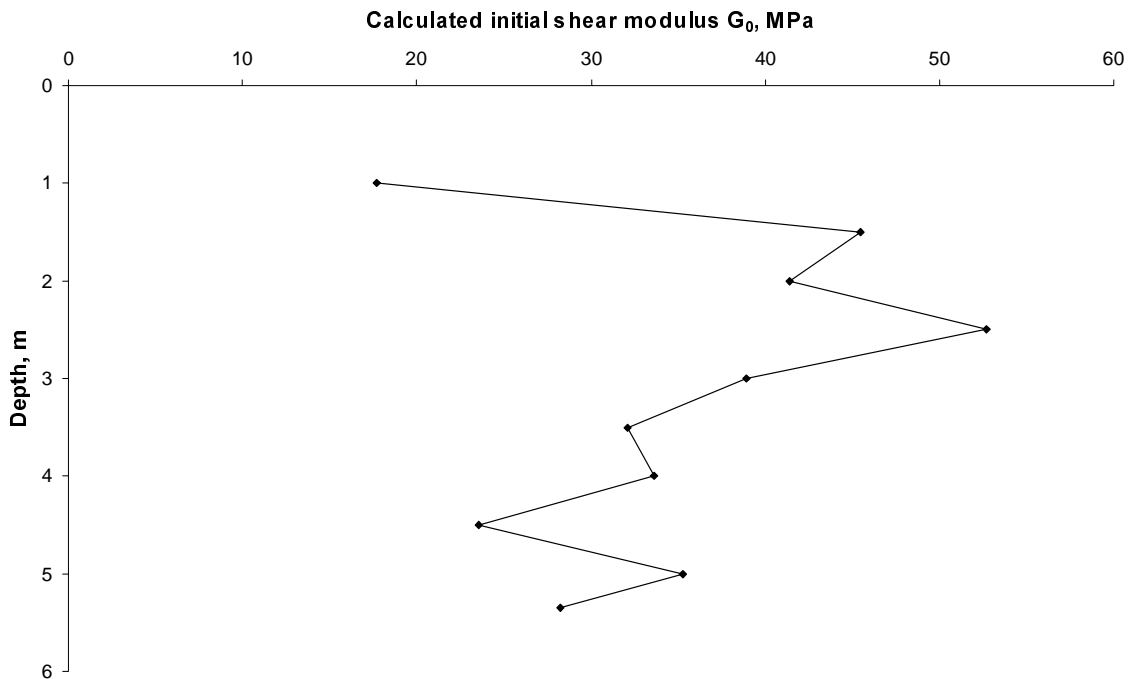


Fig. 46. Initial shear modulus at in situ stresses calculated from the pressuremeter tests.

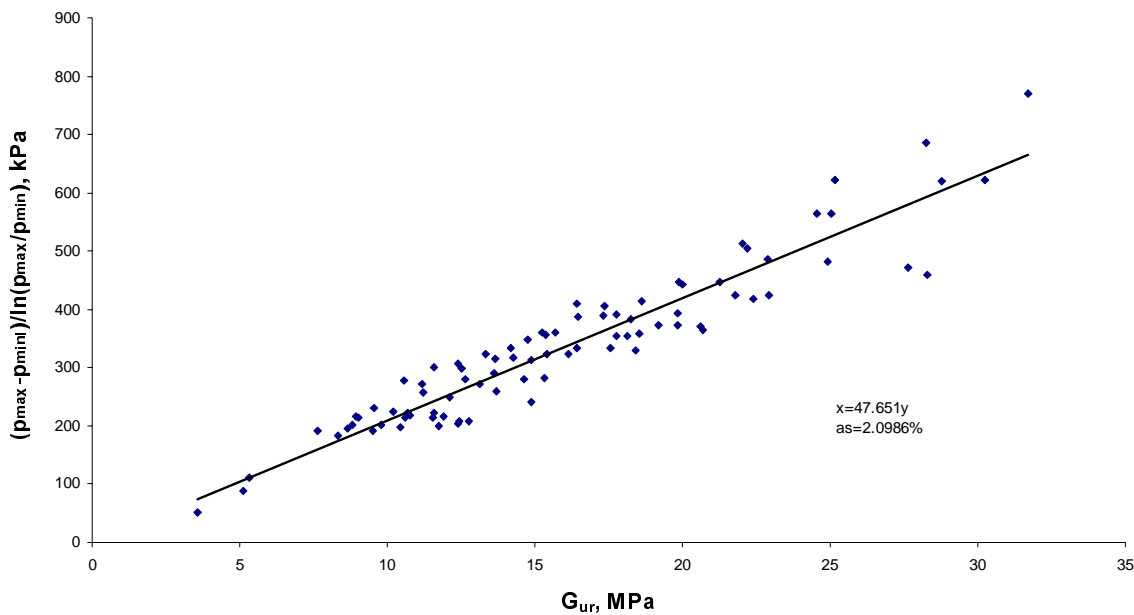


Fig. 47. Evaluation of the swelling parameter from pressuremeter tests.

Fig. 47 contains the results from all loops in the tests. Naturally, some scatter is present, which relates to variations within the tests and also variation with depth. The average values for each test depth are shown in Fig. 48.

The variation in the evaluated swelling index with depth is relatively small and it is difficult to discern any particular pattern. It may therefore be considered as a constant for the soil profile. The variation in unloading-reloading modulus is then primarily related to the different pressures at which unloading starts and the size of the unloading. The measured variation in stiffness with depth then becomes a function of the stiffness and strength of the soil as reflected by the virgin expansion curve, from which the unloading starts.

The above relation can be used to predict the variation in modulus in the unload-reload loops. In this case, it has to be assumed that the shape of the loop is inversely symmetric, i.e. that the initial stiff modulus and its decrease at unloading are reflected by an identical stiff modulus and curvature from the start of reloading. This assumption may be somewhat general, but the pos-

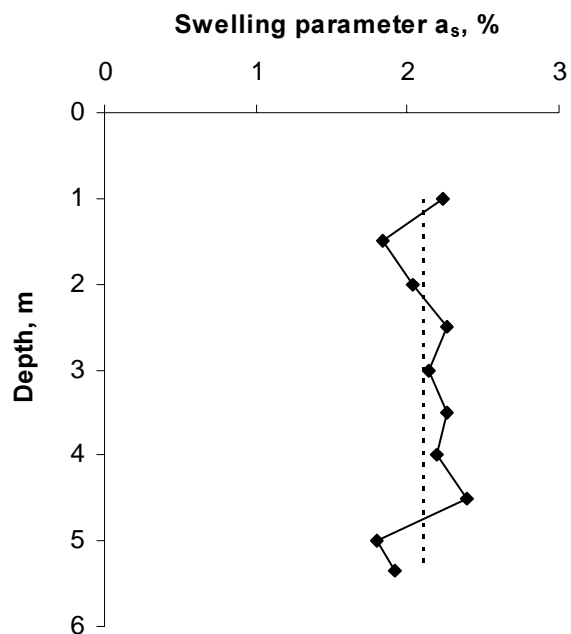


Fig. 48. Variation in swelling index with depth.

sible error decreases with strain level and is eliminated when the whole loop is considered. The initial stiff modulus at both ends of the loop becomes

$$G_0 = p'_{max} / a_s$$

For a certain decrease in radial stress to the pressure  $p'$ , the secant shear modulus can be calculated from

$$G = \frac{p'_{\max} - p'}{a_s \ln \frac{p'_{\max}}{p'}}$$

The cavity strain at the wall can be calculated from

$$\varepsilon_c = \frac{p'_{\max} - p}{2G}$$

from which the shear strain in the soil mass can be calculated by one of the empirical methods.

This has been illustrated for the results from the test at 2 metres depth at Tornhill in *Fig. 49*. As can be seen in the figure, this method describes much better what is actually measured in the main part of the unload-reload loops and covers the whole strain interval from 0.0001 to 0.01.

However, the translation to geotechnical design parameters is more uncertain since it also involves an estimation of the previous maximum normal stress in the current loading direction.

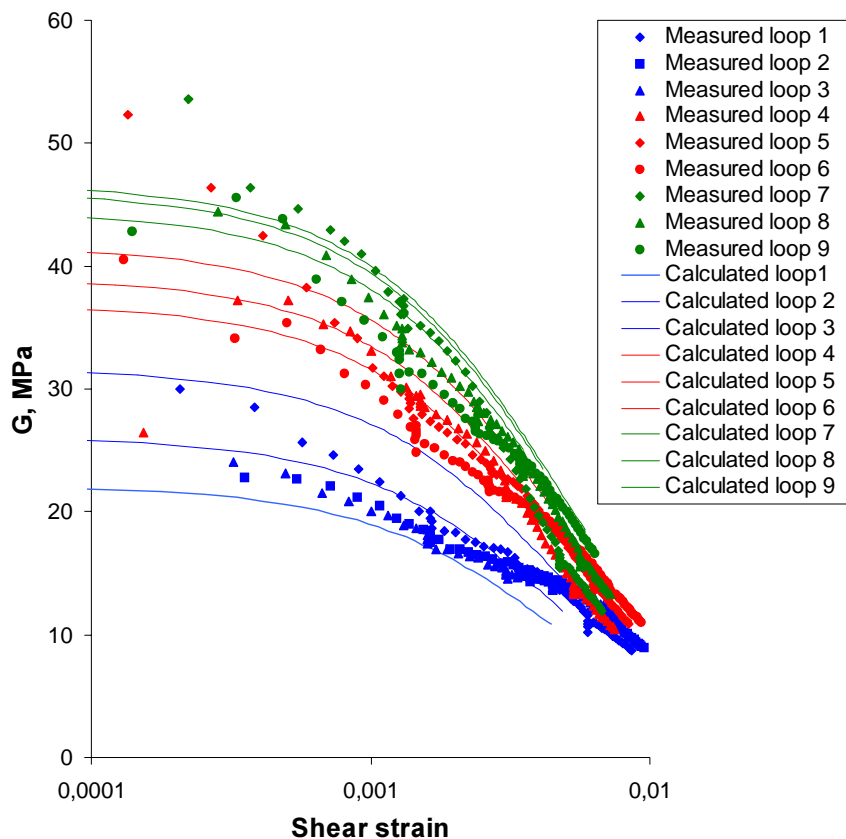


*Fig. 49. Comparison between the evaluated shear moduli in the different unloading-reloading loops at 2 metres depth at Tornhill and the estimated relations between modulus and shear strain using the swelling index.*



## 3.5 SAMPLING

### 3.51 Tube sampling

In Sweden, tube sampling in clay is normally performed with the Swedish standard piston sampler. However, in clay tills, the content of coarse particles is so great that a diameter of 50 mm is too small to obtain representative samples. Also, the equipment is not designed for this type of very stiff soil with large contents of flint and coarse objects. Even if samples could be obtained, the wear on the equipment would be considerable. For tube sampling in this type of soil, open samplers with larger diameters are normally used.

Tube sampling in the present project was performed with equipment similar to the Danish “Americanerrör”. The sampling tubes are made from ordinary thin-walled seamless stainless tubes with an inner diameter of 70 mm and a wall thickness of about 2 mm. These are cut into lengths of 600 mm. The lower end of the sampling tube is turned into a sharp edge and three holes are drilled for fixing bolts at the upper end.

The upper end of the sampling tube is threaded onto an adapter with the same outer diameter as the tube. The lower part of the adapter has been turned down to fit tightly inside the tubes over a length long enough to provide a stiff connection with proper guidance for the tube. It also contains two outer grooves with O-rings making the connection airtight. After the tube has been threaded on, it is fixed in this position by three bolts.

The adapter also contains a vertical air-water channel with a ball valve. This enables air and water on top of the sample to be flushed out when the sampler is pushed down, but shuts off and prevents the sample being sucked out during withdrawal of the sampler. The upper end of the adapter is connected to stiff drill rods. The sampler thus conforms to the normal requirements for thin walled sampling in fine grained soils, except that there is no inner clearance in the tubes above the cutting edge. Such clearances

often create more problems than benefits according to Swedish experience.

Sampling is performed from the bottom of pre-drilled holes. These can be prepared with different types of auger and stabilised in different ways. In this case, a hollow stem auger with a shaft wide enough to accommodate the sampler was used. The auger was rotated down to just above the sampling depth and then the centre part was drawn up and the sampler was lowered into the shaft, *Fig. 50*. The open-ended sampler was then pushed down 500 mm or to refusal, whichever came first. After a short rest period lasting a few minutes, the sampler was withdrawn.



*Fig. 50. Sampling operation with tube sampler in progress. The hollow stem auger is rotated down and the prepared tube sampler is suspended at the side, ready to be lowered into the shaft.*

On reaching the ground surface, the ball valve was opened, the fixing bolts removed and the sampling tube released from the adapter. The ends of the tube were then sealed and the whole tube wrapped in plastic.

This operation continued through the upper layers of Baltic clay till and mixed clay till. Sampling was performed at approximately every 0.5 metre from 1 to 6 metres depth. However, coarse objects were encountered and this resulted in most of the sampling strokes failing to fully reach the intended length of 500 mm. It also meant that at some levels it was necessary to predrill past a large object before the sampler could be lowered. Thus, this type of sampling did not provide a fully continuous profile. No attempt was made to take samples in the underlying North-east till in this way since it was considered impossible.

Afterwards, the samples were placed well protected inside their stiff sampling tubes. Their size also enabled very careful transport to the laboratory in the rear seat of a private car. At the laboratory, they were stored in a room with controlled temperature and humidity.

Most attempts at sampling had been terminated because of refusal to penetration and the cutting edges of almost every sampling tube had buckled inwards during the sampling operation. Apart from possible disturbance, this also resulted in the formation of an automatic shutter when the sampler was withdrawn. There were no indications that the samples had tended to be drawn out of the sampler during its withdrawal from the ground. Buckling of the edge apparently also directly led to refusal in penetration since no corresponding grooves in the samples could be found when these were extruded.

Before extrusion of the samples, the buckled part of the edges had to be sawn off in the workshop. The sampling tubes were then placed vertically in a special extrusion rig where they were pushed out by a hydraulic piston.

The sampling tubes can be re-used after a new cutting edge has been turned. However, it must be expected that a certain length of the tube is lost after each sampling operation and the number of times the tube can be re-used is therefore limited.

### 3.52 Core drilling

Core drilling was performed with the Geobor-S triple tube wire line core sampling system. This equipment was originally designed for taking cores in rock, but techniques for taking cores in clay tills have also been elaborated (Jonsson et al. 1995), *Fig. 51*.

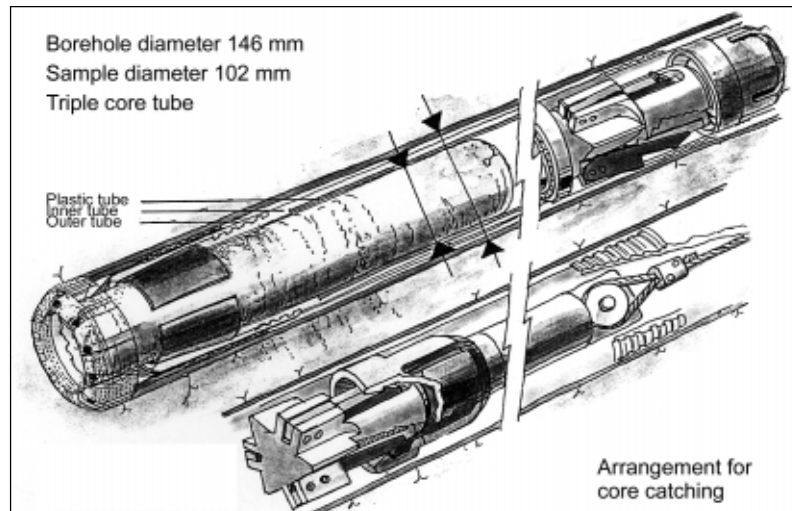
Drilling is performed with a rotating drill bit and flushing with a drilling fluid. The drilled out core has a diameter of 102 mm and is inserted into a plastic sample tube with a length of 1.5 metres. The sampler can be equipped with different types of shutter, which are selected according to the type of soil or rock in the core. After drilling out a core with the same length as the sample tube, the core is drawn up inside the tube with the aid of a wire which is first lowered inside the drill rods and hooked onto the sampling tube.

The sampling tube can be split lengthways and then opened for inspection and classification of the core material directly on site. It can also be used as an integral tube, which is an advantage when it is to be sealed and used as a container for transporting and storing the cores.

The Geobor-S equipment can be used in a wide range of stiff soils and rock. During operation, it is possible to vary the design and construction of the drill bit, the drilling fluid and its pressure and flow, the position of the inlet of the flushing fluid, the applied vertical force, the applied torque and the speed of rotation. As mentioned above, the type of shutter is also selected depending on the material in the drilled-out core.

It has been found that “impregnated drill bits with matrix quality” are required for drilling through pieces of flint in limestone, while “surface set bits” yield better core qualities in clay

Fig. 51.  
*Principle for the coring system in Geobor-S and example of a core taken in Baltic clay till. The core is taken with a split sample tube and the upper half is removed for inspection of the sample. Atlas Copco and Jonsson et al. (1995).*



till, particularly when this contains layers of coarse soils (Jonsson et al. 1995). The applied vertical force is regulated according to the stiffness of the soil or rock. The force must be sufficiently high to make the drill bit cut, but excessive force increases both the wear on the drill bit and disturbance of the soil. The flow of the flushing medium also has to be carefully controlled. A rise in the pressure indicates that the flushing channels are becoming clogged, whereas excessive pressure or flow creates excessive erosion in the soil. The other parameters must also be regulated more or less continuously as drilling proceeds and the composition of the soil or rock varies. It has been shown that high quality samples can be obtained in this way even in complex soil profiles. However, handling of the equipment then becomes more demanding and requires a very skilled and experienced operator.

Flushing with water, which is the normal drill fluid, entails an obvious risk of the soil sample absorbing water during the sampling operation. Dueck (1997) found indications that this may be the case also in clay till. Furthermore, when flushing with water, a considerable amount of water is pumped down into the ground and then flows up to the ground surface. Even if it is collected here, the drilling operation often entails a considerable soaking of the adjacent ground. The coring operation with the Geobor-S equipment in the current project was therefore moved a short

distance away from the test area where most of the other investigations and subsequent load tests were performed.

The drilling operation was performed to provide a continuous core from the ground surface through the various layers of clay till and into the bedrock. A core with a total length of about 15 metres was therefore taken. Drilling was performed with the utmost care and all the experience previously acquired was utilised. The whole operation occupied two full working days.

Success in core drilling is often measured in terms of the recovery ratio, i.e. the ratio between the length of the core brought to the ground surface in relation to the drilled length. In this respect, the operation was a total success, since the cores fully corresponded to the drilled length within the measuring accuracy, (carpenters rule). For determination of the soil profile, the samples could thus be considered to be excellent. However, the quality of soil samples for testing strength and deformation properties depends also on whether the properties have been preserved during the sampling operation and on how carefully they are transported to and stored in the laboratory and other handling before the actual tests are performed. In the Geobor-S system, which was originally designed for rock, the cores are taken in plastic sample tubes with a relatively low rigidity. The split tubes have practically no rigidity

and also the intact tubes are relatively flexible. This means that the samples can hardly be lifted and handled without some bending occurring when they contain soil samples. Their weight and length also normally prevent the most careful transport in a private car.

The cores taken in the current project were immediately sealed and wrapped in an additional sheet of plastic. They were then transported carefully to a padded section of the floor in a lorry and transported to the laboratory 400 km away, where they were stored in a room with controlled temperature and humidity before testing. The cores were removed from the tubes by slitting the tubes lengthways at two opposite sides in the workshop and then lifting off one half of the tube. They were then inspected and divided into selected samples for different types of testing. If the tests were not to be performed directly, the samples were wrapped in plastic and returned to the store room.

There is thus a considerable risk that Geobor-S samples of soils will undergo a significant amount of disturbance during transport and handling, and this should be taken into account when discussing the quality of the samples. This remark applies both in general and to the present project.

## 4. Experience from the field tests

### 4.1 GROUND WATER OBSERVATIONS

In the ground water observations, it was found that the response in open standpipes was very slow. Reliable measurements of the pore water pressure and its fluctuations in clay till therefore require the use of closed piezometers. Problems with the long-term stability of such piezometers were encountered and these are believed to be related to chemical reactions and development of gases. Great care therefore has to be taken in the selection of tips, filters and pipes in order to avoid such problems as far as possible.

### 4.2 SOUNDINGS

#### CPT-tests

CPT-tests yielded a fairly good picture of the stratigraphy and composition of the soil layers. However, the tests only penetrated the Baltic clay till and mixed clay till, and stopped at the transition to the North-east till. The reason for this stop was primarily excessive side friction on the probe itself, which could not be eliminated with measures such as friction reduction for the drill rods. CPT-tests in the North-east till would require much heavier equipment than what is readily available in Sweden, in addition to new, more robust CPT-probes designed for very high side friction. The CPT-tests should be performed with measurement of pore pressure and preferably with the use of slot filters and grease in the measuring system.

The undrained shear strength could be evaluated using relations between the Danish field vane and CPT-tests similar to those proposed by various Danish researchers. The CPT-tests provide continuous curves with depth and are more rational to perform than the vane tests, since the latter have to be performed at the bottom of pre-drilled holes.

Because of the great heterogeneity of the material, a relatively large number of tests have to be performed in order to obtain a measure of the variation and results that are representative for the bulk of the soil mass.

#### Dynamic probing tests

Dynamic probing tests can be used for all types of clay till. However, they require the rod friction to be almost completely eliminated and, particularly in the North-east till, a heavy-super heavy probing method to be used. The interpretation of the undrained shear strength in the clay till proposed by Butcher et al. (1995) yielded reasonable values.

#### Soil-rock drilling

Soil-rock drilling with continuous registration of the six drilling parameters yielded a fairly good picture of the stratigraphy and the variation in some of the soil properties. However, no quantitative values of properties could be evaluated. This is probably the most rational sounding method for obtaining an overall picture of the soil stratigraphy and the depth to bedrock. The quality of the bedrock can also be estimated with this method.

#### Seismic CPT-tests

Seismic CPT-tests could be used to determine the shear wave velocities down to the top of the North-east clay till, i.e. as deep as the probe penetrated. The scatter in the results was very large in this heterogeneous material and the signal noise was also considerable. Several tests at different points together with a substantial amount of filtering and averaging were therefore required to obtain a relevant picture of the variation in shear modulus in the profile.

### 4.3 IN SITU TESTS

#### Resistivity measurements

Geo-electrical surface measurements proved to give a good picture of the variation in the soil composition both vertically and horizontally. They are thus a useful supplement to the soundings for creating a relevant soil model for the investigated area.

#### Field vane tests

Danish field vane tests are often used as reference tests in clay till. However, they are time-consuming since they have to be performed at the bottom of predrilled holes and the scatter in the test results is often considerable. The tests are often performed in combination with sampling by auger, which makes the method more rational, but CPT-tests are still to be preferred.

#### Dilatometer tests

Dilatometer tests are rational, particularly when the reading of the values is automated, and can be performed down to the same depths as the CPT-tests. The results were surprisingly uniform and the evaluated soil profile was fairly relevant. The estimated coefficients of earth pressure were consistent with what was estimated from the pressuremeter tests and what was estimated empirically from the overconsolidation ratios obtained from oedometer tests. The overconsolidation ratios were estimated fairly well with the relations proposed by Powell and Uglow (1988) for non-fissured soils. However, the undrained shear strengths became too low when estimated with any of the commonly used methods for clay. The estimated moduli appear to be of relevant sizes, which will be discussed further when compared to the results of the plate load tests. The estimated moduli in the Baltic clay till were of approximately the same size as those measured at reloading in the oedometer tests. In the mixed clay further down, they were lower or much lower than the corresponding oedometer values. The disturbance when inserting the dilatometer blade in the mixed clay till may thus be expected to have been significant to considerable.

#### Pressuremeter tests

Pressuremeter tests have been performed according to the Menard procedure and the procedure with a number of unloading-reloading loops proposed by Ekdahl and Bengtsson (1996). Both types of test are performed in predrilled holes. Self-boring pressuremeter tests in this type of soil had previously been shown to be very difficult to perform, Skanska Teknik (1998).

The preparation of the test cavity was best performed by using a combination of an auger with hollow stem and rods and the original tool designed by Menard, (Baguelin et al 1978). The auger was then used to prepare a straight hole down to just above the test level and the Menard tool was used to prepare the final test cavity below. Thick bentonite drilling mud was used to stabilise the holes and it was found to be very important to lower the pressuremeter probe and start the test without any unnecessary delay. Because of the large content of flint particles in the soil, a "canvas cover" was used on the probe. This entailed a significant resistance to expansion in the probe itself and required very careful calibration.

The Menard type tests were straightforward to perform and interpret. There was some scatter in the results, which may be related to variation in both cavity quality and soil properties, but in general a fairly consistent picture of the variation in soil properties was obtained. This relates to both horizontal stresses, yield and limit pressures and pressuremeter moduli.

The more advanced pressuremeter tests with volume controlled expansion of the probe and several unload and reload cycles were much more time-consuming. The tests can be rationalised considerably by running them with a computer-controlled electric motor instead of manually. A programme for this purpose has recently been presented by Holmén and Lindh (1999). The same type of results as for the Menard type tests was obtained when evaluating the new tests similar to the Menard procedure. An allowance for

rate effects had to be made for the evaluation of limit pressure and undrained shear strength.

The results from the unload-reload loops were fairly consistent, particularly when the stress and strain dependence was evaluated with the proposed alternative method. The unload-reload loops are performed to enable an evaluation of the properties in an overconsolidated range in a test cavity in which the effects of disturbance when creating the test cavity have largely ceased to affect the results. This goal was apparently achieved. Also the creep effects evaluated by keeping the pressure constant during the expansion of the probe yielded consistent results.

#### 4.4 SAMPLING

##### Open tube sampling

Sampling with the open tube sampler was a relatively simple operation in the two upper layers of clay till, although it required a considerable amount of equipment. In this case, a large hollow stem auger was used for predrilling to the sampling depth. This in turn required the use of a powerful drill rig. The sampling tubes were easily prepared from standard steel tubes and the adapter for the drill rods was a fairly simple construction. However, this required access to a well-equipped workshop.

The pressing down of the thin-walled tubes was also relatively easy until large objects, which buckled the cutting edge, were encountered. This effectively stopped the penetration and in most cases determined the length of the sample. Withdrawal of the sampler did not entail any problems with retaining the samples. Neither did sealing, transportation and storage of the samples within the steel tubes present any difficulties. The quality of the samples as judged by inspection both in the field and after extrusion in the laboratory appeared to be good.

The later extrusion of the samples required access to a workshop, where the buckled ends of the tubes were first sawn off. It then required a

rig with a powerful hydraulic jack in which the tubes were placed and fixed vertically and the samples pushed up and out of the tubes. Re-use of the sample tubes then required re-turning of the cutting edges in the workshop.

##### Core drilling

Core drilling was performed with a Geobor-S triple tube wire line system. The procedure followed the recommendations given by Johnsson et al. (1996) and experienced operators at Lund University. This made it possible to obtain a continuous core with 100 % recovery ratio. The operation was time-consuming and taking a 15 m long core through the layers of clay till and one metre into the bedrock occupied two full working days, including preparations and clean-up operations.

The quality of the cores was found to vary. The first disturbance effects during sampling were found in the uppermost 1 – 1.5 metres, where the drill bit apparently did not drill through all the large objects in the soil, but partly tore them loose and mixed them into the soil mass. The consistency of this part of the core was thus considerably softer than the rest of the profile. For the rest of the layer of Baltic clay till, the quality of the cores appeared to be good. In the mixed clay till with frequent layers and pockets of coarse material, the flushing medium appears to have caused erosion. In this material, there were a number of cavities and the large pores between the coarse gravel and cobble size particles were sometimes clean or only partly filled with finer material. In the North-east clay till further down, the sample quality appears to have been good.

The samples were brought up to the ground inside plastic tubes. These were pushed out of the encasing steel tubes on a horizontal working bench. During this operation and subsequent transfer to the transport vehicle, as well as transport and handling in the laboratory, it was almost impossible to fully protect the slender 1.5 m long plastic tubes from bending moments resulting from the weight of the core itself. The handling and transport of the cores in such a way that they

remained as undisturbed as possible was thus found to be a major problem and the degree to which this was successful is uncertain. Some development of the equipment and the handling and transport procedure is called for if the equipment is to be used regularly for taking undisturbed soil samples. However, for regular samples of rock and for soil samples used only for inspection and classification, this is not a great problem.

Also the core samples required access to a workshop where the plastic tubes could be split open and the cores parted into suitable lengths for specimen preparation.



## 5. Laboratory tests

### 5.1 ROUTINE TESTS

#### General

The routine tests and classifications performed in this project were intended as supplements to the previous investigations performed by Dueck (1995). Classifications and a detailed description of the soil profile were made on the continuous core taken with the Geobor-S sampler. Some additional determinations of the grain size distribution were also made in this context in order to verify the classifications based on inspection. Routine tests and detailed classification were also performed on all specimens in the triaxial tests. This was done to enable a comparison of the results with existing empirical relations based on parameters such as void ratio, clay content and water content. Also the specimens in the oedometer tests were classified and tested in regard to density and water content. With respect to the heterogeneity of the material, the tests were as far as possible performed on the bulk of the specimen. When it was necessary to part the specimen, care was taken to ensure that the tested soil was representative of the bulk of the material. The only exceptions were determination of liquid limit, where large grains shall be excluded, and determination of specific density, where the largest particles were also excluded.

#### Classification

The continuous core obtained with Geobor-S proved to be of varying quality. The first sample down to 1.5 metres depth appeared to be somewhat remoulded. At this shallow depth, the soil was less stiff and the effective stress level was probably insufficient to keep large particles in place and allow them to be drilled through. Instead, they appear to have been torn loose and remoulded into the more fine-grained soil matrix together with some of the flushing water. This

problem appears to have been restricted to the topmost metre in the soil profile and the samples are generally of better quality further down. However, problems with erosion of some of the material in the soil matrix were also detected in coarse gravelly layers further down in the profile.

The layering found in the profile in this point was according to *Table 3*.

Examples of the cores can be seen in *Figs 52 a-h*.

The profile is in general agreement with the picture of the layering in the test field found by Dueck (1995). As has been pointed out earlier, the detailed layering varies from point to point within the test field. Therefore, the profile found in the continuous core cannot be applied to the test results from the various other tests without considerable caution. A further classification of the soil in the test field was made for the samples taken with the tube sampler. These samples were taken at the test area, but the profile is not continuous and many details, in particular zones with coarse soils, are therefore left out. It should be noted that also this profile is not necessarily quite relevant for the adjacent tests within the test area. A further classification was therefore made on samples taken with a screw auger at the centre of each plate loading test after these tests had been completed. The results of these are shown together with the results of the load tests. For the other tests, the general picture will have to suffice.

However, the classification of the samples taken with the tube sampler is fully relevant for the other laboratory tests performed on these samples. The classification for the samples at this point was as follows, (*Table 4*):

Table 3. Classification of continuous core obtained by Geobor-S.

Depth, m	Classification
0-0.15	Dark-brown <b>topsoil</b> composed by organic silty clay with infusions of sand and gravel and a high content of plant remains
0.15-0.45	Dark-brown <b>topsoil</b> composed by organic silty clay with pieces of bricks and tiles and infusions of sand, gravel and plant remains
0.45-0.70	Yellow-brown rust-stained silty <b>clay till</b> with some root threads and gravel size particles
0.70-1.08	Yellow-brown silty <b>clay till</b> rich in gravel size particles of limestone and flint with small layers or pockets of sand and some root threads
1.08-1.23	Yellow-brown silty <b>clay till</b> with particles of limestone and flint
1.23-1.55	Brown-grey <b>clay till</b> with infusions of sandy clay till and small silt pockets, some root threads and rust stains.
1.55-2.2	Brown-grey <b>clay till</b>
2.2-2.4	Brown-grey <b>clay till</b> with a thin layer of clayey silt and small pockets of silt
2.4-3.75	Brown-grey <b>clay till</b> with significant content of grains of limestone
3.75-4.1	Brown-grey <b>clay till</b> mixed with layers of gravelly soil
4.1-4.2	Brown-grey <b>clay till</b>
4.2-4.6	Brown-grey <b>clay till</b> mixed with layers of <b>gravelly soil</b>
4.6-4.8	Brown-grey sandy silty <b>clay till</b>
4.8-5.0	Brown-grey somewhat clayey silty <b>sand</b>
5.0-5.1	Brown-grey sandy silty <b>clay till</b>
5.1-5.15	Brown-grey silty <b>sand</b>
5.15-5.32	Brown-grey sandy silty <b>clay till</b>
5.32-5.38	Grey mixture of <b>gravel</b> and cobbles from clay shale and crystalline rock
5.38-5.45	Grey gravelly sandy <b>clay till</b>
5.45-5.52	Grey <b>cobble</b> (covering the whole cross section of the core)
5.52-5.84	Grey gravelly sandy <b>clay till</b> containing a drilled through <b>slice of clay shale</b>
5.84-6.45	Dark-grey sandy gravelly <b>clay till</b> with cobbles/slices of clay shale. The gravel is a mixture of crystalline rock and clay shale particles, mainly the latter.
6.45-6.5	Black slice of <b>clay shale</b>
6.5-6.95	Dark-grey gravelly silty <b>clay till</b>
6.95-7.02	Black slice of <b>clay shale</b>
7.02-7.4	Dark-grey gravelly silty <b>clay till</b> with gravel and cobble size particles of mainly clay shale
7.4-7.5	Cobble of granite covering the whole cross section of the core
7.5-8.23	Dark-grey sandy silty <b>clay till</b> with layer of silty sand and infusions of cobbles of both clay shale and crystalline rock
8.23-8.53	Dark-grey sandy silty <b>clay till</b>
8.53-8.7	Dark-grey gravelly sandy silty <b>clay till</b>
8.7-9.0	Dark-grey sandy silty <b>clay till</b> with thin layers of silty sand and infusions of a sand pocket, gravel and cobbles of clay shale
9.0-9.65	Dark grey sandy gravelly <b>clay till</b> with infusions of cobbles and a small amount of lime
9.65-10.38	Dark-grey sandy silty <b>clay till</b> with a thin layer of sand and infusions of gravel size particles of clay shale.
10.38-11.9	Dark-grey sandy silty <b>clay till</b> with several, about 50mm thick, layers of sand and one layer with rounded gravel and cobble size particles of crystalline rock
11.9-12.0	Black slice of <b>clay shale</b>
12.0-12.3	Dark-grey sandy silty <b>clay till</b>
12.3-12.6	Dark-grey gravelly sandy silty <b>clay till</b>
12.6-13.4	Dark-grey sandy silty <b>clay till</b> with a small pocket of sand
13.4-13.7	Dark-grey sandy silty <b>clay till</b> with several thin layers of sand. Infusions of gravel size particles
13.7-13.85	Dark-grey gravelly sandy silty <b>clay till</b>
13.85-	Black <b>bedrock</b> of clay shale



a) core from 0 to 0.5 metre depth showing the transition from top soil to Baltic clay till



b) core from 1.7 to 2.3 metres depth showing homogeneous clay till



c) core from 3.9 to 4.6 metres depth showing clay till mixed with layers of gravelly soil



d) core from 5.3 to 5.8 metres depth showing gravel and cobbles in the mixed till layer



e) core from 5.9 to 6.5 metres depth showing sandy, gravelly till at the bottom of the layer of mixed till



f) core from 6.5 to 7.5 metres depth showing gravelly, silty clay till with cobble size particles at the top of the North-east till



g) core from 7.5 to 9.0 metres depth showing sandy, silty North-east clay till with infusions of cobbles

h) core from 13.6 to 14.8 metres depth showing the transition from North-east clay till to bedrock of clay shale



Fig. 52 Examples of cores from the test field at Tornhill.

Table 4. Classification of samples taken by tube sampler.

Depth, m	Classification
0.8-1.1	Fine sand
1.1-2.8	Sandy silty clay till with grains of limestone
2.8-3.3	Silty clay till with grains of limestone and infusions of small sand pockets
3.3-3.4	Silty sand with infusions of clay
3.4-3.7	Silty clay till with thin layers and small pockets of silt
3.7-3.85	Sandy silty clay till
3.85-4.25	Sandy silty clay till mixed with layers of gravelly silty sand
4.24-5.1	Silty clay till with grains of limestone
5.1-5.4	Sandy clay till
5.4-5.7	Sandy clay till with coarse gravel size particles

A comparison with the classification in the previous profile shows that the main layering is the same, although the levels and composition of various layers may differ somewhat and the presence of various sand and silt layers or pockets may only be very local.

#### Grain size distribution

The grain size distributions in the layers of clay till generally coincided with the bands for the different types of clay till presented by Dueck (1995). However, when the pockets and layers of sand, silt and gravel are considered, the bulk of the material becomes somewhat coarser. This should be taken into account when the average properties of the soil mass and larger specimens are considered.

#### Density

The densities were measured on the specimen for oedometer and triaxial tests and for the core samples also as an average for the whole length of the 1.5 m long samples. The test specimens had volumes of 115.45 and 314.16 cm<sup>3</sup> for the oedometer tests on 70 and 100 mm diameter specimens respectively. The volumes for the triaxial tests were approximately 500 and 1500 cm<sup>3</sup> for the 70 and 100 mm diameter samples, depending on the height of the individual specimen.

The measured densities in the upper two layers of clay till had a slightly higher average than in the previous investigations by Dueck: 2.18 t/m<sup>3</sup> compared to 2.13 t/m<sup>3</sup>. However, the scatter in the results was considerably less and it was also possible to discern a certain trend with a higher density around 2 metres depth, decreasing to a minimum at 3 m depth and then slowly increasing with depth, Fig. 53. The selected specimens from the continuous cores showed slightly lower densities than the specimens from the tube samples. However, this is probably a result of the selection of the specimens, in which particularly uniform fine-grained sections of the cores were chosen for testing. The average densities of the cores were fully compatible with those from the tube samples. The measured densities in the core samples of North-east till were approximately 2.42 t/m<sup>3</sup>.

#### Dry density

The dry density of the specimens was determined from the volume of the specimens before testing and the dry mass of the carefully collected material after testing. The corresponding variation was found in the measured dry densities, with an average value of approximately 1.85 t/m<sup>3</sup> in the upper two layers of clay till and 2.25 t/m<sup>3</sup> in the North-east till, Fig. 54.

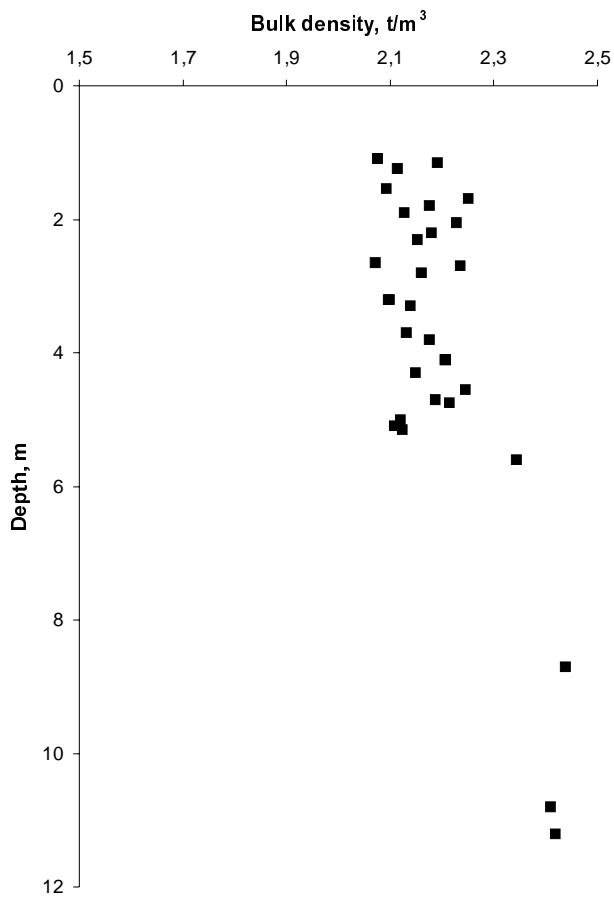


Fig. 53. Measured densities in the test specimens from the test field.

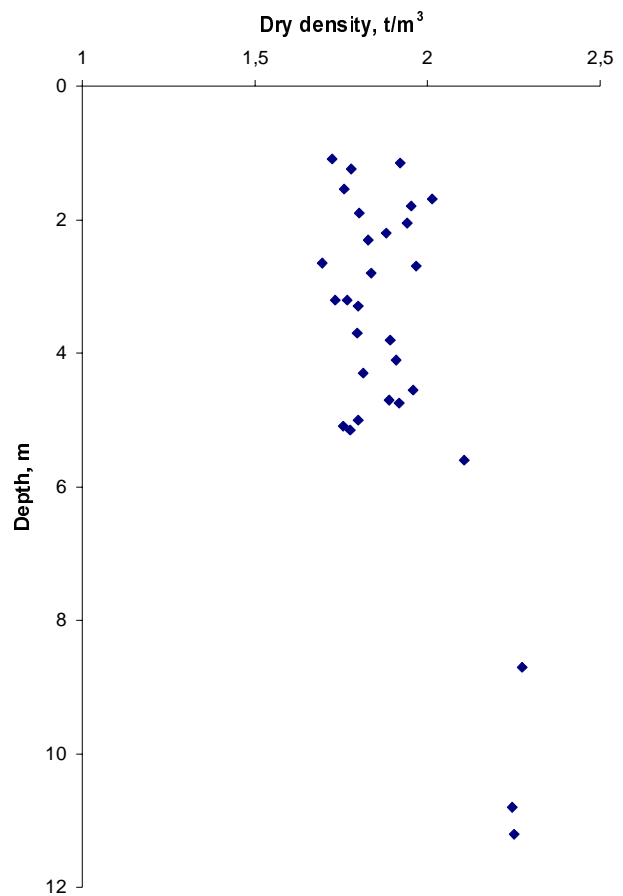


Fig. 54. Measured dry densities in the specimens from the test field.

### Particle density

The particle density was measured mainly on the finer part of the material, i.e. gravel size particles were not included. This is common practice when the results are intended to be used for evaluating grain size distributions from sedimentation analyses. The determinations were performed according to the Swedish standard method. The measured values ranged between 2.6 and 2.7 t/m<sup>3</sup>. No systematic variation with depth could be found within the investigated depth interval between 1.1 and 5.6 metres. The particle density varies with the mineral composition of the tested specimen. Since the coarsest particles were not included, the measured values may be somewhat misleading for the bulk of the material, particularly in the more gravelly specimen.

A special study was made on one of the specimen. This was first divided into different fractions and the particle density for each fraction was determined. For the finest material, where coarse sand and gravel size particles had been sorted out, a particle density of 2.68 t/m<sup>3</sup> was measured. When coarser sand particles were included, the value decreased to 2.66 t/m<sup>3</sup>. The average particle density for a large number of gravel particles was 2.68 t/m<sup>3</sup>. However, when the gravel particles were divided into different mineral groups, the particle densities varied considerably from about 2.49 t/m<sup>3</sup> in soft limestone/chalk to 2.76 in black crystalline rock. Harder limestone and clay shale had particle densities of 2.58 t/m<sup>3</sup> and 2.70 m<sup>3</sup> respectively. In order to obtain a correct value of the average particle density of the specimen, all particles would thus have to be included in the determination.

### Natural water content

The natural water content of the specimen was determined from the mass of the specimen before testing and the dry mass after testing. The scatter of the determined values is within almost exactly the same range as in the previous investigation, *Fig. 55*. The values from the specimens from the upper core samples are generally on the high side, but again this is probably a result of the selection of the specimens.

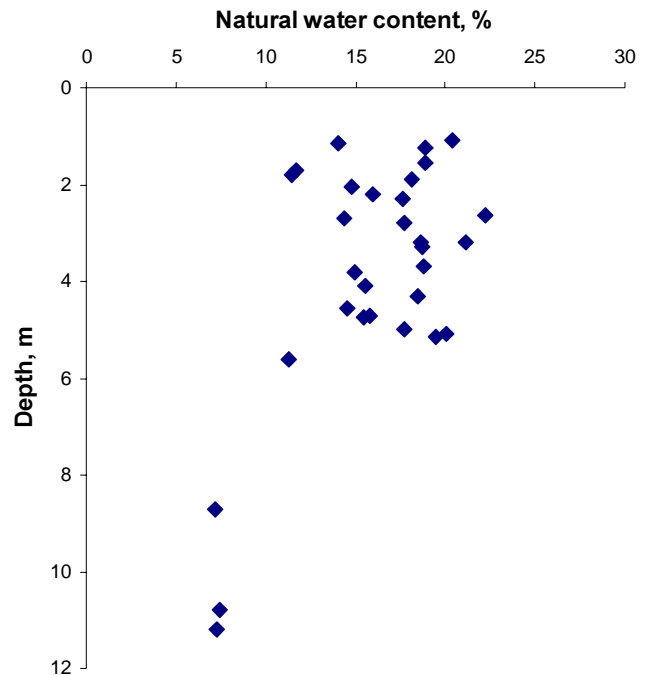


*Fig. 55. Determined natural water contents in the specimens from the test field.*

### Liquid limit

Only a few determinations were made of the liquid limit. The determined values all fell within the range of scatter in the previous investigations by Dueck (1995).

### Clay content

The clay content was determined for the triaxial test specimens. It was also determined for a number of specimens from the core samples in order to check the classification and for samples taken later by auger at the points where the load tests had been performed. A comparison with the data presented by Dueck shows that the clay contents are similar, *Fig. 56*. However, the values from the present investigation are generally on the low side and particularly the uppermost layers are considerably more sandy and less clayey than was found in the previous investigation. This can mainly be attributed to the local variation. The picture may also be somewhat affected by the sampling technique, since more of the coarse material may have been included in the samples taken by tube sampler than in those taken by auger.

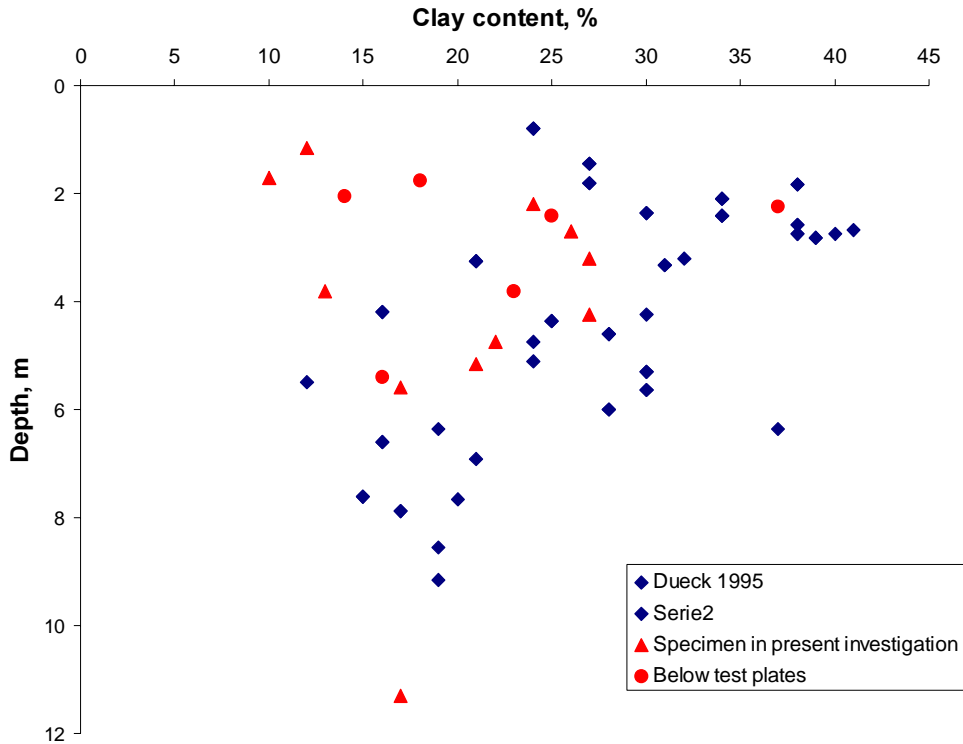


Fig. 56. Measured clay contents in specimen from the test field.

### Void ratio

The void ratio is calculated from the dry density and the particle density. The value of the particle density strongly affects the calculated void ratio. There are some doubts regarding the relevance of the determined particle density for the bulk of the material and the calculated void ratios may thus contain errors. The particle densities have therefore also been checked against the calculated saturation ratios as described below. When the calculated saturation ratios have exceeded 100 %, the particle densities have been increased somewhat, unless this in turn would yield unreasonable values in view of the soil composition and possible ranges. The void ratios for the specimens in the present investigation were similar but generally somewhat lower than in the previous investigation, Fig. 57. This is a combined result of slightly higher dry densities and somewhat lower particle densities in the present investigation.

### Degree of saturation

The degree of saturation is calculated from the dry density, the particle density and the natural water content. When calculated with the determined values for particle density, the degree of saturation in general was between 100 and 105%. There was one lower value and a few higher values. Saturation ratios higher than 100 % are impossible and indicate errors in the parameters used for the calculation. In this case, the particle density was considered as the value whose relevance might be questioned. Somewhat higher values of the particle density would yield saturation ratios of 100 % and this correction was applied for those specimens where the ratio was too high. This meant only a small correction for the majority of the determined values. However, since no particle density higher than 2.72 t/m<sup>3</sup> has been measured in this or previous investigations in this type of clay till, this value was used as an upper limit. The saturation ratios thus calculated were 100 % for the entire profile except for one specimen, in which the ratio was only about 90 %, Fig. 58. Half of this specimen con-

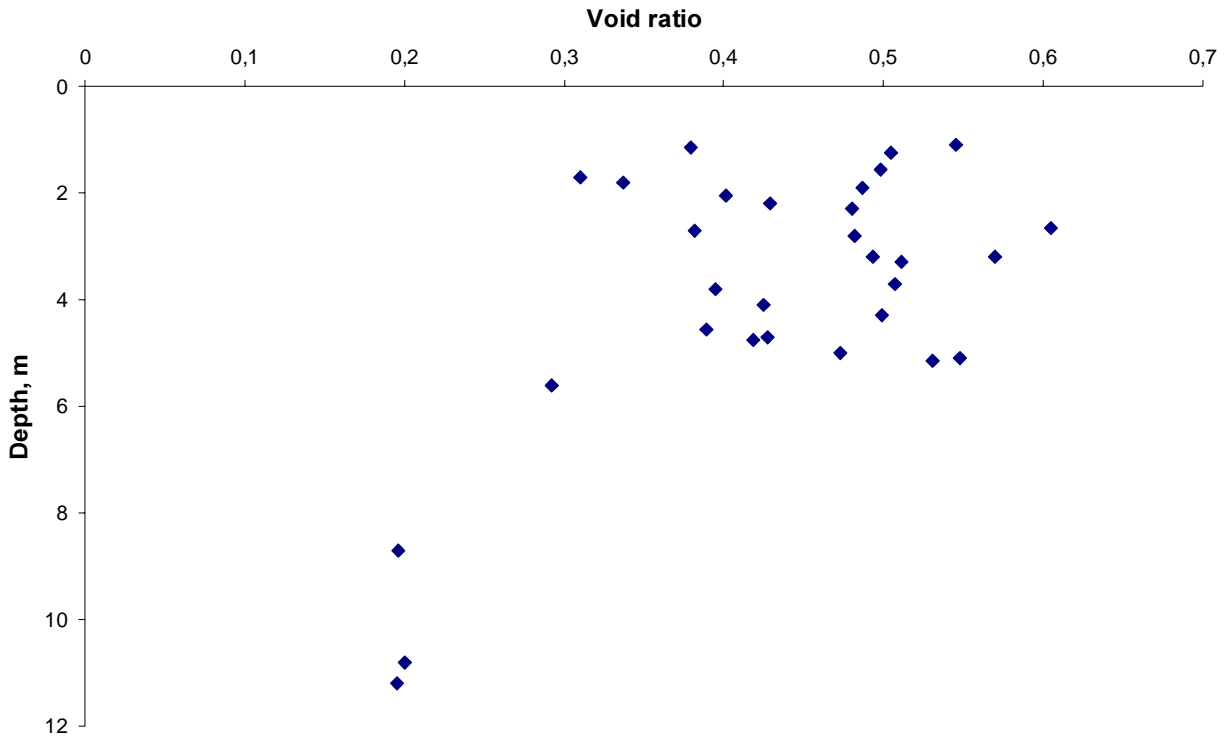


Fig. 57. Calculated void ratios in the present investigation.

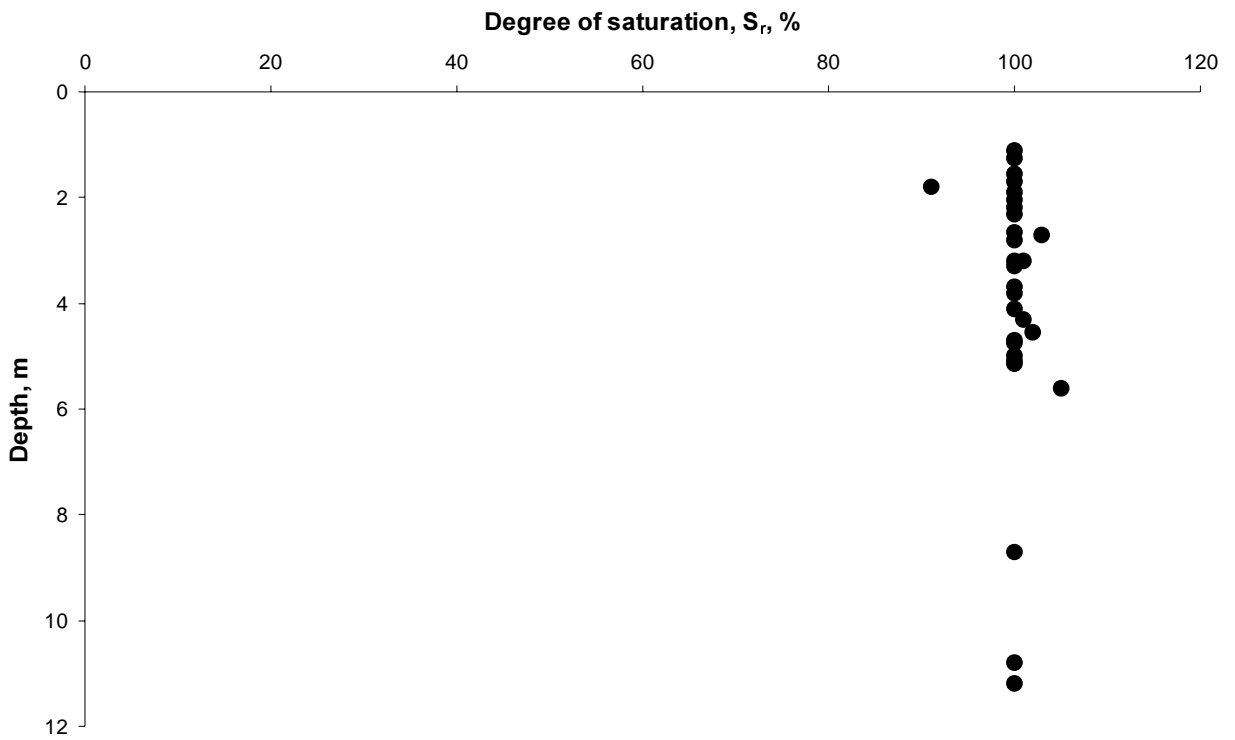


Fig. 58. Calculated degree of saturation.



sisted of sand and the capillarity of the sand was probably not high enough to fully retain the water when the specimen was pushed out of the sampling tube. At a few levels, the calculated saturation ratios are still slightly above 100%, which is believed to be related to other measuring errors. These values all relate to particularly low void ratios and the lower this ratio is, the more sensitive the calculated saturation ratio becomes to possible errors in the measurements of masses and volumes.

## 5.2 OEDOMETER TESTS

Oedometer tests were performed as incrementally loaded tests. For this purpose, two new oedometers were constructed, one for 70 mm diameter specimens and the other for 100 mm diameter specimens. The oedometer rings were thick-walled to prevent lateral expansion during the tests. The 70 mm diameter ring had a height of 30 mm and the 100 mm diameter ring a height of 40 mm.

The oedometer rings were fixed and drainage was provided at both ends of the specimen. The vertical compression of the specimen was measured by two transducers fixed on opposite sides on the ring to measure the penetration of the piston into the ring. Measuring errors arising from compliance of the apparatus were thus avoided. The loading of oedometers of this size could not be performed conveniently in the usual way with weights on balanced loading arms. Instead, two different types of pneumatic and hydraulic loading system were used.

The smallest oedometer used an existing loading frame, in which a regulated air pressure acts on a piston through a pair of bellows with very large area and thereby creates a very high and stable load. For the largest oedometer, a special loading system was constructed. In this assembly, a constant pressure device from Wykeham Farrance, originally intended for constant high pressure in triaxial cells, was used together with a high precision hydraulic cylinder. The hydraulic cylinder had a built-in return spring and a non-dismissive internal friction because of the necessary sealing.

This meant that it was relatively difficult to achieve exact predetermined load steps, particularly in the unloading-reloading loops. However, once a change in pressure had created a certain load, this remained very stable with time. The applied load was measured by load cells and recorded continuously throughout the tests in both arrangements.

For the smallest oedometer, the specimen was pushed directly from the sampling tube into the oedometer ring, which was lubricated internally with high pressure grease. The specimen was then cut off above and below the ring, and the end surfaces were carefully prepared to be smooth and flush with the ends of the ring. The oedometer ring was weighed before this operation and then again containing the prepared specimen. Smaller cavities from particles that had to be removed were filled in with as solid material as possible. In this process, some of the specimens had to be rejected because the cavities were too numerous and/or large and were thus expected to significantly influence the results. A new specimen was then prepared from the same sample tube. One tube from about 5.6 m depth had such a high content of gravel size particles that it was impossible to prepare a satisfactory specimen from the sample.

For the 100 mm oedometer, a uniform fine-grained part of the continuous core was selected and cut off. One end was then levelled sufficiently for the piece to stand steady and vertically, and the sides of the cylindrical sample were then carefully trimmed. This trimming was necessary since the shutter in the sampler creates fine grooves along the perimeter of the sample. The sample has a diameter of 102 mm and the trimming was thus limited to about 1 mm which is also sufficient to remove the grooves. The greased oedometer ring was then carefully threaded over the sample and the same procedure for preparing the end surfaces as for the smaller oedometer specimen commenced.

The oedometer ring with the specimen was then placed in the oedometer bowl on top of a dry

filter stone. A guide ring for the piston was fitted and the piston, also with a dry filter stone, was applied. The deformation transducers were fitted and the assembled oedometer was placed in the loading frame. The first load step was applied directly and water was then filled into the oedometer bowl until the specimen was fully submerged. The deformations were then studied and if there was any tendency for the sample to suck up water and swell, the load was increased to prevent this. The loading was then applied with a new doubled load step after approximately each 24 hours. At a load of about 90 % of the estimated preconsolidation pressure, an unloading cycle started with a reduction in the load of 50 % in each step down to the in situ effective vertical stress. From this point, the specimen was reloaded in the same sequence as the first loading up to the maximum stress well beyond any preconsolidation pressure. The maximum stress in the tests was between 3000 and 5000 kPa. As mentioned earlier, it was difficult to apply an exact predetermined load in the large oedometer, but the load actually achieved was measured by the load cell and achieving exactly doubled (or halved) load steps is not important.

A preconsolidation pressure was estimated before the tests on the basis of the results of the vane shear tests and the previously performed oedometer tests. This means that the preconsolidation pressures may have been exceeded before unloading in some of the tests. However, this has not obviously affected most of the evaluated parameters and it is possible to rectify the discrepancy for the others. The duration of each load step of 24 hours was followed in principle, but in some load steps, in particular directly after reversal of the loading procedure, it was possible to shorten this time since the primary deformations were soon completed and it was possible to extrapolate the small secondary creep effects with sufficient accuracy.

When evaluating a preconsolidation pressure, there should ideally be a distinct break in the stress-strain relation with a decrease in modulus when passing this yield stress. No such breaks

were obtained in the curves and the preconsolidation pressures had to be evaluated using less distinctive changes and less certain methods. Recommendations for evaluation of preconsolidation pressures in clay tills have been made by Jacobsen (1992) and Trankjaer (1996).

According to Jacobsen (1992), the preconsolidation pressure can be evaluated by the classical Casagrande construction using an additional auxiliary construction, *Fig. 59 a*. The stress-strain relation for the loading part of the curve is then plotted in log-linear scales. The ultimate straight line relation in this plot is never reached in the tests, but has to be constructed. This is done by adding a common value of stress,  $\sigma'_k$ , to all the points on the curve until this new stress-strain curve forms a straight line in the plot. The highest emphasis should then be put on the part for higher stresses to become a straight line. The preconsolidation pressure can then be estimated directly from

$$\sigma'_c = 2.5\sigma'_k$$

The straight line can also be used in a Casagrande type of evaluation. The point with minimum radius on the curve is then found at the effective vertical stress  $\sigma'_k$  and the preconsolidation pressure is found where the bisectrix of the angle between the tangent to the curve and a horizontal line from this point cuts the straight line, *Fig. 59 b*.

In international practice, the stress-strain curve is often plotted for the strains at 100 % primary consolidation, whereas in Sweden the strains at 24 hours after load application are used. Both approaches have been used for the tests in this project, but no apparent difference was obtained.

A further indication of the preconsolidation pressure can be obtained by studying the variation of the coefficient of secondary compression,  $\epsilon_s$ , in the tests. This value is then evaluated for each load step in the first loading and plotted against the applied load, *Figs 60 a and b*.

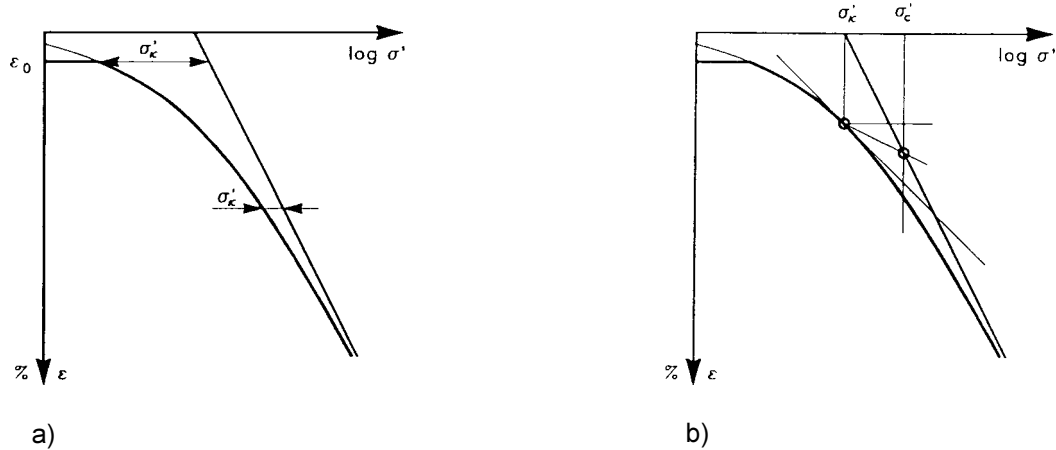


Fig. 59. Evaluation of preconsolidation pressure according to Jacobsen (1992)  
 a) Construction of the straight virgin compression line and evaluation of  $\sigma'_k$   
 b) Evaluation of preconsolidation pressure according to Casagrande with support from the previously constructed straight line and evaluated  $\sigma'_k$

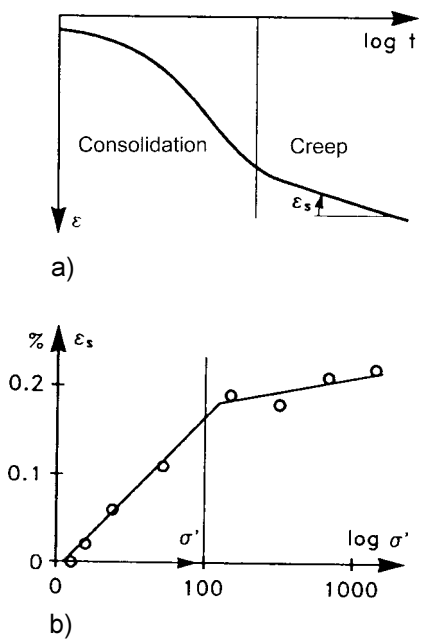


Fig. 60. Evaluation of preconsolidation pressure based on the variation in creep properties (Jacobsen 1992 based on Akai 1960).  
 a) Evaluation of coefficient of secondary compression.  
 b) Estimation of preconsolidation pressure based on the variation in creep rate.

The outcome of this method varies depending on the stability of the trends in the variation and the closeness of the nearest point to the preconsolidation pressure. In some cases, there was very good agreement between the preconsolidation pressures estimated in this and the previous ways, but in other cases the evaluation became very subjective, with a large possible interval due to the wide span between the doubled loads.

Trankjaer (1996) proposed a third method of interpreting the preconsolidation pressure. In this method, the variation of the modulus with vertical effective stress is studied. Ideally, a relatively high modulus should be measured as long as the soil is overconsolidated. At the preconsolidation pressure, there should be a decrease in modulus and for stresses above the preconsolidation pressure the modulus should increase almost linearly with the effective stress, Fig. 61. As mentioned, no such decrease in modulus was observed in the tests. The moduli for high stresses formed straight line relations with the effective stresses and the moduli at low stresses were higher than this relation. However, the evaluation of the point at which the relation connects to the straight line relation was very subjective. It could

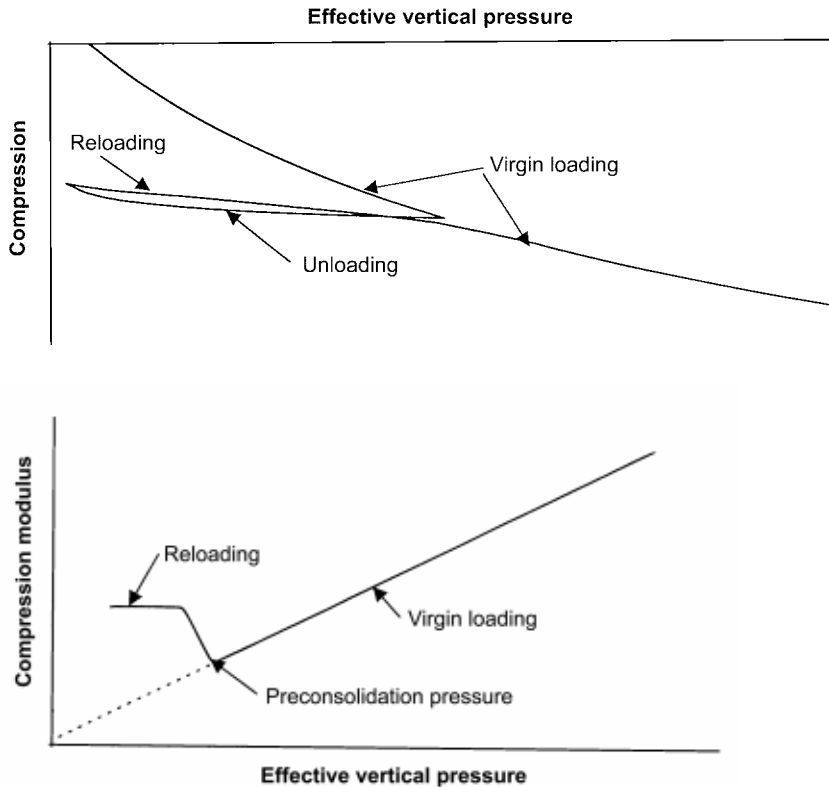


Fig. 61. Evaluation of preconsolidation pressure from variation in modulus, Trankjaer 1996.

in principle be estimated anywhere in the interval of doubled load between the last point with a modulus above the straight line relation and the first point on it.

All four types of evaluation were applied to the results of the oedometer tests and the evaluated values were weighted with the highest stress put on the first types of evaluation, Fig. 62.

The compression modulus varies with stress and depends on whether the soil is overconsolidated and in a reloading state or if it is normally consolidated and in a virgin loading state. For clays, the modulus in the virgin loading state is normally a linear function of the effective vertical stress,  $\delta M = M' \delta \sigma'$ . For coarse and stiff soils, the relation can often be approximated to  $M = M' \sigma'$ . This was also found in all oedometer tests in this project. The factor  $M'$  is a material parameter and varies with the type of soil, (Janbu 1970).

For determination of the modulus in the overconsolidated state, an unloading is performed from a stress just below the preconsolidation pressure to the in-situ effective vertical stress and the soil is then reloaded. The reloading modulus varies with the stress at which unloading starts and the stress to which unloading has been performed. It is therefore very important for these stresses to be correct if the reloading modulus, i.e. the modulus in the overconsolidated state, is to be evaluated directly from the curve.

A more general way of describing the modulus in the overconsolidated state is to make use of the empirical observation that the stress strain curve at unloading forms a straight line when the stress is plotted in a logarithmic scale, Fig. 63. The unloading modulus (or swelling modulus),  $M_s$ , can then be written as

$$M_s = \frac{\sigma'_v}{a_s}$$

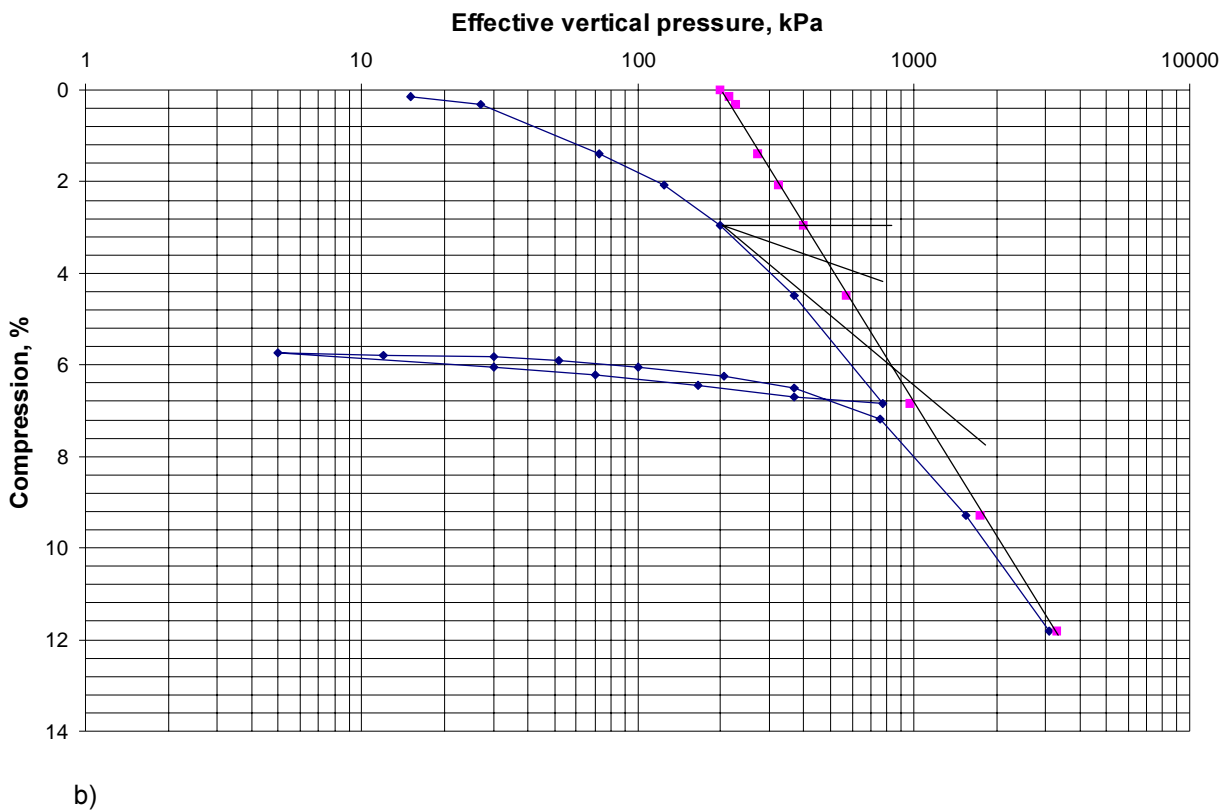
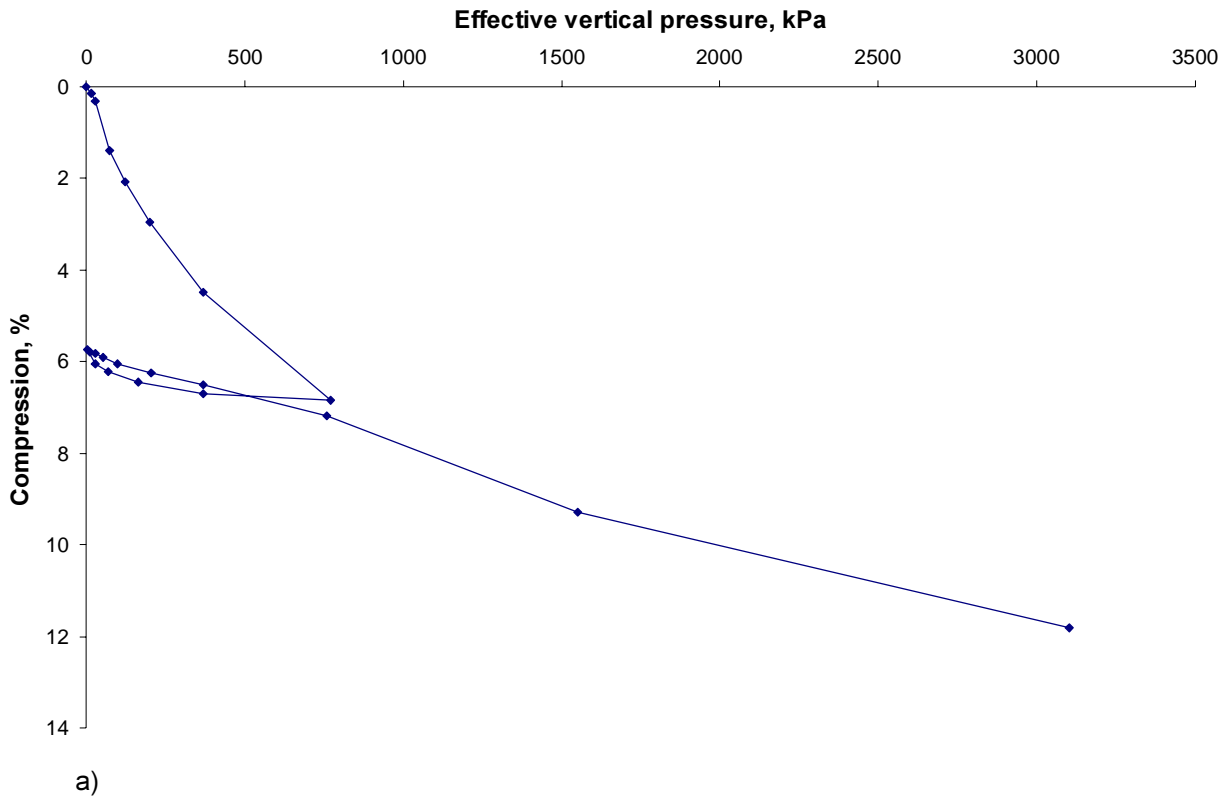
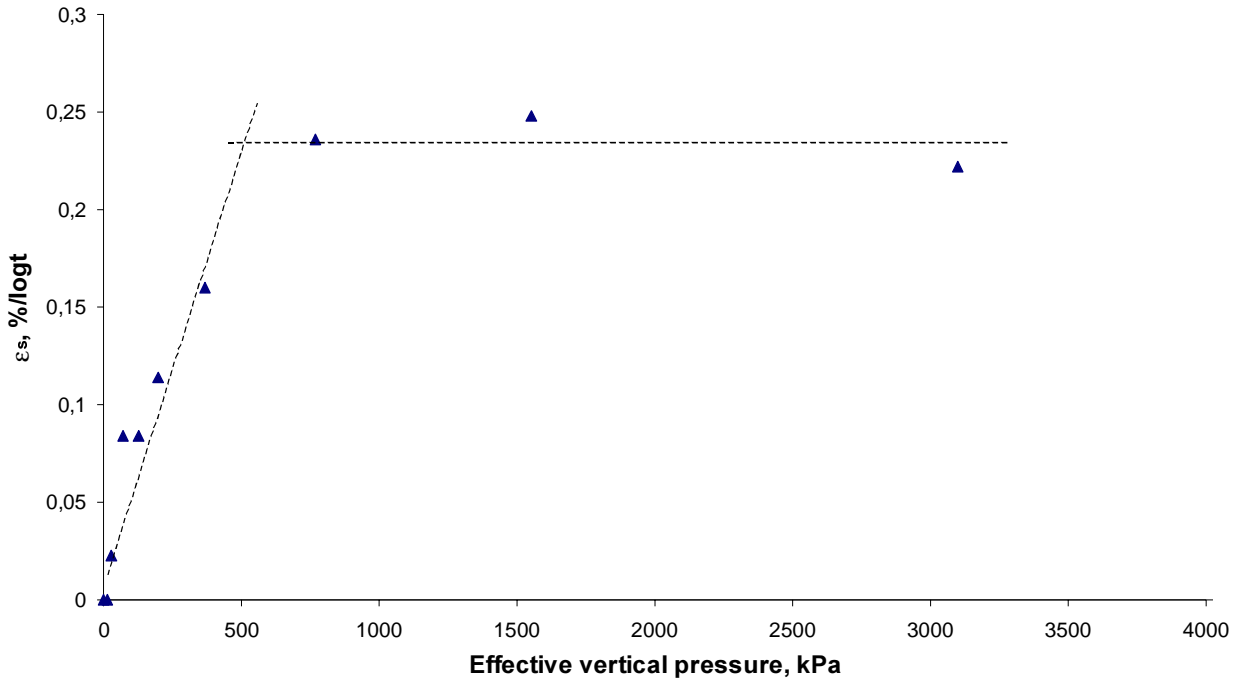
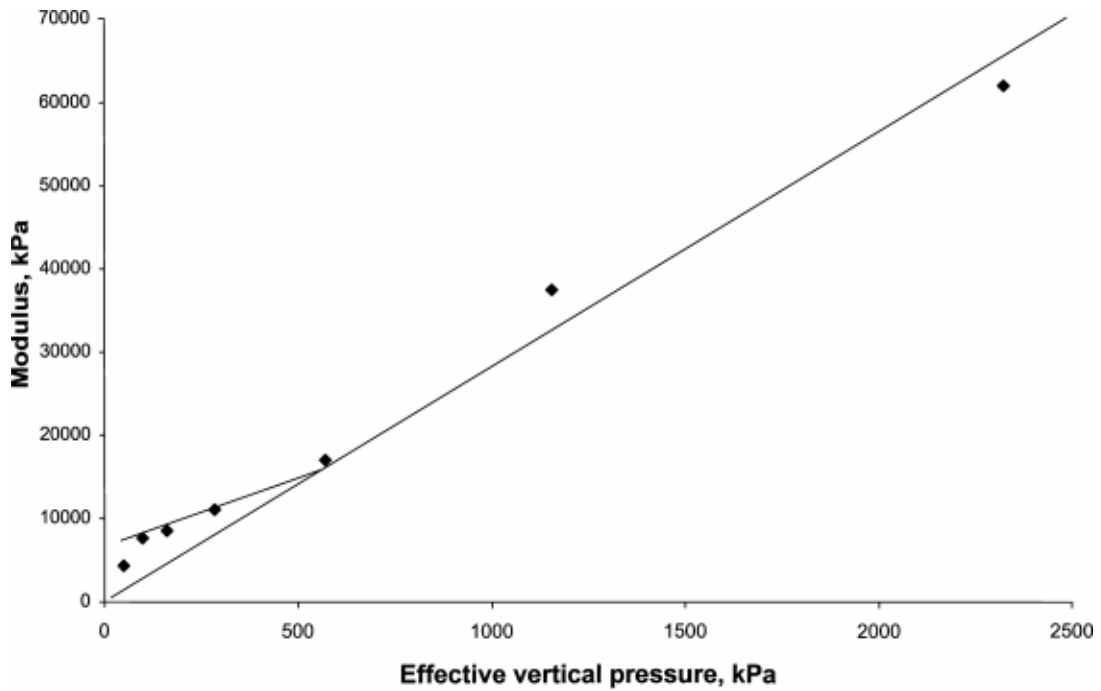


Fig. 62. Example of a result of an oedometer test on clay till, Tornhill 1.25m depth, 70 mm diameter.  
 a) Stress-strain curve in linear scales.  
 b) Stress-strain curve with stress in logarithmic scale and evaluation of preconsolidation pressure.



c)



d)

Fig. 62. c) Variation in secondary compression and evaluation of preconsolidation pressure.  
 d) Variation in modulus and evaluation of preconsolidation pressure.

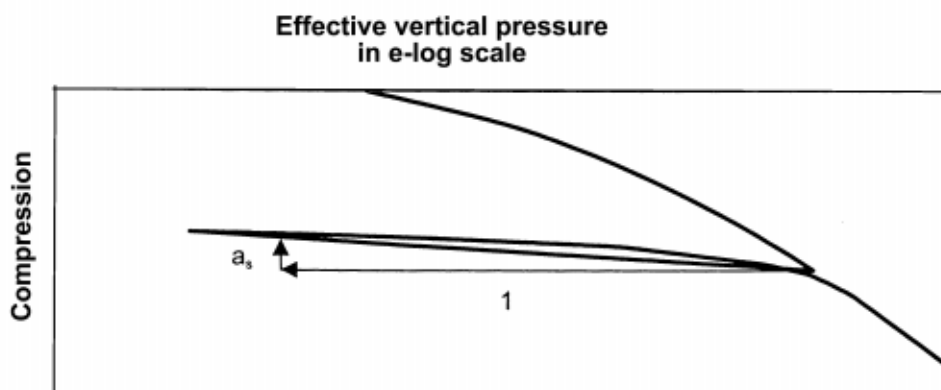


Fig. 63. Evaluation of the swelling index  $a_s$ .

The parameter  $a_s$  is the swelling index, which is a material parameter, (Larsson 1986).

At reloading, the stress-strain relation normally becomes a fairly straight line when plotted in linear scales, i.e. the modulus is almost constant, up to the point of unloading where the curve breaks and retains the relation for the first loading. If the swelling index is known, the swelling and the reloading modulus can thus be calculated for any case of unloading and reloading. Because of creep effects, the swelling does not start immediately when the stress is lowered below the preconsolidation pressure and the reloading curve does not pass through the point on the virgin compression line at the preconsolidation pressure where the unloading started. The cross-over point between the unloading and reloading curves occurs at the same strain as when unloading started, but at a pressure  $b\sigma'_c$ , where  $b$  is  $\leq 1$ .  $b$  is a material parameter which is close to 1 in coarse materials such as sand and gravel, but decreases with decreasing average grain size and increasing plasticity to about 0.8 in clays. It is about 0.9 in silts and most clay tills, and this value was found to be relevant also in the present tests.

The recompression modulus,  $M_{rl}$ , after a soil has been unloaded from the preconsolidation pressure,  $\sigma'_c$ , to a pressure  $\sigma'_{min}$  can thus be calculated from

$$M_{rl} = \frac{b\sigma'_c - \sigma'_{min}}{a_s \ln\left(\frac{b\sigma'_c}{\sigma'_{min}}\right)}$$

In some cases, particularly when the unloading has been performed to effective stresses close to zero, the recompression curve has been found to deviate significantly from the straight line relation. Also the modulus at reloading then has to be expressed as a function of stress. However, this was not found in the present series of tests.

If the unloading has started just below the preconsolidation pressure and been performed to the in situ vertical stress, the reloading modulus evaluated directly from the curve and the calculated modulus should coincide. However, the results will be different if a) the preconsolidation pressure has been misjudged prior to the test and unloading has started at higher or lower stresses than the appropriate, and b) it has been difficult to unload to the exact in situ stress, as in the case of the larger oedometer. Fig. 64 shows the directly measured values compared to those calculated using the evaluated preconsolidation pressures and swelling indexes. As can be seen, there is general agreement, but in some cases the corrections for different stresses are relatively large.

Apart from the oedometer tests in the present investigation, test results have also been reported by Dueck (1996). These results have been inter-

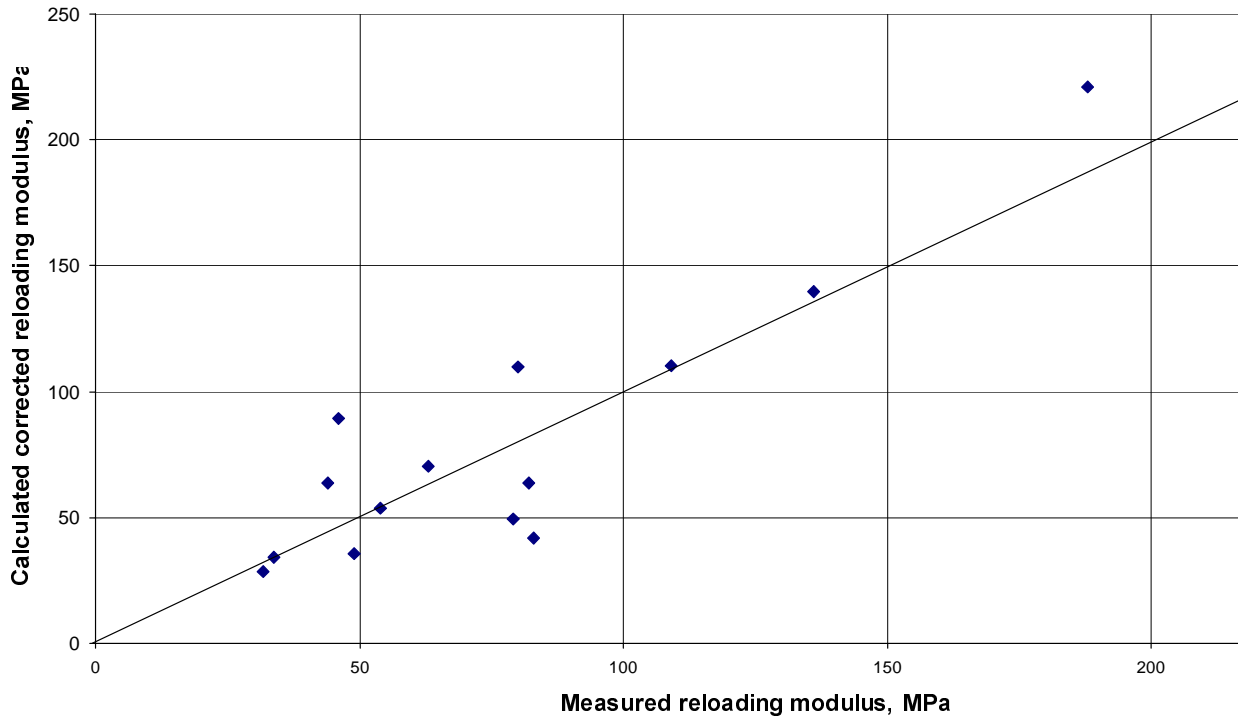


Fig. 64. Comparison between measured and calculated reloading moduli.

preted in the same way and yielded corresponding ranges of possible preconsolidation pressures. The average values obtained by the methods described above are included for purposes of comparing and supplementing the general picture.

The evaluated preconsolidation pressures form a consistent picture with a preconsolidation pressure of 600–700 kPa in the stiff layer of Baltic clay till at approximately 2 metres depth, decreasing to 400–500 kPa in the mixed till below and then increasing as the boundary to the North-east till is approached, *Fig. 65*.

The values are fairly consistent, but should be seen as minimum values since the sampling must be expected to have caused some disturbance. Even if consistent, the values are still only about 50–70 % of those evaluated empirically using the Danish relation with the field vane

$$\sigma'_c = \sigma'_0 \left( \frac{\tau_v}{0.4\sigma'_0} \right)^{1/0.85}$$

where  $\tau_v$  is the undrained shear strength measured by the vane and  $\sigma'_0$  is the effective overburden pressure.

The preconsolidation pressures evaluated from the specimen taken with the Geobor-S sampler are considerably lower in the uppermost part of the profile. This is related to the excessive disturbance caused by this sampling technique in the part of the profile with very low effective stresses. These values have therefore been disregarded. At greater depths, the quality of these samples improves. However, no tests were performed on specimens from this sampler at depths greater than 3.2 metres since it was not possible to find sections of the cores down to 6 metres depth that were sufficiently free from coarse gravel size particles to prepare specimens for the large oedometer.



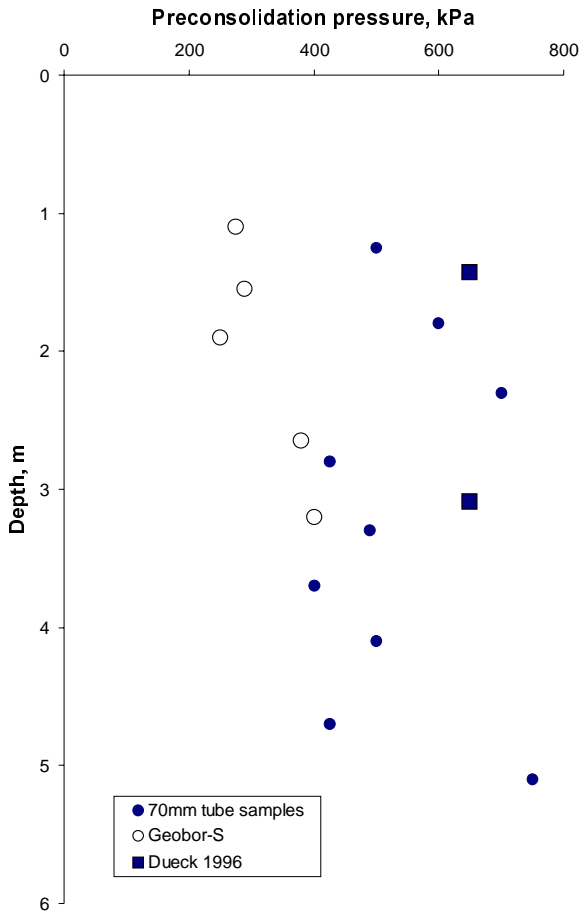


Fig. 65. Evaluated preconsolidation pressures from oedometer tests in the Baltic and mixed clay tills.

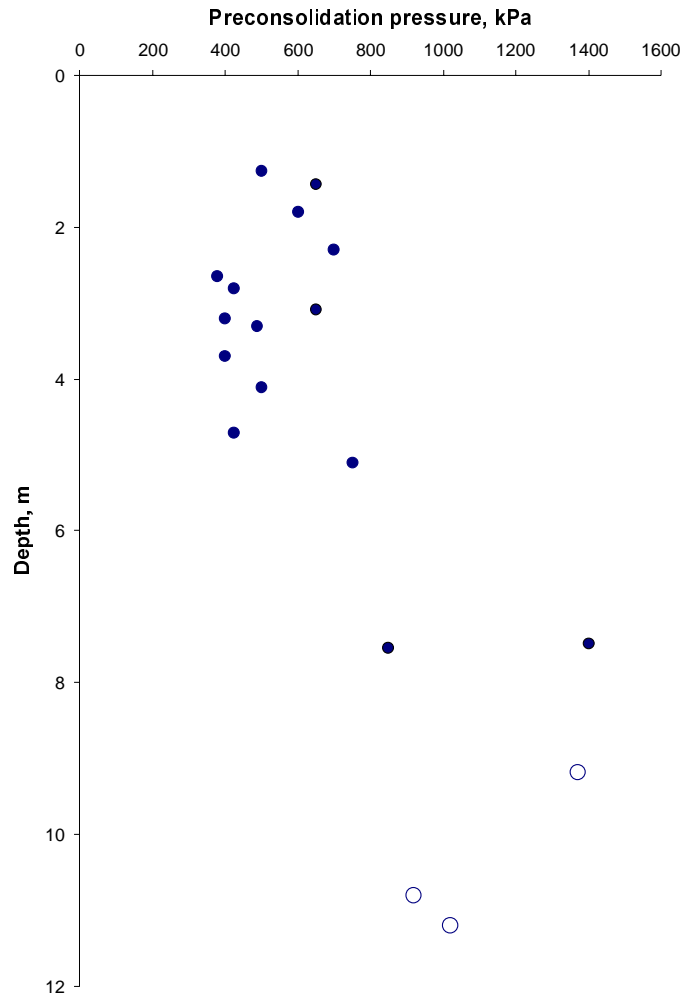


Fig. 66. Evaluated preconsolidation pressures for the soil profile at Tornhill. Filled symbols represent oedometer tests and open symbols data estimated from triaxial tests.

For the North-east till, there are only results from two oedometer tests reported by Dueck (1997). The results from these two tests differ widely. There are also results from three triaxial tests in which the specimens were consolidated for stresses lower than the preconsolidation pressure. When using the above empirical relation applied to the measured strength in relation to the consolidation stress, additional indications are obtained of the possible level of the consolidation pressure in the North-east till. The average of the data indicates a preconsolidation pressure of about 1100 kPa in this till, Fig. 66.

The modulus numbers,  $M'$ , are approximately 30 in the upper two layers of till, Fig. 67. The variation relates to the composition of the individual specimen. The values from the tests on the core samples are thus generally among the lowest, since the specimens were prepared from selected, homogeneous, fine-grained parts of the cores. The highest values are found for specimens rich in gravel size particles and specimens containing layers or pockets of sand. With regard to composition, all measured values fall within the range proposed by Janbu, (1970). Since the specimens are not fully representative of the more coarse-

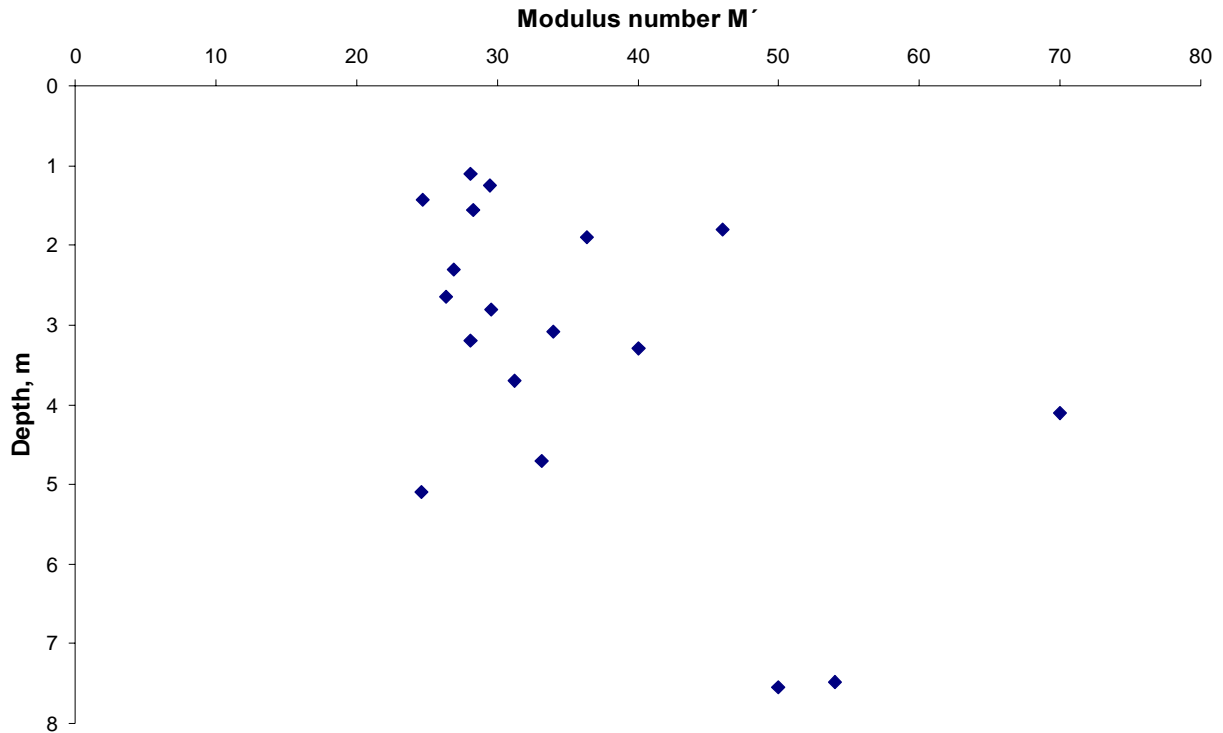


Fig. 67. Evaluated modulus numbers from the oedometer tests.

grained parts of the profile, a slightly higher average modulus number of 35, for example, would be more representative of the bulk of the upper two layers of clay till. The corresponding values from the two oedometer tests in the coarser North-east till are approximately 50.

The swelling index,  $a_v$ , also depends on the composition of the soil: the coarser the material, the lower the swelling index. A tentative relation between the swelling index and the average grain size,  $d_{50}$ , was presented by Larsson (1986). According to this relation, swelling indexes between 0.1 and 0.7 %, with an average of 0.3 %, might be expected for the grain size distributions measured in the profile. From the tests, swelling indexes between 0.08 and 0.65 % were evaluated, with an average of 0.27 %. The lowest values were obtained in specimens containing layers or pockets of sand. A more detailed comparison cannot be made since the grain size distributions for the individual oedometer specimens were not determined.

### 5.3 TRIAXIAL TESTS

The triaxial tests in this project were primarily performed on the samples from the tube sampler. This is because these samples, based on the results from the oedometer tests, were judged to be of better quality in the upper layers and also because some erosion appeared to have occurred in the core samples from the coarser layers further down. A small number of additional tests were performed on samples from the cores in the North-east till, which were judged to be both of better quality and the only type of samples available for this type of material. The triaxial tests previously performed by Dueck (1997) were all performed on specimens taken with the Geobor-S sampler.

Most of the new tests were performed as consolidated undrained tests with a relatively high back-pressure. The high back-pressure was not primarily required for saturation, since the specimens were fully saturated in their natural condition, but to ensure that no negative pore pressures would

develop during the tests. The previous tests by Dueck were performed according to Danish practice as  $CU_{u=0}$  tests, in which the pore pressure is zero throughout the test and the volume of the specimen after consolidation is kept constant through regulation of the cell pressure.

The specimens were pushed out from the sampling tubes and the end surfaces were prepared in the same way as the oedometer specimen. For the core samples, a uniform part of the core was selected after the tube had been split and the core was then parted and the specimen lifted out. No trimming of the sides was performed and generally there were no cavities that had to be filled in. The intended height of the specimen was twice the diameter, but the final height was often considerably shorter because of large gravel size particles encountered in the intended end surfaces.

The base pedestals and the top caps in the triaxial apparatuses were supplied with polished stainless steel plates in order to reduce the end friction. An arrangement recommended by authors such as Lacasse and Berre (1988) and DeGroot and Sheahan (1995) was used with greased rubber

membranes between the specimen end surfaces and the polished steel plates, and with filter paper strips on the specimen periphery in contact with ring-shaped filters at the rear of the polished plates, *Fig. 68*.

The specimens were first consolidated for a vertical stress of about 90 % of the preconsolidation pressure evaluated from the oedometer tests with a  $K_0$  value of 0.5. The consolidation was performed stepwise and during this process a check was made to ensure that the axial and volumetric strains were small and compatible. The strains at the end of the consolidation were typically about 2 %. In a few of the tests, the strains tended to be excessive at the end of the consolidation and the final stresses were then slightly reduced.

After the first consolidation, the samples were brought back to in situ stresses. According to the test results, the horizontal stresses are higher than the vertical stresses in the field. The stresses in the triaxial tests were therefore brought back to isotropic stress conditions corresponding to the estimated horizontal stresses. No attempt was made to create a condition with lower vertical stresses since this was expected to create more problems than benefits.

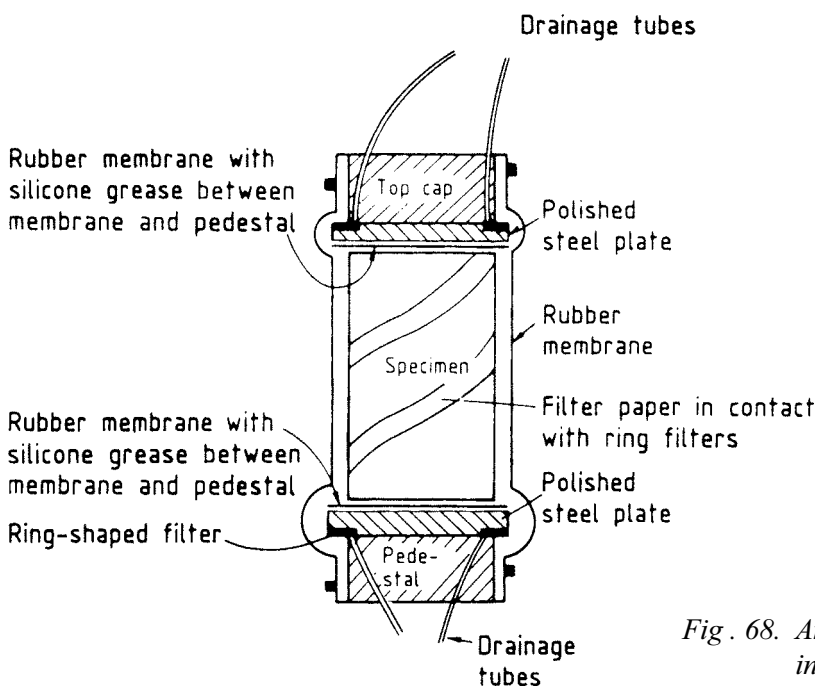


*Fig. 68. Arrangement for reducing end friction in triaxial tests*

After the consolidation stages, the specimens were subjected to compression tests with constant rate of axial deformation. The undrained tests were performed with the normal rate of deformation of 0.6 %/hour and the drained tests were run ten times slower to ensure full drainage. These rates are more or less standard rates in the SGI laboratory. The rates were also checked against estimated coefficients of consolidation to ensure that they would provide the required degrees of pore pressure equalisation and excess pore pressure dissipation respectively.

The undrained tests were run to an axial compression of 15 %. At this strain, all the samples except one had passed failure or asymptotically approached an end value. All the samples also showed a pronounced dilatant behaviour. No peak strengths were developed in the tests. After an initial stiff response in approximately the first 0.5 % of axial compression, where the pore pressure increased, there was a significant change in the stress-strain curve with a much slower increase in shear stress with strain and the pore pressures started to decrease. This decrease in pore pressure continued until both the stress-strain and the pore pressure-strain relations had asymptotically reached their end values, *Fig. 69*.

The corresponding stress-paths showed a steep rise towards the failure line within the first “elastic” part of the test and just after yield attained a straight line relation corresponding to the failure conditions in terms of fully mobilised effective shear strength parameters, *Fig. 70*.

The arrangement for reducing end friction appeared to perform well since uniform specimens deformed in a uniform way, i.e. they remained as straight cylinders for most of the tests. In some cases, single shear planes developed at the very end of the tests well after the maximum shear stress had been reached. However, the “frictionless” end surfaces were no guarantee for a uniform deformation of the specimen. Several specimens contained layers of different materials and the deformations after yield then became concentrated to the weakest of these layers, *Fig. 71*.

Some specimens also contained single large gravel particles located asymmetrically in the specimen. This eventually led to tilting of the specimen, causing it to partly slide off the end plates. This also facilitated the formation of a single shear surface at the end of the test.

The measured undrained shear strengths varied in the same way as the preconsolidation pressures, *Fig. 72*. The measured undrained shear strength was thus about 175 kPa in the Baltic clay till, decreasing to about 120 kPa in the mixed clay till and then increasing in the transition to the North-east till. The only exception to this picture was a specimen from 3.8 m depth. This specimen contained an unusually high amount of sand and gravel size particles and was very close to the boundary of what should be classified as clay till. The shear stress continued to increase and the pore pressures to decrease also at large strains, and no end value seemed to be approached within the testing range. The specimen deformed in a fairly uniform manner, but at the end of the test, coarse particles could be seen to protrude from the soil mass and the specimen had started to tilt, *Fig. 73*. Results from the triaxial tests performed by Dueck (1997) have been included for comparison. These tests were carried out for a different purpose and somewhat different consolidation stresses were therefore used, which may have affected the results to some degree. Only tests in which the preconsolidation stresses have not been exceeded during the consolidation have been included.

A comparison has been made between the measured shear strengths and empirically expected strengths with consideration to preconsolidation and overconsolidation ratio.

TRIAXIAL TEST

Tornhill				Date	2000-08-31
				Project No	1-9905-310
Bore hole	Depth	Designation		Approved by	
1	2,2 m	Clay till			
Test date	Height	Type of test	Drainage conditions	Consolidation stresses	
2000-03-21	139,8 mm	Active	Undrained	$\sigma'_1$	60 kPa
Performed by	Diameter	File name		$\sigma'_2$	50 kPa
LMO MLU	69,8 mm	L-315f.tri		Pore pressure 300 kPa	
Remarks					

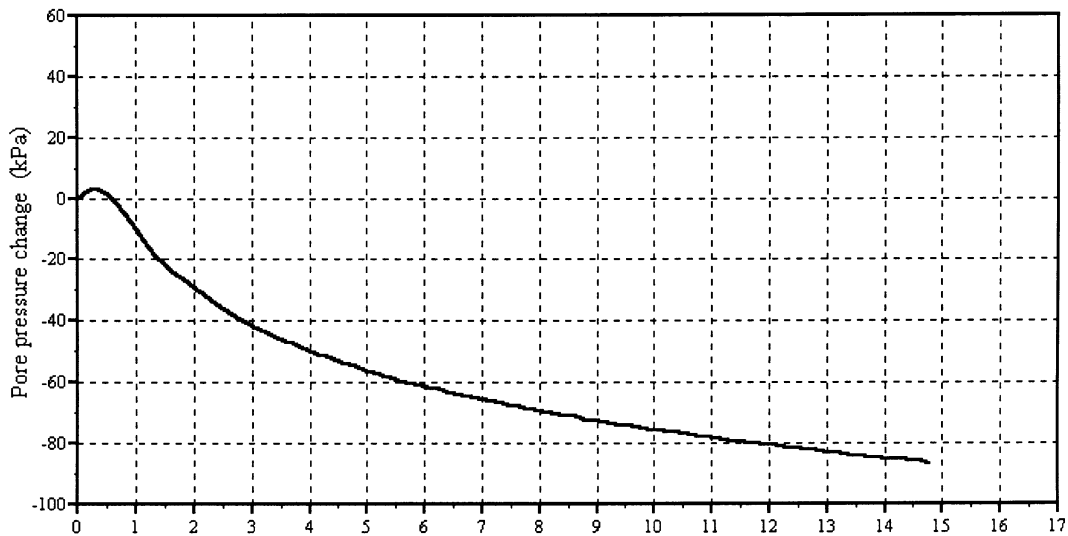
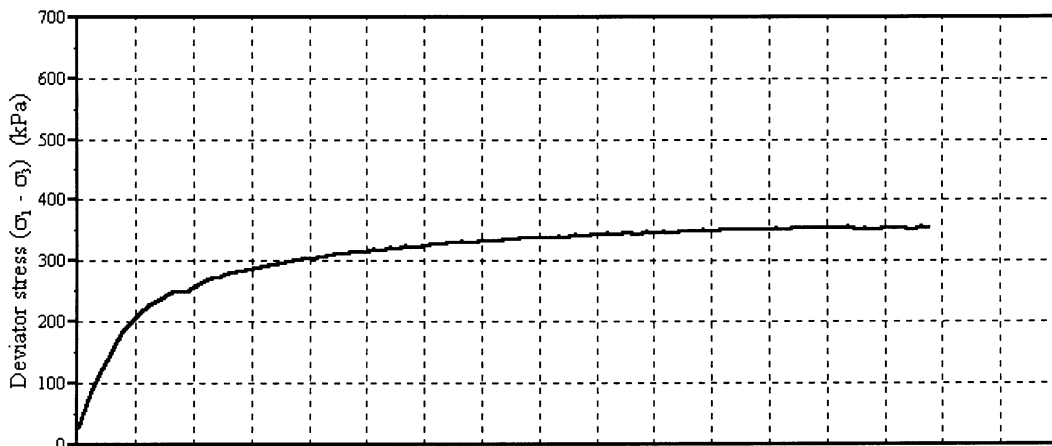


Fig. 69. Example of a result from an undrained triaxial test on clay till from Tornhill

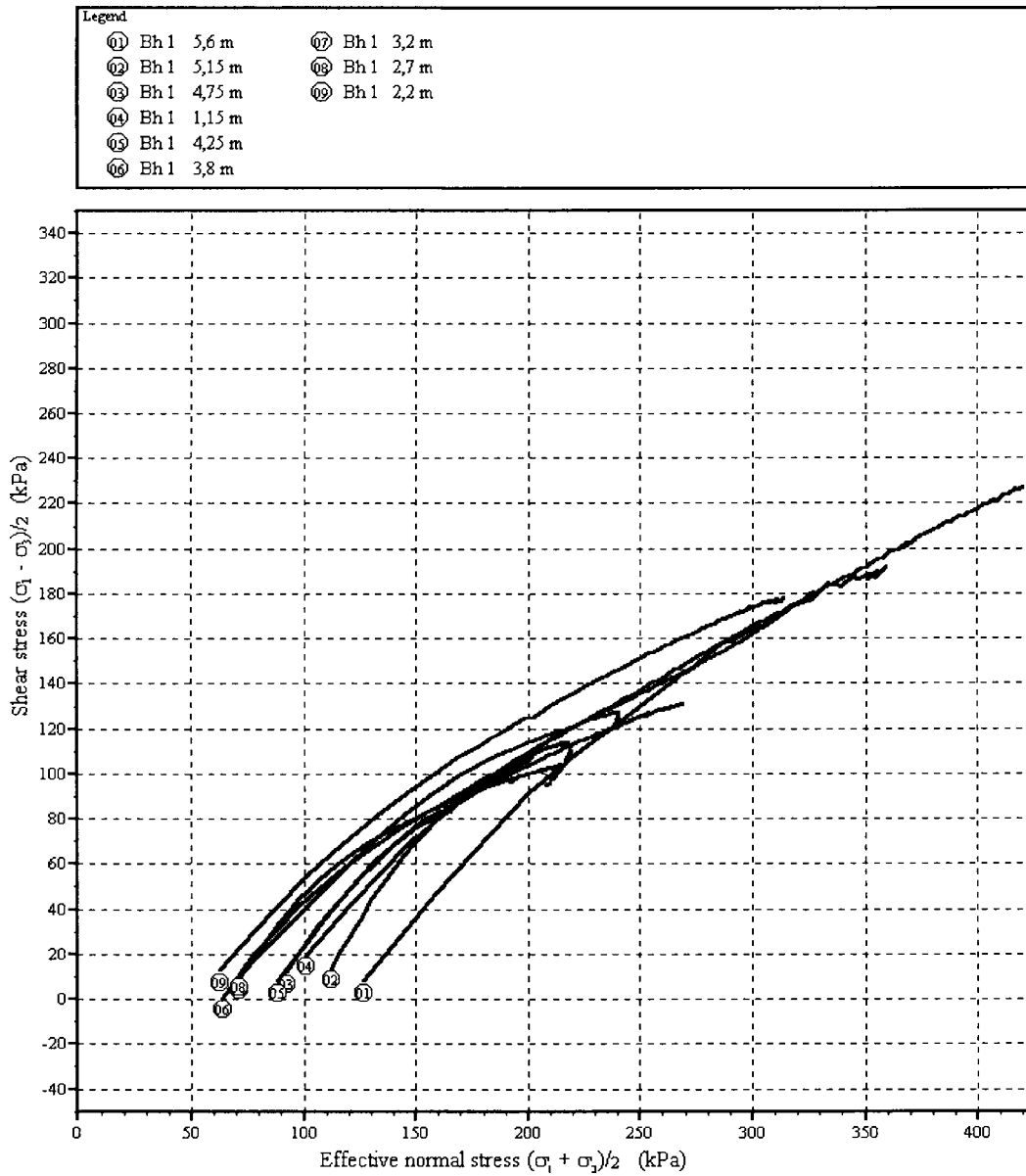


Fig. 70. Stress paths from the undrained triaxial tests in Baltic and mixed clay till.



Fig. 71.  
Two-layer specimens  
after testing.

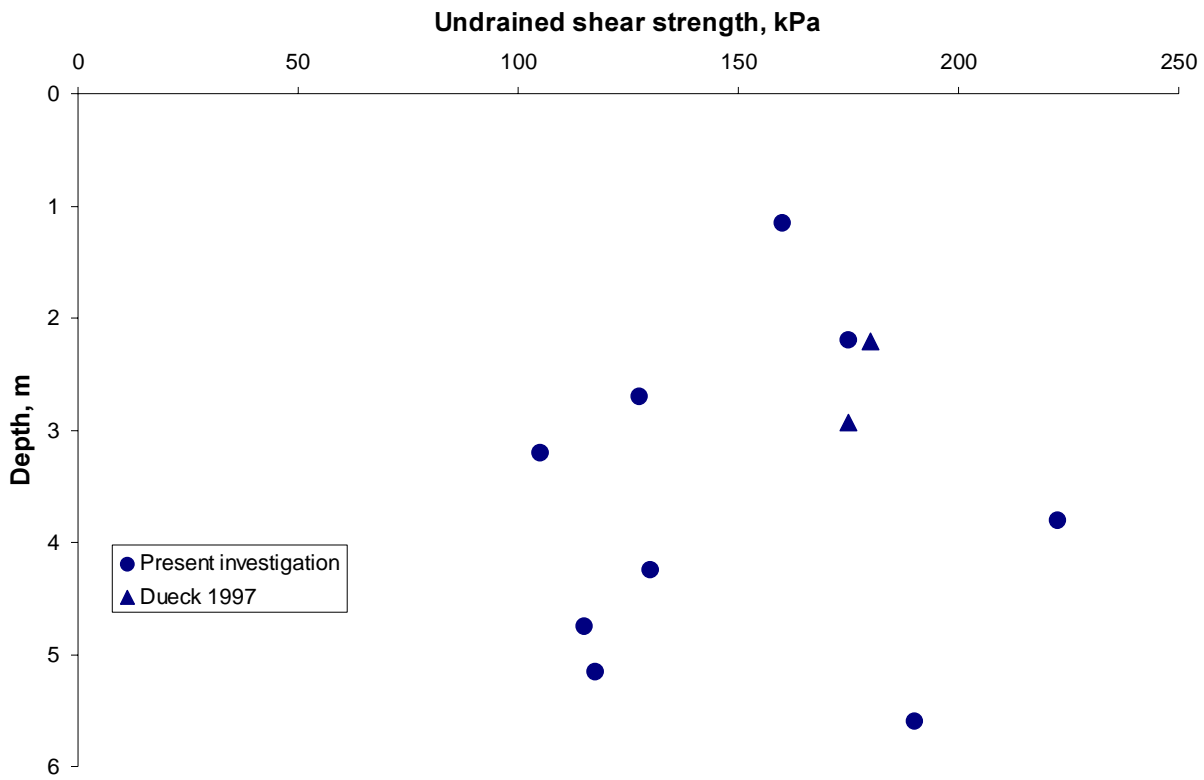


Fig. 72. Measured undrained shear strengths  
from the triaxial tests



Fig. 73.  
The specimen from  
3.8 metres depth  
after testing.

According to Danish experience, (Steenfelt and Foged (1992), the undrained shear strength,  $c_u$ , can be evaluated from

$$c_u = a\sigma'_{v0}OCR^\Lambda$$

The exponent  $\Lambda$  is assumed to be 0.85, which is a fairly normal value also for other types of clay. The normal value of  $a$  is given as 0.4.

A back calculation has been made of the value of  $a$  using the consolidation stresses and the imposed overconsolidation ratio in the first step of the consolidation together with the measured undrained shear strength and the value 0.85 for  $\Lambda$ . This gives an average value of  $a$  of 0.41, excluding the odd value for 3.8 metres depth, Fig. 74. The measured strength values are thus to

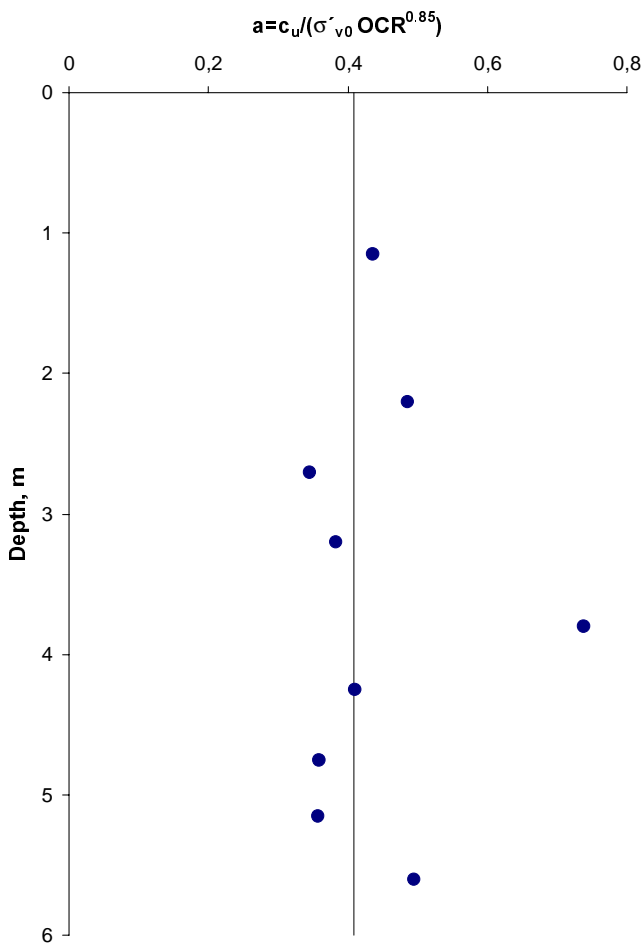


Fig. 74. Estimation of factor  $a$  from the triaxial tests.

be considered as normal for the stress history. In Danish practice, the above relation is often used to estimate the preconsolidation pressure using undrained shear strengths from field vane tests. The specimens are then reconsolidated for 90 % of this pressure before being brought back to the in situ stresses and tested. This procedure, if applied in the present project, would most probably have resulted in very good correspondence between the strengths measured in the field vane tests and the triaxial tests. However, it would also have led to excessive strains during consolidation and would not have yielded an independent measure of the strength based on “undisturbed” sampling and laboratory testing. The estimation of the shear strength would then in both cases be based mainly on the results of the field vane tests.

There is thus a considerable difference between the shear strengths as measured by triaxial tests in the laboratory using results from oedometer tests for determination of stress history and the shear strengths measured by field vane tests in the field. This difference may be attributed partly to disturbance of the samples during sampling, transport and handling, and partly to uncertainties in the evaluation of the oedometer tests. However, it is difficult to estimate the degree to which the difference can be attributed to the respective cause and the exact relevance of the results from the field vane tests.

The additional triaxial tests on North-east till were performed on specimens consolidated for effective stresses corresponding approximately to the in situ stresses. The specimens were thus not initially reconsolidated to estimated preconsolidation stresses. A similar test had also been performed by Dueck (1997). The results from these tests yielded undrained shear strengths between 550 and 825 kPa. These values may be considered to be on the low side since a proper reconsolidation had been omitted. The only type of available reference data consists of the results of the dynamic probing tests, which indicated undrained shear strengths of about 1000 kPa throughout the layer of North-east clay till.



The effective strength parameters were estimated from the stress paths. The stress paths for all the tests in the Baltic and mixed clay tills formed fairly straight line relations for the failure states, with inclinations corresponding to a friction angle of  $30^\circ$ , Fig. 70. The variation could mainly be interpreted as a variation in the effective cohesion intercept  $c'$ . In the tests on North-east till, the stress paths indicated friction angles of  $32-33^\circ$ .

In Swedish practice, the cohesion intercept  $c'$  for clay is normally evaluated empirically from the preconsolidation pressure or the undrained shear strength as  $0.03\sigma'_c$  or  $0.1c_u$ . A comparison between the evaluated values of  $c'$ ,  $c_u$  and  $\sigma'_c$  from the laboratory tests in the present project yields the average relations  $c'/\sigma'_c = 0,027$  and  $c'/c_u = 0,08$ , Fig. 75. There is a considerable spread in the measured relations, but the common relations

appear to be useful also for a rough preliminary estimate in these types of clay till.

Two different sets of empirical relations have previously been elaborated for clay till to link the undrained shear strength, the effective friction angle and the cohesion intercept with other soil properties. These are the Danish Jacobsen (1970) and the Swedish Hartlén (1974) relations. According to Jacobsen, the shear strength properties can be estimated from the void ratio  $e_k$ , ( $\approx e_0$ ), using the formulas

$$c_u = 10 \cdot e^{(0,77 \cdot e_k^{-1,2})}, kPa$$

$$c' = 430 \cdot e^{(-7,3 \cdot e_k)}, kPa$$

$$\phi' = 35,3 - 9 \cdot e_k, ^\circ$$

$e$  = the base of the natural logarithm, (= 2.718)

The corresponding, more elaborate formulas proposed by Hartlén take both void ratio, water content,  $w_\rho$ , and clay content,  $l_c$ , into account. The clay content is calculated from material passing the 20 mm sieve.

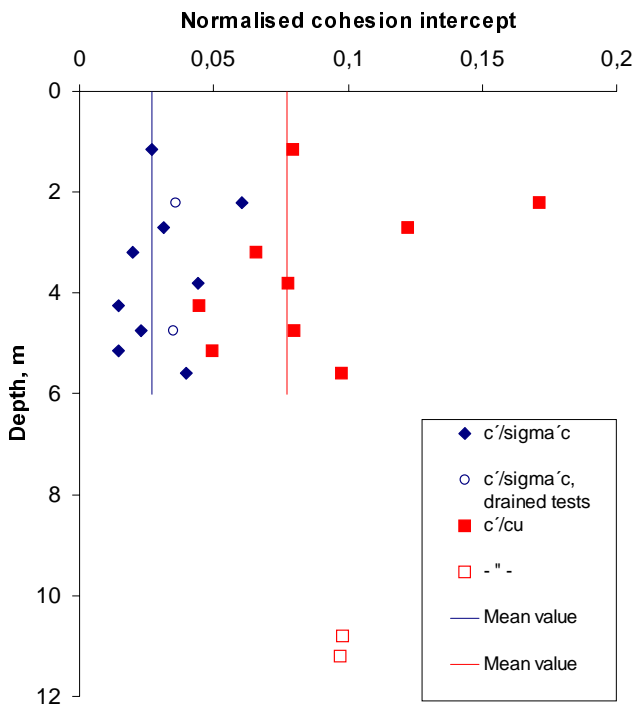


Fig. 75. Relations between effective cohesion intercept, preconsolidation pressure and undrained shear strength measured in the laboratory tests on clay till from Tornhill.

$$c_u = 18 \cdot w_0^{-2.05} \cdot e_0^{-1.88} \cdot l_c^{2.66}, kPa \quad c_u \leq 200kPa$$

$$c' = 3 \cdot w_0^{-3.23} \cdot e_0^{-2.12} \cdot l_c^{4.19}, kPa \quad \text{if } c' \leq 20kPa$$

$$c' = -24 - 140 \cdot \log w_0 - 80.9 \cdot \log e_0 + 155 \cdot \log l_c, kPa \quad \text{if } 20kPa < c' \leq 50kPa$$

$$\phi' = 22 \cdot w_0^{0.166} \cdot e_0^{-0.139} \cdot l_c^{-0.311}, ^\circ \quad 24^\circ < \phi' < 33^\circ$$

A comparison with the measured values shows that the empirically estimated undrained shear strengths in the Baltic and mixed clay tills are generally lower than the measured values, *Fig. 76*. This is in spite of the fact that the values measured in the triaxial tests may already be considered to be on the low side. For the North-east till, the strengths estimated with Hartlén's relation were about the same as the measured values. However, this relation is not intended for such high strengths. In this till, Jacobsen's relation yields values about four times greater than those measured in the tests.

A comparison between measured and estimated values of the effective cohesion shows that the values estimated by Jacobsen's relation are generally about twice as great as the measured values. Hartlén's relation yields values with about the same average trend as the measured values, but the scatter is high, *Fig. 77*. The two highest values from the North-east till are actually above the range for Hartlén's relation, which is intended only for values up to 50 kPa.

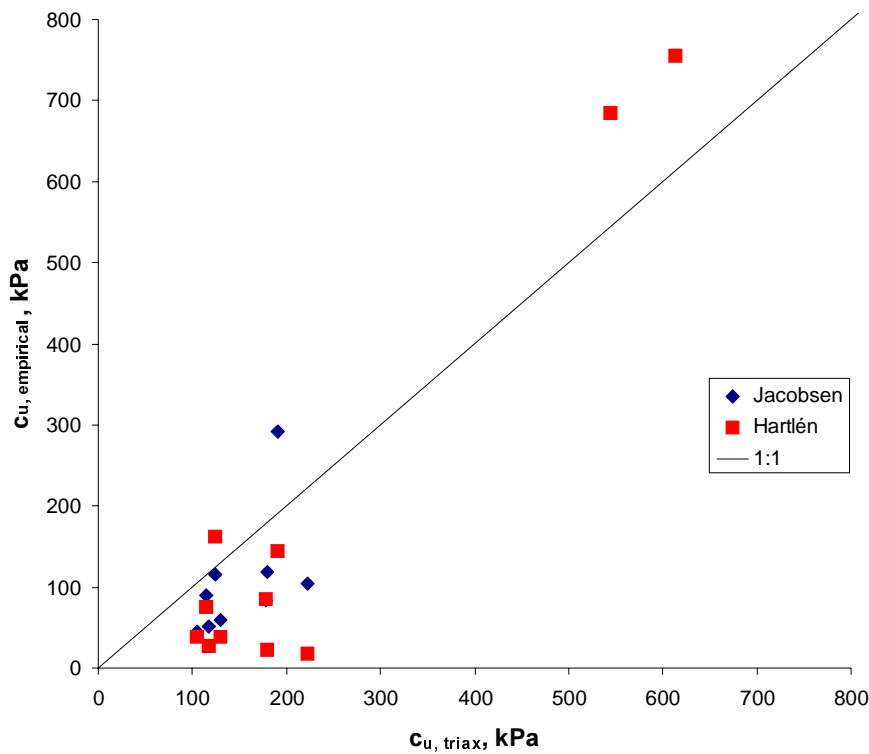


Fig. 76. Comparison between undrained shear strength measured in the laboratory and empirically estimated values. (Values for the North-east till estimated by the Jacobsen relation are omitted because they are far outside the ranges of the plot).

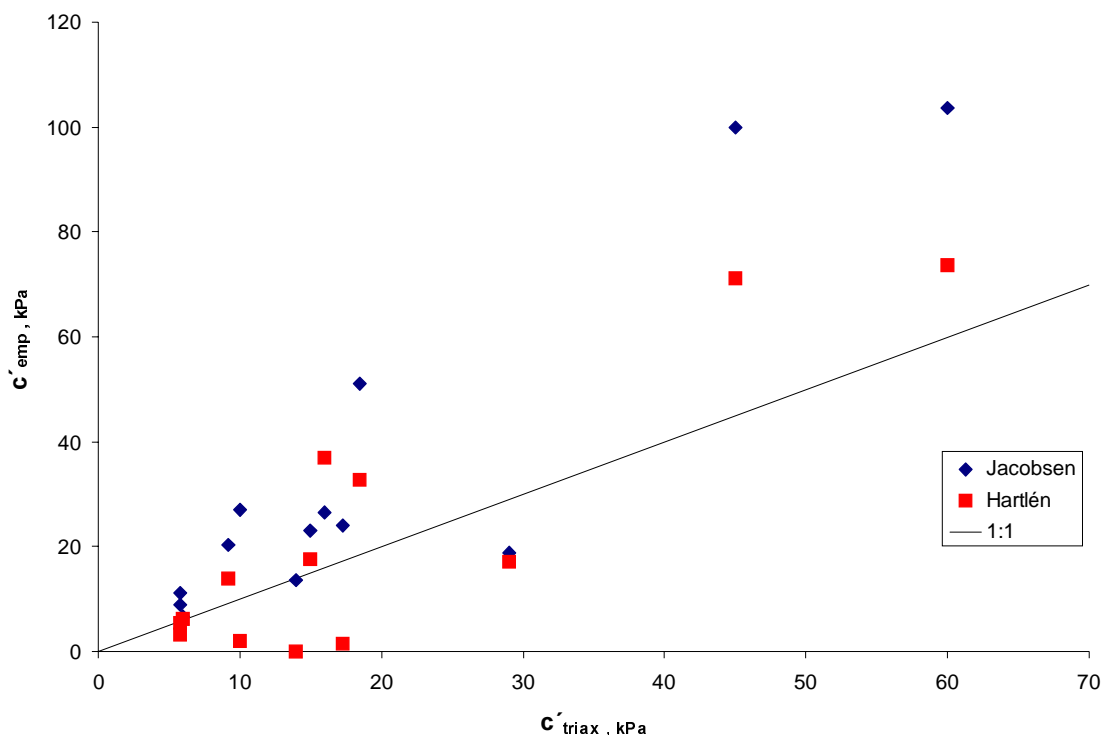


Fig. 77. Comparison between effective cohesion intercepts measured in the laboratory and empirically estimated values.

The span for the measured friction angles was very narrow,  $30^\circ$  in the Baltic and mixed clay tills and  $32^\circ$ – $33^\circ$  in the North east till. The ranges for the estimated friction angles were also very narrow,  $30^\circ$  to  $33.5^\circ$  for Jacobsen's relation and  $30.5^\circ$  to  $33^\circ$  for Hartlén's relation. However,  $33^\circ$  is the upper limit for Hartlén's relation and this had to be applied for most of the tests. In this way, a fairly good correlation was obtained, with slightly higher estimated values than those measured, Fig. 78.

The general outcome of this comparison is that the accuracy of both types of empirical estimations proposed for clay till was poor. The empirical relation proposed by Hartlén and which has been extensively used in this part of south-west Sweden yielded values of the undrained shear strength which in general were too low. The scatter in the relation between measured and estimated effective cohesion was larger than for the simple relation normally used for clays in Sweden and the more elaborate estimation of the effective friction angle did not improve the simple as-

sumption of a constant friction angle of  $30^\circ$  in Swedish clays.

The drained triaxial tests were performed mainly in order to check the relevance of the effective strength parameters evaluated from the undrained tests also for drained conditions. Three such tests were performed as supplements to the undrained tests. However, one of the specimens buckled at an early stage in the test and thus only two of the results are relevant. The stress strain curves from these tests also showed a dilatant behaviour after a small deformation with elastic compression. The maximum rate of dilation then occurred at a relatively small axial deformation and the maximum value of shear stress was reached within 3 % of axial deformation. The tests were terminated after 5 % axial deformation and the deformations up to this point were uniform, with the specimens remaining as straight cylinders.

The specimens in the two tests came from different levels in the Baltic and mixed clay till, but the

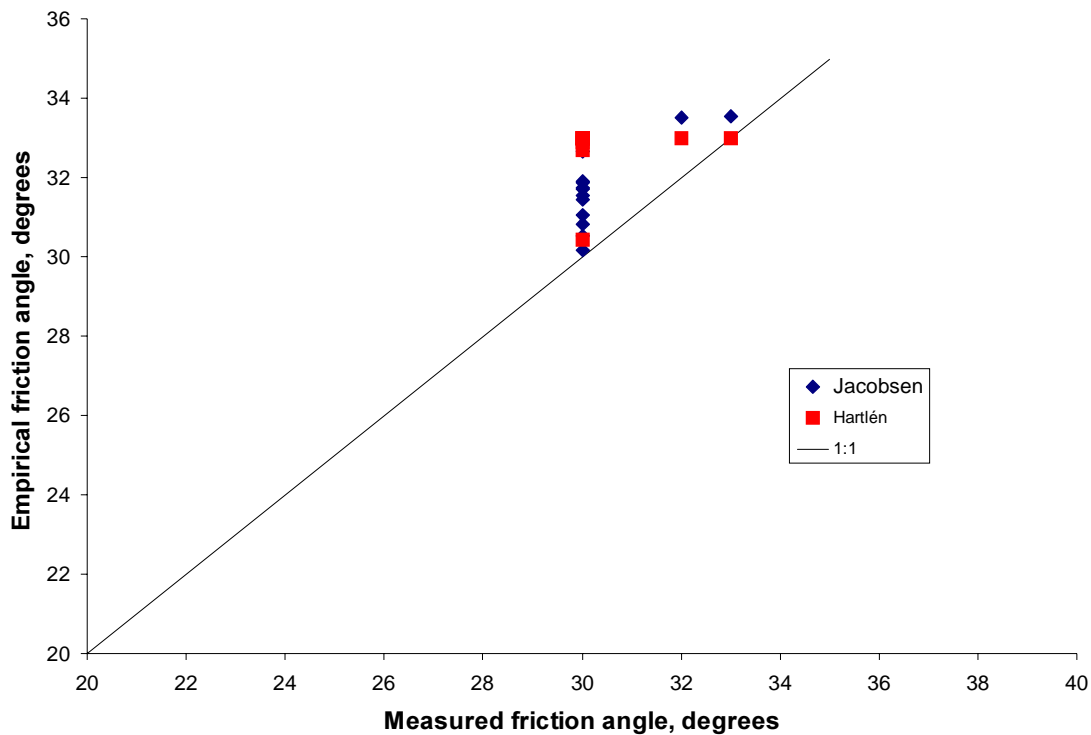


Fig. 78. Comparison between effective friction angles measured in the laboratory and empirically estimated values.

preconsolidation pressures were about the same. Two options of interpretation were possible, either connecting the two failure points and evaluating parameters  $c'$  and  $\phi'$  disregarding the difference in material, or assuming the friction angle to be  $30^\circ$  and evaluating parameter  $c'$  only. In this case, the choice did not make any difference. The evaluated friction angle was  $30^\circ$  and the cohesion intercepts 14 and 15 kPa. The normalised cohesion intercepts are shown together with those from the undrained tests in Fig. 75 and no significant difference can be observed.

### Moduli from triaxial tests

The modulus of elasticity was evaluated according to Duncan and Chang (1970). In this procedure, the secant modulus is continuously evaluated as

$$E = \frac{\sigma_1 - \sigma_3}{\epsilon_1}$$

The inverse of the modulus,  $1/E$ , is then plotted against the axial strain,  $\epsilon_1$ , and the parameters  $E_0$  and  $b$  are evaluated, Fig. 79.

The secant modulus for any strain level can then be estimated from

$$E = \frac{E_0}{1 + bE_0\epsilon_1}$$

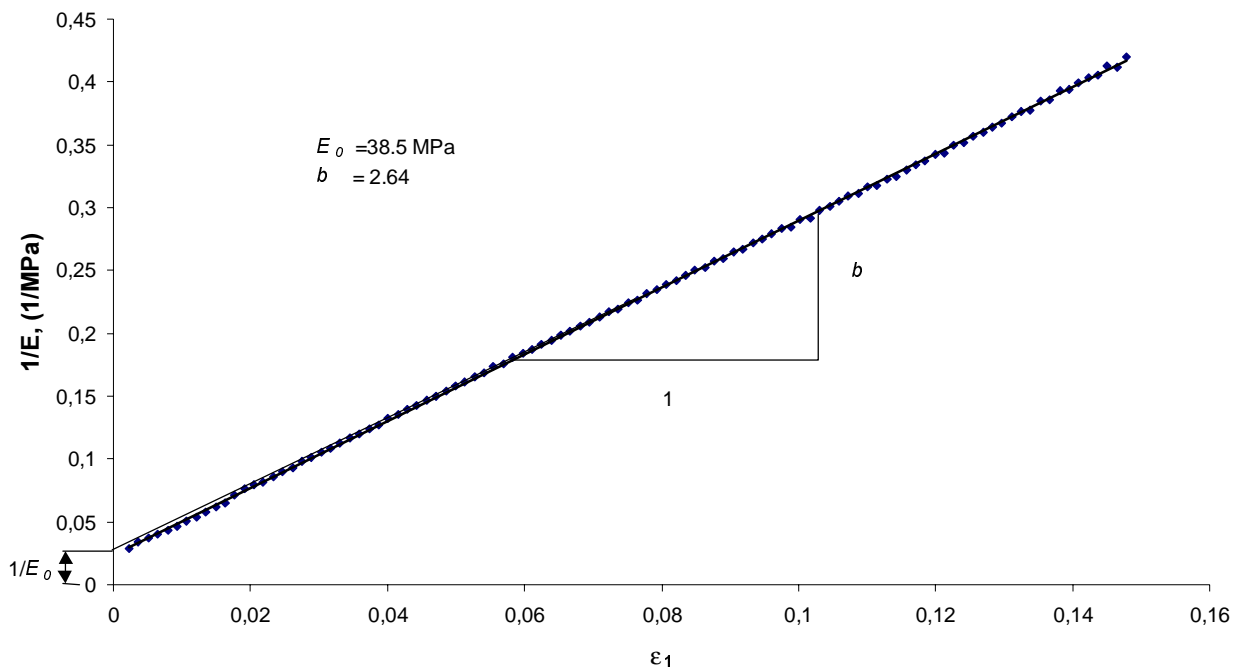


Fig. 79. Evaluation of parameters  $E_0$  and  $b$ . Data from the undrained triaxial tests on a specimen from 2.2 m depth at Tornhill.

The evaluation is sensitive to possible errors in the measurement of deformation in terms of compliance of the system and imperfect fitting between the specimen ends and the end plates. The evaluation is therefore normally restricted to strains larger than 1 per cent in the ordinary triaxial set up. The range can be increased to somewhat smaller strains by using internal transducers inside the cell mounted on the specimen. However, this also limits the upper working range, which has to be large for clay till specimens.

The evaluation was performed for all undrained tests on Baltic and mixed clay tills. The fit of a straight line to the plotted relations varied. For some of the tests, the fit was good from very small strains and throughout the test. For other tests, the straight line relations held only for the first part of the tests and in a few tests, there was hardly any straight line relation to be found at all. For the latter curves, only the slope of the curve

at an inflexion point and at relatively small strains could be evaluated. The evaluated values of  $E_0$  and  $b$  have been weighted with consideration to the portion of the curve for which they are relevant and are plotted in *Fig. 80. a* and *b*.

There may be a certain trend in the results with relatively high initial moduli in the Baltic clay till and lower values in the mixed clay till, which increase again as the transition to the North-east till is approached. In a similar way, the  $b$ -values may be found to be lower in the Baltic clay till, higher in the mixed clay till and then decreasing again with depth. However, the values are dependent on effective stress, stress history, the composition of the particular specimen and the degree of disturbance caused by sampling and handling, and the scatter is large.

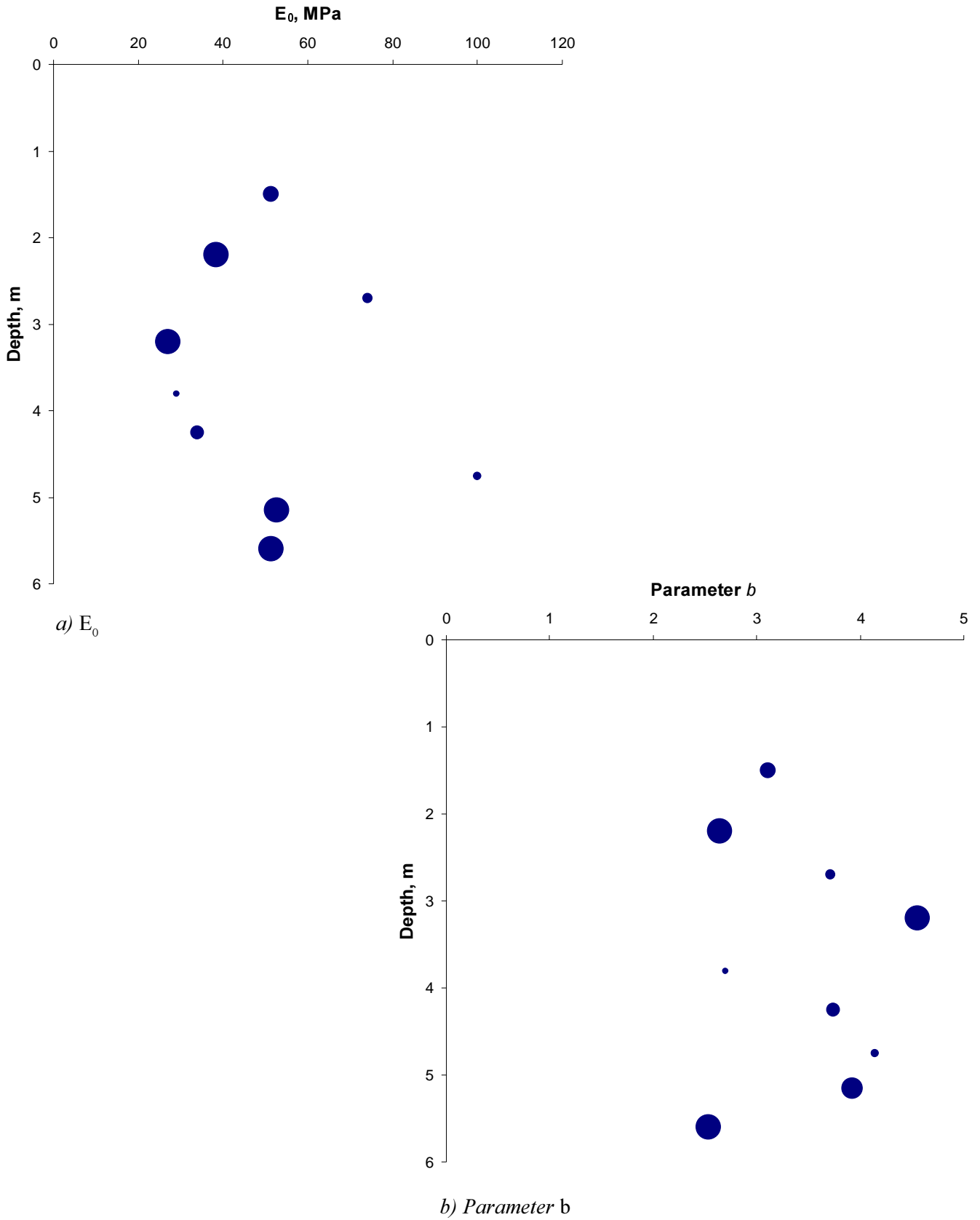


Fig. 80. Evaluated parameters for description of the modulus of elasticity from undrained triaxial tests. The size of the symbols represents the allotted weight for the results.

## 6. Experiences from the laboratory tests

### 6.1 HANDLING OF SOIL SAMPLES

The handling of the samples in the laboratory entailed some difficulties, which are not encountered for more normal soil samples. The 1.5 m long slender tubes with core samples weighed up to 30 kg and were very difficult to handle without introducing bending moments. Both types of sampling tubes had to be brought into the workshop before the samples could be taken out. The buckled part of the steel tubes had to be sawn off before the sample could be pushed out whereas the plastic tubes had to be cut through lengthways at two opposite sides. One half of the tube could then be lifted off and the sample could be parted into selected portions. All this had to be done without disturbing the samples and without losing some of the water content before the test specimens could be prepared in the laboratory. This required a fair amount of time and auxiliary equipment and great care.

### 6.2 ROUTINE TESTS

Due to the heterogeneity of the soil, relatively large specimen had to be used to obtain representative values of bulk density, dry density and water content. These determinations were made on the entire specimens for oedometer- and triaxial tests and thus on volumes ranging from about 115 cm<sup>3</sup> to 1600 cm<sup>3</sup> and dry weights ranging from about 250 g to 4 kg.

For accurate determination of dry weights and water contents in clays, the samples should be allowed to cool off in desiccators, which put new demands on the sizes of the latter. The determination of water content could also be affected by layers or lenses of coarser material which could not fully retain the water when taken out of the sampling tubes.

At determination of particle density, quite different values may be obtained depending on what part of the soil mass is included in the test. The

clay till consists of a heterogeneous mixture of clay to gravel size particles with occasional cobbles and boulders. The origin of the individual particles varies from different crystalline rocks to different sedimentary rocks and the sedimentary rocks have yielded particles ranging from chalk to flint. The determined particle density could thus vary significantly from specimen to specimen and may not even be fully representative for the whole specimen since not all grain sizes were included in the tested material.

The calculated void ratios and saturation ratios are very sensitive to the particle density and possible errors in the determinations of water content and dry density. The sensitivity increases with decreasing void ratio.

The classification of the material is difficult because of the heterogeneity and a full description of the soil profile requires continuous cores.

### 6.3 OEDOMETER TESTS

Oedometer tests were performed on both tube samples and core samples. The tube samples were pushed directly from the sampling tubes into the oedometer ring. The specimen preparation was thus limited to creating smooth end surfaces flush with the ends of the oedometer ring. This preparation should be limited to prevent loss of water and other disturbances during the preparation. Some protruding coarser objects have to be removed and replaced during this operation but this should be limited as far as possible. Samples in steel tubes could not be inspected beforehand. This entailed that a large number of intended specimens had to be rejected and new portions of the sample had to be pushed out and the preparation retried. For one of the samples from the mixed clay till, it was not possible to find any portion from which an oedometer specimen could be prepared.

The specimen from the core samples had to be trimmed slightly also on the periphery before they could be fitted into the oedometer ring. The depth of this trimming was restricted to about 1 mm. Both this and the subsequent trimming of the end surfaces were facilitated by the fact that the samples could be inspected beforehand and that particularly fine-grained and homogeneous portions could be selected.

The oedometer tests have been evaluated using a great number of approaches; even more than are presented in this report. In general, none of these methods gave clear indications of the preconsolidation pressure and the results of a number of approaches had to be gathered and weighed before the combined results could yield a probable value. The other evaluated parameters in terms of modulus number, swelling index and creep rate were within the limits of what would be expected from empirical experience.

### 6.4 TRIAXIAL TESTS

The triaxial tests entailed similar problems of creating smooth and parallel end surfaces. An excess of coarse particles in an intended end surface could normally be remedied by decreasing the height of the specimen. The tests were performed with "friction free" end plates and the deformation of the specimen appeared to be uniform for most of the test. However, because of the heterogeneity of the soil, the specimens often tended to tilt at the end of the tests and they then also tended to slide off the end plates. This seemed to be restricted to what happened at large strains after failure had occurred. It is often recommended to use some type of pins at the centre of the end surfaces to prevent the specimen from sliding on the end plates. This was not considered to be feasible in the clay till with its abundance of coarser particles.

The smallest specimen sizes with 70 mm diameter may be considered as minimum sizes for this type of material. In fact, the results of the test with the coarsest material showed that the specimen size in this case was too small. The 70 mm size should therefore preferably be limited to

non-gravelly soils and larger specimen should be used in tests on coarser material.

The results of the triaxial tests were normal with respect to the measured preconsolidation pressures. However, since the latter were considerably lower than what was empirically estimated from the field tests, also the undrained shear strength values were correspondingly lower. According to the results, the effective shear strength parameters may be estimated with the same empirical relations that are normally used for other types of clay in Sweden.



## 7. Plate loading tests

### 7.1 PRINCIPLE OF THE PLATE LOADING TESTS

The plate loading tests were performed in order to check the applicability of different methods of estimating bearing capacity and settlements for shallow foundations on clay till. The tests were performed as a series of tests on square plates with dimensions chosen in such a way that ultimate bearing capacity failure was expected to be reached for at least the smallest plate and with such variations that the effect of the stresses extending to various depths could be studied. The largest plate also had dimensions similar to an ordinary foundation.

Foundations in Sweden are made so deep that they are unaffected by frost action, which normally means a foundation level 1.1 – 2.5 m below the ground surface, unless special precautions are taken. In the plate loading tests, it was also desired to lay the plates on top of fairly homogeneous soil below the top soil and desiccated crust in order to facilitate interpretation of the results. In ordinary foundations, part or all of the excavation for the foundation is often back-filled after the foundation work has been completed.

Much of the loading equipment is standard for this type of test, which sets limits on possible dimensions and maximum loads. The loading equipment consisted of a system of beams, ground anchors and hydraulic jacks and pumps. The main beams consisted of three 17 m long steel profiles which could be bolted together. Such beams are kept in Swedish National Rail Administration depots distributed throughout the country for use in temporary emergency repairs of railway lines and can often be made available for loading tests. Because of the high loads, a secondary system of beams was placed across and on top of the main beams over the largest plate. The ends of the beams were placed on sup-

ports consisting of wooden rafts of the type normally used to support excavators on soft ground. In this case, they were used to provide firm and level bases, and the number of rafts at the ends can also be adjusted to place the beams in a horizontal position. The required reaction force can be provided by dead-weights or by ground anchors. In this case, it was considered unsuitable to use dead-weights and a system of eight ground anchors was installed. The ground anchors consisted of tie rods, which were lowered in pre-drilled holes down to 10 metres in the bedrock and then fixed by pumping in cement grout. The ground anchors were placed in pairs, one on each side of the ends of the beam systems, and extended well above the beams. Shorter beams were placed across the ends of the beam systems and were tied down with a pre-stress in the tie rods in order to secure the system.

The dimensions of the reaction system made it possible to install three plates measuring 0.5 x 0.5 m, 1 x 1 m and 2 x 2 m in a row along the main beams without significant interference in terms of the same soil mass being affected by the different load tests. The distances between the plates and the loading sequence were also adjusted to minimise the influence from a preceding load test on the results from the following load tests. Thus, the smallest plate was placed at one end of the row, the largest plate was placed approximately in the middle but somewhat closer to the smallest plate, and the intermediate plate was placed at the other end of the row. The plates were then tested in a sequence with the smallest plate first and the largest plate last.

No large amount of backfill was put in place after the plates had been installed. The plates were installed 0.2 m deeper than the rest of the excavation and only the gaps left after removal of the moulds were filled in.

The load on the plates was provided by hydraulic pumps and jacks. According to Swedish practice, the load in tests on friction soils is normally applied in steps with a duration long enough to enable a study of the creep rate of the deformations (Bergdahl et al. 1993). For cohesive soils, a longer duration is required to permit for full dissipation of excess pore pressures and related consolidation if the drained properties are to be studied. A minimum of ten steps is normally used to enable evaluation of both load settlement curves and failure loads. In tests on friction soils and in undrained tests on clays, a duration for each load step of about 8 minutes is normally considered sufficient. In the present series of tests, the tests were performed in steps with durations that were determined with respect to the measured pore pressures and time settlement curves. The durations of the load steps were therefore somewhat shorter for the first load steps and then increased at higher loads as the time-settlement relations changed. The durations were thus mainly 2 hours for the 0.5 m square plate, 4 hours for the 1 m square plate and 6 hours for the 2 m square plate. The duration of the load steps in the unloading and reloading loops was only about 12 minutes for each step. The pore pressure in the soil below the plate was measured during the tests in order to verify that full excess pore pressure dissipation was achieved.

Different systems for application of both constant static loads, cyclic loads and dynamic loads by hydraulic jacks have been developed at the Institute. In this case, an electronically operated system was used in which the load was measured and regulated by means of an electronic load cell. Because of the high loads and pressures and the long duration of the tests, a back-up system for maintaining oil pressure was installed which was automatically engaged if the pressure should drop. This proved to be well-advised, since the first oil pump failed at the end of the series of tests.

## 7.2 INSTALLATION OF PLATES AND INSTRUMENTATION

The reinforced concrete plates were to be cast in place at the bottom of excavated pits. The ground water observations in previous years had shown that the free ground water level would normally be about 2 m below the ground surface in summertime. However, the spring this year was wet, with a ground water level at the ground surface, and no significant lowering of the ground water was observed during the period of the investigations and subsequently. An attempt was made to lower the ground water locally by excavating large holes to 2 metres depth at the ends of the intended excavation for the tests and pumping out the water from the bottom of these. This continued for a couple of weeks, but no effect was observed at the observation points in the test area. Time was then running short and it was decided to perform the excavation and to try to keep the water out and preserve the soil properties at the bottom of the excavation in the usual way. This entailed the excavation of ditches and pumping at the bottom of the excavation, while minimising the length of the periods between excavation and reloading by installation of the plates.

The excavation work was started using an excavator to about 0.2 m above the foundation level. A 1.3 metre deep pit with base dimensions of about 13 x 5 metres was thus excavated. The slopes at one of the long sides had an inclination of about 1:1 but the slopes at the other sides were steeper. Care was taken to perform the last part of this excavation smoothly without excessive deepening of the pit in the separate digging operations. At two opposite corners of the excavation, holes were dug to 2 metres depth and the pumps were lowered into these. Ditches were then dug along the sides of the excavation. The further 0.2 metre of excavation for the tests plates was carried out manually, *Fig. 81*. The prefabricated moulds were then put in place.

After the excavation work, part of the instrumentation below the plates was installed. This consisted of settlement gauges. In this stiff soil, the



Fig. 81. Excavation for the plates at Tornhill.

installation required the drill rig to be lowered into the excavation. This required great care with installation of rails for the rig to run on in order not to disturb the bottom of the excavation.

The instrumentation under each of the plates was to consist of three settlement gauges placed at different depths and one piezometer. However, the disturbance at installation appeared to be relatively large and therefore only one settlement gauge was installed under the smallest plate. The settlement gauges consist of short augers, which are screwed down into the soil. The rods are encapsulated in a plastic tube and the annulus is filled with grease. When the auger has been screwed into place, the plastic tube is retracted over a distance corresponding to the intended range of measured settlements. The rods and protecting tubes are extended to pass through the concrete plate.

The settlement gauges were placed close to three corners of the plates in the so called “characteristic point” for stresses and settlements, i.e. at a perpendicular distance of  $0.13b$  from adjacent sides of the plate (where  $b$  is the width of the plate). One gauge for each plate was placed with its centre at a depth of about 0.15 metre below the base. The reason for this was to obtain a check on possible excessive deformations resulting from disturbance of the bottom of the pit in spite of the careful excavation. The other two gauges were placed at depths within the depth interval down to  $2b$  below the plates.

After installation of the instrumentation, reinforcing bars were placed in the moulds and concrete was pumped in. Apart from the settlement gauges below the plates, the total settlements of the plates were measured on rods fixed in the concrete at each corner of the plate.

The work of installing the moulds, instrumentation and, reinforcement, in addition to pouring the concrete, was a fight against time owing to water seepage. The pumps and ditches needed constant monitoring since parts of the slopes continuously collapsed as water continued to seep in on the lower parts of the slopes. There was also a rain shower during this period. The bottom of the excavation was checked carefully just before the concrete was poured to estimate the extent of the softening. Although the surface itself was then very soft, the obvious effect extended only to about 10 mm depth below. The ground water conditions were measured with tensiometers and pore pressure probes below the excavation and in the slopes. The free ground water level in the slopes was found to be about 1 m below the ground surface. Below this level, water seeped into the excavation and above it the pore pressures were negative, corresponding to negative hydrostatic pressures from this level. Below the bottom of the excavation, the pore pressures were slightly artesian and thus there was an upward gradient with water seeping very slowly up towards the surface.

Piezometers were installed beneath the plates in order to check that the tests were drained and that all excess pore pressures had dissipated at the end of each load step. The piezometers were electrical and were intended to be installed at depths where the pore pressures could be expected to be highest with consideration to stress increases and drainage paths. The piezometers were pushed in at the corners where no settlement gauges had been installed and with such inclinations that they would be positioned centrally beneath the plates. After pushing the piezometer into place, the drill rods were retracted, leaving only the piezometer connected to a wire and the signal cable in the ground. However, this operation had to be performed with the drill rig standing on the slope of the excavation and the resistance of the soil was so great that the intended depths could not always be fully reached.

The concrete plates were 0.5 metre thick. One day after casting the plates, the moulds were removed and the gaps between the plates and the surrounding soil in the excavation were filled in with excavated soil. The work with setting up the reaction, loading and measuring systems was then commenced.

### 7.3 INSTALLATION OF THE REACTION SYSTEM

The eight ground anchors had been installed by PEAB Grundteknik about one month in advance. The ground surface at each pair of ground anchors was now scraped off and levelled. A number of wooden rafts, or “excavator mats”, were then stacked and adjusted in such a way that the top surfaces of the stacks were at the intended levels and horizontal. The three railway bridge beams were placed side by side with the ends resting on the stacks at the ends of the excavation and then bolted together. Their common centre line was carefully aligned with the centre line of the row of plates. Two short beams were then placed on top and across the ends of the large beams, and were connected to the tie rods from the ground anchors. Above the centre of the largest plate, two other beams were placed on top of and across the railway bridge beams with their ends resting on the two stacks of excavator mats at the sides of the excavation. The ends of these beams were connected to the corresponding tie bars in the same way as the ends of the long beams. The tie rods were pre-stressed and the whole reaction system was thereby fixed, *Fig. 82*.



*Fig. 82.*  
*Reaction system*  
*being mounted.*

## 7.4 INSTALLATION OF THE LOADING SYSTEM

The loading system used for the tests at Tornhill consisted of a hydraulic pump and electronically operated regulation valves, two hydraulic jacks for different load ranges, corresponding load cells for measuring the load and providing the signal for regulating the hydraulic pressure, and a computer for data collection and regulation of the loading process. A back-up system for the hydraulic pressure was also installed.

For the two smaller plates, a circular stress distribution plate was centred directly on the concrete. The load cell and the jack were then positioned on this plate and on top of them further plates were laid as required to fill the gap up to the reaction beams. For the largest plate, an additional square stress distribution steel plate covering a large part of the top surface was laid in position before the above mentioned assembly was put in place. In order to distribute the load on the reaction beams evenly, a short beam was fixed under and across them at the loading point.

### Measuring system

The measuring system consisted of the computerised data collection and load regulation system, the load cells, the piezometers and the displacement transducers. The displacement transducers were fixed on special measurement beams (ladders), whose ends rested on the ground outside the area affected by the particular test. The displacement transducers measured the movements of the top of the plate and the settlement gauges in relation to this ladder. The whole system was protected from sun and weather by tarpaulins, using the reaction beams as a ridge. The measurement beam was supplied with a fixed vertical scale and was continuously levelled by a high precision instrument in order to check that the reference level was stable, *Fig. 83*.



*Fig. 83.*  
*Installation of the measuring system.*

### Loading procedure

The load tests were to be performed in steps with maintained constant loads. In order to ascertain that all excess pore pressures would dissipate during the time for each load step, a number of preliminary calculations were made using somewhat conservative assumptions. On the basis of these calculations, a tentative schedule was set up where each load step for the smallest plate was to be applied for 2 hours. The corresponding times for the middle and the largest plates were 4 hours and 6 hours respectively.

Preliminary calculations of the bearing capacity had given widely differing results depending on which strength parameters were used. However, the preconsolidation pressure in the upper part below the plate was estimated to be at least 650 kPa and the calculated bearing capacities were somewhat or much higher than this value. For the first test plate, which was the smallest 0.5 x 0.5 metre plate, it was therefore decided to start with load steps of 25 kN, corresponding to 100 kPa, which would give the desired minimum of eight load steps.

The first load test resulted in failure after ten load steps and it was decided to make the steps somewhat smaller in the next test. The 1 m x 1 m plate was thus loaded in steps of 75 kN corresponding to 75 kPa. No direct failure was obtained in this test, but the frequently used failure criterion of the settlement being equal to 10 % of the plate width was approached.



Fig. 84. Deflections in the reaction beams at the end of the loading test on the largest plate.

The maximum design load for the reaction system varied depending on where the load was applied. The tie rods were designed to take a maximum force of 500 kN each. However, this force could not be mobilised simultaneously in every rod and it was difficult to estimate the interaction within the beam system. For the 1 m x 1 m plate, the load was applied about midway on the free span of the large beams between their ends and the crossing beams above the 2 m x 2 m plate. The pair of tie rods at the ends of the beams would have to take about half of the applied load and with a possible imbalance in the system, one of them might have to take more than the other. The loading of the 1 m x 1 m plate was therefore stopped at a load of 1350 kN.

For the 2 m x 2 m plate, the main load would be taken by the crossing beams and their tie rods. A contribution would also be obtained from the long railway bridge beams, but this would require a fairly large deflection because of the long span. The crossing beams and their tie rods were designed for a maximum load of 2000 kN. The loading of the large plate was applied in steps of 200 kN, corresponding to 50 kPa, and no failure was expected. The loading was continued up to a total load of 2800 kN, where it was stopped because of large and permanent deflections in the crossing reaction beams, *Fig. 84*.

The settlements and pore pressures were studied continuously during the load steps. During the initial steps of each test, the settlements essentially stopped within a short time. The time-settlement curves then showed straight-line relationships between log time and settlement, with very low creep rates. At the same time, the piezometer readings showed that no or only very small excess pore pressures developed and that these appeared to dissipate rapidly. It was thus possible to shorten the first load steps in each series. The time settlement curves then gradually changed in such a way that the time required to reach a straight-line settlement-log time relationship increased and the duration of the load steps was increased. However, the times in the preliminary schedule did not have to be exceeded.

## 8. Results of the plate load tests

### 8.1 GENERAL

The load tests were performed as planned without any serious mishaps. The only significant practical problem was the continuous struggle to keep the ditches and pumping wells open. The first hydraulic pump failed at one stage, but the automatic back-up worked and this did not affect the tests. A slow drift in two of the piezometers was also observed. However, this was so slow that it did not affect the interpretation of the results in any significant way.

### 8.2 0.5 X 0.5 METRE PLATE

The loading of the smallest plate was performed with an initial step of 10 kN, a second of 15 kN up to 25 kN and thereafter in steps of 25 kN. After the initial step, each step was applied for 2 hours. In order to check the elastic properties, an unloading and reloading cycle was also performed with a duration of each step of only

12 minutes. This cycle was performed in steps of 25 kN from the end of the step with 150 kN load down to 25 kN and then to 10 kN, and with the same reloading sequences. These loads do not include the weight of the plate itself or the weight of the hydraulic jack and other parts in the loading system. Together, they created an additional load of about 12.5 kN on the smallest plate.

After the unloading and reloading cycle, loading continued in steps of 25 kN with 2 hours duration. In the last load step with a load of 250 kN, the settlements continued with a constant rate for approximately half an hour, whereupon they started to accelerate and failure developed. The failure was still slow and the plate settled vertically without any tilting, *Fig. 85*. As failure proceeded, a pattern of radial cracks developed at the ground surface around the plate.

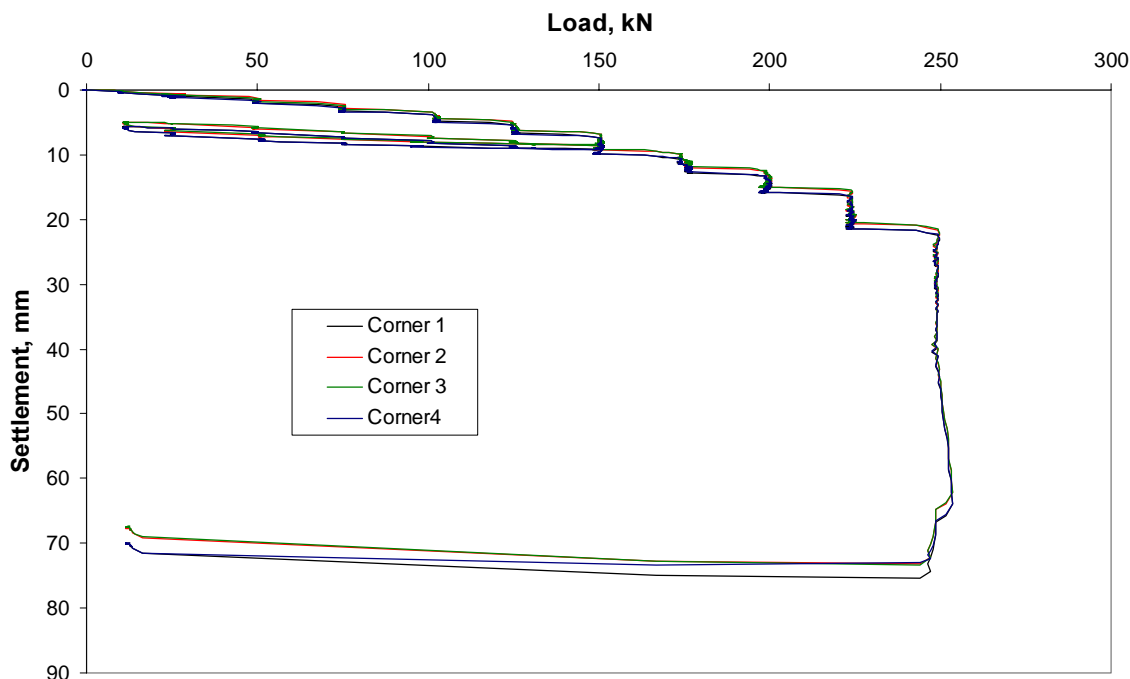


*Fig. 85. Load - settlement curves for the four corners of the 0.5 x 0.5 metre plate at Tornhill.*

## Results plate load test

Only one settlement gauge was installed under this plate. It was located at a depth of about 0.14 m below the plate, or 0.3 times the plate width. The measurements showed that initially almost all settlements occurred within this depth and by the end of the test, just before failure, about 50 % of the total settlements had occurred in this depth interval, *Fig. 86*.

The time - settlement curves for each load step, except the last, started with a certain curvature but eventually formed straight lines in a settlement - log time plot, *Fig. 87*. The time until this stage was reached increased successively as the load increased. The shape of the initial curve depended on the time for load application and how the zero time was selected. However, this did not significantly affect the evaluated creep rates or settlements at the end of the load steps.

The evaluated slopes of these lines constitute a measure of the creep rate in the load steps. The creep rates increase continuously with increasing load. The relation is smoothly rounded and there

is no particular point where there is a significant change in behaviour and thereby an indication of a creep failure load until the penultimate step. In this step there is a significant increase in the creep rate and failure may be considered to have started already in this step. *Fig. 88*.

Under the assumption that the pattern in the measured time-settlement curves continues, the measured creep settlement rates enable an extrapolation of the measured (or extrapolated) settlements after 2 hours to expected settlements after 10 years, which is the time perspective normally considered in settlement predictions. Both the measured 2-hour curve and the extrapolated 10-year curve for settlement versus load are smoothly rounded without any sign of a bearing capacity failure for loads up to 200 kN, *Fig. 89*. Above this load, the creep settlements increase considerably and the extrapolated 10-year settlements almost reach the failure criterion for settlements, amounting to 10 % of the plate width as early as at a load of 225 kN.

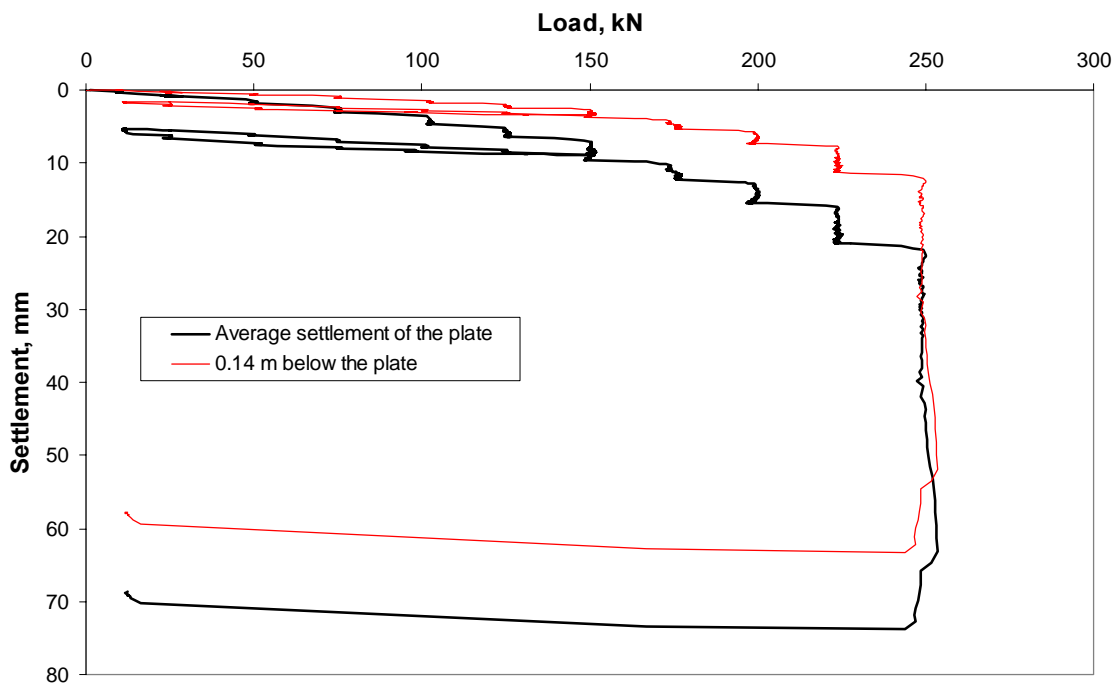


*Fig. 86. Measured settlement of plate and settlement gauge below the 0.5 x 0.5 metre plate at Tornhill.*



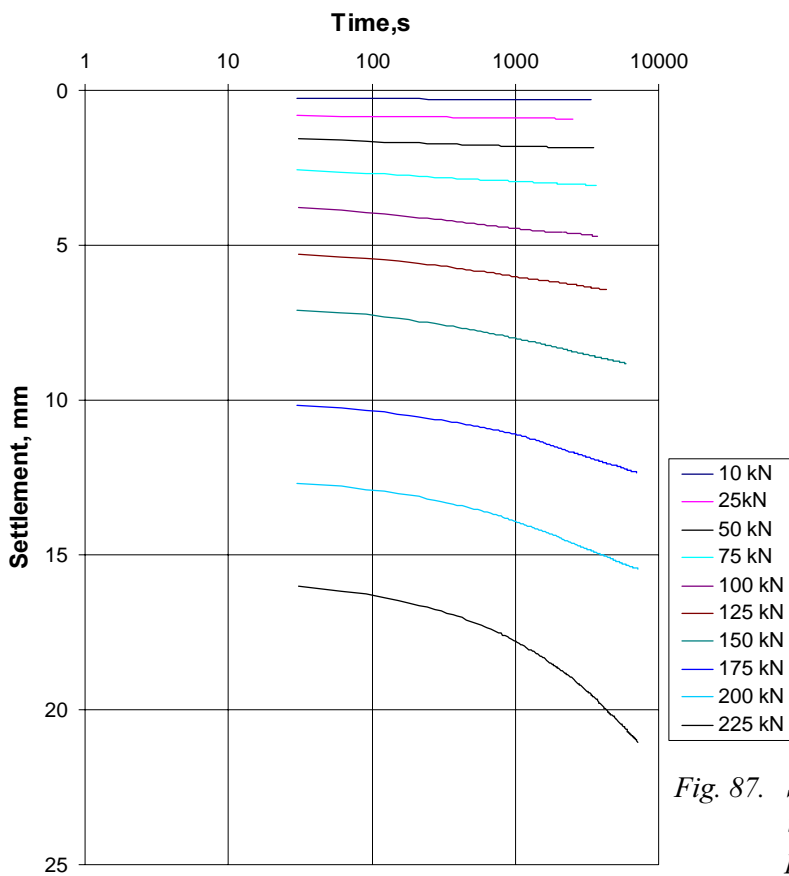


Fig. 87. Settlement - log time curves measured in the load test on the 0.5 x 0.5 metre plate at Tornhill.

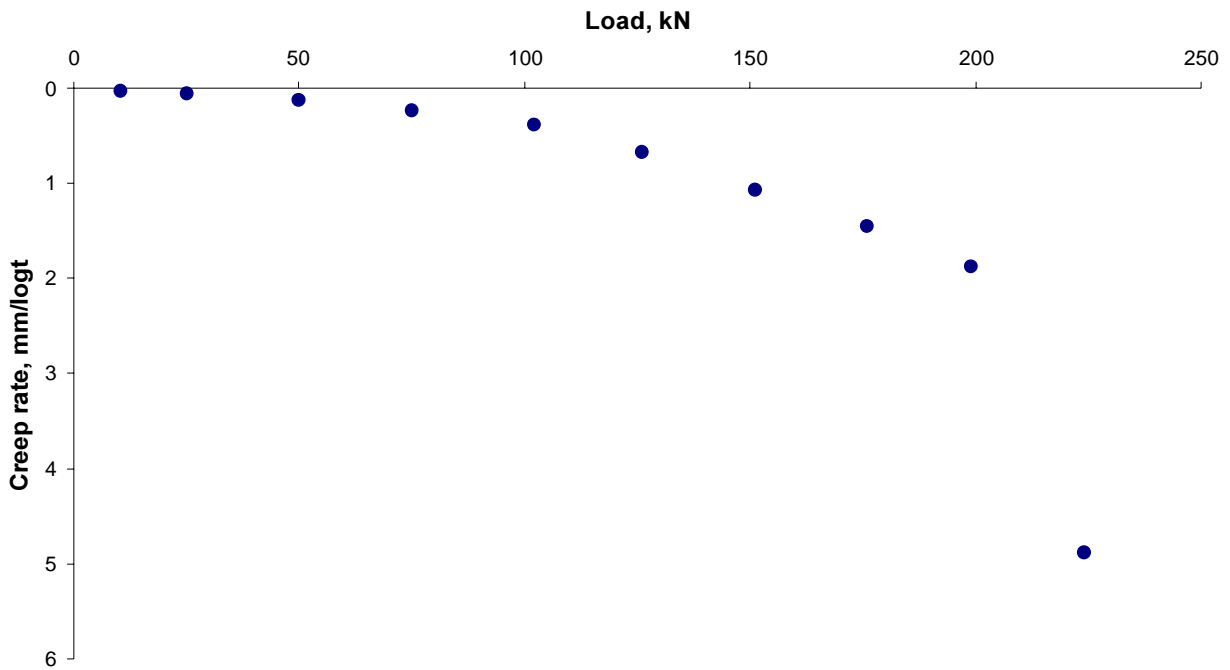


Fig. 88. Rate of creep settlements versus load measured in the load test on the 0.5 x 0.5 metre plate at Tornhill.

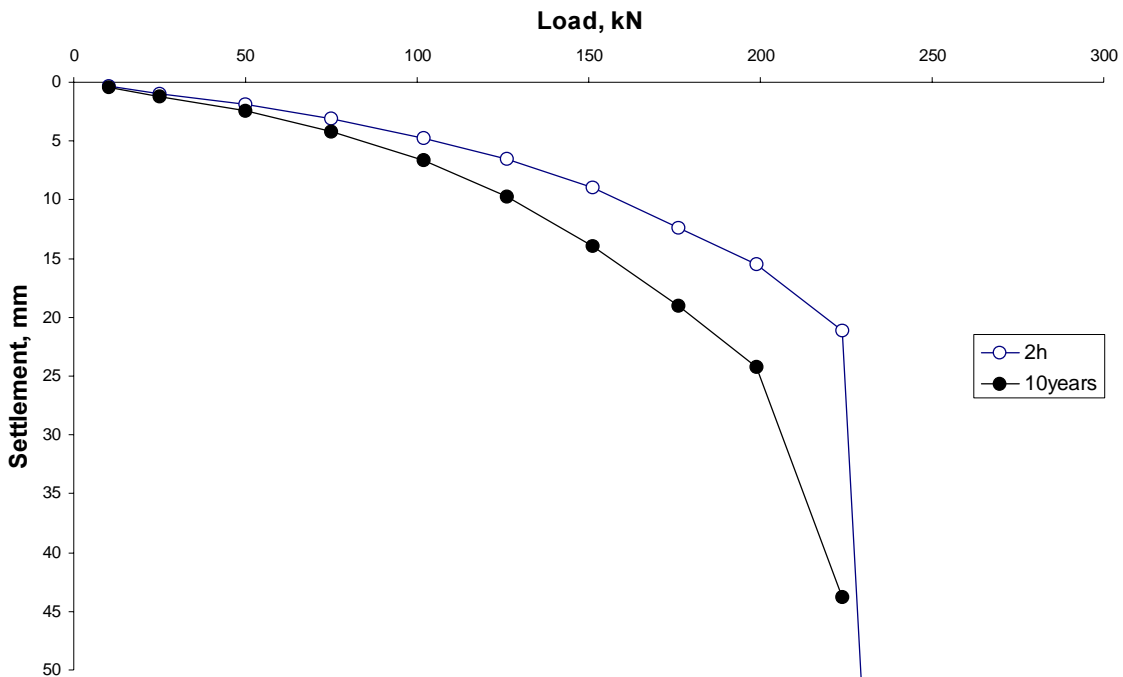


Fig. 89. Measured and extrapolated load - settlement curves in the load test on the 0.5 x 0.5 metre plate at Tornhill.

The time dependence of settlements in coarse soils is normally estimated by assuming that the calculated settlements for a certain time can be adjusted to another time by applying the formula

$$S_t = S_0 \left( 1 + c \cdot \log \frac{t}{t_0} \right)$$

where  $S_t$  = settlement at time  $t$

$S_0$  = settlement at time  $t_0$

$c$  = constant

From the load steps, the constant  $c$  has been calculated versus the total settlement at the end of the current load step. The values are somewhat sensitive to the time used as a reference, which in this case has been set to  $t_0=1$  year. The results from the current load test yield a factor  $c$  with an average value of approximately 0.07. However, the value appears to increase gradually with the load from a minimum of 0.04 to a maximum of 0.09 before creep failure is approached and the value becomes even higher, Fig. 90.

The measured excess pore pressures were very small. They were insignificant in the first two load steps and then increased sufficiently to enable monitoring of the pore pressure generation and dissipation. The pore pressures increased only about 0.5 kPa in each load step and were then seen to dissipate fully within the 2-hour periods with constant load. In the unloading and reloading loop, the times for the load steps were shorter and this dissipation then took place only partly. The excess pore pressure thus fell gradually to about -1.5 kPa at the end of the unloading and then gradually rose to about 1 kPa in the last steps of the reloading. When the 2-hour duration of the load steps was resumed, the excess pore pressures also returned to 0.5 kPa and dissipated within the load step. In the last load step, the pore pressure generation changed and the excess pore pressures became negative when failure occurred, Fig. 91.

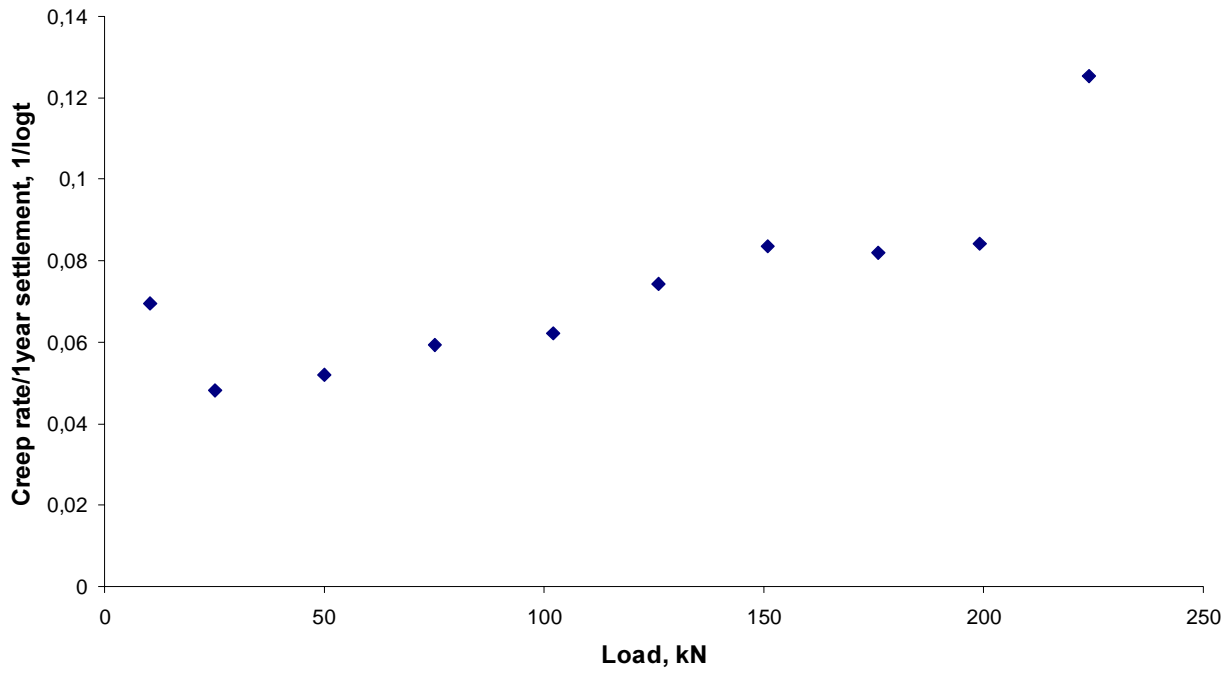


Fig. 90. Relative creep settlement rate versus load in the load test on the 0.5 x 0.5 metre plate at Tornhill

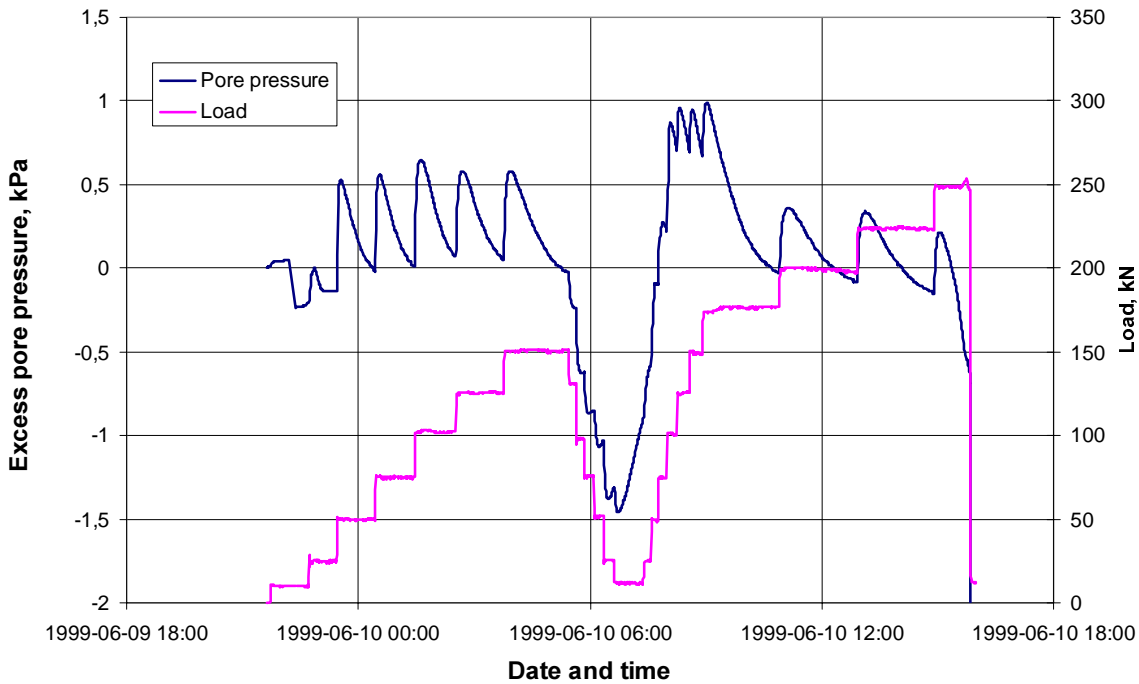


Fig. 91. Measured pore pressure changes during the load test on the 0.5 x 0.5 metre plate at Tornhill.

On the basis of the pore pressure measurements, the load test can thus be considered to have been a drained test and the time chosen for load application was found to be well suited.

### 8.3 1 X 1 METRE PLATE

Loading of the 1 x 1 metre plate was performed in steps of 75 kN up to a total load of 1350 kN. The load was applied for 4 hours in most of the steps. An unloading-reloading cycle was performed from 300 kN load with a duration of 12 minutes for each step. The test was terminated at 1350 kN load, when the average total settlement was 88 mm. The failure criterion for a settlement, amounting to 10% of the plate width, was then well exceeded for the extrapolated 10-year settlements. The plate settled straight down without any significant tilt, *Fig. 92*.

The measurements of the deep settlement gauges showed that the settlements started just below the plate and then spread downwards with increasing load, but only just reached a level of 2.0 m (=2.0*b*) below the plate. By the end of the test,

when the total settlements were 88 mm, only 2 mm of settlement had occurred at 2 metres below the plate, *Fig. 93*.

Also in this case, the settlement - log time curves for the load steps eventually formed fairly straight lines and it was possible to evaluate the creep rates, *Fig. 94*.

The curve for the creep rate versus load formed a curve with a distinct break at a load of about 700 kPa, *Fig. 95*. Up to this point, the curve had been smoothly rounded and after this point it changed to a significantly steeper but fairly straight line. Thus, there is no indication of an imminent creep failure in the measured creep rates.

Both the measured average 4-hour settlements and the extrapolated 10-year settlements show smoothly rounded curves versus load without any indication of an imminent bearing capacity failure before the test was stopped at 1350 kN load, *Fig. 96*. However, the failure criterion for a settlement, amounting to 10 % of the plate width,

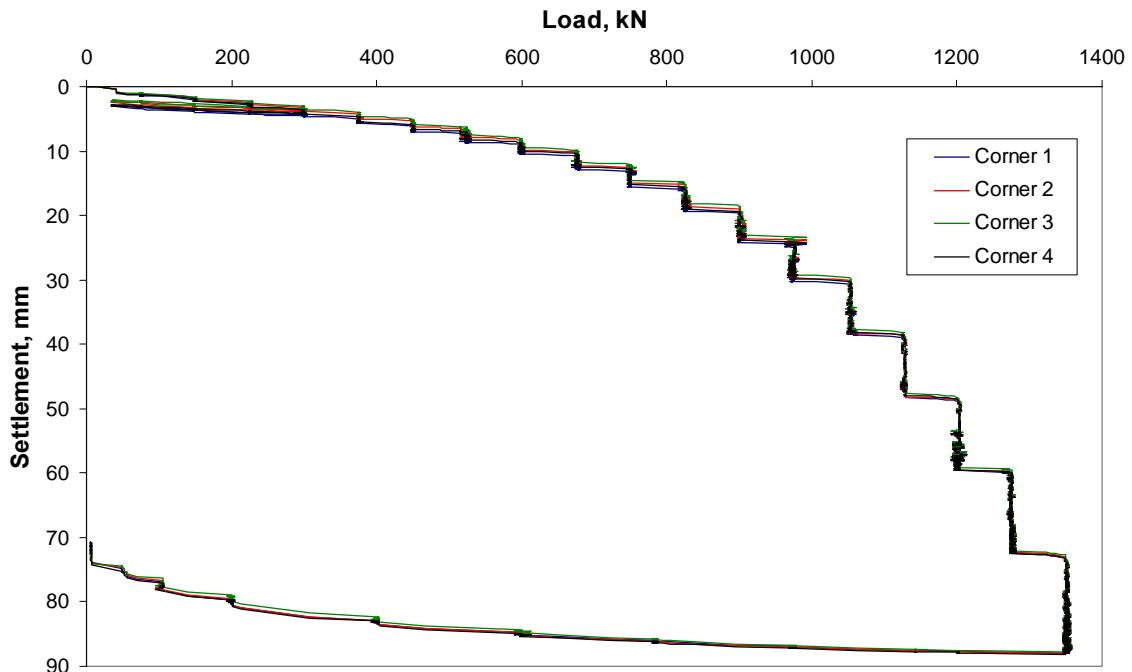


Fig. 92. Load - settlement curves for the four corners of the 1 x 1 metre plate at Tornhill.

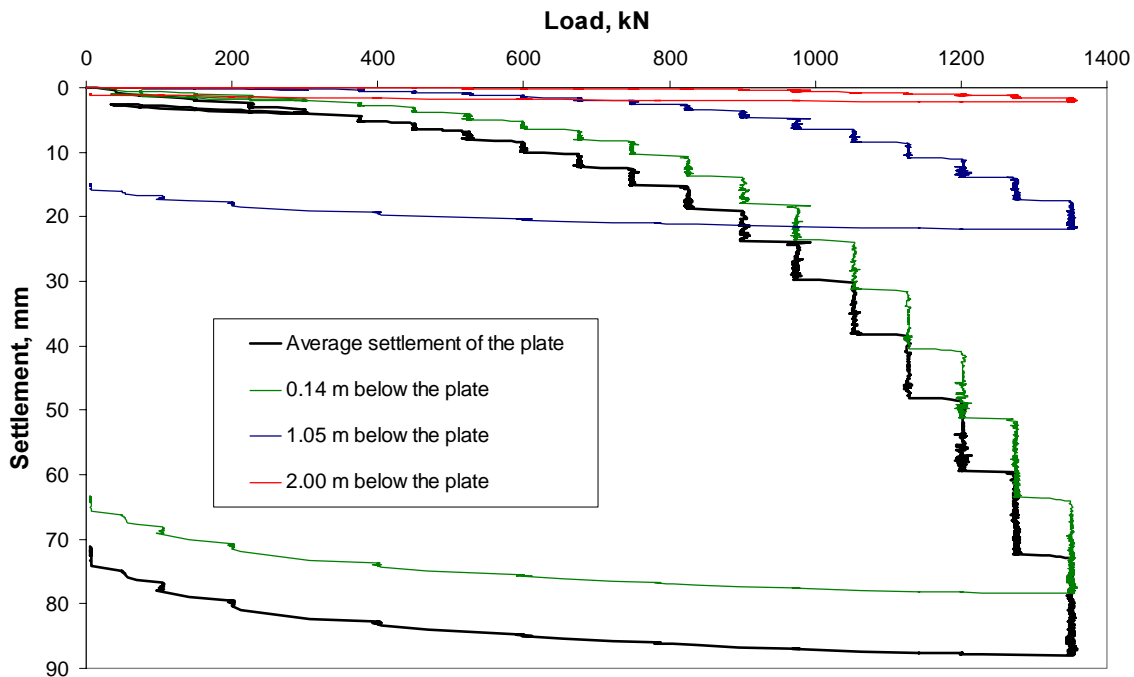


Fig. 93.  
Measured settlements at different levels below the plate in the 1 x 1 metre plate at Tornhill.

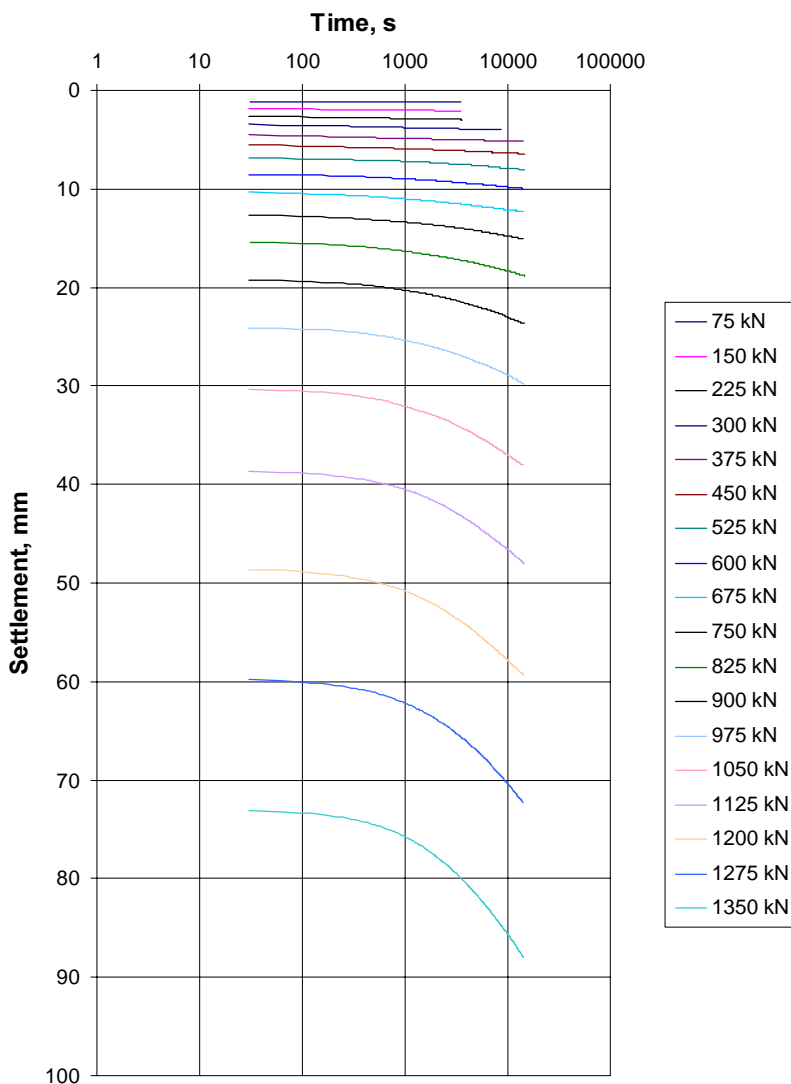


Fig. 94.  
Settlement - log time curves measured in the load test on the 1 x 1 metre plate at Tornhill.

**Results plate load test**

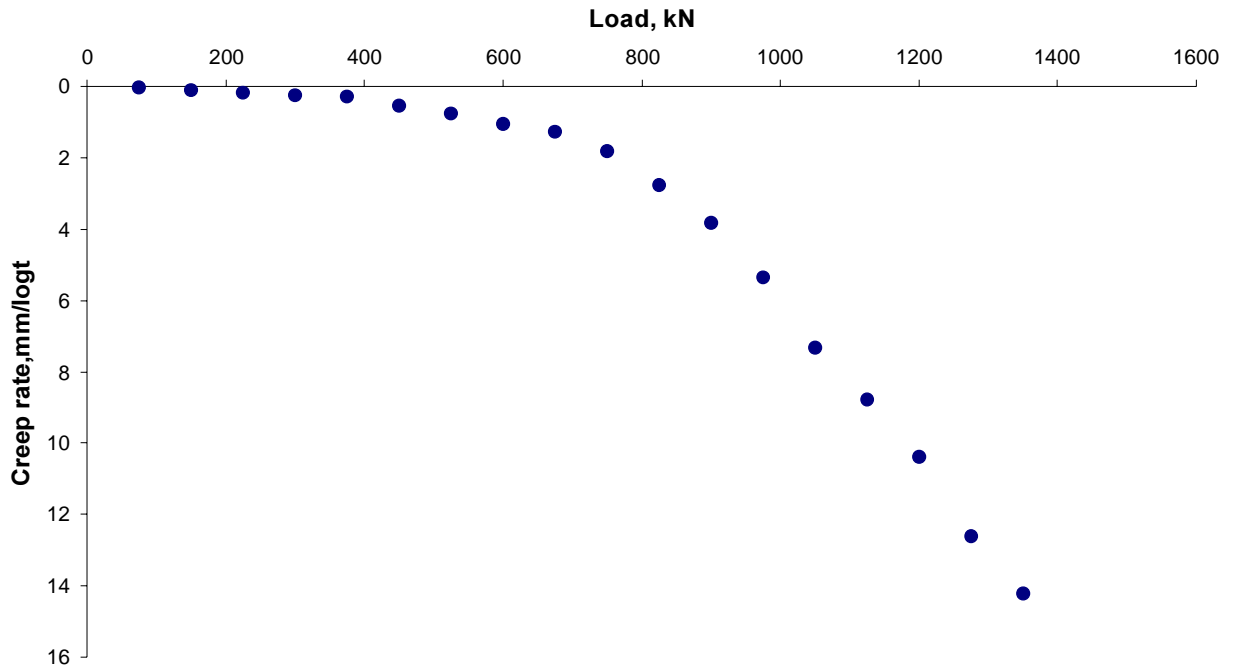


Fig. 95. Rate of creep settlements versus load measured in the load test on the 1 x 1 metre plate at Tornhill.

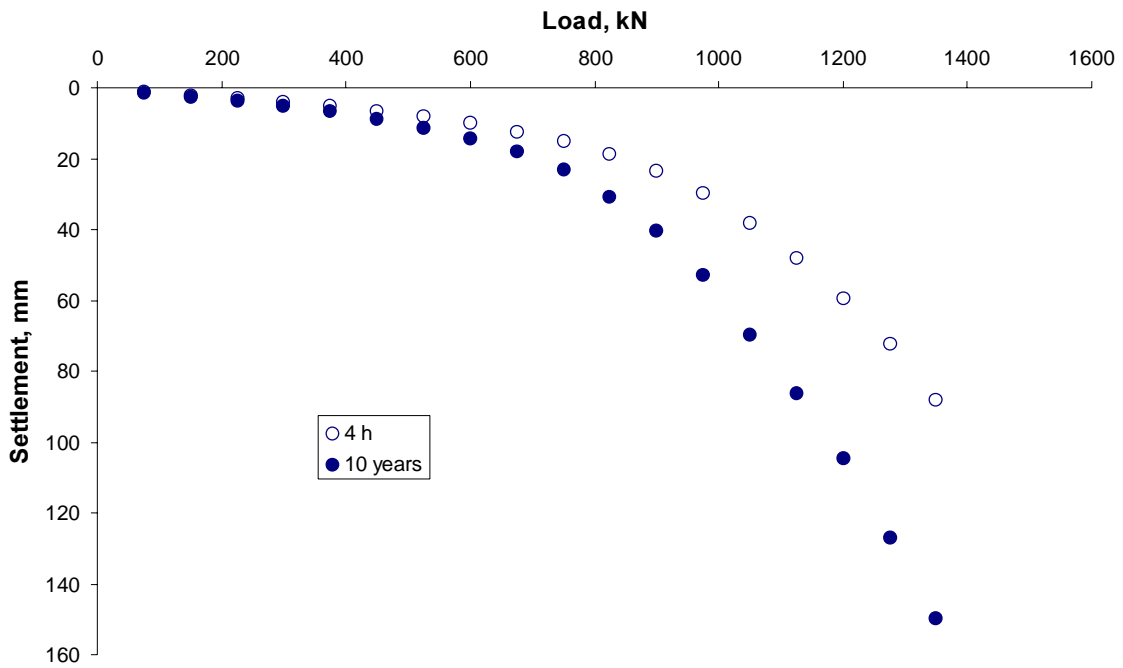


Fig. 96. Measured and extrapolated load - settlement curves in the load test on the 1 x 1 metre plate in the test field at Tornhill.

had been passed at a load of 1200 kN for the 10-year settlements. The load - settlement curves and the previously shown creep curve may be interpreted as indicating that a preconsolidation pressure was exceeded at a load of approximately 700 kN, or 700 kPa in vertical stress.

Parameter  $c$ , which describes the creep rate in relation to the total settlement, was found to increase linearly with the load. The value increased from 0.03 at the start of loading to about 0.11 at the break in the creep-load curve. It then remained fairly constant for the steps with higher loads, *Fig. 97*.

The piezometer below the plate recorded a pore pressure increase of about 3.5 kPa during the test period. However, this increase was mainly linear with time and continued also during the periods of constant load, when the pore pressure should

instead have decreased. The pore pressure increase also largely remained after the final unloading of the plate when negative excess pore pressures ought to have been registered. Most of the recorded increase in pore pressure is therefore believed to have been an electronic drift with a continuous zero shift. If this is assumed to have been linear with time and to amount to the recorded excess pore pressure after unloading, a corrected curve can be obtained, *Fig. 98*. Only extremely small excess pore pressures then remain and the only significant changes are the decreasing and returning pore pressures in the faster unloading-reloading loop and the decrease at final unloading. In either case, corrected or uncorrected, the generated pore pressures are so small that the test can be considered fully drained.

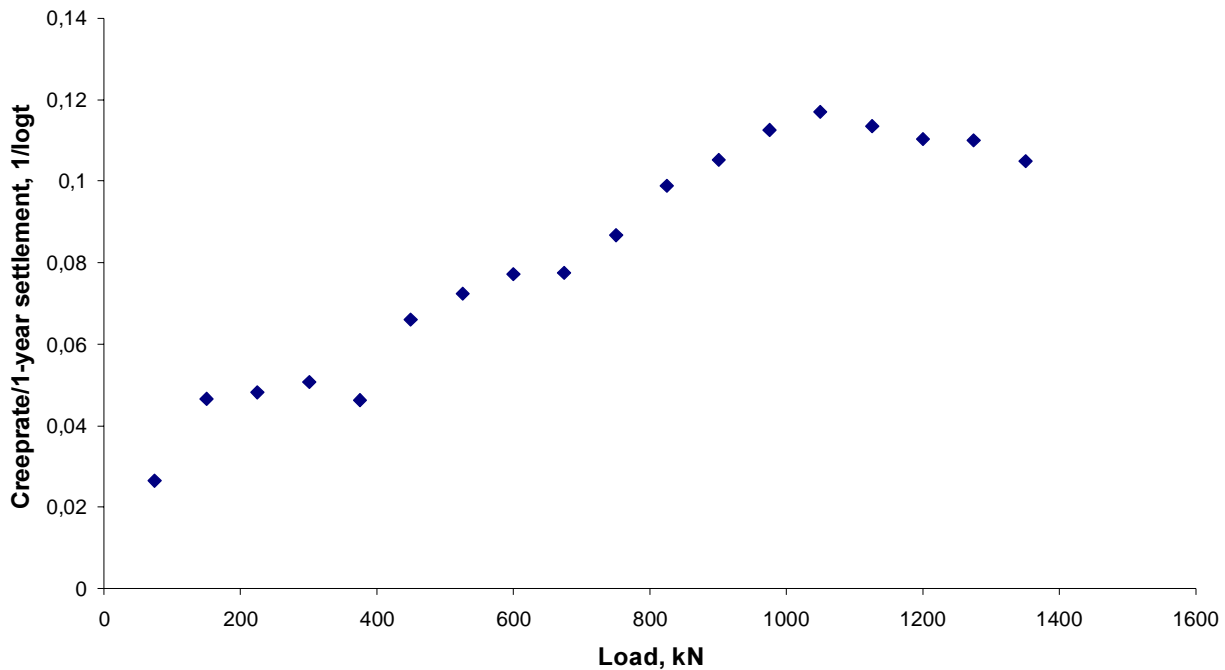


*Fig. 97. Relative creep settlement rate versus load in the load test on the 1 x 1 metre plate at Tornhill.*

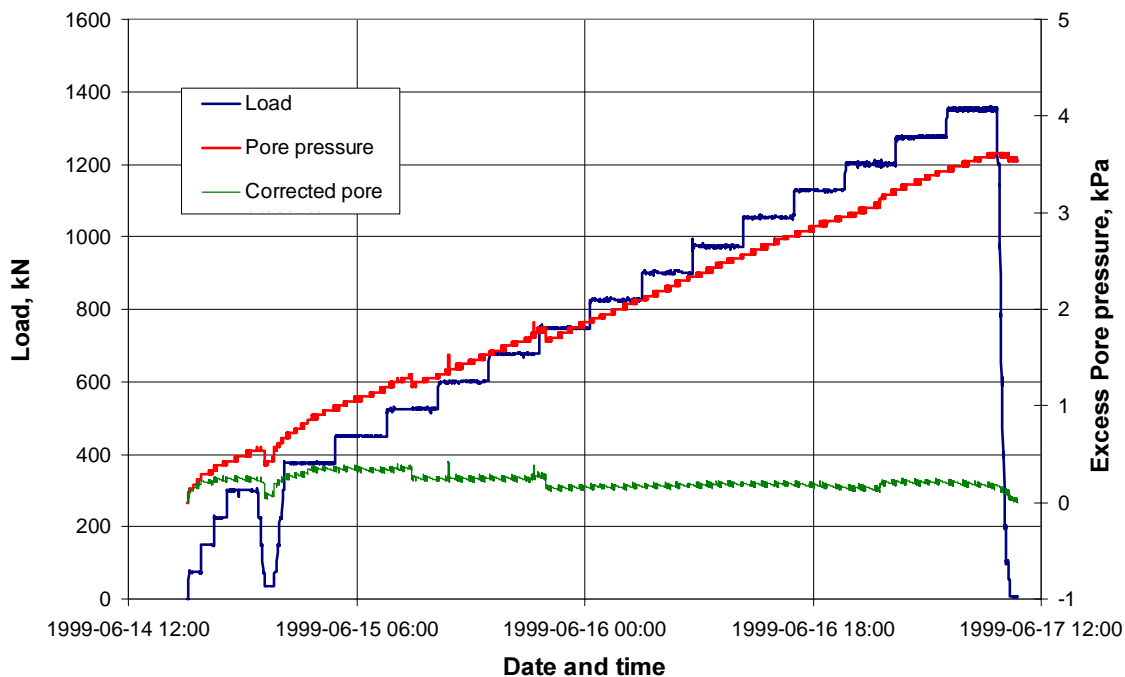


Fig. 98. Measured pore pressure changes and corrected excess pore pressures in the load test on the 1 x 1 metre plate at Tornhill.

#### 8.4 2 X 2 METRE PLATE

The load test on the 2 x 2 metre plate was performed with load steps of 200 kN and a duration usually of 6 hours. No unloading - reloading was performed in this test. The test was stopped at a load of 2800 kN owing to excessive deformations in the reaction system. The settlements then amounted to 56 mm and the plate had settled almost vertically without any significant tilting, Fig. 99.

The settlements versus depth showed the same pattern, with settlements starting just below the plate and then spreading downwards with increasing load. When the test was stopped at 2800 kN load, the settlement at 2 metres depth below the plate, i.e. a depth equal to the plate width, was only 6.2 mm or 11 % of the total settlement, Fig. 100.

Also in this case, the settlements in the load steps eventually formed the typical straight-line relations in the settlement - log time plots, Fig. 101.

The evaluated creep rates are plotted versus applied load in Fig. 102. The relation is smoothly curved with continuously increasing creep rates at increasing load and no breakpoint can be clearly discerned. There may possibly be a break for the last step, but this is not clear enough to be considered a fact.

The measured and extrapolated load - settlement curves are smoothly rounded without any indication of an imminent bearing capacity failure, Fig. 103.

The rate of the creep settlement in relation to the settlement is about the same as for the previous tests, Fig. 104.

The measured excess pore pressures were similar to those measured in the previous test, Fig. 105. On the same grounds, a zero drift may be expected to have occurred during the testing period, but in this case it does not appear to have been quite linear versus time. However, the measured ex-



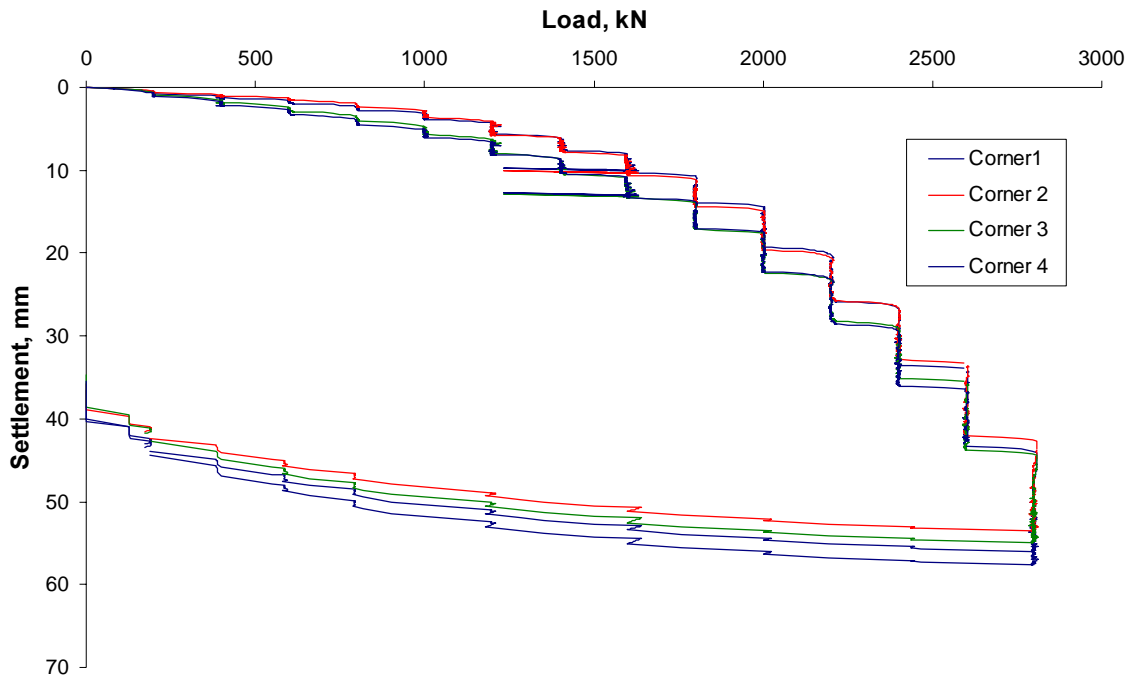


Fig. 99. Load - settlement curves for the four corners of the 2 x 2 metre plate at Tornhill.

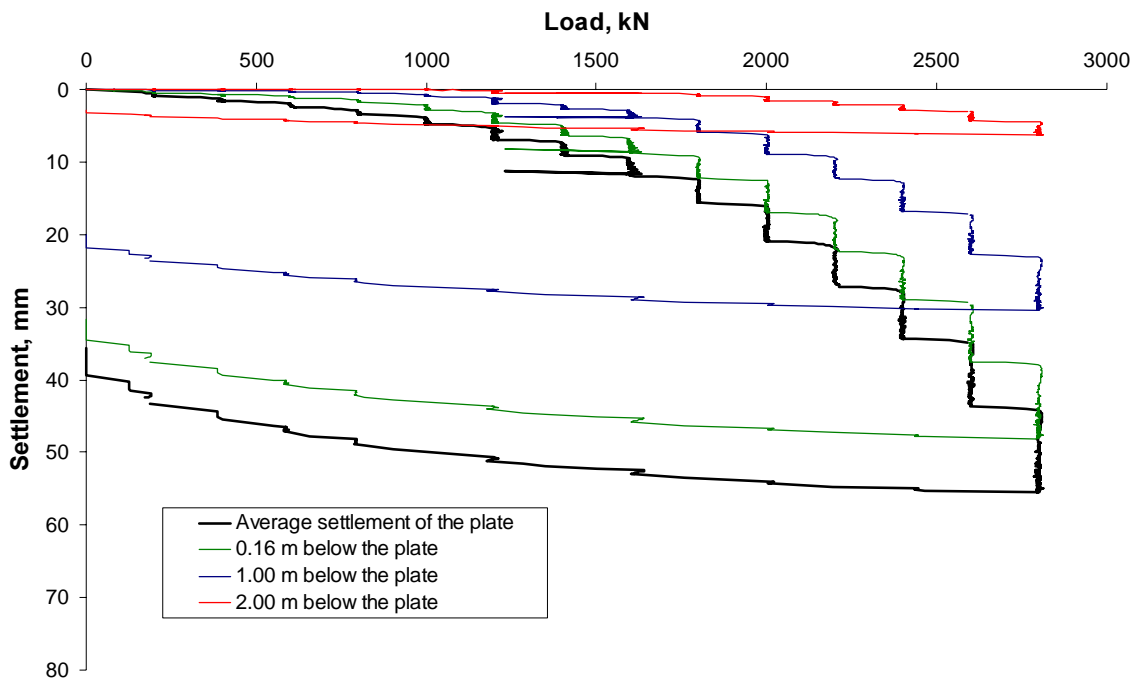


Fig. 100. Measured settlements at different levels below the plate in the 2 x 2 metre plate at Tornhill.

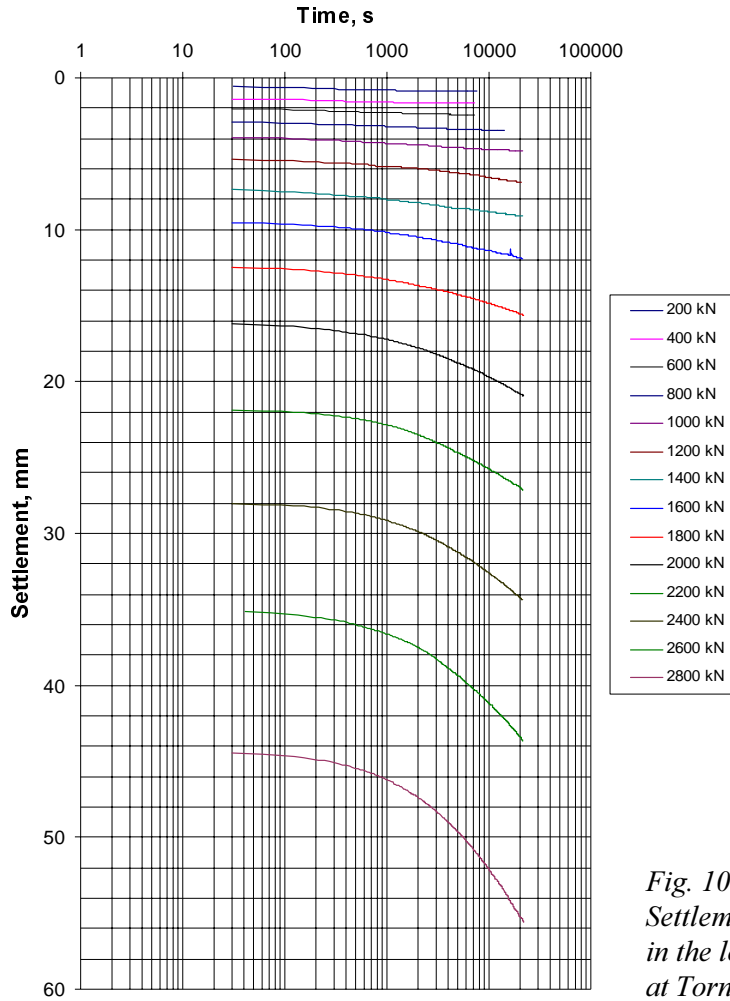


Fig. 101. Settlement - log time curves measured in the load test on the 2 x 2 metre plate at Tornhill.

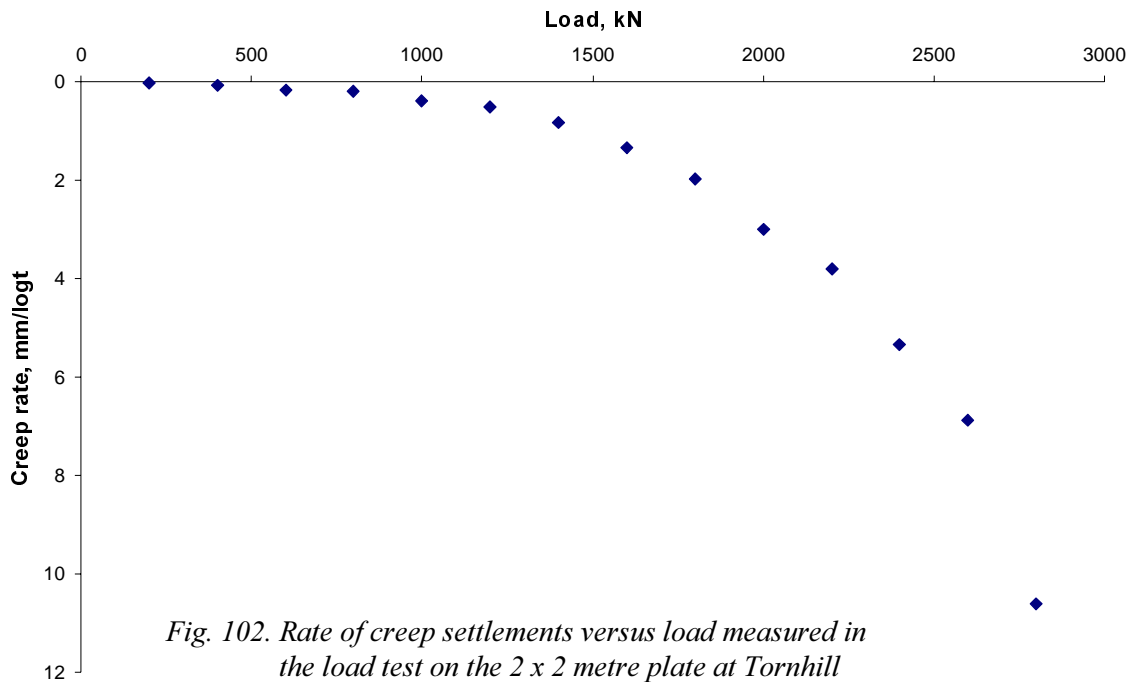


Fig. 102. Rate of creep settlements versus load measured in the load test on the 2 x 2 metre plate at Tornhill

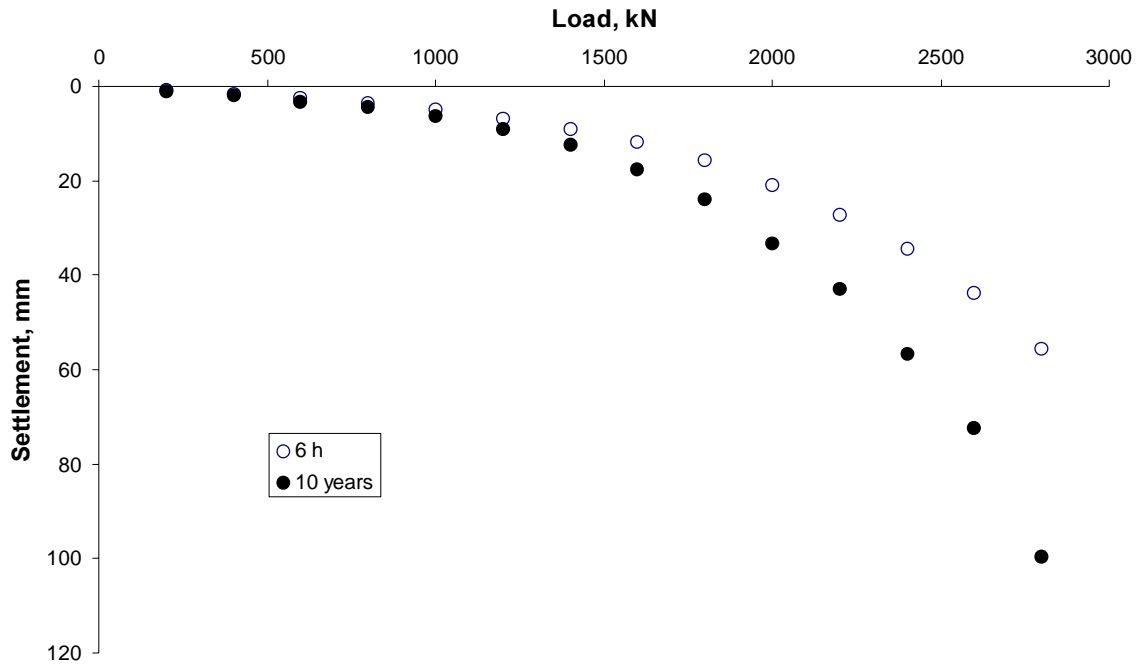


Fig. 103. Measured and extrapolated load - settlement curves in the load test on the 2 x 2 metre plate at Tornhill.

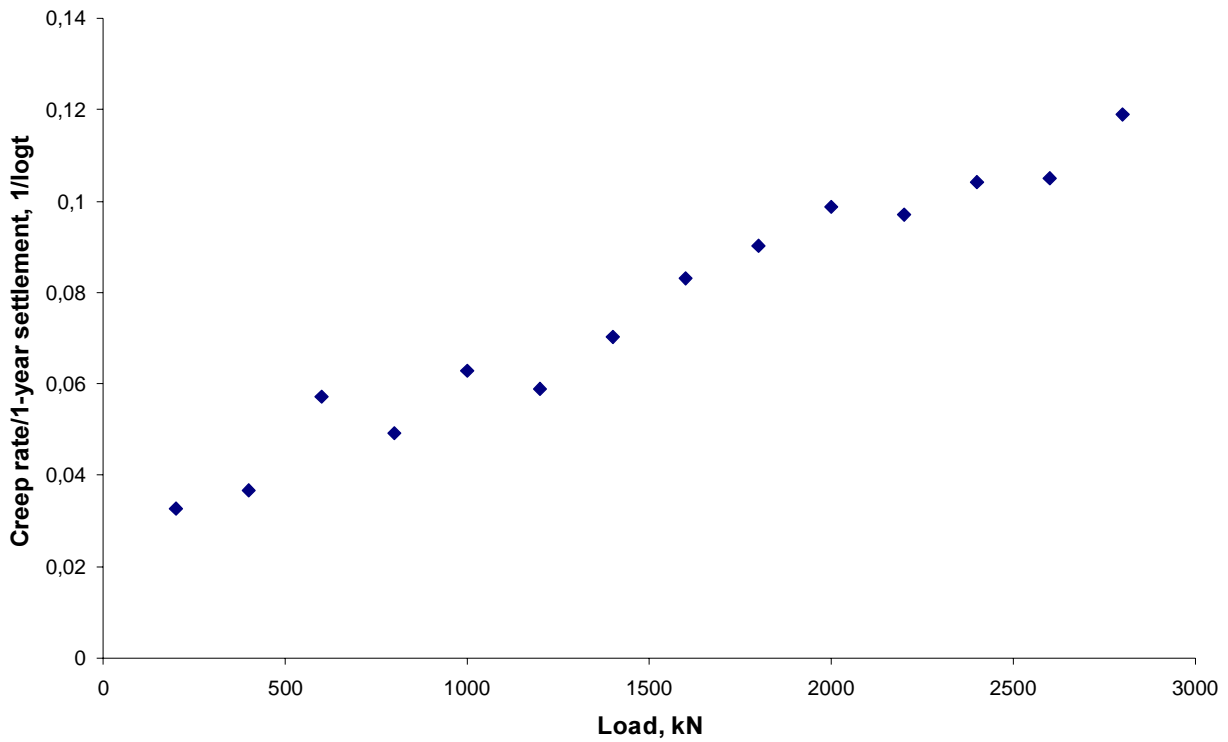


Fig. 104. Relative creep settlement rate versus load in the load test on the 2 x 2 metre plate at Tornhill.

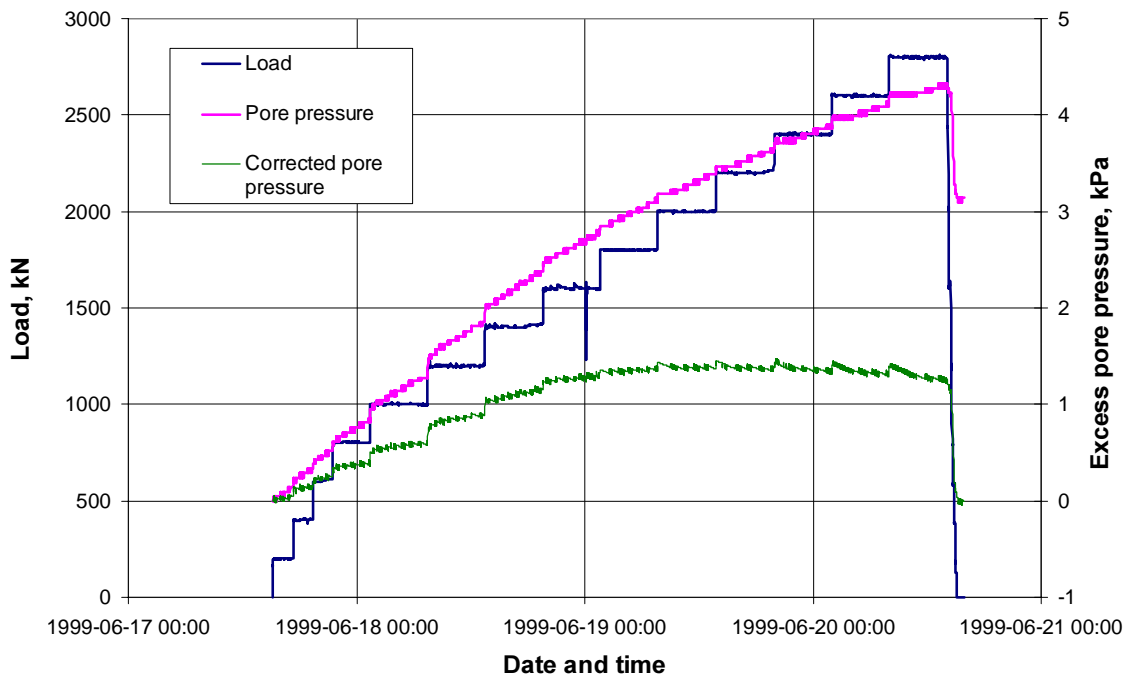


Fig. 105. Measured pore pressure changes and corrected excess pore pressure in the load test on the 2 x 2 metre plate at Tornhill.

cess pore pressures are very small and when the same correction is applied most of them disappear. From the curve, it can still be seen that there is a small increase in the pore pressure each time the load is increased and that this excess pore pressure dissipates during the load step. No significant excess pore pressures accumulated during the test and the load test can be regarded as a drained test.

### 8.5 SETTLEMENT DISTRIBUTION IN THE LOAD TESTS

The settlement distributions measured in the tests show that all significant settlements occurred within a depth of  $2b$  under the plates, Fig. 106. However, it should also be observed that the distribution of settlements with depth changes with the applied load, with more settlements occurring at greater depths as the load increases. The distribution shown in the figure refers to settlements in the stress regions where no preconsolidation stresses or creep failure loads have been exceeded.

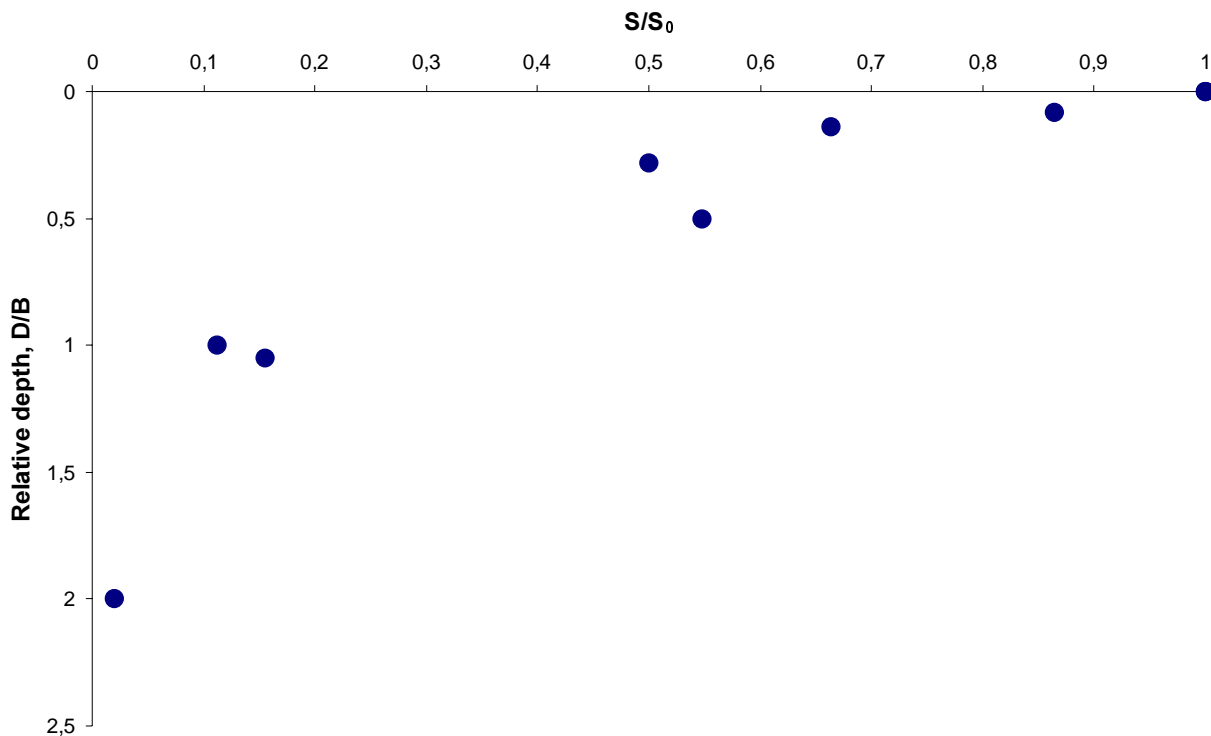


Fig. 106. Settlement distribution with depth measured in load tests at Tornhill.

## 8.6 COMMENTS ON THE PLATE LOAD TESTS

The tests were performed as planned and the plates settled vertically without any significant tilting. Actual failure was obtained for the smallest plate, whereas only the “failure load” at a relative settlement of 0.1 times the plate width was obtained for the medium size plate and the corresponding value could be extrapolated from the largest plate. However, the load - settlement curves were fairly steep at the ends of both tests and it was also possible to make a general estimate of the “ultimate failure load”. All three tests could be considered drained tests.

The relative settlements for the three plates were uneven, *Fig. 107*. The response under the 1.0 m x 1.0 m plate, which was located furthest to the east in the row, was considerably stiffer, with smaller settlements than for the other two plates. The reason for this can be found in the composi-

tion of the soil below the plates. When pumping holes had previously been dug outside the excavated area in the attempt to lower the ground water table, a large pocket of almost clean sand was found in the hole to the east of the excavation. At the same time, homogeneous clay till was found in the hole to the west. A varying composition of the material in the floor of the excavation was also observed. After the plate tests, continuous samples were taken with a screw auger at the centre of the removed plates down to a depth of twice the plate width. The results of the soil classification and the determined water contents and liquid limits clearly show that the soil in the affected compressible layers was considerably coarser below the 1.0 m x 1.0 m plate than below the other two plates, *Table 5*. These differences should be considered when comparing the results to calculated settlements and bearing capacities.

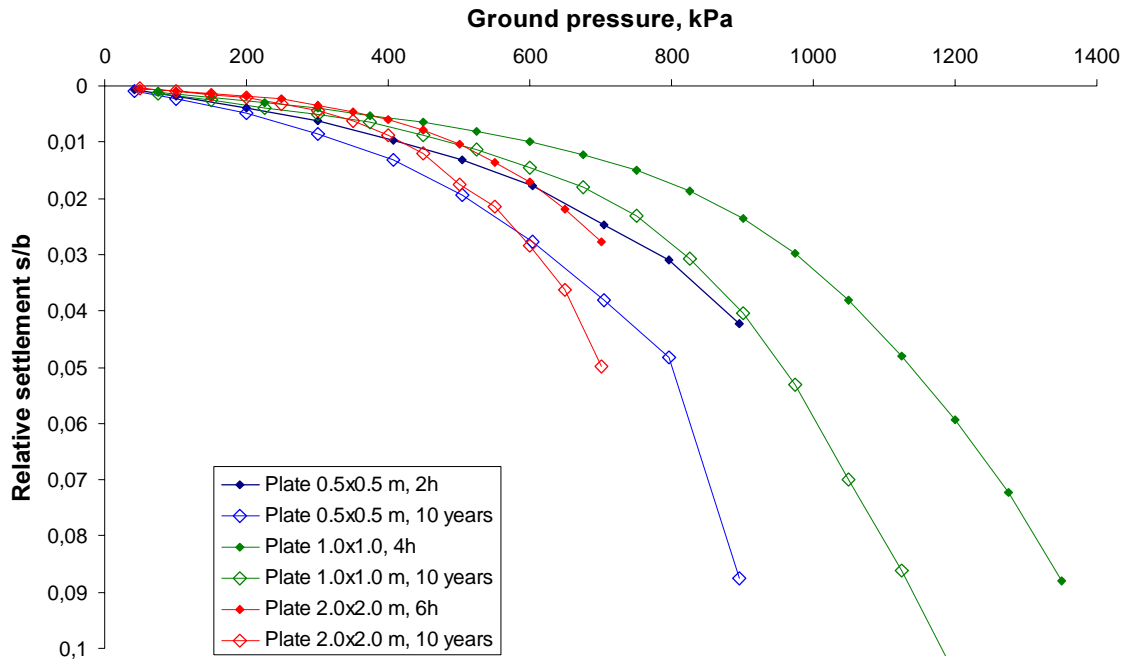


Fig. 107. Relative settlements below the plates.

Table 5. Soil profiles below the plates.

Relative depth	Plate 0.5 x 0.5 m			Plate 1.0 x 1.0 m			Plate 2.0 x 2.0 m			
	D/B	Soil type	w <sub>N</sub> , %	w <sub>L</sub> , %	Soil type	w <sub>N</sub> , %	w <sub>L</sub> , %	Soil type	w <sub>N</sub> , %	w <sub>L</sub> , %
0-0.25		Clay Till	22	42	sa si Clay Till	15	22	Clay Till	20	43
0.25-0.5		-"	22	42	-"	15	22	-"	20	43
0.5-0.75		-"	22	42	cl Sand Till	10		-"	17	31
0.75-1.0		cl sa Silt	15		sa Clay Till	14	25	-"	17	31
1.0-1.25		Clay Till	16	36	-"	14	25	sa si Clay Till	17	23
1.25-1.5		-"	16	36	si Clay Till	16	35	-"	18	26
1.5-1.75		-"	16	36	-"	16	35	-"	18	26
1.75-2.0		-"	16	36	si Sand	18		sa gr cl Till	13	17

All tests showed more or less pronounced breaks in the curves, indicating a creep load or passing a preconsolidation pressure. These breaks occurred in the ground pressure interval of about 600 – 800 kPa and thus generally correspond to the estimated level of the preconsolidation pressures from the oedometer tests. However, the preconsolidation pressures were only exceeded in su-

perficial layers and the change in modulus when passing the preconsolidation pressure is relatively moderate. At these ground pressures, also most of the estimated bearing capacity was mobilised. The break in the curves may thus also be related to a yield for excessive shear stresses in the ground.

## 9. Comparison between predicted and measured settlements and bearing capacity

### 9.1 SETTLEMENTS

The settlements have been calculated on the basis of the oedometer and triaxial tests in the laboratory and the pressuremeter and dilatometer tests in the field. A calculation has also been made on the basis of the initial shear modulus measured by the seismic CPT-tests and empirical relations for its decline with increasing strains.

#### Oedometer tests

The common method of calculating settlements using theory of elasticity and moduli from oedometer tests yielded values that were too small in relation to the measured settlements except for very small loads. In these calculations, the re-loading moduli estimated from parameters determined in the unloading-reloading loops were used up to the estimated preconsolidation pressures. For higher stresses, use was made of the moduli for the normally consolidated state calculated by the estimated modulus numbers and the current effective vertical stress.

A correction of the calculated settlements for creep effects measured in the oedometer tests approximately doubles the calculated settlements in a 10-year perspective when settlements for stresses above the preconsolidation pressure are considered. However, in most of the load steps, the effective vertical stresses remained below the preconsolidation pressures and in those steps where they were exceeded, this only occurred in a narrow zone just beneath the plate. The creep effects for stresses below the preconsolidation pressure are small and so is therefore the possible correction.

A much better estimation of the actual settlement curves was obtained when the empirical Jacobsen (1967) correction was applied. This correction is based on the estimated safety factor against bearing capacity failure. In this case, the

drained bearing capacity was calculated to be critical and approximate values of this, (see Chapter 9.2, Table 10), were used to estimate the safety factors.

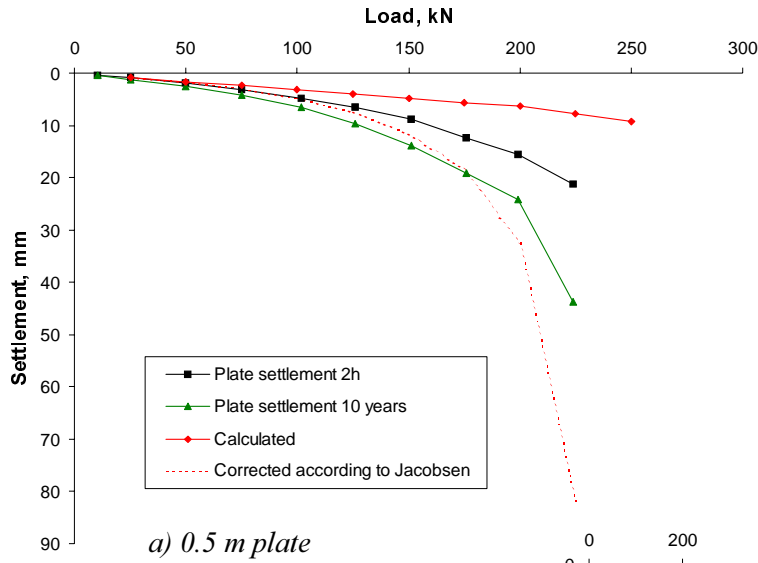
From the observations made during the tests, the loading tests were also considered to be drained. The Jacobsen correction factor includes observations of real full-scale constructions and should be fairly relevant for the design settlements, which normally refer to the 10-year settlements. In view of the heterogeneity of the soil in the test field, the correspondence between settlements estimated in this way and the extrapolated 10-year settlements from the plate load tests must be considered to be good, *Fig. 108. a-c*. The largest difference was obtained for the 1.0 x 1.0 m plate, which can at least partly be attributed to the soil conditions beneath this plate.

The corresponding empirical correction based on results from sands and silts proposed by Larsson (1996) was found to be inapplicable to the results from the clay till.

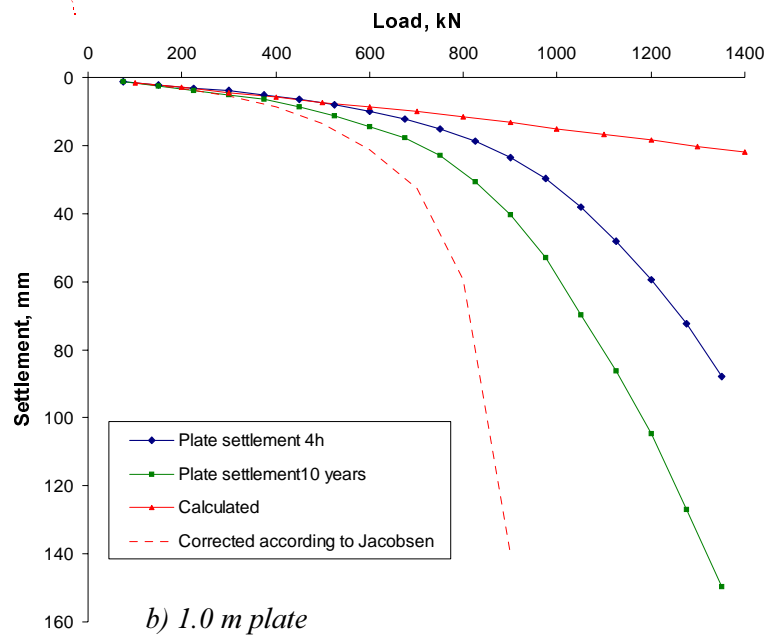
#### Dilatometer tests

The results from dilatometer tests are interpreted to yield compression moduli compatible to the oedometer moduli. These moduli are correspondingly used in the same type of calculations. For clays, the interpreted moduli may be assumed to be valid in the overconsolidated range for stresses below the preconsolidation pressure, which in principle should be relevant for the current cases.

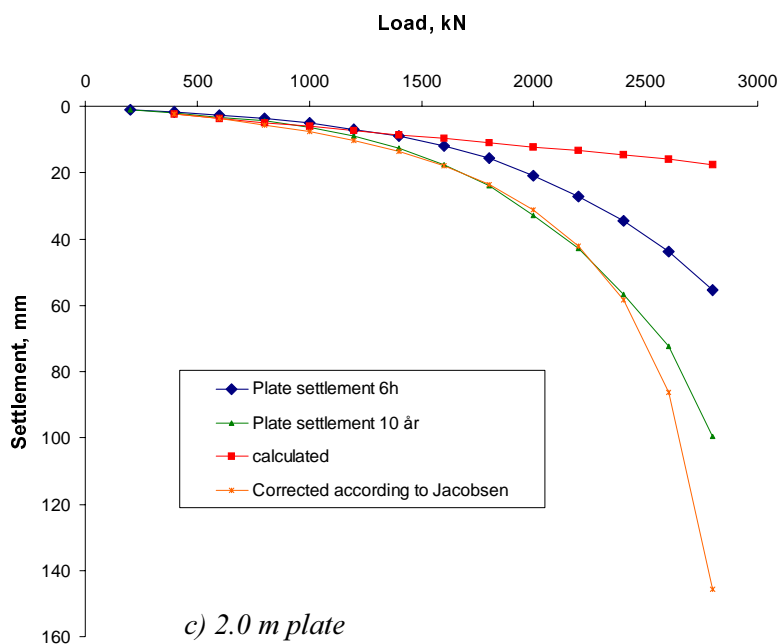
The oedometer moduli and the dilatometer moduli were generally of similar sizes. However, the dilatometer tests were performed in the natural ground before the excavation was made, whereas the oedometer tests were performed and interpreted to include this unloading. The moduli in the oedometer tests were also interpreted from



a) 0.5 m plate



b) 1.0 m plate



c) 2.0 m plate

Fig. 108. Comparison between measured and extrapolated settlements and settlements calculated from results from oedometer tests.



the unloading-reloading loop, where the disturbance effects are largely eliminated. Possibly as a consequence of this, the dilatometer moduli were higher than the oedometer moduli in the upper part of the profile and then became lower further down. This variation can also be seen in the calculated settlements, in that the settlements for the smallest plate calculated on the basis of dilatometer moduli become significantly smaller than those measured and calculated from oedometer test results. Beneath this plate, only the uppermost part of the profile was affected by the load. For the larger plates, where larger parts of the profiles were affected, the calculated settlements became more similar. Since the moduli evaluated from the dilatometer tests correspond to oedometer moduli, it should be appropriate to apply the Jacobsen correction also in these calculations. This is verified by the comparison with the load test results, *Fig. 109*.

Also the calculated settlements from the dilatometer tests can thus be considered to be fairly relevant after a correction according to Jacobsen (1967). However, effects of softening because of unloading and other changes in the conditions in relation to those prevailing during the test cannot be taken into account.

## Pressuremeter tests

### Menard procedure

The traditional way of calculating settlements from results from pressuremeter tests is the semi-empirical Menard procedure. This calculation yields a straight load-settlement relation and the calculated settlements should be applicable for normal ground pressures and the design time for the construction, i.e. about 10 years. The normal ground pressures should in this case be up to 400 kPa, which corresponds to loads of 100, 400 and 1600 kN on the respective plates. A comparison with the measured and extrapolated load settlement relations shows that this is mainly the case also in the current case, *Fig. 110*. The main difference involves the smallest plate, where the calculated settlements are on the low side. This may to some extent be attributed to the softening because of the excavation.

The Menard procedure involves the use of a rheological factor  $\alpha$ , which is selected on the basis of soil type and the relation between the pressuremeter modulus,  $E_M$ , and the net limit pressure,  $p_L^*$ , evaluated from the test results. In the current case, the soil classification “overconsolidated clay” would yield an  $\alpha$ -factor of 1, whereas the average  $E_M/p_L^*$  relation of just below 16 would yield an  $\alpha$ -factor of 2/3. Calculations have been made using both factors and the  $\alpha$ -factor of 1 was found to be most appropriate.

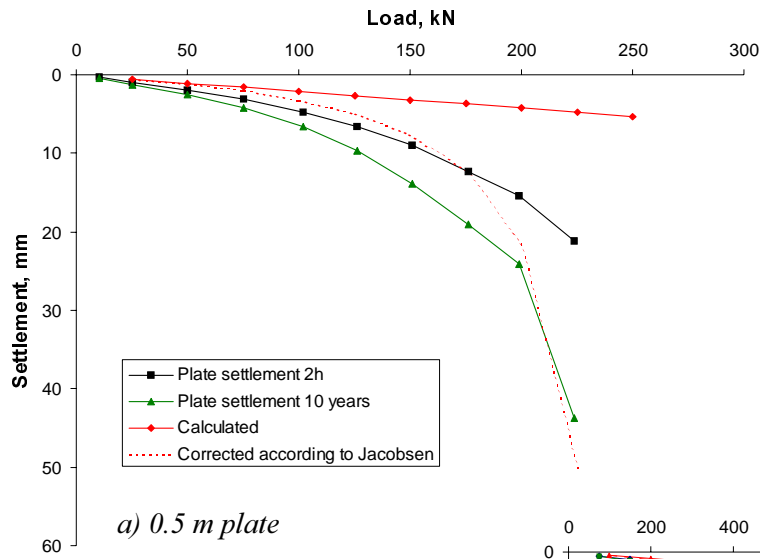
Since the calculations with the Menard procedure yield linear load-settlement relations, the settlements for small loads become overpredicted and the settlements for higher loads than the normal ground pressures become underestimated.

### Briaud procedure

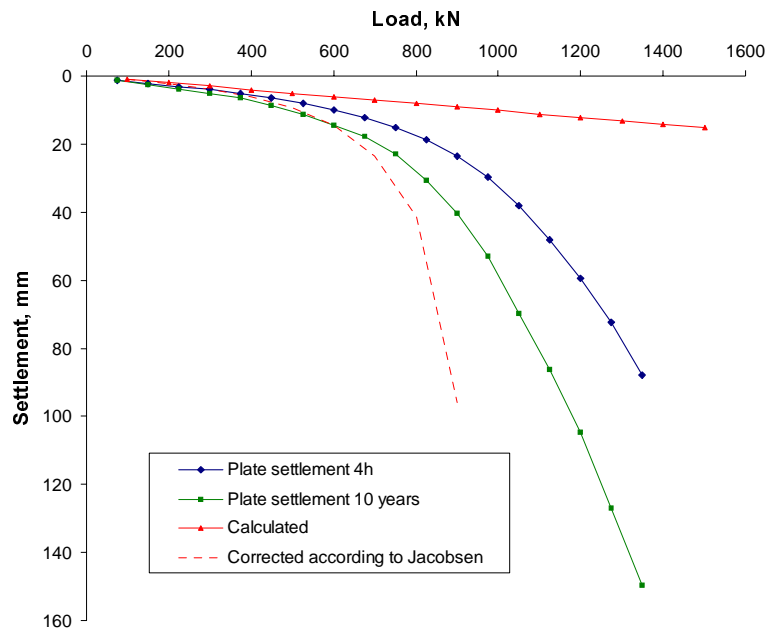
The Briaud procedure uses a weighted average of the actual pressuremeter curves as described in appendix. The results from all Menard pressuremeter tests have therefore been corrected and plotted according to Briaud’s procedure, *Fig. 111*.

The results have then been weighted in relation to their influence for the particular plate and combined into average pressuremeter curves for each plate, *Fig. 112*.

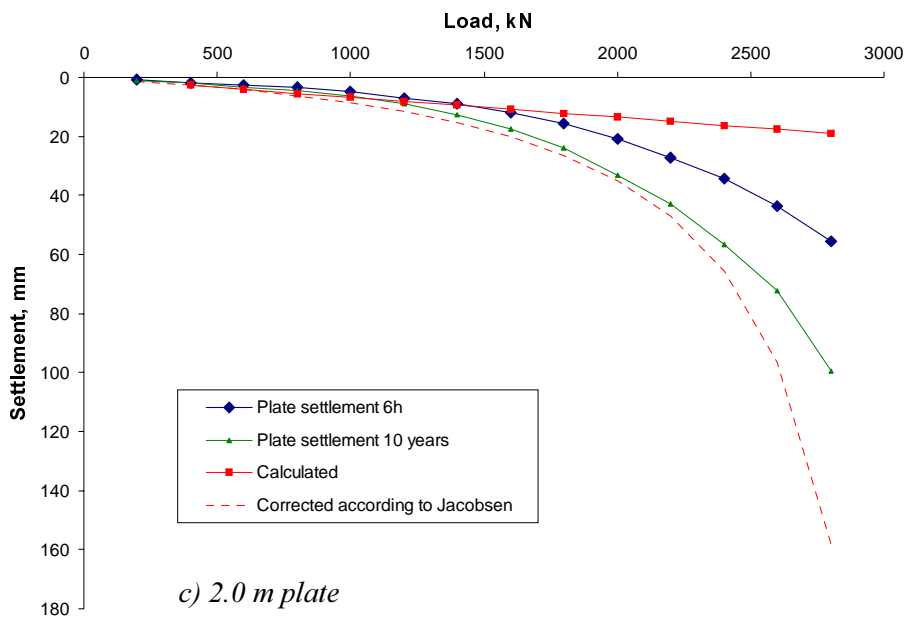
The average pressuremeter curves have then been converted into load-settlement curves according to Briaud. For this purpose, both the conversion factors proposed by Briaud (1995) and the factors later suggested by Larsson (1997) have been applied. For transformation of the 1-minute readings in the pressuremeter tests to the actual loading times in the plate load tests and to 10-year values, an exponent  $n_{pmt}$  of 0.047 has been used. This value was evaluated from holding periods during the new type of pressuremeter tests. The scatter was relatively small. In the translation, both the value of 0.047 and twice this value, as proposed by Briaud, have been used as exponents.



a) 0.5 m plate



b) 1.0 m plate



c) 2.0 m plate

Fig. 109. Comparison between measured and extrapolated settlements and settlements calculated from results from dilatometer tests.

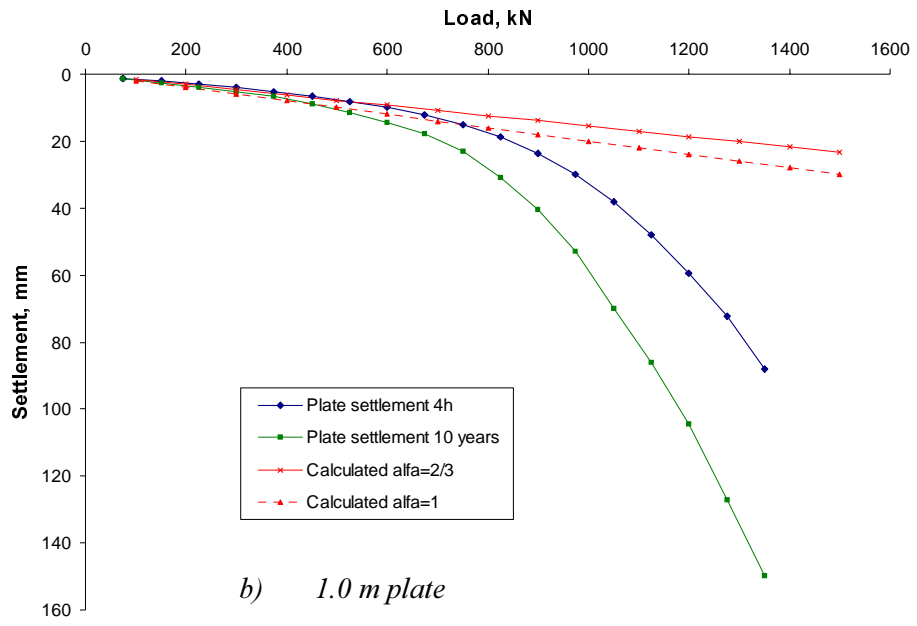
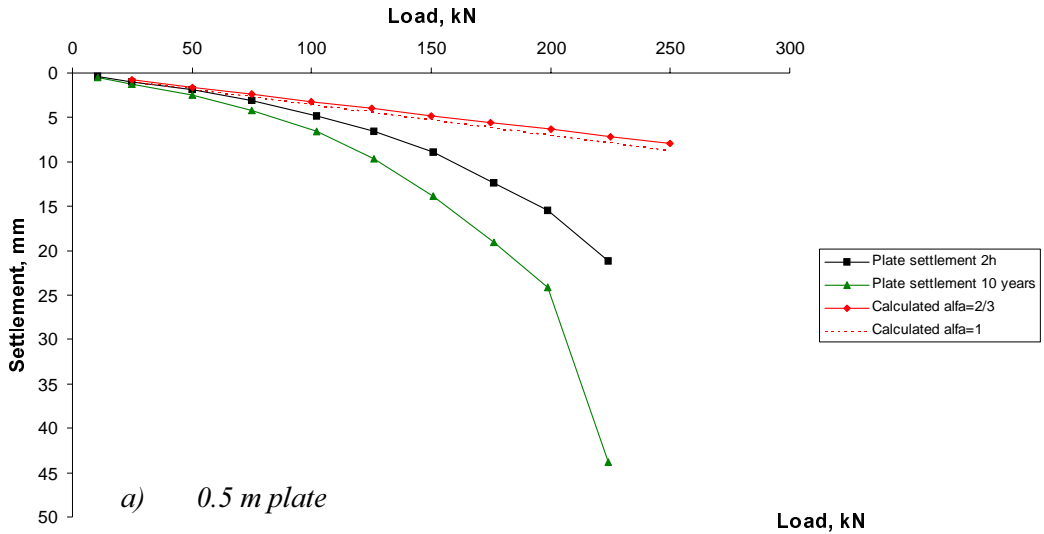
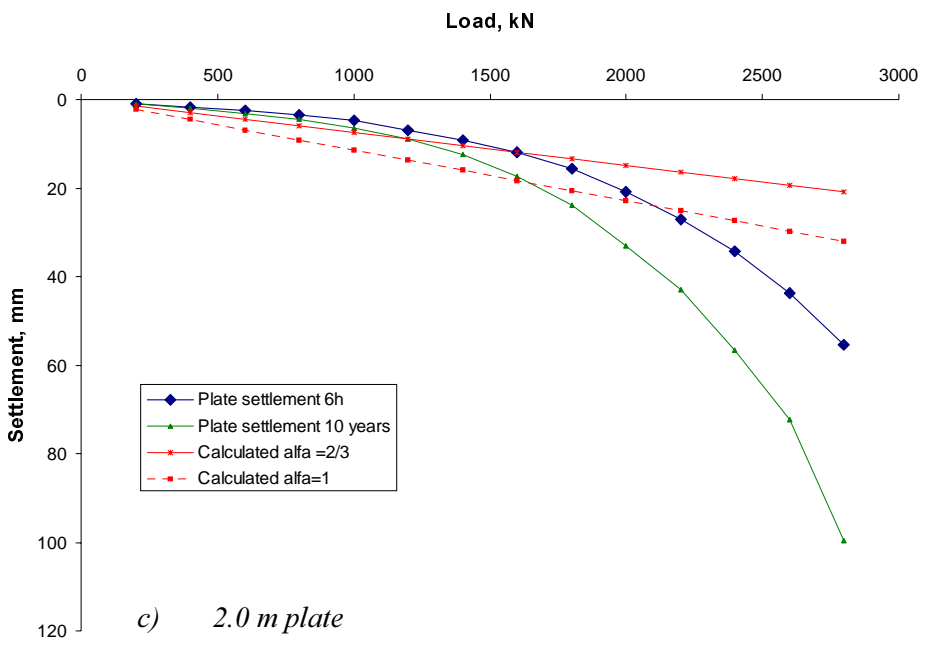


Fig. 110.  
Comparison between measured and extrapolated settlements and settlements calculated from Menard pressuremeter tests.



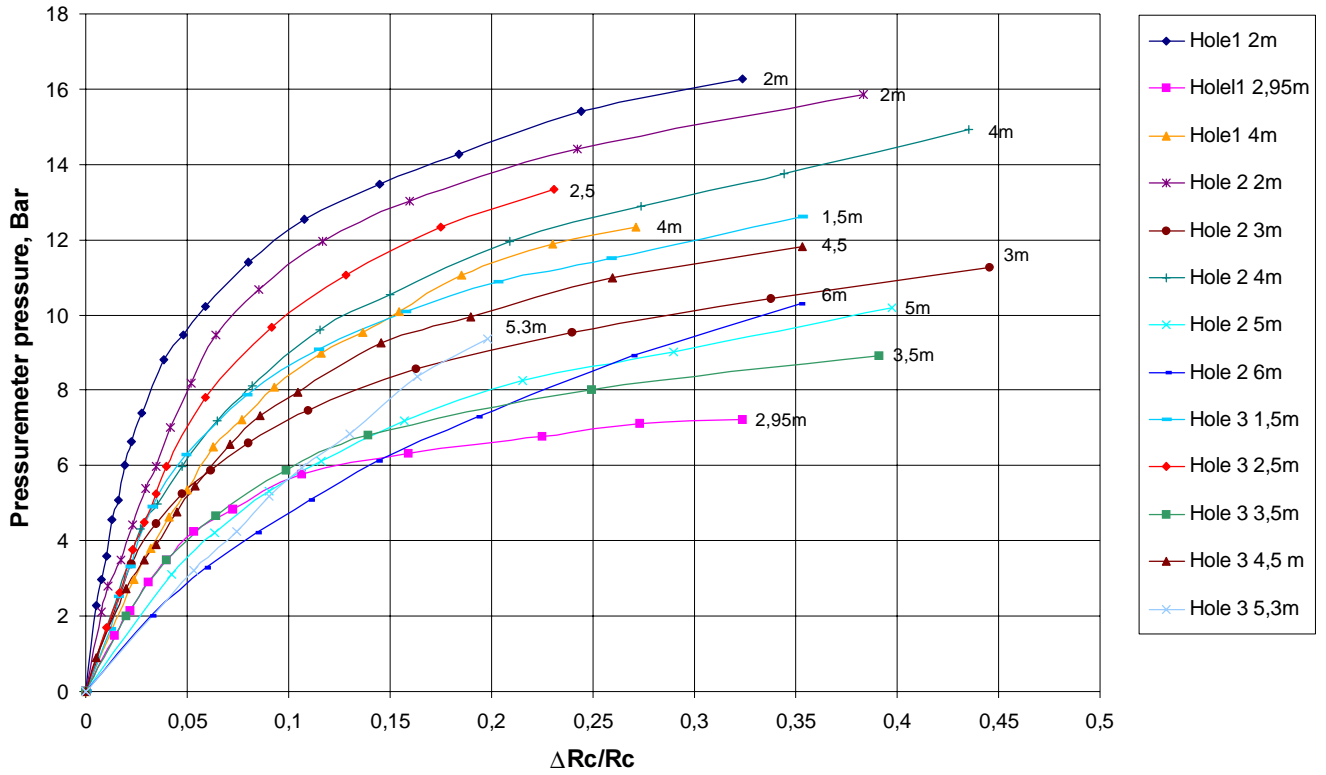


Fig. 111. Pressuremeter curves plotted according to Briaud.

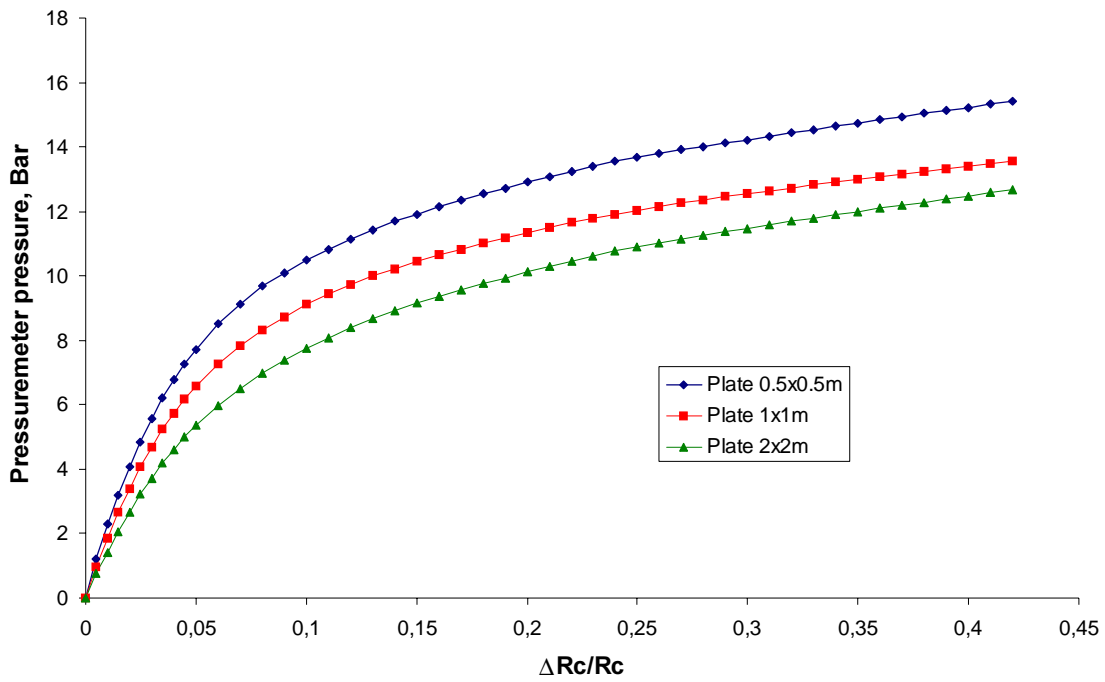
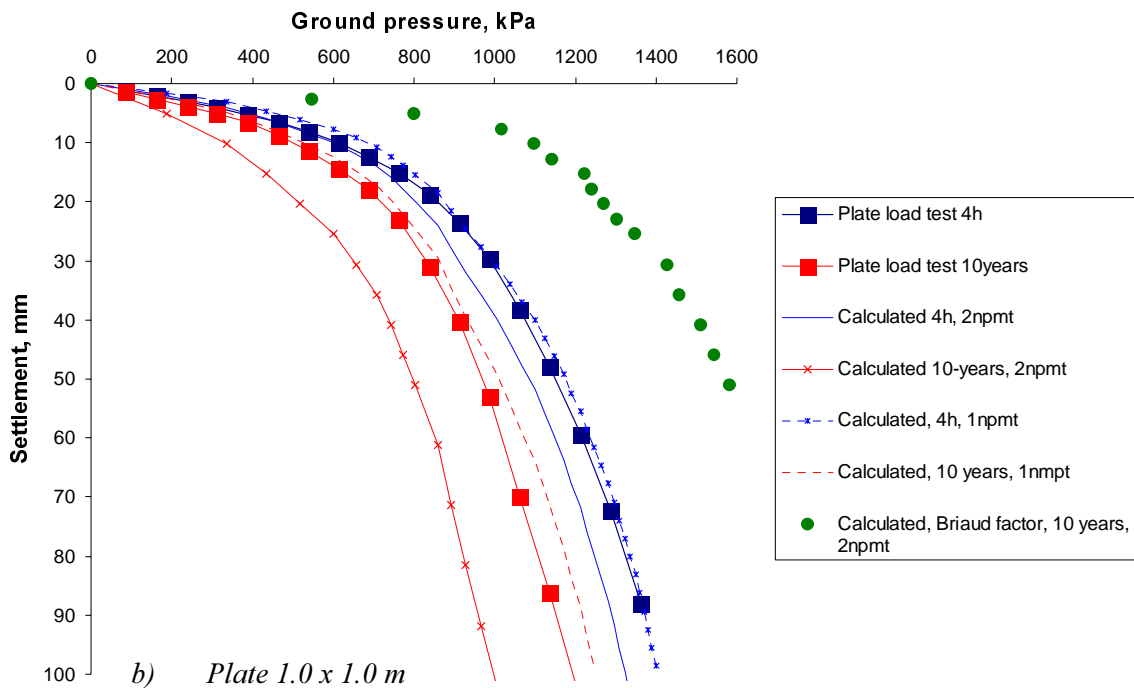
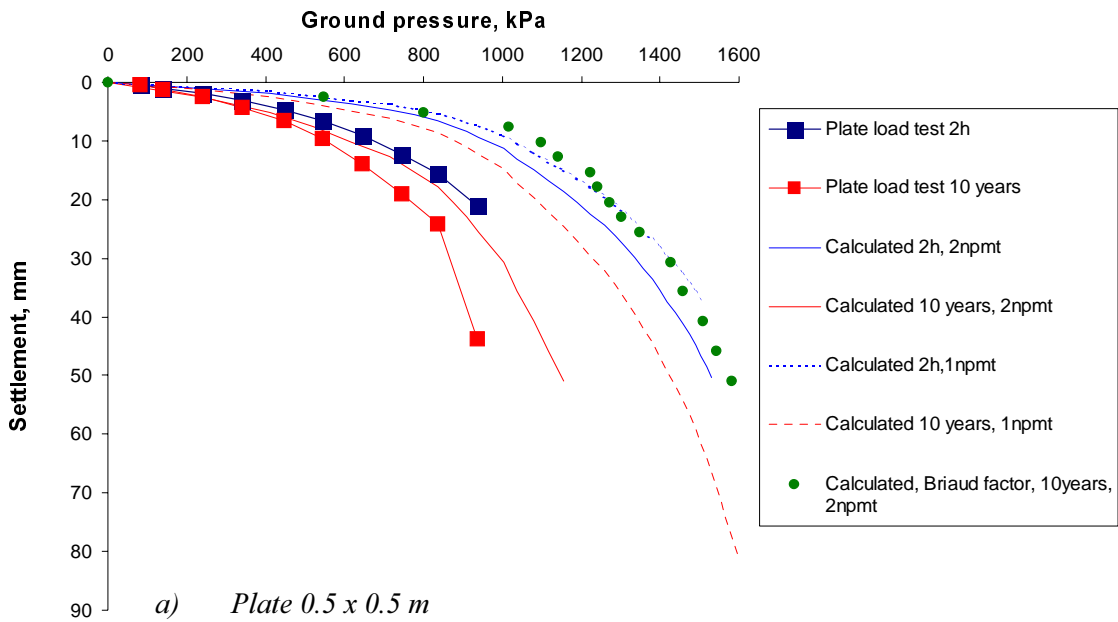


Fig. 112. Average pressuremeter curves for the three plates.

The calculated load-settlement curves are compared to the results from the plate load tests in *Fig. 113 a-c*.



*Fig. 113. Comparison between measured and extrapolated load settlement curves from the plate load tests and relations calculated on the basis of ordinary pressuremeter tests according to the Briaud procedure. Unless otherwise stated, the SGIΓ-factors, (Larsson (1997)), have been used.*

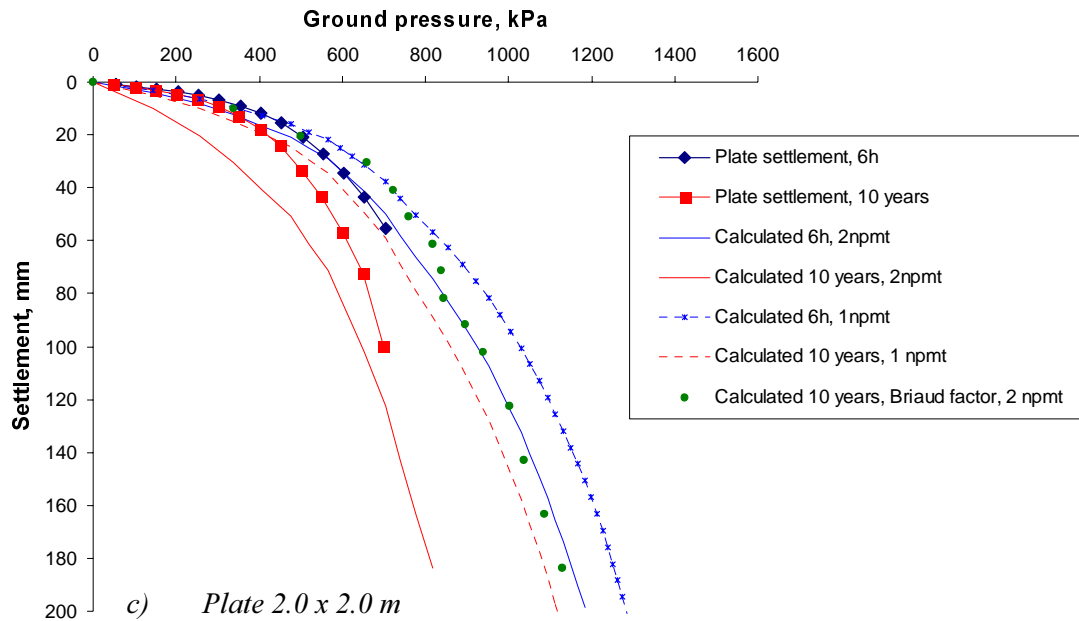


Fig. 113. Comparison between measured and extrapolated load settlement curves from the plate load tests and relations calculated on the basis of ordinary pressuremeter tests according to the Briaud procedure. Unless otherwise stated, the SGI  $\Gamma$ -factors, (Larsson (1997), have been used.

The comparisons showed directly that the  $\Gamma$ -factors proposed by Briaud (1995) for sand were too large for the clay till. This was mainly found also for silts and sands in Sweden and was then tentatively attributed to the quality of the test cavity (Larsson 1997). Since test cavities in stiff clay may be expected to be of higher quality than in sands, the  $\Gamma$ -factors may be expected to be smaller. The factors proposed by Larsson appear to be of the right size also for the clay till in the current investigation, but the spread in the results is too large to enable a more exact evaluation. In the presented figures, the calculations using Briaud factors are only shown for 10-year settlements estimated with a maximum time exponent of  $2 \times 0.047$ . The other curves calculated with these factors are located further up and to the right in the diagrams.

The use of a doubled time exponent appears to be somewhat exaggerated, while most of the results indicate that the evaluated exponent from the tests is not quite sufficient. Except for the smallest plate, where the results may be seriously affected by unloading effects from the excavation, the use of the evaluated exponent directly as it is appears to yield more relevant results in terms of settlements within normal loading ranges. However, the real load settlement curve becomes steeper at higher loads and this time correction of the test results may not be sufficient for estimation of the failure load.

The calculations using the Briaud procedure with SGI conversion factors and the measured time relation thus predict fairly well the actual shapes of the load-settlement curves. However, possible effects of an excavation entailing swelling and softening after the tests have been performed cannot be taken into account and the failure load may be somewhat overestimated.

### **Ekdahl and Bengtsson procedure**

The evaluation and calculation procedure proposed by Ekdahl and Bengtsson (1996) has been used for the results from the pressuremeter tests with the new equipment. The calculations have been made with the FLAC finite difference programme and the load steps have been considerably smaller than in the originally proposed procedure. The calculations have been performed with the parameters determined from the unloading-reloading loops and the time dependence determined from the holding tests performed as part of the test procedure.

In the calculations, the stress conditions in the ground have been simulated starting with the initial stresses evaluated from the various field tests and followed by the excavation. The plate load has then been applied. One of the problems in the calculations has been the assumption about the stress transfer between the plate and the ground. The plates were placed in slightly larger holes extending 0.2 m deeper than the rest of the excavation. The gaps between the plates and the surrounding soil were filled in after the moulds had been removed. The assumed stiffness in the refilled material, even if low, had a significant effect on the calculated load transfer and settlements. However, it was difficult to estimate this stiffness and the shear strength parameters between the plate and the back-filled soil outside. In the final calculations, the stress transfer from the sides of the plates to the surrounding soil was therefore assumed to be zero. The assumed shear strength of the material also had an effect on the calculated stress transfer within the soil, since very high shear stresses developed beneath the edges of the plates. Based on the observations during the tests, the drained shear strength was assumed to be most relevant and was therefore used. Higher stress transfer and shear strength would have allowed more of the load to be transferred to the soil outside the plate, resulting in lower stresses and strains beneath it. The stiffness of the plate itself had to be assumed to be very high to avoid a significant calculated bending of the plate.

The calculations have been performed in accordance with the original procedure outlined in appendix “Calculation methods”. In this case, the calculated load-settlement curves assumed shapes of the same pattern as the load tests, i.e. successively bending downwards, in contrast to previous calculations for clay tills. The reason for this is that the tests in the current investigation yielded higher initial moduli, larger reductions in moduli with strains and smaller increases in moduli with increasing stresses compared to the previous tests. For higher loads, the calculated stress-strain curves are also somewhat affected by the shear strength being exceeded locally beneath the edges of the plates, which results in larger shear strains and larger reductions in shear modulus.

The compatibility of the calculated results with the actually measured settlements varies. For the smallest plate, the calculated settlements became very similar to the measured values in the normal working range, but larger at higher loads, where they rapidly increased, leading to failure for excessive deformations. For the 1 x 1 m plate, which was lying on coarser soil and had the stiffest response, the calculated settlements became larger than the actually measured values throughout the loading range and for the largest plate, the calculated settlements became more similar to, but still larger than, those measured,

*Figs 114 a-c.*

In the original Ekdahl and Bengtsson procedure and calculation programme, the shear moduli are reduced in relation to the calculated vertical strains. If, instead, the reduction is made on the basis of calculated shear strains, the calculated settlements become larger and the load-settlement curves bend off much more sharply at a critical load, *Fig. 115 a-c*. This is related to the large shear strains, particularly when the shear strength beneath the edges of the plates is exceeded. The calculated settlements thereby show a poorer correlation with those measured in the plate load test results.

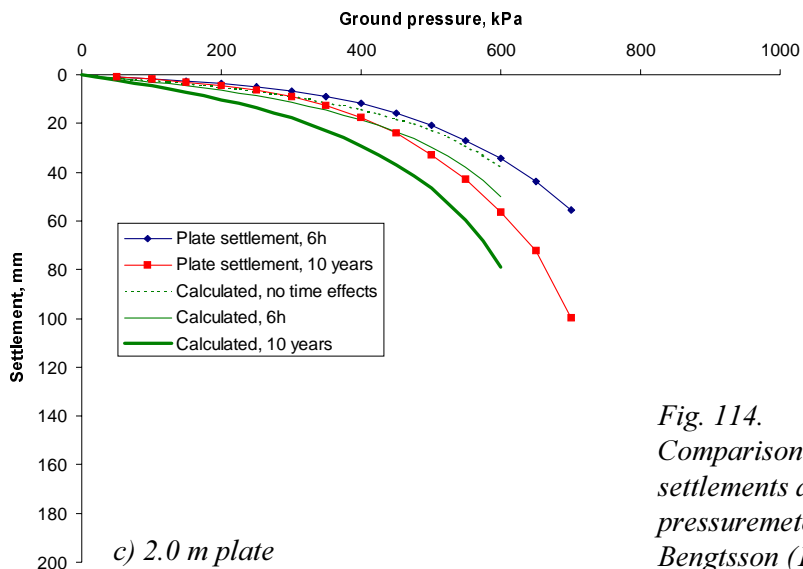
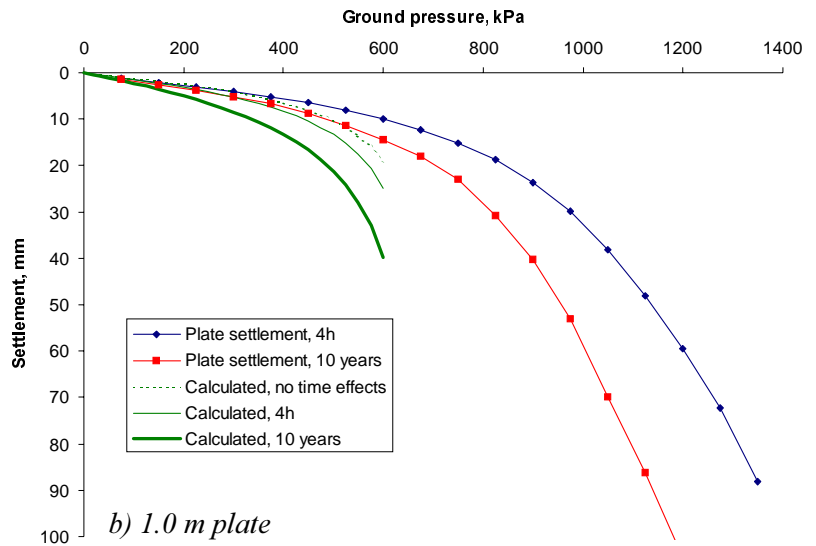
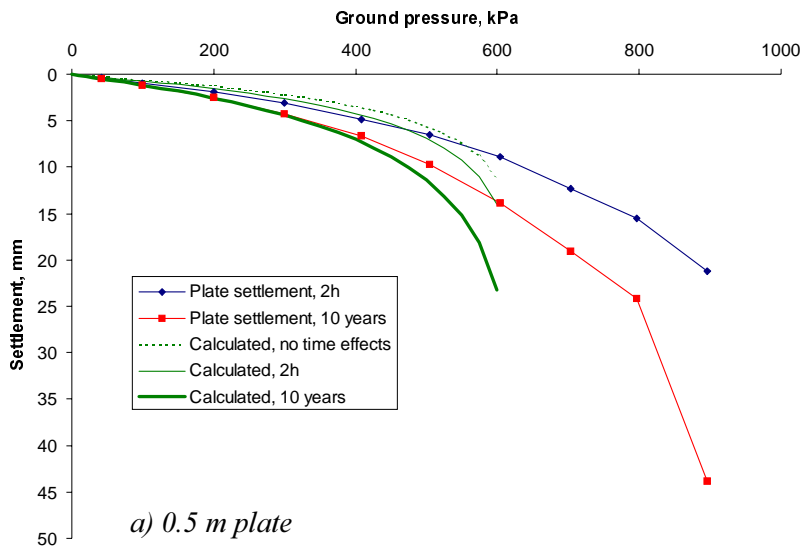


Fig. 114. Comparison between measured and extrapolated settlements and settlements calculated from new pressuremeter tests following the Ekdahl and Bengtsson (1996) procedure.



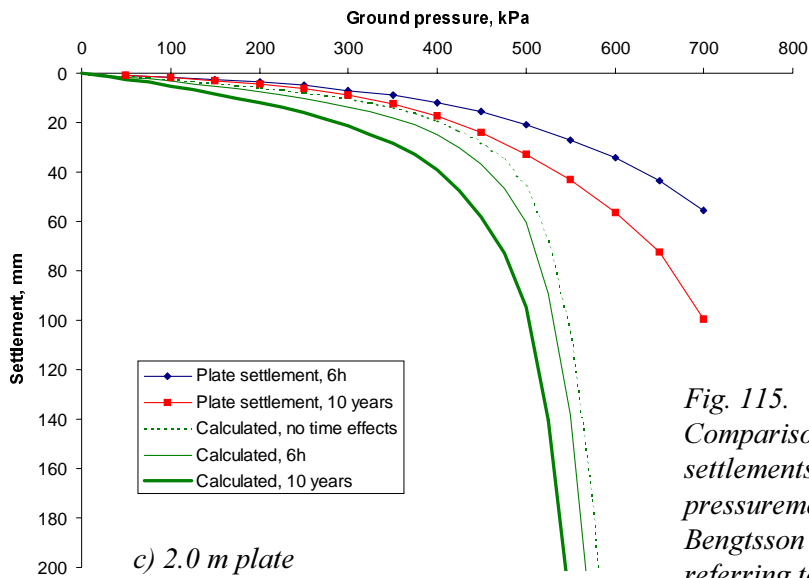
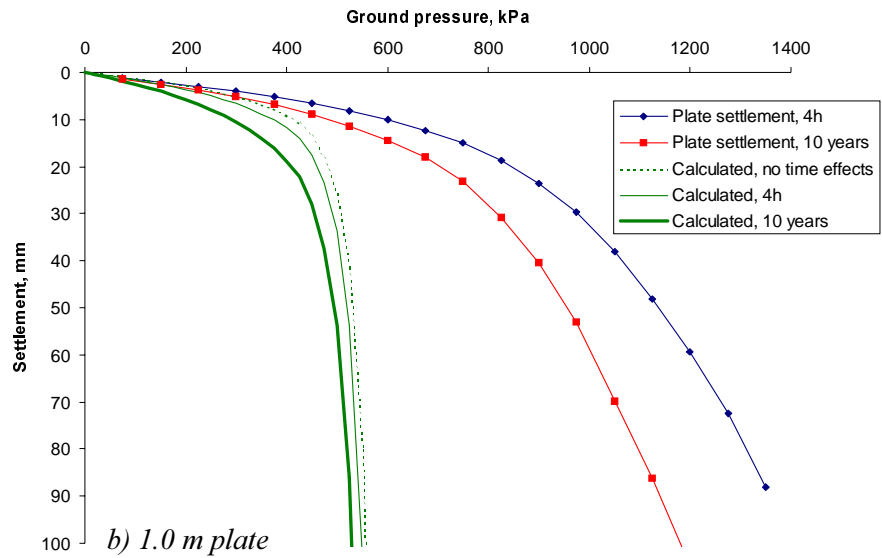
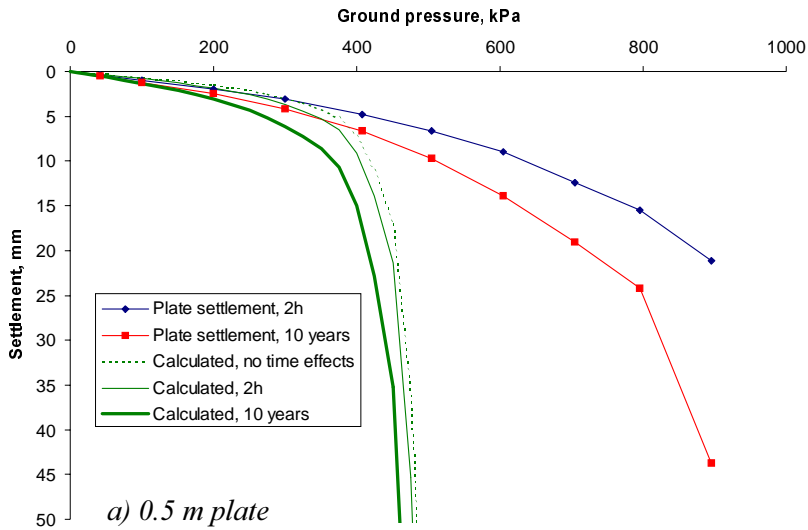


Fig. 115. Comparison between measured and extrapolated settlements and settlements calculated from new pressuremeter tests following the Ekdahl and Bengtsson (1996) procedure but using moduli referring to shear strain.

As stated above, the calculations are very sensitive to assumptions about load distribution and shear strength. A load transfer between the sides of the plates and the surrounding soil results in lower stresses beneath the plates, a higher critical load and a smaller curvature of the load-settlement curve up to this load. An assumption of higher shear strength also increases the critical load and lessens the curvature. The relevance of the measured moduli and the method for calculating settlements is thereby primarily reflected in the first part of the curves for relatively low stresses. The remainder of the calculated curves become more and more dependent on the assumptions on load transfer and shear strength as the stresses increase.

#### **Calculations using the alternative interpretation of the new pressuremeter tests**

The same calculations as in the previously described procedure have been made using the alternative formulation of the variation of the modulus described in "Evaluation of moduli at small strains". In these calculations, also the preconsolidation pressures determined from the oedometer tests have to be introduced. They are used in calculating both the initial modulus and its decline as the preconsolidation pressure is re-approached during loading. These calculations thus become very sensitive both to the determination of the preconsolidation pressure and the calculation of the stress distribution and current stress level in the ground. On the other hand, they are less sensitive to the assumption on shear strength since the reduction in modulus is related to stress and not to strains.

The formulation of the modulus in practice leads to failure when passing the preconsolidation pressure. The calculations cannot therefore be continued for stresses higher than the preconsolidation pressure without introducing another modulus formulation for higher stresses. This has not been done here. The calculations have thus been performed up to the vertical stress where the preconsolidation pressure is exceeded in the uppermost layer. The calculations yield smaller

settlements until the preconsolidation pressure is approached and a more brittle behaviour when passing a critical creep pressure than the calculations with the previous formulation of the modulus, *Fig. 116*. The relation between the two types of calculations varies with the assumptions on load transfer and shear strength.

#### **Calculations based on the results of triaxial tests**

The calculation procedure has also been used together with the modulus parameters evaluated from the triaxial tests. The triaxial tests were mainly undrained, but the emphasis in the evaluation was put on relatively small strains, where the difference between drained and undrained moduli is small. The modulus parameters were assumed to relate to 1-day deformations and the 10-year settlements have been calculated on the assumption of a 10 % increase per log cycle of time. These calculations also produced load-settlement curves of similar shapes to the measured curves. In general, the results were very similar to those calculated from the pressuremeter test results using the Ekdahl and Bengtsson procedure and moduli related to shear strains and the soil response in the load tests showed a significantly higher stiffness than the calculated response, *Fig. 117*. Once again, the results are very dependent on the assumptions on load transfer and shear strength.

#### **Calculation with moduli from seismic cone tests**

A final calculation with the same calculation procedure was made using moduli estimated from the seismic cone tests. In these tests, only the initial shear modulus  $G_0$  at very small strains is measured. This value then has to be converted to a modulus that varies with strain by using empirical relations.

According to Hardin and Drnevich (1972), the change in modulus with shear strain can be expressed by the modified hyperbolic stress-strain relation

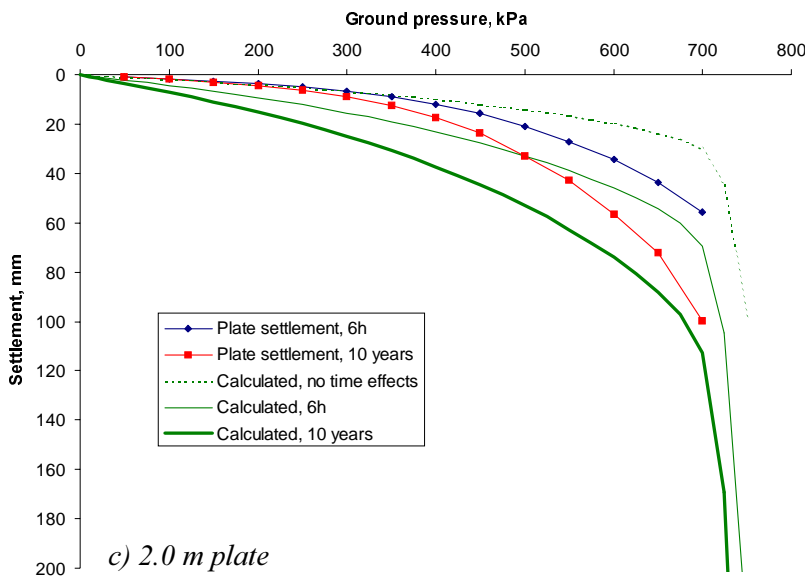
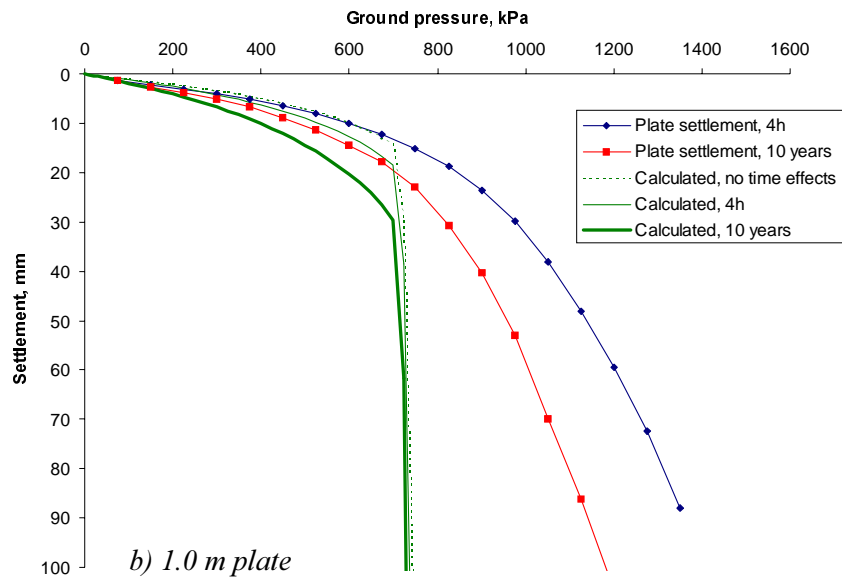
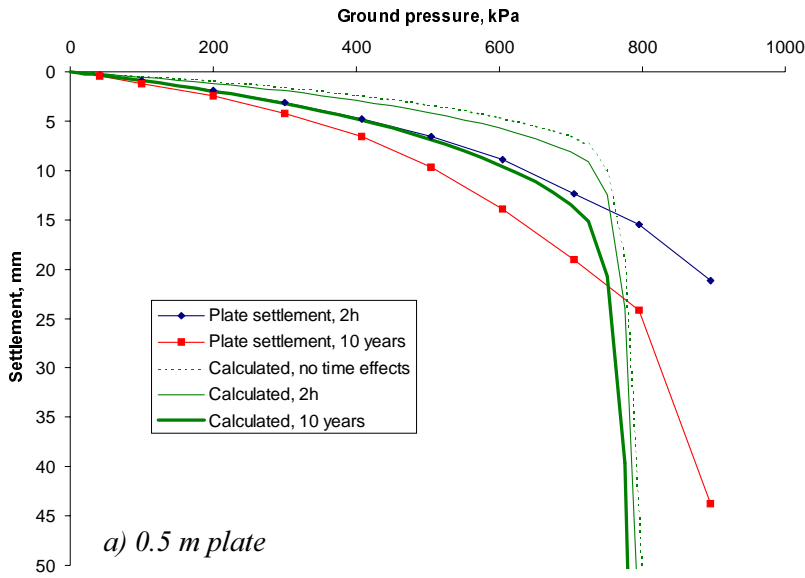


Fig. 116. Comparison between measured and extrapolated settlements and settlements calculated from the new pressuremeter tests and the alternative formulation of the modulus.

Comparison ...

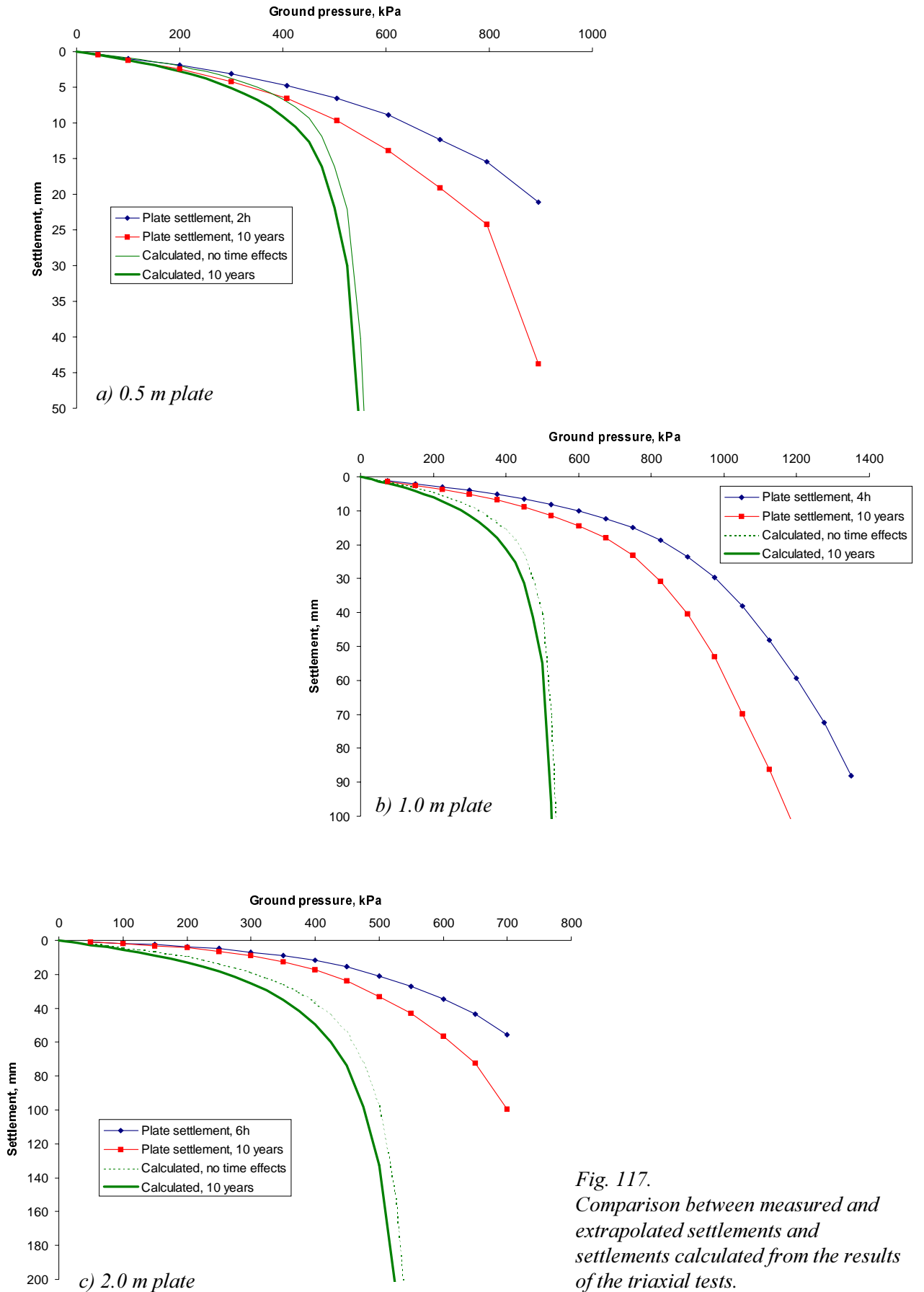


Fig. 117. Comparison between measured and extrapolated settlements and settlements calculated from the results of the triaxial tests.

$$G = \frac{G_0}{1 + \gamma_h}$$

where

$$\gamma_h = \frac{\gamma}{\gamma_r} \left( 1 + ae^{-b \frac{\gamma}{\gamma_r}} \right)$$

In this expression

$\gamma$  = shear strain

$\gamma_r$  = reference strain,  $\tau_{max}/G_0$

$a$  and  $b$  = material constants. For saturated clay,

$$a \approx 1 \text{ and } b \approx 1.3$$

$e$  = base of the natural logarithm,  $\approx 2.72$

For  $\tau_{max}$ , the undrained shear strength may be used. An estimation of the undrained shear strength is obtained directly from the results of the seismic cone penetration test and these values have been used in the present calculations.

The Hardin and Drnevich relation is an average relation, which should be modified with respect to the composition of the particular clay. The variation in modulus versus shear strain for different types of clayey soils has been presented by Vucetic and Dobry (1991). In the present soil profile, an average value of the plasticity index would be about 12 %. The curve corresponding to this plasticity index according to Vucetic and Dobry is almost identical to the curve obtained if a shear strain of  $2.2\gamma$  is used in calculating the actual shear modulus with the given equation, *Fig. 118*.

The modulus - strain curves estimated in this way are shown in *Fig. 119*.

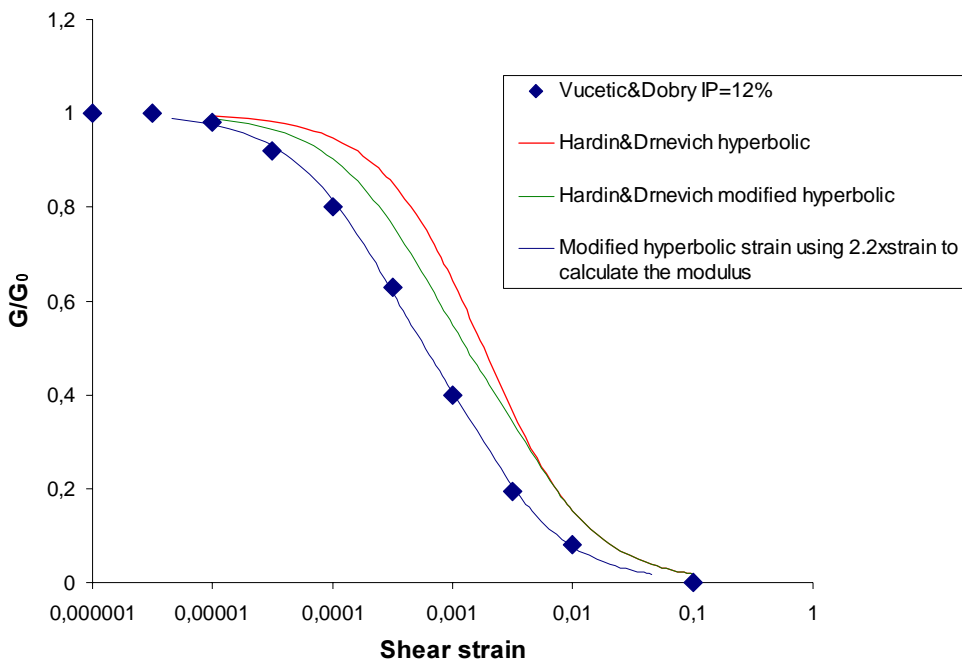


*Fig. 118. Comparison between the modulus-shear strain relation for  $I_p = 12\%$  given by Vucetic and Dobry and the hyperbolic and modified hyperbolic relation obtained by the Hardin and Drnevich equations.*

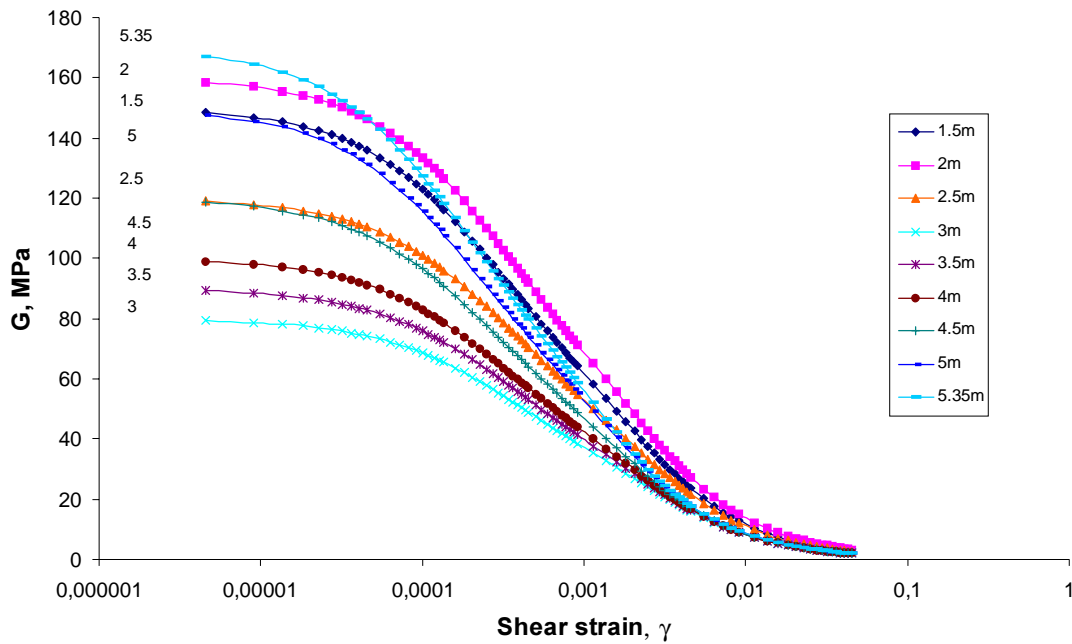


Fig. 119. Modulus-strain relations estimated from initial shear moduli from seismic cone tests and Vucetic and Dobry's empirical relations for modulus reduction with strain.

Use of the initial shear modulus entails a very stiff calculated initial response, which then breaks down with increasing stresses and strains. The initial moduli determined by the seismic cone are several times larger than the corresponding moduli from the pressuremeter or triaxial tests. However, the empirical relations imply that these high moduli are rapidly reduced when the stresses increase, particularly in low plastic soils. Compared to the other types of tests, the initial shear modulus is determined at very rapid loading and the time corrections would be considerable. However, there are no guidelines for how such a correction should be performed. In this case, the seismic loading has been assumed to correspond to a time of about 1 millisecond and the conversion to plate loading times has been made using a time exponent of 0.05.

The calculations yielded load-settlement relations that were initially stiffer than those measured, but which then sharply bent off at a critical pressure, Fig. 120. Considering the very large and crude correction for time effects, the relevance of these calculations may be seriously questioned.

### Comments on the settlement calculations

For reasons described earlier, the reference data from the plate load tests contained a considerable scatter. The comparison between calculated and measured settlements should be made with this in mind.

The earlier, best-proven methods for estimating settlements in this type of soil are using oedometer tests or Menard pressuremeter tests. When the empirical correction factor proposed by Jacobsen (1967) was applied, the straightforward calculation using oedometer moduli proved to give the best overall fit to the measured settlements. However, even if the calculations are simple, the cost for taking undisturbed samples and performing an adequate number of oedometer tests for obtaining the required parameters is high. A fairly good estimation of the settlements was also obtained when using oedometer moduli evaluated from dilatometer tests and treated in the same way as those estimated from the oedometer tests. The cost for obtaining these moduli is much less, but no other reference data exist for this type of soil to verify that this agreement is general.

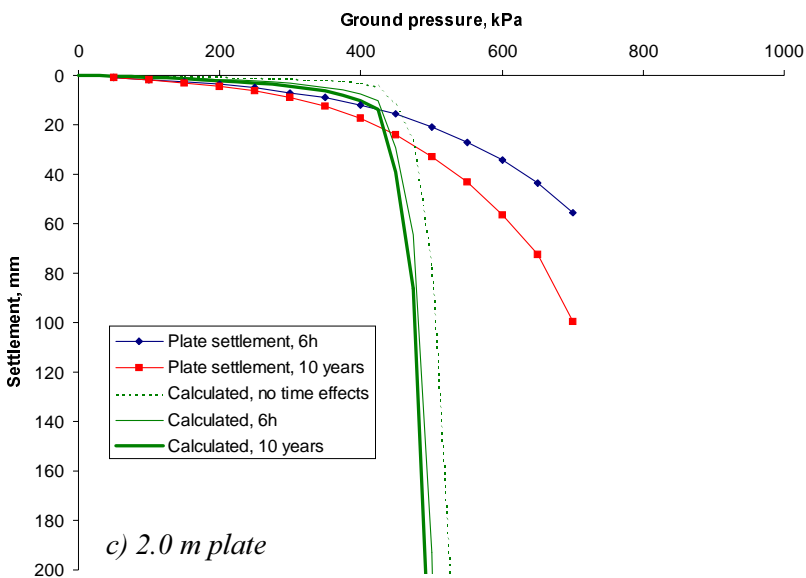
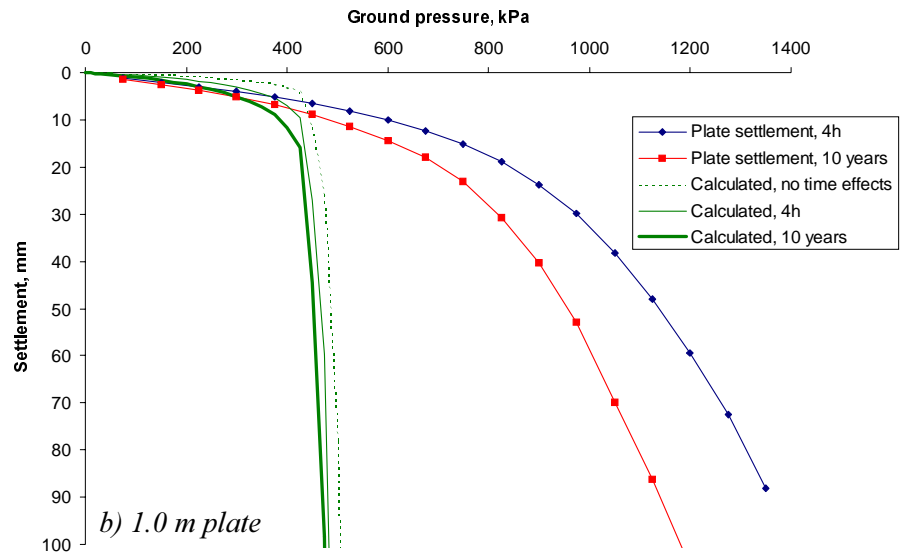
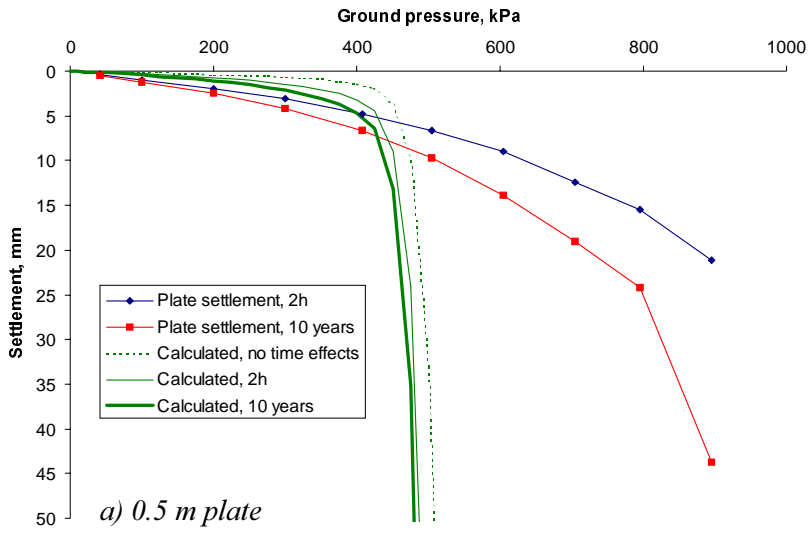


Fig. 120.  
Comparison between measured and extrapolated settlements and settlements calculated from the results of the seismic cone tests.

The Menard type of pressuremeter test, evaluation and calculation yields straight-line load-settlement relations that are intended to yield relevant settlements within the normal range of permitted loads. This was found also in this case. The cost for this procedure is higher than for the dilatometer tests, but still relatively low. The Briaud procedure of calculating settlements from the same type of pressuremeter tests yielded load-settlement curves more similar in shape to the measured curves and thereby provided somewhat better predictions for the whole loading range. This assumes that the SGI factors and a time exponent of  $1 \cdot n_{\text{pmt}}$  are used. The cost for this procedure is only marginally higher than for the Menard procedure.

Calculations using the Ekdahl and Bengtsson procedure for results from the new type of pressuremeter tests yielded load-settlement curves of the same shape and settlements approximately equal to or somewhat larger than the measured values. This assumes that the original procedure is followed. A stricter evaluation of the decrease in modulus based on shear strains yielded higher settlements and poorer correlation with the measured settlements. The cost for performing and evaluating the tests is considerably higher than for the traditional pressuremeter tests, and the time and cost for performing the modelling and calculation are also considerable.

Calculations using moduli from the alternative method of interpretation yielded somewhat smaller settlements with a similar or slightly better correlation with the measured values, but in this case also the preconsolidation pressure had to be determined, which entails a much higher cost.

Calculations of the same type using modulus of elasticity from triaxial tests also yielded load settlement curves with shapes similar to those measured, but with larger settlements at the corresponding loads. When using these moduli, the initial stiffness in the soil was missed and the calculated load-settlement curves were steeper than those measured throughout the loading

ranges. The results were very similar to those obtained when using new pressuremeter tests and evaluating the decrease in modulus from calculated shear strains. The cost for taking undisturbed samples and performing the required laboratory tests is higher than for performing the new type of pressuremeter tests.

The calculations using moduli estimated from the seismic cone tests yielded an initially much stiffer response to the load than measured. The estimation of the variation in modulus with strain relies entirely on empirical relations and the translation to relevant loading times for a construction is hitherto very uncertain. The usefulness of the method with present knowledge must therefore be questioned. However, the cost for obtaining the moduli is very moderate.

The correlations for the calculations with advanced numerical methods based on moduli varying with strain are heavily dependent on assumptions concerning stress transfer and shear strength in the soil. In this case, no stress transfer was assumed and the drained shear strength as determined in laboratory tests was used. Because of the shallow foundation depth and the low overburden pressures, this strength became relatively low and significantly less than any estimation of the undrained shear strength. Assumptions of higher load transfer and shear strengths would have improved the correlations between the settlements calculated in this way and the measured values. However, it would not have improved the correlation between the calculated and observed settlement distributions. In the calculations, the settlements became more concentrated to the zone closest to the plate as the load increased. In the load tests, the settlements started directly beneath the plate and then spread downwards as the load increased.

It is also very difficult to find a sound basis for an assumption of a significant load transfer and shear strength higher than the drained parameters in the present case.



## 9.2 BEARING CAPACITY

The bearing capacity is traditionally calculated as an ultimate load on the basis of the measured shear strength of the soil. In the current load tests, failure was obtained only for the smallest plate. Probable ranges for the failure load could be obtained by extrapolation of the load-settlement curves from the other two plates. It should be observed that the failure obtained in the load test on the smallest plate was a punching type failure and not the classical shear surface assumed in most bearing capacity theories.

Other criteria for “failure” or “creep” loads are often used. The alternative “failure” load is then normally given as the load for which a certain relative settlement is obtained. A criterion of  $s/b = 0.1$  is often used, i.e. the settlement amounts to 10 % of the foundation width. For this criterion, the question arises concerning which time perspective should be applied. Since a settlement of this size is considered to cause the construction to cease to function, the lifetime of the construction (normally set to about 10 years) should instead be taken into account. Creep failure is evaluated from the shapes of the load-settlement curve and the load-creep rate curve. Creep failure is then estimated at a point where there is a significant break in the curves and both settlements and creep increase more rapidly than according to the trend before this load. Unless there is a brittle failure in the soil beneath the plate, the alternative failure load is not directly related to the shear strength of the soil but has to be calculated from a load-settlement calculation taking the curved load-settlement relation into

account. The creep load may be associated with mobilisation of a certain degree of the shear strength or local failure in the soil mass, but can also be associated with exceeding of the preconsolidation pressure.

From the plate loading tests, it was possible to estimate the following approximate failure and creep ground pressures beneath the plates (*Table 6*):

Calculations of ultimate failure loads in clay till are usually made both for undrained and drained conditions using undrained shear strength and drained effective shear strength parameters. The lowest bearing capacity obtained from these calculations, after application of appropriate safety factors or safety coefficients, is then used as design failure load. No such factors or coefficients are applied in comparisons with results from load tests to check the calculation methods.

The undrained shear strength has been determined in different ways yielding very different results. These can be divided into three main groups:

- Field vane tests and CPT-tests. Since the evaluation of the CPT-tests is calibrated against the field vane test, there is no significant difference in these results.
- Pressuremeter tests evaluated according to Menard or Mair and Wood. Both evaluation methods yield approximately the same results.

*Table 6. Estimated failure and creep pressures from the load tests.*

Plate	Ultimate failure kPa	$s = 0.1b$ , load test, kPa	$s = 0.1b$ , 10 years kPa	Creep pressure kPa
0.5 x 0.5	950	950	910	800
1.0 x 1.0	1600	1400	1150	700
2.0 x 2.0	950	950	780	800

- Triaxial tests and pressuremeter tests evaluated according to Briaud (1992) which in this case yielded values of similar sizes.

Other evaluations of the undrained shear strengths by alternative methods for pressuremeter tests or from dilatometer tests yielded considerably higher or lower values respectively.

The weighted undrained shear strengths for the relevant soil volume beneath the plates and the corresponding calculated bearing capacities are shown in *Table 7*.

The only calculated bearing capacities calculated on the basis of undrained shear strength that were the same size as the measured values were those calculated on the basis of results from triaxial tests (or pressuremeter tests with the strength evaluated according to Briaud (1992)). Bearing capacities evaluated from the commonly used field vane tests were much too high. However, the results from the plate load tests showed that these tests should be considered as drained tests. Their results in terms of ultimate bearing capacity cannot therefore be used to estimate the relevance for various undrained strength determinations.

The corresponding calculations with drained effective shear strength parameters have been performed with a friction angle of 30° and various assumptions about the effective cohesion  $c'$ . The latter parameter is dominant in the current case because of the low overburden pressures in the excavation. The effective cohesion has been estimated in five different ways:

- as evaluated from the triaxial tests
- estimated empirically as 0.03 times the pre-consolidation pressure from oedometer tests
- estimated empirically as 0.1 times the undrained shear strength from field vane tests
- estimated empirically from void ratio, water content and clay content according to Hartlén (1974)
- estimated empirically from the void ratio according to Jacobsen (1967)

The estimated relevant effective cohesion and the corresponding calculated bearing capacities are shown in *Table 8*.

*Table 7. Undrained shear strengths and calculated bearing capacities for the test plates.*

Plate	Undrained shear strength, kPa		
	Field vane and CPT tests	Pressuremeter test (Menard and Mair&Wood)	Triaxial test and pressuremeter test (Briaud)
0,5 x 0,5	360	275	175
1.0 x 1.0	360	275	175
2.0 x 2.0	290	220	145
	Bearing capacity, kPa		
0,5 x 0,5	2537	1939	1236
1.0 x 1.0	2381	1820	1160
2.0 x 2.0	1861	1573	933

Table 8. Estimated effective cohesion and calculated drained bearing capacity for the test plates.

Plate	Triaxial test	Effective cohesion, kPa			
		$0.03 \times \sigma'_c$	$0.1 \times c_{\text{uvane}}$	Hartlén	Jacobsen
0.5 x 0.5	20	19.5	36	24	23
1.0 x 1.0	20	19.5	36	24	23
2.0 x 2.0	16.5	18	29	18	19
		Bearing capacity, kPa			
0.5 x 0.5	868	849	1485	1020	974
1.0 x 1.0	840	823	1419	983	940
2.0 x 2.0	741	784	1178	794	819

A comparison with the plate test data shows that all the calculated bearing capacities are fairly relevant, except for those using empirical estimations from field vane tests, which are too high. In this context, it should be remembered that the soil below the 1.0 x 1.0 m plate is considerably coarser, and thereby probably more dilatant with higher effective cohesion, than the general soil conditions in the test field.

The ultimate bearing capacity has also been calculated from pressuremeter tests according to Menard. These calculations yielded the following results (Table 9):

Table 9. Bearing capacities for the test plates calculated from pressuremeter tests according to Menard.

Plate	Bearing capacity, kPa
0.5 x 0.5	1568
1.0 x 1.0	1318
2.0 x 2.0	1082

The results from these calculations are generally too high. The discrepancy decreases with depth and the correlation may be influenced by the effect of the excavation. The pressuremeter tests were performed at higher overburden pressures and initial horizontal stresses than the plate load tests. However, there is no method that can correct for this.

The “failure” loads at the deformation criteria  $s = 0.1b$  can only be calculated with methods that take the curved load-settlement relation into account. These are the methods using moduli from oedometer tests together with Jacobsen’s correction factor, the Briaud method for calculation of settlements from pressuremeter tests and the advanced methods using moduli that vary with strain. The “failure” loads thus calculated and the creep loads estimated from the shapes of the calculated load-settlement curves are given in Table 10.

The corresponding calculations using the alternative formulation of the moduli from pressuremeter tests result in creep pressures of 700 kPa and failure stresses of 725 kPa for all three plates. However, this is a direct result of reaching the estimated preconsolidation pressures.

Table 10. Calculated “failure” pressures and estimated yield stresses for the load plates.

Method	Plate	s/b = 0.1 time for load test, kPa	s/b = 0.1, 10 years, kPa	Creep pressure, kPa
Oedometer modulus, Jacobsen correction	0.5 x 0.5		825	750
	1.0 x 1.0		825	750
	2.0 x 2.0		720	600
Briaud, pressuremeter test	0.5 x 0.5	1600	1400	850
	1.0 x 1.0	1400	1250	850
	2.0 x 2.0	1300	1100	650
Ek Dahl and Bengtsson, new pressuremeter	0.5 x 0.5	650	635	575
	1.0 x 1.0	650	635	575
	2.0 x 2.0	650	635	575
Triaxial modulus	0.5 x 0.5	560	540	450
	1.0 x 1.0	530	520	450
	2.0 x 2.0	530	520	450

**Comments on the calculations of bearing capacity**

The calculated ultimate bearing capacities were best estimated using the general bearing capacity and drained shear strength parameters. The pore pressure measurements and the time-settlements observations during the tests also indicated that the load tests were to be considered as drained.

Failure in terms of creep load and excessive settlements was estimated fairly well by using oedometer test results and Jacobsen’s empirical correction. The creep load could also be estimated using Briaud’s method of calculating settlement based on pressuremeter tests. However, the almost brittle failure after exceeding this load could not be fully estimated by this method.

The creep load almost coincided with the preconsolidation pressures estimated from the oedometer tests. It is still difficult to estimate the degree to which this yield occurred because a preconsolidation pressure was exceeded and the degree to which it was related to development of plastic zones beneath the edges of the plates where the yield limit in terms of shear stresses had been exceeded. According to the correlations between calculated and observed settlements, these critical shear stresses are higher than the failure stresses calculated using the estimated drained shear strength parameters.

## References

- Akai, K. (1960).** Die strukturellen Eigenschaften von Schluff. Mitteilungen, Heft 22, Technische Hochschule, Aachen.
- Andersen, K.H., Kleven, A. and Heien, D. (1988).** Cyclic Soil Data for Design of Gravity Structures. ASCE, Journal of Geotechnical Engineering, Vol. 114, No.5, 1988.
- Atkinson, J.H. and Little, J.A. (1988).** Undrained Triaxial Strength and Stress-Strain Characteristics of a Glacial Till Soil. Canadian Geotechnical Journal, Vol. 25, No.3.
- Atkinson, J.H. and Sällfors, G. (1991).** Experimental Determination of Stress-Strain-Time Characteristics in Laboratory and In-Situ Tests. General Report. Proceedings, 10th European Conference on Soil Mechanics and Foundation Engineering, Florence, Vol. 3.
- Baguelin, F., Jezequel, J.F., LeMee, E. and LeMehaute, A. ((1972).** Expansion of Cylindrical Probes in Cohesive Soils. ASCE, Journal of the Soil Mechanics and Foundation Division, Vol. 98, No. SM11, Nov. 1972.
- Baguelin, F., Jézequel, J.F. and Shields, D.H. (1978).** The Pressuremeter and Foundation Engineering. Trans. Tech. Publications.
- Baziw, E.J. (1993).** Digital Filtering Techniques for Interpreting Cone Data. ASCE, Journal of Geotechnical Engineering, Vol. 119, No. 6, 1993.
- Bergdahl, U. (1984).** Geotekniska undersökningar i fält. Swedish Geotechnical Institute, Information No. 2, Linköping.
- Bergdahl, U., Ottosson, E. och Malmborg, B.S. (1993).** Plattgrundläggning. Svensk Byggtjänst, Solna.
- Berre, T. (1982).** Triaxial Testing at the Norwegian Geotechnical Institute. Geotechnical Testing Journal, Vol. 5, No. 1/2, 1982.
- Berre, T. (1988).** Effekt av prøvehøjde og endefriksjon ved treaxialforsøk og enaksiale trykkforsøk. Nordiske geoteknikermøte 10, NGM-88, Oslo, Artikler og "poster"-sammandrag.
- Berre, T. (1995).** Methods for Triaxial Compression Tests on Water-Saturated Soils. 11th European Conference on Soil Mechanics and Foundation Engineering, Copenhagen, Workshop 2: Standardisation of Laboratory Testing, Report prepared by the European Technical Committee ETC 5.
- Briaud, J.-L. (1992).** The Pressuremeter. A.A. Balkema, Rotterdam.
- Briaud, J.-L. (1995).** Pressuremeter Method for Spread Footings on Sand. The Pressuremeter and its New Avenues, Bailly (ed.), Balkema, Rotterdam.
- Briaud, J.-L., Lytton, R.L. and Hung, J.T. (1983).** Obtaining Moduli from Cyclic Pressuremeter Tests, ASCE, Journal of Geotechnical Engineering, Vol. 109, No. GT5.
- Briaud, J.-L., Cosentino, P.J. and Terry, T.A. (1987).** Pressuremeter Moduli for Airport Pavement Design and Evaluation. FAA Report DOT/FAA/PM-87-10. Civil Engineering Department, Texas A&M University, College Station.
- Brinch-Hansen, J. (1961).** A General Formula for Bearing Capacity. Danish Geotechnical Institute, Bulletin No. 11, Copenhagen.
- Brown, J. D., and Meyerhof, G. G. (1969).** Experimental Study of Bearing Capacity in Layered Clays. Proceedings, Seventh International Conference on Soil Mechanics and Foundation Engineering, Mexico City, Vol. 2, pp. 45-51.

- Burland, J.B. (1989).** The Ninth Bjerrum Memorial Lecture: Small is Beautiful - the Stiffness of Soils at Small Strains. *Canadian Geotechnical Journal*, Vol. 26, pp. 499-516.
- Butcher, A.P., McElmeel, K. and Powell, J.J.M. (1995).** Dynamic Probing and its Use in Clay Soils. *Proceedings, International Conference on Advances in Site Investigation Practice*, London, Vol.2.
- Butcher, A.P. and Powell, J.J.M. (1995).** Effects of Geological History on the Dynamic Stiffness in Soils. *Proceedings, 11th European Conference on Soil Mechanics and Foundation Engineering*, Copenhagen, Vol. 1.
- Butcher, A.P. and Powell, J.J.M. (1995).** Practical Considerations for Field Geophysical Techniques used to Assess Ground Stiffness. *Proceedings, International conference on advances in site investigation practice*, London, Vol.2.
- Campanella, R.G., Robertson, P.K. and Gillespie, D. (1986).** Seismic Cone Penetration Tests. *Proceedings of In Situ 86', a Specialty Conference on Use of In Situ Tests in Geotechnical Engineering*, Balcksburg, Virginia. ASCE, New York.
- CEN (1994).** Eurocode 7: Geotechnical design - Part 1: General rules. *European Committee for Standardization*, Brussels.
- Clarke, B.G. (1995).** *Pressuremeters in Geotechnical Design*. Blackie Academic & Professional, London.
- DeGroot, D.J. and Sheahan, T.C. (1995).** Laboratory Methods for Determining Engineering Properties of Overconsolidated Clays. *Engineering Properties and Practice in Overconsolidated Clays*, Transportation Research Record, No. 1479.
- DGF Feltekomité (The field committee of the Danish Geotechnical Society) (1993).** *Refernceblad for vingeforsøg*. Referenceblad 1, Revision1, Dansk Geoteknisk Forening, København.
- Dueck, A. (1995).** Reference Site for Clay Till. Lund Institute of Technology, Lund University, Department of Geotechnology, LUTVDG/TVGT -3025-SE.
- Dueck, A. (1997).** Egenskaper i lermorän. En laboratoriestudie utförd vid Laboratoriet for Fundering, Aalborgs Unviversitetscenter. Lund Institute of Technology, Lund University, Department of Geotechnology, LUTVDG/TVGT-3028-SE.
- Dueck, A. (1998).** Shear Strength and Matrix Suction in Clay Tills - Triaxial Test Procedures to evaluate Shear Strength of Clay Tills from Southwestern Sweden. *Diss*, Lund Institute of Technology, Lund University, Department of Geotechnology, Lund.
- Dueck, A. och Garin, H. (1995).** Pressometerförsök i fast lera och lermorän - Samarbetprojekt mellan Institutionen för Geoteknologi, Lunds tekniska högskola och Skanska Teknik AB Malmö. Lund Institute of Technology, Lund University, Department of Geotechnology, LUTVDG/TVGT-3022-SE.
- Duncan, J.M. and Chang, C.-Y. (1970).** Non-linear Analysis of Stress and Strain in Soils. *ASCE, Journal of the Soil Mechanics and Foundation Division*, Vol. 96, No. SM5.
- Ekdahl, U. (1997).** Kung Oscars bro - Planskild korsning i Lund. *Grundläggningdagen 97, Rätt i grunden; 2. Nyhetspasset - GD 97*, Stockholm. Svenska Geotekniska Föreningen, Linköping.
- Ekdahl, U. och Bengtsson, P.-E. (1996).** Ny metod att räkna sättningar vid plattgrundläggning. *Väg- och Vattenbyggaren*, Nr. 3, 1996.
- Ekdahl, U., Lindh, P. och Jonsson, A. (1996).** Väst kustbanan, Kävlinge - Lund; Kompletterande geoteknisk undersökning. PEAB Grundteknik, Malmö.
- Fredlund, D. G. and Rahardjo, H. (1993).** *Soil Mechanics for Unsaturated Soils*. Wiley and Sons, New York.

- Foged, N. og Steinfeld J.S. (1992).** An Engineering Approach to Preloaded Clay Till Strength. Nordiske geoteknikermøde, NGM-92, Aalborg, DGF-Bulletin No. 9, Vol. 1/3.
- Gibson, R.E. and Andersson, W.F. (1961).** In Situ Measurements of Soil Properties with the Pressuremeter. Civil Engineering and Public Works Review, London, Vol. 56, No. 658, May 1961.
- Hansbo, S., and Sällfors, G. (1984).** Jordmekanik. (Soil Mechanics). Handboken Bygg, Geoteknik, Kapitel G 05, Liber Förlag, Stockholm
- Hardin, B.O. and Drnevich, V.P. (1972).** Shear Modulus and Damping in Soils: Design Equations and Curves. ASCE, Journal of the Soil Mechanics and Foundation Division, Vol. 98, No. SM7.
- Hartlén, J. (1974).** Skånska moränlerors hållfasthets- och bärighetsegenskaper. Diss. Chalmers University of Technology, Department of Geotechnical Engineering, Göteborg.
- Hird, C.C., Powell, J.J.M. and Yung, P.C.Y. (1991).** Investigations of the Stiffness of a Glacial Clay Till. Proceedings, 10th European Conference on Soil Mechanics and Foundation Engineering, Vol. 1. Florence.
- Holmén, M. och Lindh, P. (1999).** Automatisering av en pressometer. Geo'99 - Geotekniska forskardagar. Swedisk Geotechnical Institute, Varia No. 485, Linköping
- Jacobsen, M. (1967).** Morænelerers geotekniske egenskaber. Diss. Danish university of Technology, København. Reprinted by Aalborg University Centre 1994.
- Jacobsen, M. (1970).** Strength and Deformation Properties of Preconsolidated Moraine Clays. Danish Geotechnical Institute, Bulletin No. 27, København.
- Jacobsen, M. (1975).** Nogle danske morænelerers styrke- og deformationsegenskaber. Nordiske geoteknikermøde i København.
- Jacobsen, M. (1992).** Bestemmelse av forbelastningstryk i laboratoriet. 11. Nordiske Geoteknikermøde, NGM-92, Aalborg, Vol. 2/3.
- Jacobsen, M. (1992).** Karakteristiske belastningstilstande for moræneler. 11. Nordiske Geoteknikermøde, NGM-92, Aalborg, Vol. 2/3.
- Jardine, R.J. (1991).** Strain-Dependent Moduli and Pressuremeter Tests. Discussion. Géotechnique, Vol. 41, No. 4, pp 621-626.
- Janbu, N. (1963).** Soil Compressibility as Determined by Oedometer and Triaxial Tests. European Conference on Soil Mechanics and Foundation Engineering, Wiesbaden, Vol.1.
- Janbu, N. (1970).** Grunnlag i geoteknikk. Tapir forlag. Trondheim
- Jelinek, R. (1951).** Der Einfluss von Gründungstiefe und begrenzter Schichtmächtigkeit auf die Druckausbreitung im Baugrund. Bautechnik, Vol. 28, Heft 6, 1951.
- Jonsson, A., Andersson, B. och von Strokirch, C. (1995).** A Method Study of Geobor S - a Triple Tube Wire Line Coring System, performed in Limestone and Clay Till. Lund Institute of Technology, Lund University, Department of Geotechnology, LUTVDG/TVT G - 5040-SE.
- Jørgensen, M. og Denver, H. (1992).** CPT-Tolkningsprocedurer. 11. Nordiske Geoteknikermøde, NGM-92, Aalborg, Vol.1/3.
- Kammer Mortensen, J., Hansen, G. og Sørensen, B. (1991).** Correlation of CPT and Field Vane Test for Clay Tills. Dansk Geoteknisk Forening, DGF Bulletin Nr.7. København.
- Karlsson, R. and Hansbo, S. (1984).** Soil Classification. Swedish Council for Building Research, T21:1982. Second Edition, Revised in 1984. Stockholm.
- Kondner, R.L. (1963).** Hyperbolic Stress-Strain Response: Cohesive Soils. ASCE, Journal of the Soil Mechanics and Foundation Engineering Division, Vol. 89, No. SM1, 1963.
- Kristensen, P.S., Erichsen, L. og Sørensen, C.S. (1992).** Great Belt - Foundation of the West Bridge. 11. Nordiske Geoteknikermøde, NGM-92, Aalborg, Vol. 1/3.

- Lacasse, S. and Berre, T. (1988).** Triaxial Testing Methods for Soils. Advanced Triaxial Testing of Soil and Rock. ASTM Special Technical Publication STP 977.
- Ladanyi, B.(1972)** In Situ Determination of Undrained Stress- Strain Behaviour of Sensitive Clays with the Pressuremeter. Canadian Geotechnical Journal, Vol. 9, No. 3, Aug. 1972.
- Ladd, C.C. and Foott, R. (1974).** New Design Procedure for Stability of Soft Clays. ASCE, Journal of the Geotechnical Engineering Division, Vol. 100, No. GT7.
- Larsson, R. (1981).** Drained Behavior of Swedish Clays. Swedish Geotechnical Institute, Report No. 12, Linköping.
- Larsson, R. (1986).** Consolidation of Soft Soils. Swedish Geotechnical Institute, Report No. 29, Linköping.
- Larsson, R. (1989).** Dilatometerförsök - En in-situ metod för bestämning av lagerföljd och egenskaper i jord. Utförande och utvärdering. Swedish Geotechnical Institute, Information No. 10, Linköping.
- Larsson, R. (1992).** CPT-sondering. Utförande - utförande - utvärdering. En in-situ metod för bestämning av jordlagerföljd och egenskaper i jord. Swedish Geotechnical Institute, Information No. 15, Linköping.
- Larsson, R. (1992).** Deformationsegenskaper i jord - Deformationsmoduler och enkla jordmodeller med speciellt avseende på relativt små deformationer inom det "elastiska" området. Chalmers University of Technology, Department of Geotechnical Engineering, Report B 1994:6. Göteborg.
- Larsson, R. (1997).** Investigations and Load Tests in Silty Soils - Results from a Series of Investigations in Silty Soils in Sweden. Swedish Geotechnical Institute, Report No. 54, Linköping.
- Larsson, R. (2000).** Lermorän - en litteraturstudie; Förekomst och geotekniska egenskaper. Swedish Geotechnical Institute, Varia No. 480, Linköping.
- Larsson, R., Bergdahl, U. and Eriksson, L. (1984).** Evaluation of Shear strength in Cohesive Soils with Special Reference to Swedish Practice and Experience. Swedish Geotechnical Institute, Information No. 3. Linköping.
- Larsson, R., Löfroth, B. och Möller, B. (1995).** Processing of Data from CPT Tests. International Symposium on Cone Penetration Testing, CPT'95, Vol.2, Linköping.
- Larsson, R. och Mulabdic, M. (1991).** Shear Moduli in Scandinavian Clays. Swedish Geotechnical Institute, Report Nr. 40, Linköping.
- Larsson, R. och Mulabdic, M. (1991).** Piezocone Tests in Clay. Swedish Geotechnical Institute, Report Nr. 42, Linköping.
- Leveen, F. och Palm, M. (2000).** Utvärdering av kombinerad resistivitets- och CPTU-sond. Lund Institute of Technology, Lund University, Department of Geotechnology, Lund.
- Luke, K. (1996).** Cone Factors from Field Vane and Triaxial Tests in Danish Soils. XII Nordiska Geoteknikermötet, NGM-96, Reykjavik.
- Mair, R.J. and Wood, D.M. (1987).** Pressuremeter Testing. Ciria, Butterworths, London.
- McManis, K.L. and Lourie, D.E. (1995).** Issues and Techniques for Sampling Overconsolidated Clays. Engineering properties and practice in overconsolidated clays, Transportation Research Record, No. 1479.
- Marchetti, S. (1980).** In Situ Tests by Flat Dilatometer. ASCE, Journal of the Geotechnical Engineering Division, Vol. 106, No. GT3
- The Menard pressuremeter (1975).** Interpretation and Application of Pressuremeter Test Results to Foundation Design. Menard General Memorandum D. 60. AN Sols Soils No. 26 - 1975.
- Palmer, A.C. (1972).** Undrained Plane-Strain Expansion of a Cylindrical Cavity in Clay: A Simple Interpretation of the Pressuremeter Test. Géotechnique, Vol. 22, No. 3, Sept. 1972.



- Powell, J.J.M. and Butcher, A.P. (1991).** Assessment of Ground Stiffness from Field and Laboratory Tests. Proceedings, 10th European Conference on Soil Mechanics and Foundation Engineering, Florence, Vol.1.
- Powell, J.J.M. and Butcher, A.P. (1997).** Determining the Modulus of the Ground from In-Situ Geophysical Testing. Proceedings, 14th International Conference on Soil Mechanics and Foundation Engineering, Hamburg, Vol. 1.
- Powell, J.J.M. and Uglow, I.M. (1988).** The Interpretation of the Marchetti Dilatometer Test in UK Clays. Penetration Testing in the UK. Thomas Telford, London.
- Riggins, M. (1981).** The Viscoelastic Characteristics of Marine Sediments in Large Scale Simple Shear. Diss. Civil Engineering, Texas A&M University.
- Roque, R., Janbu, N. and Senneset, K. (1988).** Basic Interpretation Procedures of Flat Dilatometer Tests. Proceedings of 1st International Symposium on Penetration Testing, Orlando, Florida, Vol. 1.
- Schmertmann (1978).** Guidelines for Cone Penetration Tests, Performance and Design. Federal Highway Administration, Report FHWA-TS-78-209, Washington.
- SGF:s fältkommitté (The Field Committee of the Swedish Geotechnical Society) (1998).** Rekommenderad standard för Jord-bergsondering, (Jb-sondering). Svenska Geotekniska Föreningen, Linköping.
- SGF:s laboratoriekommitté (The Laboratory Committee of the Swedish Geotechnical Society) (1996).** Bestämning av kompressionmodul,  $M_v$ , för överkonsoliderad jord. Meddelande från laboratoriekommittén. Svenska Geotekniska Föreningen, Linköping.
- Skanska Teknik (1998).** Pressometerundersökning i lermorän. Skanska Teknik AB, Geoteknik och Grundläggning, Malmö.
- Steenfelt, J.S. and Foged, N. (1992).** Clay Till Strength - SHANSEP and CSSM. Nordiske geoteknikermøde i Aalborg, DGF-Bulletin No. 9, Vol. 1/3.
- Steenfelt, J.S. og Sørensen, C.S. (1995).** CPT - Contraption for Probing in Tills? International Symposium on Cone Penetration Testing, CPT'95, Vol.2, Linköping
- Svensson, M. (1999).** Ytvågsseismik - magi eller ett verktyg inom geotekniken. Bygg & Teknik, Vol. 91, Nr.1.
- Svensson, M. (2000).** Surface Wave Seismics - A Comparison between In Situ Shear Moduli determined by SASW-Technique and Other Methods. In preparation.
- Swedish Geotechnical Society (1993).** Recommended Standard for Cone Penetration Tests. Report 1:93, Linköping.
- Swedish Geotechnical Society (1995).** Rekommenderad standard for dilatometerförsök. Report 1:95, Linköping.
- Swedish Standard SS 02 71 14 (1977).** Geotekniska provningsmetoder - Skrymdensitet. (Geotechnical Test - Bulk Density). Swedish Building Standards Institution, Stockholm.
- Swedish Standard SS 02 71 16 (1977).** Geotekniska provningsmetoder - Vattenkvot och vattenmättnadsgrad. (Geotechnical Test - Water Content and Saturation Ratio). Swedish Building Standards Institution, Stockholm.
- Swedish Standard SS 02 71 18 (1989).** Geotekniska provningsmetoder - Konsistensgränser. (Geotechnical Test - Consistency Limits). Swedish Building Standards Institution, Stockholm.
- Swedish Standard SS 02 71 24 (1992).** Geotekniska provningsmetoder - Kornfördelning, Sedimentering - Hydrometermetoden. (Geotechnical Test - Particle Size Distribution, Sedimentation Test - Hydrometer Method). Swedish Building Standards Institution, Stockholm.
- Swedish Standard SS 02 71 29 (1992).** Geotekniska provningsmetoder - Kompressionsegenskaper - ödometerförsök med stegvis pålastning - kohesionsjord. (Geotechnical Test - Incrementally Loaded Oedometer Tests). Swedish Building Standards Institution, Stockholm.

- Trankjaer, H. (1995).** Forbelastet moraenellers deformationsegenskaber. Diss. Laboratoriet for Fundering, Aalborg University. Aalborg.
- Trankjær, H. (1996).** Deformationsmodel for intakt moræneler. XII Nordiska Geoteknikermötet, NGM-96, Reykjavik.
- Tremblay, M. (1990).** Mätning av grundvattenninå och portryck. Swedish National Road Administration - Vbg, Publication 1990:41, Borlänge. Also in Swedish Geotechnical Institute, Information No. 11, Linköping.
- Tscheng, Y. (1957).** Fondations Superficielles en Millieu Stratifié. Proceedings, Fourth International Conference on Soil Mechanics and Foundation Engineering, London, Vol. 1, pp. 449 - 452
- Vesic, A. (1973).** Analysis of Ultimate Loads of Shallow Foundations. ASCE, Journal of the Soil Mechanics and Foundation Division, Vol. 99, No. SM1, Jan. pp. 45-73.
- Vucetic, M. and Dobry, R. (1991).** Effect of Soil Plasticity on Cyclic Response. ASCE, Journal of Geotechnical Engineering, Vol. 117, No. 1, Jan. 1991.
- Wood, D. M. (1990).** Strain-Dependent Moduli and Pressuremeter Tests. Technical note, Géotechnique, Vol. 40, No.3. (Discussion in Géotechnique Vol. 41, No. 4.)
- Wroth, C.P. (1982).** British Experience with the Self-Boring Pressuremeter. Proceedings, Symposium on the Pressuremeter and its Marine Applications. Institut de Petrole, Laboratoire des Ponts et Chaussées, Paris.
- Öberg, A-L. (1997).** Matrix Suction in Silt and Sand Slopes; Significance and Practical Use in Stability Analysis. Thesis. Department of Geotechnical Engineering, Chalmers University of Technology, Gothenburg

# Appendix

# Calculation methods for prediction of settlements and bearing capacity

## A.1 GENERAL

Ekdahl and Bengtsson (1996) presented a new method of calculating settlements of foundations on clay till based on results from pressuremeter tests and Jacobsen (1967) had previously presented an empirical chart for correction of settlements calculated for the same case on the basis of reloading modulus from oedometer tests. Apart from this, there are no special methods for calculation of bearing capacity and settlements in clay till.

Because of its loading history, the clay till is normally overconsolidated to such an extent that only the compression characteristics in the reloading mode are of interest for normal foundations. Furthermore, because of the heterogeneity and the high moduli, the soil in many respects often behaves more like a silt than a clay. In this project, those methods designed particularly with clay till in mind have been tested. An investigation has also been made of the extent to which methods normally used for silts and other overconsolidated clays can be applied to clay till. The conditions and properties of the clay till in Tornhill are sometimes far outside the restrictions normally applying to their use. Thus, the results in the present investigations do not reflect the general applicability of the methods to the areas for which they are intended.

Some methods are general and are intended to cover all types of soil and geometric conditions. As its name implies, the “general equation for bearing capacity” is thus intended for all soils and conditions. In this equation, both empirically estimated shear strength parameters and parameters determined by more elaborate testing may be introduced. Also the Menard type of pressuremeter test and the related method of calculation of bearing capacity are intended to be generally applicable. The new interpretation and calculation

method for pressuremeter tests presented by Briaud (1995) was, on the other hand, originally proposed to be valid only under certain conditions in sand, and has later been extended to silt (Larsson 1997).

For calculation of settlements, the methods using theory of elasticity to estimate the distribution of the stress increase and moduli are applicable to all types of soil. The moduli may then be evaluated semi-empirically from dilatometer tests or measured in oedometer tests, triaxial tests or in unload-reload loops in pressuremeter tests, among other methods. As before, the calculation methods based on pressuremeter tests according to Menard are general, but the Briaud method has so far been restricted to sand and silt.

## A.2 PREDICTION OF SETTLEMENTS

### Calculations based on stress distribution according to theory of elasticity and moduli

Settlements can be calculated using theory of elasticity to estimate the distribution of the stresses and moduli ( $E$  or  $M$ ) to describe the stiffness of the soil. For widespread flexible loads, such as wide fills, the variation in the stress distribution is calculated both with depth and distance across the area. The settlements may then be calculated with moduli determined semi-empirically from dilatometer tests or pressuremeter tests or directly from unload-reload loops in pressuremeter tests, or in the laboratory by oedometer tests or triaxial tests. In the latter cases, the variation in moduli with stress may also be taken into account. For high fills, the shear strength below the edges of the fills may be mobilised to such a degree that allowance has to be made for lateral movements in the soil.

For rigid footings, the stress distribution is calculated below the characteristic point. Ideally, the oedometer modulus  $M$  should be used for wide-spread loads and the modulus of elasticity  $E$  for narrow footings. This distinction is not always made in practice, except in more elaborate analyses using more advanced calculation methods. The settlements are calculated using moduli determined as above. For pressuremeter tests, also other calculation methods are used. For rigid footings of limited width in relation to the compressible soil layer, the mobilisation of the shear strength increases as the vertical stress increases and the same increase in the soil stiffness because of the increasing vertical stress as in the oedometer case can not be counted upon. On the contrary, a strain softening with a gradually decreasing modulus with increasing load and settlement must be taken into consideration. This can be done by making iterative calculations in which the calculated settlements are matched with the moduli at the corresponding strains.

The settlements are calculated from

$$s = \sum_0^z \frac{\Delta\sigma_z'}{E_z} \Delta z \quad \text{or} \quad s = \sum_0^z \frac{\Delta\sigma_z'}{M_z} \Delta z$$

and the calculation is made over a depth  $z$  which at least comprises all depth intervals in which the increase in effective vertical stress is  $\geq 10\%$ . Another way of limiting the depth for which the settlements are calculated is to use the empirical observations that for square or circular footings there are normally no significant settlements below a depth of twice the width of the footing under its base. The corresponding limiting depth for strip foundations is four times the foundation width, (Schmertmann 1978).

Some types of estimation of moduli yield values that can be used to calculate the 10-year settlements. In other cases, a similar type of correction for time as in the Schmertmann (1978) method has to be used, i.e. a 20% increase in settlement per increase in log time, a modulus which is a function of time or some other corresponding method.

The real load-settlement curves for footings on thick deposits of compressible soil are curved, which means that settlement predictions using a constant modulus will normally overestimate the actual settlements at small loads and underestimate them at high loads. The Swedish handbook for design of shallow foundations, (Bergdahl et al. 1993), recommends that if the load is increased above 2/3 of the design failure load, the empirical moduli should be reduced by 50% for the higher load. However, since the design calculations involve a large number of partial safety factors depending on the particular construction and the risk involved, this is rather difficult to translate into general terms enabling a comparison to be made against the results of load tests, for example. A very approximate translation would be that the breaking point where the modulus should be reduced corresponds to the permissible ground pressures according to the old building codes, which in turn implies that this correction would normally not be applicable to ordinary constructions.

A study of the results in previous projects together with plate loading tests performed by SGI on sands and silts, as well as other empirical observations, has shown that the load-settlement curves have a parabolic shape. The same observation was made by Jacobsen (1967) for foundations on clay till. Based on a large number of settlement observations, he proposed that the settlements calculated on the basis of reloading moduli determined in oedometer tests should be corrected. The correction factor increases with increasing mobilisation of the bearing capacity, *Fig. 121*, and thus provides the observed curved load-settlement relation.

For sands and silts, the settlements calculated with stress distribution according to theory of elasticity and using the most relevant estimates of the constant moduli coincide with the actual settlements at a relative settlement of about  $0.014b$  (Larsson 1997). Based on these results, it was proposed that the settlements could be calculated according to the following procedure:

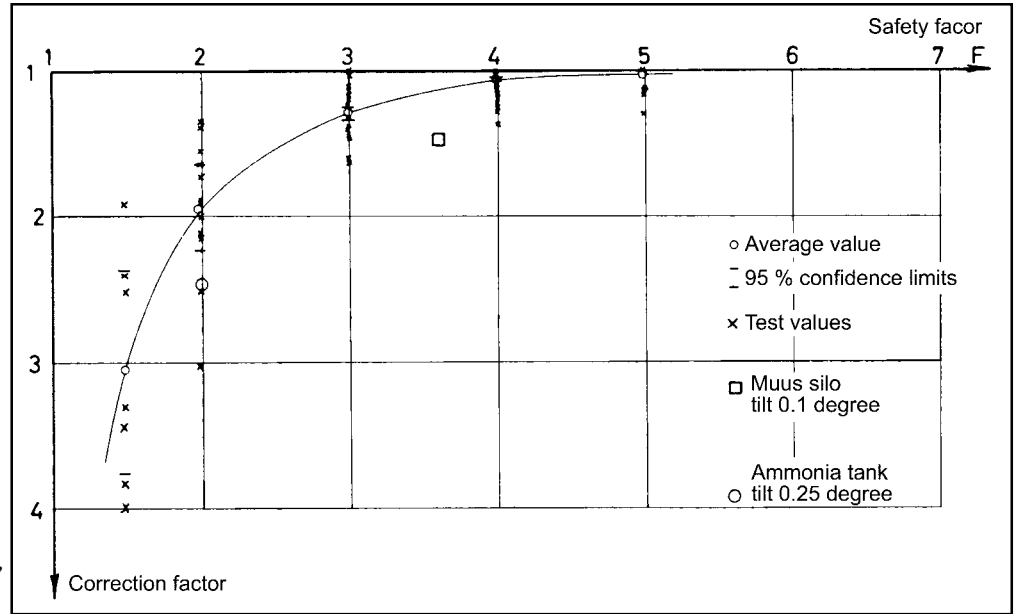


Fig. 121. Empirical correction factor for settlements of foundations on clay till calculated with reloading moduli from oedometer tests, (Jacobsen 1967).

1. A settlement factor,  $F_s$ , comprising the thickness of the compressible layer contributing to the settlements, the stress distribution and the compression moduli is calculated as

$$F_s = \sum_0^z \frac{f_z \Delta z}{E_z}$$

where  $f_z$  = influence factor under the characteristic point in the centre of the sublayer  $\Delta z$  according to theory of elasticity.

2. A reference stress,  $q_{ref}$  which gives the reference settlement  $s_{ref} = 0.014b$  is calculated as

$$q_{ref} = 0.014b / F_s$$

3. The relative settlement  $s/b$  for all other applied stresses up to failure is calculated as

$$\frac{s}{b} = 0.014 \left( \frac{q}{q_{ref}} \right)^2$$

### Calculation of settlements of footings based on Menard type pressuremeter tests

Calculation of settlements of footings based on pressuremeter tests is usually performed according to Menard (1975) and Baguelin et al. (1978). The 10-year settlement is then calculated as

$$s = \frac{2}{9E_d} \Delta p b_0 \left( \lambda_d \frac{b}{b_0} \right)^\alpha + \frac{\alpha}{9E_c} \Delta p \lambda_c b \quad , \text{ m}$$

where

$E_d$  = weighted harmonic mean value of measured pressuremeter moduli  $E_{pm}$  down to a depth of  $8b$  below the foundation level, kPa

$E_c$  = harmonic mean value of measured pressuremeter moduli  $E_{pm}$  down to depth  $b/2$ , kPa

$b_0$  = reference width = 0.6 m

$b$  = width of foundation, m

$\alpha$  = rheological factor depending on soil type and the relation  $E_{pm}/p_1^*$ , Table 11

$\lambda_d$  and  $\lambda_c$  = shape factors, see Table 12

$\Delta p$  = net ground pressure ( $p' - p'_0$ ), kPa

$p'_0$  = effective overburden pressure at the foundation level, kPa

Table 6. Rheological factors according to Baguelin et al. (1978).

Soil Type	Peat		Clay		Silt		Sand		Sand and gravel	
	$E_M/\rho_1^*$	$\alpha$	$E_M/\rho_1^*$	$\alpha$	$E_M/\rho_1^*$	$\alpha$	$E_M/\rho_1^*$	$\alpha$	$E_M/\rho_1^*$	$\alpha$
Over-consolidated			>16	1	>14	2/3	>12	1/2	>10	1/3
Normally consolidated		1	9-16	2/3	8-14	1/2	7-12	1/3	6-10	1/4
Weathered and/or remoulded			7-9	1/2		1/2		1/3		1/4
Rock			Extremely fractured		Other		Slightly fractured or extremely weathered			
			$\alpha = 1/3$		$\alpha = 1/2$		$\alpha = 2/3$			

Table 7. Shape factors according to Baguelin et al. (1978).

$L/B_s$	Circle	1	2	3	5	20
$\lambda_d$	1	1.12	1.53	1.78	2.14	2.65
$\lambda_c$	1	1.10	1.20	1.30	1.40	1.50

The first term in the equation relates to the increasing shear stresses (settlements related to changes in shape) and the second to the increase in normal stresses (settlements due to volumetric compression).

In most soils, the moduli vary with depth but, provided that this variation is within limits, the equivalent moduli  $E_d$  and  $E_c$  can be used in the calculation.

For calculation of  $E_d$  and  $E_c$ , the soil below the foundation level is divided into 16 fictitious sub-layers with thickness  $b/2$ , Fig. 122.

If several determinations of the pressuremeter modulus have been made in the main layers indicated in Fig. 122, the harmonic mean value in the layer  $E_i$  is first calculated. A harmonic mean value  $\bar{x}$  is calculated from

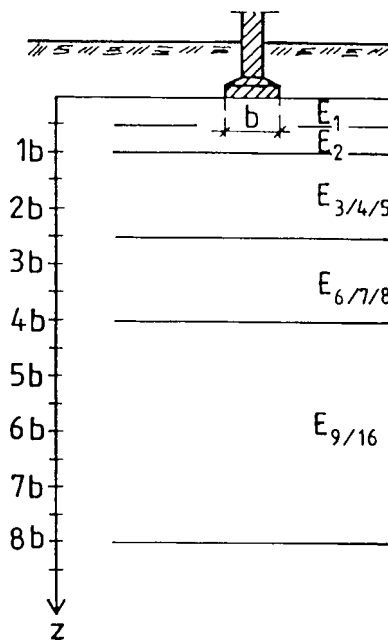


Fig. 122. Division of the soil into fictitious sub-layers for calculation of  $E_d$  and  $E_c$ , Baguelin et al. (1978).

$$\frac{1}{x} = \frac{1}{n} \left( \frac{1}{x_1} + \frac{1}{x_2} + \dots + \frac{1}{x_n} \right)$$

$E_c$  and  $E_d$  are then calculated from

$$E_c = E_1$$

and

$$E_d = \frac{4}{\frac{1}{E_1} + \frac{1}{0.85E_2} + \frac{1}{E_{3,4,5}} + \frac{1}{2.5E_{6,7,8}} + \frac{1}{2.5E_{9/16}}}$$

In cases where pressuremeter tests have not been performed to the full depth of  $8b$ , the weighting of the measured moduli can be performed according to Menard (1975).

For foundations with a smaller embedment than the plate width, the calculated settlement is increased by the percentages given in *Fig. 123*.

When there is a large variation in pressuremeter moduli with depth, i.e. when two separate geological deposits with very different properties are involved, this calculation model may not be suitable. The calculation is then performed for a two-layer system or for a soft layer at arbitrary depth according to Baguelin et al. (1978).

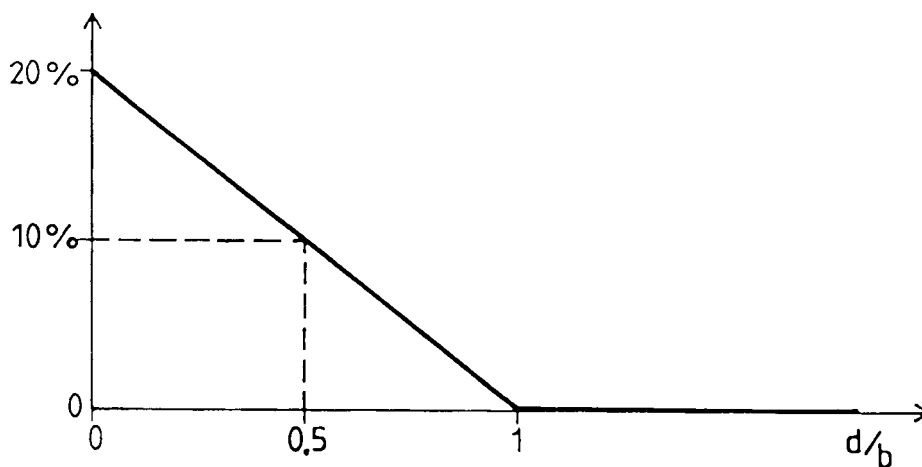


*Fig. 123. Increase in settlement at superficial foundation depths in per cent according to Baguelin et al. (1978).*

### The Briaud method of calculating settlement and bearing capacity from results of pressuremeter tests

The Menard method of interpreting the pressuremeter test and using the results entails that bearing capacity and settlements are calculated separately without relating to each other. The bearing capacity is thus calculated on the basis of  $p_l$  as the ultimate bearing capacity without regard to the size of the settlements that occur before then and the settlements are calculated on the basis of  $E_{pm}$  using a constant modulus without regard to its change with the shear stress level.

Briaud (1995) observed that the pressuremeter test, also when performed according to the Menard procedure, provides a complete stress-strain curve and presented a method for converting this into a continuous load-settlement curve for footings.

The principle of the method is that the relative displacement  $\Delta R_c/R_c$  measured in the pressuremeter test for an increase in radial pressure  $p_{pm}$  can be transformed to a relative settlement,  $s/b$ , for an increase in vertical pressure on a footing,  $p_{footing}$ . The transformation uses the equations



$$p_{\text{footing}} = \Gamma p_{\text{pmt}}$$

and

$$\frac{s}{b} = \frac{\Delta R_c}{4.2 R_c}$$

where

- $s$  = settlement of footing
- $b$  = width of footing
- $R_c$  = radius of the cavity in the pressuremeter test
- $\Delta R_c$  = increase in radius in the pressuremeter test
- $p_{\text{pmt}}$  = pressure in the pressuremeter test corresponding to  $\Delta R_c/R_c$
- $p_{\text{footing}}$  = footing pressure corresponding to  $s/b$
- $\Gamma$  = transformation function, which depends on  $s/b$

The procedure is started by plotting the pressuremeter curve as  $\Delta R_c/R_c$  versus  $p_{\text{pmt}}$  instead of the normal Menard curve with volume versus pressure. The cavity radius  $R_c$  at zero pressure is found by plotting the relative change in pressuremeter radius  $\Delta R_p/R_p$  and extrapolating the shape of the curve after initial seating errors back to zero pressure, Fig. 124.

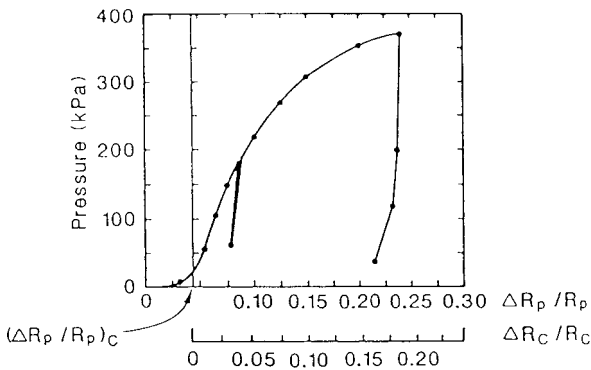


Fig. 124. Plotting of pressuremeter curve and evaluation of  $R_c$ .

The pressuremeter curves over a depth of  $3b$  below the foundation level are then weighted with respect to an assumed distribution of the influence, which is similar to that proposed by Schmertmann (1978), Fig. 125.

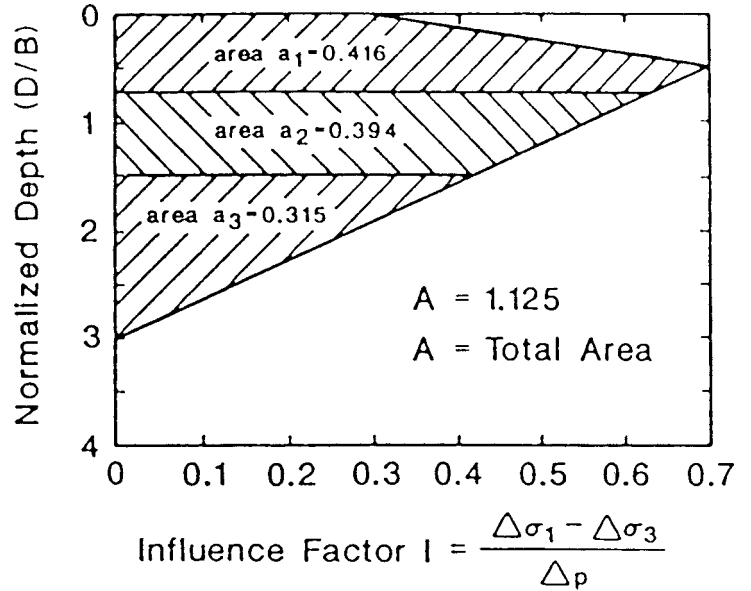


Fig. 125. Recommended distribution of the influence factor and example of allocation of influence areas  $a_i$ .

The various pressuremeter curves are weighted into an average curve by allocating an influence area to each curve corresponding to the test level and the distances between the test depths. For each value of  $\Delta R_c/R_c$  the average  $p_{\text{pmt}}$  is then calculated as

$$p = \frac{1}{A} \sum p_i a_i$$

where

- $p_i$  = pressure at  $\Delta R_c/R_c$  in test  $i$
- $a_i$  = allocated influence area for test  $i$
- $A$  = total allocated influence area

and the average pressuremeter curve is thus generated, Fig. 126. It is an advantage if a sufficient number of test curves are available so that the influence of a possible non-representative test is subdued.

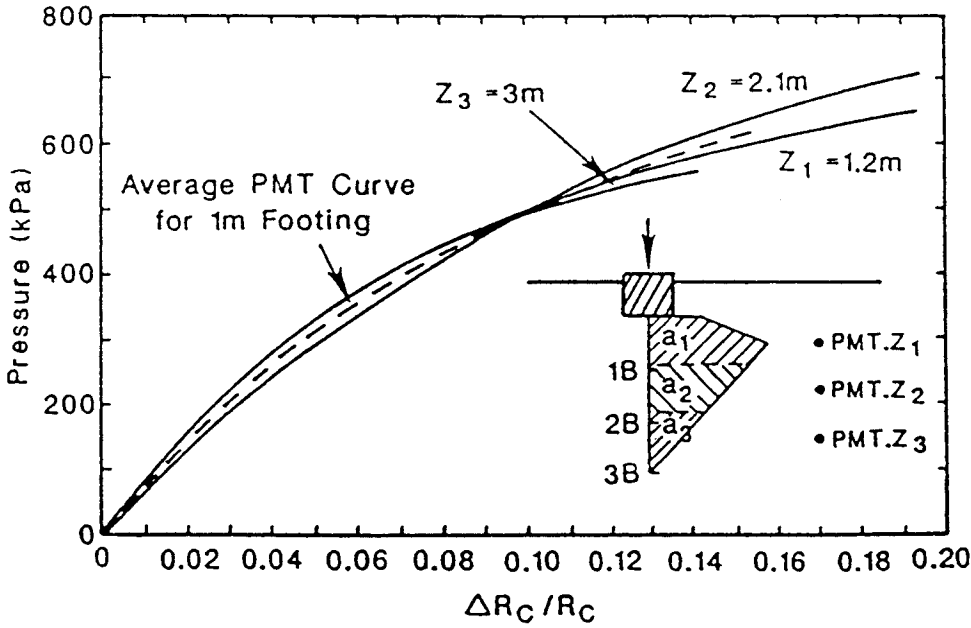


Fig. 126. Generation of the average pressuremeter curve for a footing.

The relative load-settlement curve is now constructed by using the function  $\Gamma$ . A tentative curve for the variation of this function was proposed by Briaud (1995) and this was modified by Larsson (1997) with respect to experience from tests on Swedish sands and silts, Fig. 127.

For larger deformations, the factor  $\Gamma$  is fairly constant. However, for small deformations it rapidly increases. The  $\Gamma$ -factor thereby increases the curvature of the already rounded pressure-relative displacement curves from the pressure-

meter tests. The resulting load-settlement curve becomes a shape with an initially stiff response of the soil to the applied load, after which the settlements accelerate with increasing load. The method is applicable for relative settlements up to  $0.1b$ , where failure because of excessive settlements is considered to occur.

One problem with the method arises from the time effects. The time steps in a pressuremeter

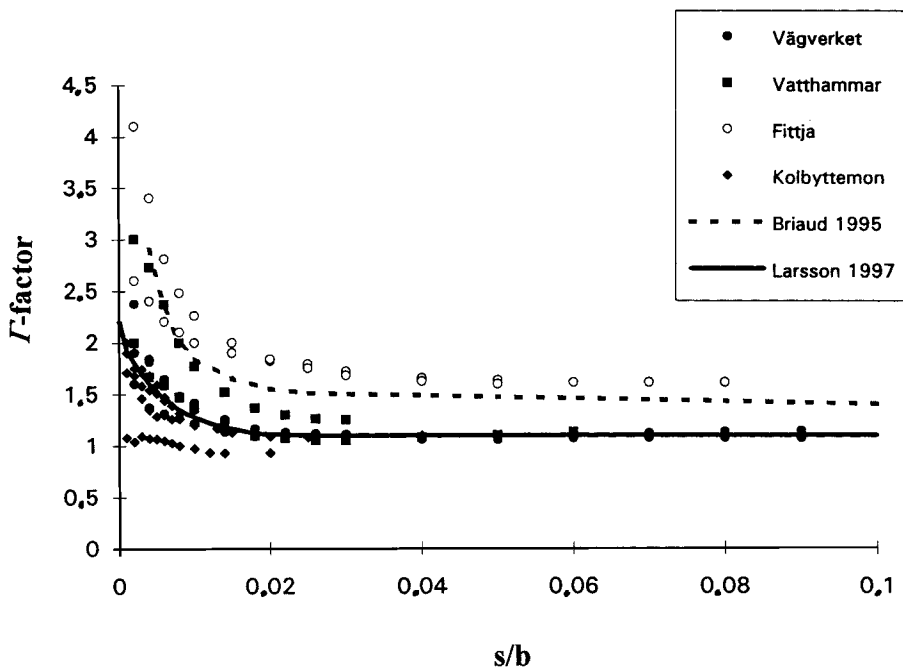


Fig. 127. The transformation function  $\Gamma$  according to Briaud (1995) and Larsson (1997).

test are often only applied for one minute and settlements of a footing are normally calculated for a 10-year perspective. Briaud proposed that the pressures in some of the steps in the pressuremeter test should be held constant long enough to enable an evaluation of the creep exponent  $n_{pmt}$

$$\Delta R_{c(t)} = \Delta R_{c(1\text{minute})} \left( \frac{t(\text{minute})}{1\text{minute}} \right)^{n_{pmt}}$$

This procedure was used in the tests with the new pressuremeter in the present investigations.

From comparisons with a number of load tests, Briaud proposed that the settlements of the test footings could be calculated as

$$s_{(t)} = s_{(1\text{minute})} \left( \frac{t(\text{minute})}{1\text{minute}} \right)^{2n_{pmt}}$$

Briaud found this to apply in comparisons with load tests with a duration of up to 30 minutes. Similar corrections are used also when transforming 1-year settlements to 10-year settlements and 100-year settlements respectively. However, transformation of a 1-minute settlement to a 10-year settlement involves 6 – 7 orders of magnitude in time and is thus a considerable source of error.

The Briaud method was evaluated in a study of the results of the previous plate load tests on sand and silt, (Larsson 1997). It was then not possible to evaluate the method proposed by Briaud for transformation of the pressuremeter test results with regard to time because the required holding tests for evaluation of the exponent  $n_{pmt}$  were missing. Like the Menard interpretation and settlement calculation, the calculation by the Briaud method appears to be sensitive to the quality of the predrilled hole. A new transformation function was therefore proposed, based on the Swedish results. In the Menard procedure, there are certain possibilities for compensating for the quality of the hole by selecting the rheological factor  $\alpha$  accordingly, but for the Briaud method no such method has been elaborated.

## New approaches to taking the variation in modulus with stress and strain into consideration

Another method of calculating settlements in overconsolidated soils from the results of pressure meter tests has been proposed by Ekdahl and Bengtsson (1996). The method uses the moduli determined from the repeated unloading and reloading cycles at several stress levels in the related proposal for a new testing procedure, see “Pressuremeter tests: New pressuremeter”. This procedure allows an evaluation of both the increase in modulus of elasticity with increasing normal stresses and its decrease with increasing shear strains. The calculation method has been shown to give promising results in clay till. However, the original method appeared to require some modification with respect to the relations between the influence of the decrease in modulus with increase in shear strain and the simultaneous increase in stiffness because of the increasing stress level. This proved to be the case for the foundations with limited widths for which it was tested and where the calculated load-settlement curves tended to bend off in the wrong direction.

The method is based on stress calculations from theory of elasticity, whereby both increases in vertical and horizontal directions are calculated continuously with depth. The stresses are calculated under the “characteristic” point where the stress (and settlement) is independent of the rigidity of the foundation. When the foundation is embedded in the ground, an increased depth  $kz$ , which is a function of the relation between foundation width and embedment depth, is calculated according to Jelinek (1951) and used in the stress calculation. The vertical strain is then calculated as

$$\Delta \varepsilon_z = \frac{1}{E_z} \left( \Delta \sigma_z - \nu (\Delta \sigma_x + \Delta \sigma_y) \right)$$

Where  $\Delta \sigma_x$ ,  $\Delta \sigma_y$  and  $\Delta \sigma_z$  are the stress changes in  $x$ ,  $y$  and  $z$  directions.  $E_z$  is the modulus of elasticity at depth  $z$  and  $\nu$  is the Poisson’s ratio

The increase in mean stress level  $\Delta\theta_q$  caused by the external load is  $(\Delta\sigma_x + \Delta\sigma_y + \Delta\sigma_z)/3$ .

The proposed calculation process is as follows:

- The bearing capacity of the foundation is calculated according to the Menard procedure for results from pressuremeter tests.
- A load increment equal to 10 % of the bearing capacity is selected.
- The stress increases in the ground resulting from the load increment are calculated
- The stress level is calculated as the initial stress at depth  $z$  in the ground,  $\sigma'_{z0} (1+2K_0)/3$ , plus half of the increase in stress level caused by the external load.  $\sigma'_{z0}$  is the in situ vertical stress and  $K_0$  is the in situ coefficient of earth pressure.
- Values of  $E_z$  are assumed on the basis of the stress levels, assumed strain levels and the relations between these parameters and the moduli evaluated from the pressuremeter tests.
- The strains are calculated as described above and compared to the assumed strain levels. An iterative procedure is then used to match the moduli and the strains. When these converge, the actual moduli and strains are found and the settlement of the foundation is obtained by integration over the depth of influence. This depth is limited according to Schmertmann (1978).
- The procedure is repeated successively for equally large load increments until a complete load-settlement curve is obtained.

In principle, the calculation method described above can be used also for other test results, such as results from triaxial tests. Also other formulations of the variation in modulus depending on shear stress, strain and normal stresses level can be evaluated from e.g. the pressuremeter tests

and used in the calculation method. The calculation of stresses may have to be modified depending on the geometry of the loading, the depth of the compressible layers and the stratigraphy of the soil. The relative influence of stress, strain and time on the moduli may have to be modified and empirical correction factors may also have to be introduced, but the general calculation procedure will still be useful.

The calculated strains and settlements need to be modified with respect to time in order to yield values that are relevant for the design life of a foundation. This can be done by using any of the aforementioned methods of describing time effects. The time aspects in this correction will depend on how fast the test was performed, in which the modulus was determined. Normally, the settlement calculations refer to 10-year settlements. When using a correction of the modulus with respect to time, this can be done already when the moduli are introduced into the calculations and no subsequent correction is then necessary.

A very approximate way of estimating the variation in modulus in stiff soils is to use the initial shear modulus  $G_0$  together with empirical knowledge about the variation of this modulus with mobilisation of the shear strength. The shear modulus can then be converted to a correspondingly changing modulus of elasticity and the settlements can be roughly estimated. However, this requires a coupling to a model for calculating the related settlements caused by volumetric compression or, alternatively, this compression must be so small that it can be neglected. Furthermore, the time effects will have to be considered. When measuring  $G_0$  by seismic methods, the time involved in the measurement is only a fraction of a second and the conversion to 10-year deformations is not straightforward.

### A.3 PREDICTION OF BEARING CAPACITY

#### The general bearing capacity equation

The general equation for bearing capacity is based on the original Prandtl formula, which has been supplemented with correction factors for inclined load, eccentric load, depth of embedment, shape of the foundation, inclined ground surface, inclined base of the foundation and layered soil profile, (Brinch-Hansen 1961 and 1973, Brown and Meyerhof 1969, Tscheng 1957, Vesic 1973). The correction factors are partly based on experimental results and slightly different bearing capacity factors have also been proposed. In Sweden, the factors given by Hansbo and Sällfors (1984) in the BYGG engineering handbook have recently been updated by Bergdahl et al. (1993) in the new handbook for shallow foundations. A new and partly different proposal for bearing capacity and correction factors has subsequently been presented by CEN (1994).

According to Bergdahl et al., [the general equation](#) can be written

$$q_b = cN_c\xi_c + qN_q\xi_q + 0.5\gamma' b_{ef} N_\gamma \xi_\gamma$$

where

- $q_b$  = ground pressure at failure, kPa
- $c$  = cohesion, part of the shear strength, kPa
- $q$  = overburden pressure at the foundation level, kPa
- $\gamma'$  = effective unit weight of the soil below the foundation level, kN/m<sup>3</sup>
- $b_{ef}$  = effective width of the foundation, m (at centric loading  $b_{ef} = b$  and at eccentric loading  $b_{ef} = b - 2e_b$ , where  $e_b$  = eccentricity, m)

$N_c, N_q, N_\gamma$  = bearing capacity factors being functions of the effective friction angle in the soil as described below

$\xi_c, \xi_q, \xi_\gamma$  = correction factors for conditions differing from those for which the bearing capacity factors were elaborated

$$\xi_c = d \cdot s \cdot i \cdot g \cdot b_c$$

$$\xi_q = d \cdot s \cdot i \cdot g \cdot b_q$$

$$\xi_\gamma = d \cdot s \cdot i \cdot g \cdot b_\gamma$$

where  $d, s, i, g,$  and  $b$  are correction factors for **d**epth of embedment, **s**hape of foundation, **i**nclined load, **g**round surface and **b**ase respectively.

For the current investigation, the latter three corrections are not relevant.

The first term in the general equation relates to the contribution of the cohesion,  $c$ , in the soil, the second to the contribution from the overburden pressure at the foundation level,  $q$ , and the third to the contribution from the weight of the wedge of soil sliding out from below the foundation at failure,  $\gamma$ , [Fig. 128](#).

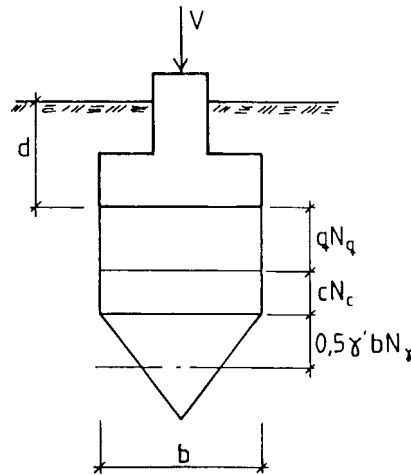


*Fig. 128. Bearing capacity - schematic principle of the general equation.*

In its basic form, the general equation is valid for an infinitely long foundation placed directly on the ground surface and loaded by a centric load. Differing conditions can be taken into account by multiplying the bearing capacity factors  $N_c, N_q$  and  $N_\gamma$  by the correction factors ( $\xi$ ).

In cohesive soils and undrained conditions, the friction angle is assumed to be zero, whereby  $N_\gamma$  becomes zero and  $N_q = 1$ . The equation is then reduced to

$$q_b = cN_c \xi_c + q \xi_q$$

In cohesionless soil, ( $c = 0$ ), the equation becomes

$$q_b = qN_q \xi_q + 0.5\gamma' b_{ef} N_\gamma \xi_\gamma$$

### Bearing capacity factors

The bearing capacity factors,  $N$ , are calculated as follows:

In undrained conditions, i.e.  $\phi' = 0$

$$N_c^u = \pi + 2$$

$$N_q^u = 1$$

$$N_\gamma^u = 0$$

In drained conditions

$$N_c = (N_q - 1) \cot \phi'$$

$$N_q = \frac{1 + \sin \phi'}{1 - \sin \phi'} e^{\pi \tan \phi'}$$

$$N_\gamma = F(\phi') \left[ \frac{1 + \sin \phi'}{1 - \sin \phi'} e^{\left(\frac{3\pi}{2} \tan \phi'\right)} - 1 \right]$$

where  $F(\phi') = 0.08705 + 0.3231 \sin(2\phi') - 0.04836 \sin^2(2\phi')$ .

### Determination of the relevant vertical stress at the foundation level

In undrained conditions, the bearing capacity is dependent on the total vertical stress at the foundation level

$$q = \gamma d_{min}$$

where  $d_{min}$  is the minimum foundation depth, see Fig. 129.

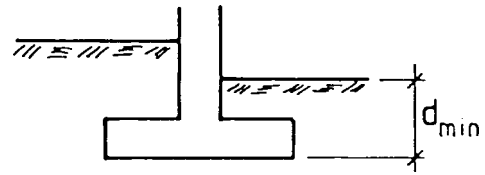


Fig. 129. Determination of minimum foundation depth.

In drained conditions, the bearing capacity is dependent on the effective vertical stress at the foundation level  $q'$ . If the foundation level is located below the free ground water level, the relevant effective vertical stress, which replaces  $q$  in the equation, becomes  $q' = q - u$ , where  $u$  is the pore water pressure at the foundation level. In the case of negative pore pressures, the total overburden pressure  $q$  is used in the equation and the effect of the negative pore pressure is converted to a “false cohesion” as described below.

### Determination of relevant unit weight of the soil below the foundation

When the free ground water level is located deeper than  $b_{ef}$  below the foundation level, the unit weight  $\gamma$  is introduced in the calculations. When the free ground water level is located at or above the foundation level, the effective unit weight  $\gamma'$  should be used, provided that the ground water conditions are hydrostatic. In non-hydrostatic conditions, a corresponding unit weight  $\gamma_i$  may be used

$$\gamma_i = \gamma - \gamma_w(1 + i)$$

where

$\gamma_w$  = unit weight of water, kN/m<sup>3</sup>  
 $i$  = hydraulic gradient  $\Delta H/d$  in the upward direction

$\Delta H/d$  = change in hydraulic head per unit depth, m/m

When the free ground water level is located within  $b_{ef}$  below the foundation level, a relevant value of  $\gamma_{eq}$  between  $\gamma$  and  $\gamma'$ , which is weighted over the depth  $b_{ep}$ , is used.

### Correction for foundation depth, $d$

The shear strength of the soil above the foundation level also contributes to the bearing capacity. This is taken into account by using the following correction factors:

$$N_c: \quad d_c = 1 + 0.35 \frac{d}{b_{ef}} \quad ; d_c \leq 1.7$$

$$N_q: \quad d_q = 1 + 0.35 \frac{d}{b_{ef}} \quad ; d_q \leq 1.7$$

$$N_\gamma: \quad d_\gamma = 1$$

### Correction for foundation shape, $s$

The basic equation is valid for an infinitely long strip foundation. For other shapes, corrections have to be applied. According to Lee et al. (1983) the following correction factors apply

$$N_c: \quad s_c = 1 + 0.2 \frac{b_{ef}}{l_{ef}} \quad \text{if } \phi' = 0$$

$$s_c = 1 + \frac{N_q}{N_c} \frac{b_{ef}}{l_{ef}} \quad \text{if } \phi' \neq 0$$

$$N_q: \quad s_q = 1 + (\tan \phi') \frac{b_{ef}}{l_{ef}}$$

$$N_\gamma: \quad s_\gamma = 1 - 0.4 \frac{b_{ef}}{l_{ef}}$$

In all cases  $b_{ef} \leq l_{ef}$

Further correction factors,  $i$ ,  $g$  and  $b$ , and corrections for dry crust or coarse soil on soft clay, which are not relevant for the current investigation, are described in Bergdahl et al. (1993), among others.

### Estimation of the effect of negative pore pressures

The effect of negative pore pressures (matrix suction) on the bearing capacity can be very great. Before this effect is utilised in a design, it has to be ascertained that the matrix suction is maintained at all times. Furthermore, a determination must be made of the minimum values that can safely be counted upon. Unless this has been clarified, the effect of matrix suction should not be taken into account.

When evaluating plate loading tests and also certain other field tests such as screw plate tests and pressuremeter tests, the matrix suction prevailing at the time of the test has to be considered. According to Fredlund and Rahardjo (1993), the effect of the matrix suction can be converted into a "false cohesion". According to Öberg (1997), this can be calculated from

$$c_a \approx (u_a - u_w) S_r \tan \phi'$$

where

$c_a$  = apparent cohesion  
 $u_a$  = pore air pressure, normally assumed to be equal to the atmospheric pressure  
 $u_w$  = pore water pressure  
 $S_r$  = saturation ratio  
 $\phi'$  = friction angle

According to the pore pressure measurements, there were no effects of natural matrix suction in the ground during the investigations and load tests in the present project.

**Calculation based on pressuremeter test results**

The bearing capacity of foundations on silt can be estimated on the basis of pressuremeter tests according to Menard (Baguelin et al. 1978). The calculation is based on the evaluated limit pressures according to

$$q_u = q + N_p (p_l - p_0) = q + N_p p_l^*$$

where

$N_p$  = bearing capacity factor in the interval 0.8 to 8.0, depending on soil type, foundation shape and embedment depth, *Fig. 130*.

$p_0$  = total horizontal stress in the soil =  $K_0(\gamma z - u) + u$

$q$  = total overburden pressure at the foundation level

$p_l^*$  = net limit pressure ( $p_l - p_0$ ), alternatively the equivalent net limit pressure  $p_{le}^*$ , see below

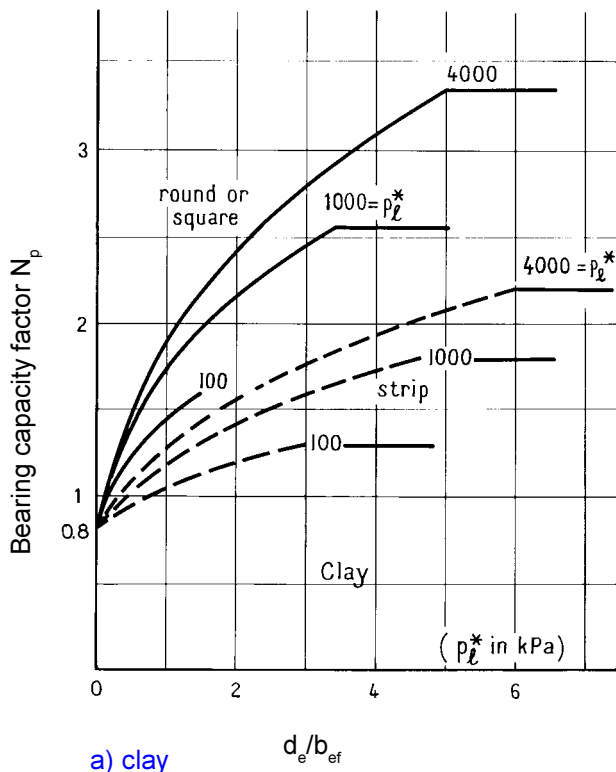


*Fig. 130. Bearing capacity factor  $N_p$  as a function of foundation shape and embedment depth for clay. (Baguelin et al. 1978)*

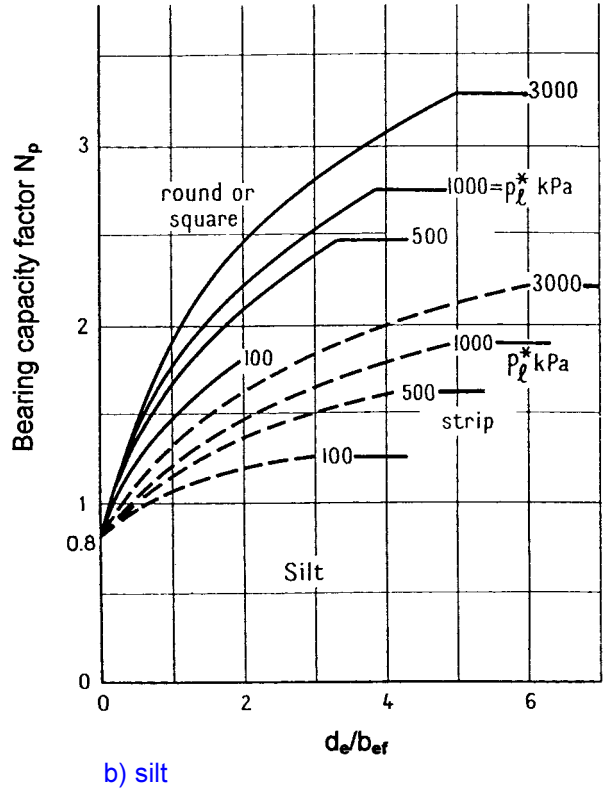


*Fig. 130. Bearing capacity factor  $N_p$  as a function of foundation shape and embedment depth for silt. (Baguelin et al. 1978)*

The bearing capacity factor  $N_p$  may be corrected for eccentric load, inclined load and sloping ground surface as described by Baguelin et al. (1978) and reproduced by Bergdahl et al. (1993). However, this is not relevant for the present investigation.

The bearing capacity equation assumes a specific constant value of the net limit pressure  $p_l^*$ . However, the bearing capacity is assumed to be influenced by the strength of the soil over a depth of  $3b$ ,  $1.5b$  above the foundation level and  $1.5b$  below. If the soil is not homogeneous over this depth, a relevant equivalent value,  $p_{le}^*$ , has to be calculated, *Fig. 131*.



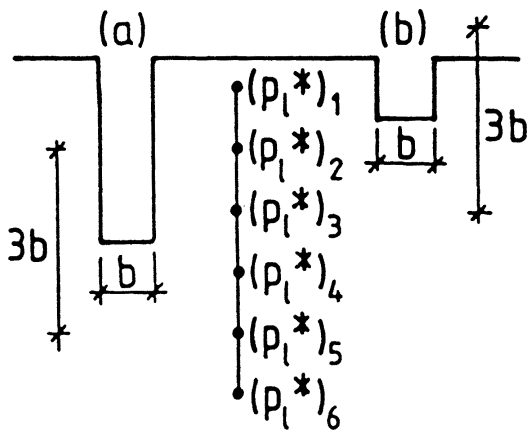


Fig. 131. In calculation of the equivalent net limit pressure, all tests within  $\pm 1.5b$  from the foundation level are taken into consideration.

$$p_{le}^* = [p_{11}^* \cdot p_{12}^* \cdot p_{13}^* \cdot \dots \cdot p_{1n}^*]^{1/n}$$

The differences between single values and  $p_{le}^*$  should not be greater than 40 %, otherwise there will be a risk of misleading results.

When the limit pressure varies with depth, the actual foundation level is replaced by an effective foundation level  $d_e$  calculated as

$$d_e = \sum_{i=1}^n \Delta z_i \frac{(p_i^*)_i}{(p_{le}^*)}$$

This calculation does not take permissible settlements into account.

### Calculation of bearing capacity with respect to settlement criteria

Most methods of calculating bearing capacity refer to real failure because the available shear strength is exceeded. However, in many cases the deformations preceding real failure are so large that all acceptable criteria for maximum settlements have been passed long before this stage. The bearing capacity can therefore also be defined in terms of acceptable loads for which only small and generally tolerable settlements will occur, or in terms of a maximum settlement which is so large that for all practical purposes failure can be considered to have occurred. A common limit for the latter criterion is that the relative settlements amount to 10 % of the plate width,  $s = 0.1b$ . Depending on the particular case, the generally tolerable settlements are given in a form such as 25 – 50 mm or a percentage of the plate width.

Generally acceptable loads which can be applied without causing any harmful settlements have previously been given in the Swedish building codes. These loads have then been based on the type of soil, the geometric conditions for the foundation and the results of common types of tests. The new building codes require bearing capacity to be calculated both in terms of failure loads in an ultimate failure state and acceptable settlements in a serviceability state with different criteria depending on the type of construction and the risk involved. This puts high demands on the ability to correctly predict the settlements over a wide range of loads and relative settlements. The available methods which have a potential to meet these requirements are the method of predicting settlements using evaluated moduli and taking into account the curved load-settlement relation, the Briaud method of predicting settlements based on pressuremeter tests and the more advanced methods of taking the change in modulus with strain into account. All these methods are described in the previous part of this chapter.